Final Report
Contract DOT-HS-031-1-126
UM-HSRI-PF-72-3-1

Limit Handling Performance as Influenced by Degradation of Steering & Suspension Systems

Volume 1 of 2
Research Study

P.S. Fancher
R.D. Ervin
P. Grote
C.C. MacAdam
L. Segel

Highway Safety Research Institute
The University of Michigan
Huron Parkway and Baxter Road
Ann Arbor, Michigan

November 1972

Prepared for
National Highway Traffic Safety Administration
U.S. Department of Transportation
Washington, D.C. 20591

TECHNICAL REPORT STANDARD TITLE PAGE

1. Report No.	2. Government Accession No.	3. Recipient's Catalog No.
UM-HSRI-PF-72-3-1		

4. Title and Subtitle	5. Report Date
Limit Handling Performance as Influenced by Degradation of Steering and Suspension Systems	November 1972
	6. Performing Organization Code

7. Author(s)	8. Performing Organization Report No.
P.S. Fancher, R.D. Ervin, P. Grote, C.C. MacAdam, L. Segel	UM-HSRI-PF-72-3-1

9. Performing Organization Name and Address	10. Work Unit No
Highway Safety Research Institute The University of Michigan Huron Parkway and Baxter Road Ann Arbor, Michigan 48105	11. Contract or Grant No. DOT-HS-031-1-126
	13. Type of Report and Period Covered Final Report 6/71 to 11/72
12. Sponsoring Agency Name and Address National Highway Traffic Safety Administration U.S. Department of Transportation Washington, D.C. 20591	14. Sponsoring Agency Code

15 Supplementary Notes

16. Abstract

The influence of degradations in steering and suspension system (S/SS), components on limit handling behavior of passenger vehicles is examined by means of analysis, simulation, laboratory measurement, and full-scale testing. The major single conclusion deriving from this study is that vehicle handling performance at the limits of tire-road adhesion is negligibly influenced by degradation in S/SS components, both singly and in combination. A principal exception, as indicated by a positive sensitivity in certain performance measures, is degraded shock absorbers.

In view of the findings, it appears that benefits to the vehicle-in-use safety program deriving from additional research on this specific topic would be minimal.

17. Key Words	18. Distribution Statement
Vehicle mechanics, open-loop measures, component degradation, steering, suspension system	Unlimited Availability

19. Security Classif. (of this report)	20. Security Classif. (of this page)	21. No. of Pages	22. Price
Unclassifed	Unclassified		

Form DOT F 1700.7 (8-69)

TABLE OF CONTENTS

TABLE OF CONTENTS (Cont)

The contents of this report reflect the views of the Highway Safety Research Institute which is responsible for the facts and the accuracy of the data presented herein. The contents do not necessarily reflect the official views or policy of the National Highway Traffic Safety Administration.

FOREWORD

The research study reported herein was supported by the National Highway Traffic Safety Administration of the U.S. Department of Transportation. The contract technical manager was Lloyd H. Emery.

This project was directed by the Highway Safety Research Institute of The University of Michigan at Ann Arbor.

The simulation study was conducted with the support of the facilities and staff of the Bendix Research Laboratories at Southfield, Michigan. The testing activity was conducted with the support of the facilities and staff of the Texas Transportation Institute (TTI) at College Station, Texas.

In November, 1971, a pilot test program was begun at TTI, permitting preliminary developments in test practice, as well as an examination of various degraded component conditions. A supplemental testing activity followed, beginning in March 1972, intending to resolve certain anomalies in the pilot test program data through an extensive set of tire properties experiments. In August, 1972, a full-scale test program was initiated, completing in September with the acquisition of a data set representing the influence of steering and suspension system degradation on the limit handling performance of two contemporary passenger vehicles.

ACKNOWLEDGEMENTS

The preparation of the literature review in this study was the responsibility of Mr. C. Winkler.

The test vehicles used in this study were prepared and initially outfitted under the direction of Mr. J. Boissonneault.

The laboratory measurement of steering and suspension system parameters was directed by Mr. J. Wirth, with assistance by Mr. Takeo Tohmiya, a visiting engineer from the Toyota Motor Company and Mr. Eugen Negros, a visiting Fulbright Fellow from the Bucharest Polytechnic Institute in Romania.

The design and preparation of mechanical simulations of degraded components was the responsibility of Mr. Earl Klager.

The design of the electronics system in the new automatic vehicle controller was the responsibility of Mr. James Ackley.

The implementation of the hybrid computer simulation at the Bendix Research Laboratory was performed by Mr. J. R. Hartz under the direction of Dr. J. G. Elliott.

Special acknowledgement is due to the test subcontractor, Texas Transportation Institute (TTI). In particular, Dr. R. Young, Mssrs. R. Zimmer, L. Milberger, M. White, and D. Cangelose of the TTI staff contributed extraordinary efforts to the success of the test activity.

Particular acknowledgement is due to Mr. Robert Hegel, of the Monroe Auto Equipment Corporation, for his active cooperation throughout the study, in the planning and fabrication of realistically degraded shock absorbers.

We also wish to express sincere thanks to Mr. Mark Waghorn, and the Leslie Hartridge Corporation, for the provision of shock absorber test equipment.

Additionally, measurement apparatus and training of technicians was provided by the Bear Equipment Company.

1. INTRODUCTION

This report presents findings, conclusions, and recommendations derived by the Highway Safety Research Institute (HSRI) in a research study for the National Highway Traffic Safety Administration (NHTSA) entitled "Component Degradation, Inspection Equipment: Steering and Suspension System Performance." The primary objective of the study was to determine, through open-loop testing, how various realistic types, degrees, and combinations of steering and suspension system component degradation affect objective and quantitative measures of vehicle performance in the conduct of accident avoidance or limit maneuvers.

This report presents material which can be more fully understood if the reader is acquainted with the concepts and methods put forth in a companion study sponsored by NHTSA and entitled "Vehicle Handling Performance" [7]. The vehicle test procedures and data processing methodology that were developed and applied in the companion study have also been used in this program. Accordingly, the primary objective of this investigation can be more explicitly expressed as determining the influence of steering and suspension system degradation on limit maneuver performance as measured by the following six vehicle handling test procedures:

- straight line braking
- braking in a turn
- roadholding in a turn
- trapezoidal steer
- sinusoidal steer
- drastic steer-brake

It should be noted that the data library generated in this study contains measurements of vehicle handling performance exhibited at the limits of tire-road adhesion. It follows that limit maneuver measures do not constitute an evaluation of the handling properties manifested in normal driving, but rather characterize the emergency maneuvering capability of the tire-vehicle system. Further, the term "open-loop" should be used in referring to these measures since the driver has been removed as an active element in the system.

In order to attain the desired objective within the prevailing constraints on time and money, it was necessary that a balanced program of analysis, laboratory testing, computer simulation, and field testing be employed, as a result of the large number of steering and suspension system degradation modes that were originally specified by NHTSA to be addressed in this program. In addition to determining the influence of

- worn ball joints
- worn tie-rod ends
- loose wheel bearings
- loose steering gear
- front-end misalignment (toe, caster and camber)
- degraded shock absorbers
- wheel mass imbalance

both singly and in combination, it was expressly requested that brake imbalance be considered as a degradation mode which, in combination with steering and/or suspension system degradations, could augment the influence of these degradations

on limit maneuvering performance. Requests were also made for HSRI to investigate the influence of long shackles (as used by "car buffs" to provide space for large tires on rear axles) and loose roll bar bushings on limit maneuver performance.

Given the geometric progression existing between the number of test runs and the size of the test matrix, HSRI structured a research approach to determine a cost-effective, full-scale test activity. This approach (namely, the overall research plan) is summarized in Section 2. The analytical, laboratory measurement, and simulation phases of this plan are described in Section 3. The pilot test program, conceived as an essential element of the overall plan, is treated in Section 4 and the results deriving from the full-scale test program are given in Section 5. Conclusions and recommendations are presented in Section 6.

Ten appendices are included in this report. Appendix I constitutes the survey of the literature that was made in the early stages of the study. Appendices II through IV treat matters related to vehicle simulation. Appendices V through IX are devoted to vehicle testing subjects. Appendix X is in a separate volume, and contains graphical presentations of the limit maneuver performance numerics that were yielded by the response time histories measured during the full-scale test program.

2. STRUCTURE OF THE RESEARCH STUDY

The major challenge presented by this study derived from the size of the matrix of degradation conditions to be examined. It was determined that adequate consideration of the most important elements of this matrix could only be assured through the exercise of a multi-stage screening process by which the vast majority of degradation modes could be shown to be negatively related to vehicle performance. It was hypothesized that this effective reduction of the matrix would follow from certain precepts of vehicle mechanics which suggested that vehicle limit performance could be shown to have a negligible sensitivity to many degradations of steering and suspension system components. The principle observation, by which negative sensitivities might be expected to predominate, derives from the phenomenon of tire shear force saturation. Since the maneuvering envelope of the pneumatic-tired motor vehicle is determined primarily by the order and distribution with which tire shear forces saturate, it follows that any change in vehicle limit performance must derive from a significant adjustment in tire forces under conditions of high angular slip (at which side force is quite insensitive to small changes in slip angle) and under conditions of longitudinal slip approaching wheel lockup. To the degree that degradation conditions would not cause significant changes in slip, tire forces would not be modified in any significant way at the limit of performance and the postulated lack of sensitivity would prevail.

Additionally, it was clear that many of the degradation modes could be represented by a common functional relationship. Steer indeterminacy thus is a generic representation of steering gear box lash, steering gear box looseness, tie rod end lash, wheel bearing play, etc.

The examination of basic sensitivities to generic degradation modes was undertaken by simulation. The findings deriving from the simulation study were then used to structure a program of pilot testing, by which the validity of the simulation was assessed, and a quantification of certain performance sensitivities was obtained. These combined results were then used to structure a full-scale test program in which two vehicles were subjected to a comprehensive set of tests to provide solid experimental data indicative of the sensitivity of vehicle performance to critical degradations across a broad range of limit maneuvering conditions.

In each of these program stages, certain component degradation states were evaluated which represented the virtually maximum level of wear or deterioration as was felt to be achievable without jeopardizing structural integrity. This concept of a virtually maximum level of wear constituted the means by which artificial degradation of components was scaled, and thus represents a key element in the selected approach. The premise that a finding of negative sensitivity is indisputably solid and sufficiently general only if it is based upon a demonstration of insensitivity for the maximally degraded species appears to be rational and defensible. Thus, ball joints and tie-rod ends were fabricated with ball studs ground down until structural continuity was threatened. Likewise, shock absorber degradation, wheel imbalance, brake imbalance, and other degradation modes were represented by extreme levels of deterioration. If vehicle performance exhibited a positive sensitivity to an imposed maximum level of component wear, as was found to be the case for shock absorber degradation, other non-maximum degradation levels were examined. The mechanical means by which various levels of component degradation could be introduced into a vehicle are presented in Appendix V.

3. TEST PLAN DEVELOPMENT ACTIVITIES

The scheme for relating limit maneuvering performance to steering and suspension system degradations originally envisioned the testing of eight vehicles in an O.E. and a degraded state. As was discussed in Section 2, the number of experimental variables is so large that the development of an efficient test plan becomes an overriding requirement. In addition, it was necessary that additional methods other than direct testing in the field be brought to bear. Consequently, a balanced program of analysis, simulation, laboratory tests, and field tests was conceived in order that field testing of the eight vehicles (called out in the contract between the University and Department of Transportation) could be held to minimal levels.

The eight vehicles specified as the test sample for this investigation were selected by DOT to match the six vehicles used in a related study [2], with two vehicles being added to supplement the various suspension and steering system design configurations represented by the original six vehicles. These eight vehicles are listed below together with a brief description of their design features.

1. Ford Mustang

   Front suspension: coil spring on upper A-arm, strut-type lower control arm, and telescoping shock absorbers.

   Rear suspension: semi-elliptic leaf springs, rigid axle, telescoping shock absorbers.

   Steering: hydraulic cylinder assisted linkage behind front wheel centerline.

2.	Chevrolet Station Wagon	Front Suspension: upper A-arm, coil spring on lower A-arm, telescoping shock absorbers. Rear suspension: semi-elliptic leaf springs, rigid axle, telescoping shock absorbers. Steering: integral power assisted gear box with linkage behind front wheel centerline.
3.	Dodge Coronet	Front suspension: upper A-arms, longitudinal torsion bars on strut-type lower control arm, telescoping shock absorbers. Rear suspension: semi-elliptic leaf springs, rigid axle, telescoping shock absorbers. Steering: integral power assisted gear box with linkage behind front wheel centerline.
4.	Ambassador	Front suspension: coil spring on upper A-arm, strut-type lower control arm, telescoping shock absorbers. Rear suspension: 4-trailing locating links, rigid axle, coil springs, telescoping shock absorbers. Steering: integral power assisted gear box with linkage ahead of front wheel centerline.

5.	Oldsmobile F-85	Front suspension: coil spring on lower A-arm, upper A-arm, telescoping shock absorbers. Rear suspension: coil springs, rigid axle, 4-trailing locating links, telescoping shock absorbers. Steering: integral power assisted gear box with linkage ahead of front wheel centerline.
6.	Volkswagen 1500 Beetle	Front suspension: McPherson strut including telescoping shock absorbers and coil springs. Rear suspension: swing axles with trailing arms, transverse torsion bars, and telescoping shock absorbers. Steering: manual gear box with asymmetrical linkage behind front wheel centerline.
7.	Austin America	Front suspension: front wheel drive, two wishbones, strut on lower frame, hydrolastic. Rear suspension: independent trailing arms, hydrolastic. Steering: manual, rack and pinion design.
8.	Ford Pick-up Truck	Front Suspension: coil springs on twin I beam, telescoping shock absorbers. Rear suspension: semi-elliptic leaf springs, rigid axle, telescoping shock absorbers. Steering: hydraulic cylinder assisted linkage behind front wheel centerline.

The above eight vehicles (1971 models) were procured for this program and provided both the requirements and the data needed to execute a methodology designed to yield maximum information on, and understanding of, performance-degradation interactions without exceeding time and funding restrictions.

The methodology designed to achieve program objectives consisted of a number of steps. The steps employed to design a full-scale test program involved four specific activities, each being an essential element of the overall plan. These activities (or methodological steps) are described below. In summary form, they were:

(1) The various suspension and steering system designs contained in the eight-vehicle sample were analyzed to characterize their functional mechanical properties in both the OEM and the degraded condition.

(2) The existing hybrid vehicle dynamics simulation was augmented and refined to explicitly represent the functional characteristics identified in (1).

(3) The simulation was exercised to examine in a comprehensive manner the influence of suspension and steering system degradation on limit maneuver performance.

(4) Pilot tests were conducted to develop experimental techniques and to confirm the trends indicated in the simulation exercises.

The first two methodological steps, cited above, constituted the development of a simulation capability in excess of that which had been developed earlier under NHTSA auspices [4]. This activity is summarized in Section 3.1 below, with additional details being given in Appendix III. Application of a simulation methodology required that vehicle parameter data be acquired. This activity is summarized in Section 3.2 below, with further details being given in Appendix II. (An extensive set of parameter data, applicable to the eight vehicles in the study sample, will also be found in this Appendix.) The results of the simulation study are discussed in Section 3.3, a complete presentation of these findings being relegated to Appendix IV. The findings of the pilot test program are presented separately in Section 4, rather than being included in this section of the report.

3.1 SIMULATION REFINEMENTS

The mechanical properties of steering and suspension system components were analyzed to develop mathematical descriptions of (1) the functional characteristics of degraded ball joints, tie-rod ends, wheel bearings, steering gear, and shock absorbers and (2) the influence of wheel alignment variables, wheel-mass imbalance and brake-torque imbalance.

Degraded ball joints, tie-rod ends, wheel bearings, and steering gear all contribute to producing play or looseness in the steering system. Degraded ball joints and wheel bearings also contribute to play in front-wheel camber angle. These play phenomena are handled in the simulation as free play which treatment represents a somewhat more drastic behavior than actually occurs in use because looseness in these components is accompanied by load-lash effects due to spring loading.

A model of the steering system was developed to include the influence of play in the steering gear box separately from play due to wheel bearings, ball joints and tie-rod ends. This model is fully described in Appendix III.

Wheel camber angle was treated in the augmented simulation as the sum of the non-degraded camber angle (as determined by suspension deflection) and an amount of camber due to play in the wheel bearings and ball joints. The polarity of the camber angle offset due to play changed with the polarity of the side force acting on the tire.

Damping forces created at the wheel by shock absorbers were computed by taking into account the mounting angle of the shock absorber and the effective gear ratio of the mounting location. The damping at the wheel was represented in the simulation by piecewise linear approximations to the shock absorber performance data acquired by laboratory measurements (see Section 3.2.3). Degraded shock absorber forces were represented in the simulation as fractions of the O.E. force. It should be noted, however, that the shock absorbers used in the test program were degraded in a more realistic fashion.

Misalignment of the front wheels was modeled by defining parameters that quantify the change in wheel alignment from the specified O.E. value. These parameters are symbolized by:

EK1 and EK2	for toe changes at the right and left front wheels, respectively
THE1 and THE2	for caster changes at the right and left front wheels, respectively
FEE1 and FEE2	for camber changes at the right and left front wheels, respectively

Wheel imbalance was treated as a rotating force at the wheel rim. The magnitude of this force was given by

$$m_{\ell} R_{rim}[(RPS)_i]^2$$

where m_{ℓ} is the mass imbalance, R_{rim} is the rim radius, and $(RPS)_i$ is the wheel angular velocity. A rate resolver circuit [5] was used to determine the horizontal and vertical components of this force. The moment of this force about the king pin was included in the steering system calculations.

A capability for simulating brake imbalance was achieved by extending the existing simulation to provide (1) brake-line pressure input to each wheel and (2) a pressure-torque relationship for each wheel.

In addition to the aforegoing refinements, the existing simulation was also modified and extended to include the mechanical properties of independent rear suspensions and to provide a means for simulating

(1) anti-pitch effects

(2) a variety of front and rear roll-center locations

(3) long shackles (as employed to locate the leaf spring used in rear suspensions)

(4) worn roll-bar bushings

(5) different tire force characteristics, front and rear.

3.2 LABORATORY MEASUREMENTS OF STEERING AND SUSPENSION SYSTEM PARAMETERS

To accomplish this task, two temporary laboratory facilities were fabricated. They consisted of

(1) a device for measuring steering system properties, and

(2) a set-up for measuring suspension properties.

Both facilities and their use in this program are described below. An existing high performance laboratory testing machine was employed to measure the force-velocity characteristics of shock absorbers, new and degraded.

3.2.1 STEERING SYSTEM MEASUREMENT TECHNIQUES. Figure 3.1 is a photograph of the test set-up used for steering system measurements. The design permits a pure torque to be applied to one front wheel on the vehicle, with the steering wheel held fixed and the other front wheel free to rotate about its steering pivot. The front wheels are resting on specially prepared turn and slide tables. (About 8 ft/lbs of torque are required to rotate these turn and slide tables under an 800 lb. vertical load.) A turn-buckle is used to increase or decrease the tension in the cable and thereby increase or decrease the torque applied to the wheel. Cable tension is measured with a load cell. By measuring the steer angle of each wheel as a function of the applied torque, the compliance in the steering linkage and in the steering column can be calculated, provided the steering gear ratio and linkage ratio are known.

The influence of steering-gear play, tie-rod end play, and loose ball joints on the relationship between steering torque and steer displacement were measured with this device. Since a considerable amount of coulomb friction is distributed at various locations in the steering system, different levels of torque are needed to overcome this friction, thereby permitting a particular type of play to show up in the test

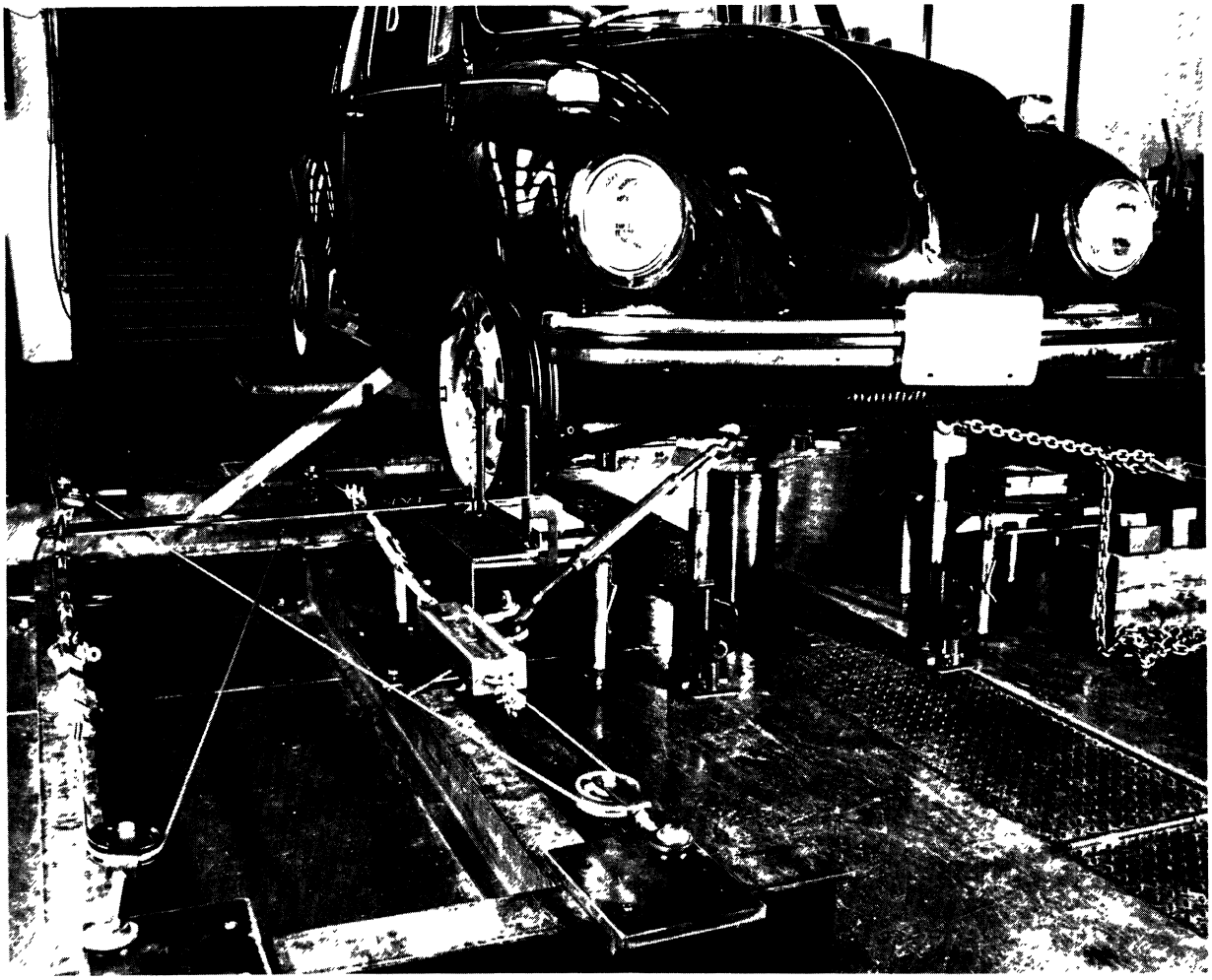

Figure 3.1. Steering system measurement fixture

result. Also, a worn "ball" in spring-loaded ball joints (and in tie-rod ends) results in what appears to be more of a change in steering compliance than additional free play.

A typical set of test results are plotted in Figure 3.2. In this example, the steering gear box adjustment was backed off to give the free play shown, approximately ±0.014 radians at the front wheels. These data, as obtained on a Chevrolet station wagon, yielded a steering-column stiffness of 1290 in.lb./rad. and a steering-linkage stiffness of 391,000 in.lb./rad.

3.2.2 SUSPENSION SYSTEM MEASUREMENTS. To obtain suspension characteristics, the sprung mass of the vehicle under test was held in place by various arrangements of chains, cables, and supports while a front wheel, independent rear wheel, or rear axle was moved up from the rebound bump stop into the jounce bump stop. Both kinematic and mechanical properties were measured: (1) wheel toe, camber, and steer effects as functions of jounce/rebound displacement and (2) the spring rate, bump stop location, bump stop rate, and coulomb friction characteristics of the suspension.

A typical set of data used for determining spring rate, roll-stabilizer rate, coulomb friction, and bump stop characteristics for an independent front suspension vehicle is given in Figure 3.3. The stabilizer bar rate was determined by holding one front wheel fixed while moving the other front wheel and making measurements with and without the stabilizer bar being attached.

Figure 3.4 shows a typical test arrangement as set up for a Ford Mustang. The test equipment located under the left front wheel consists of scales, turn and slide table, and hydraulic jack. Each vehicle tested presented its own particular problems with respect to setting up the required

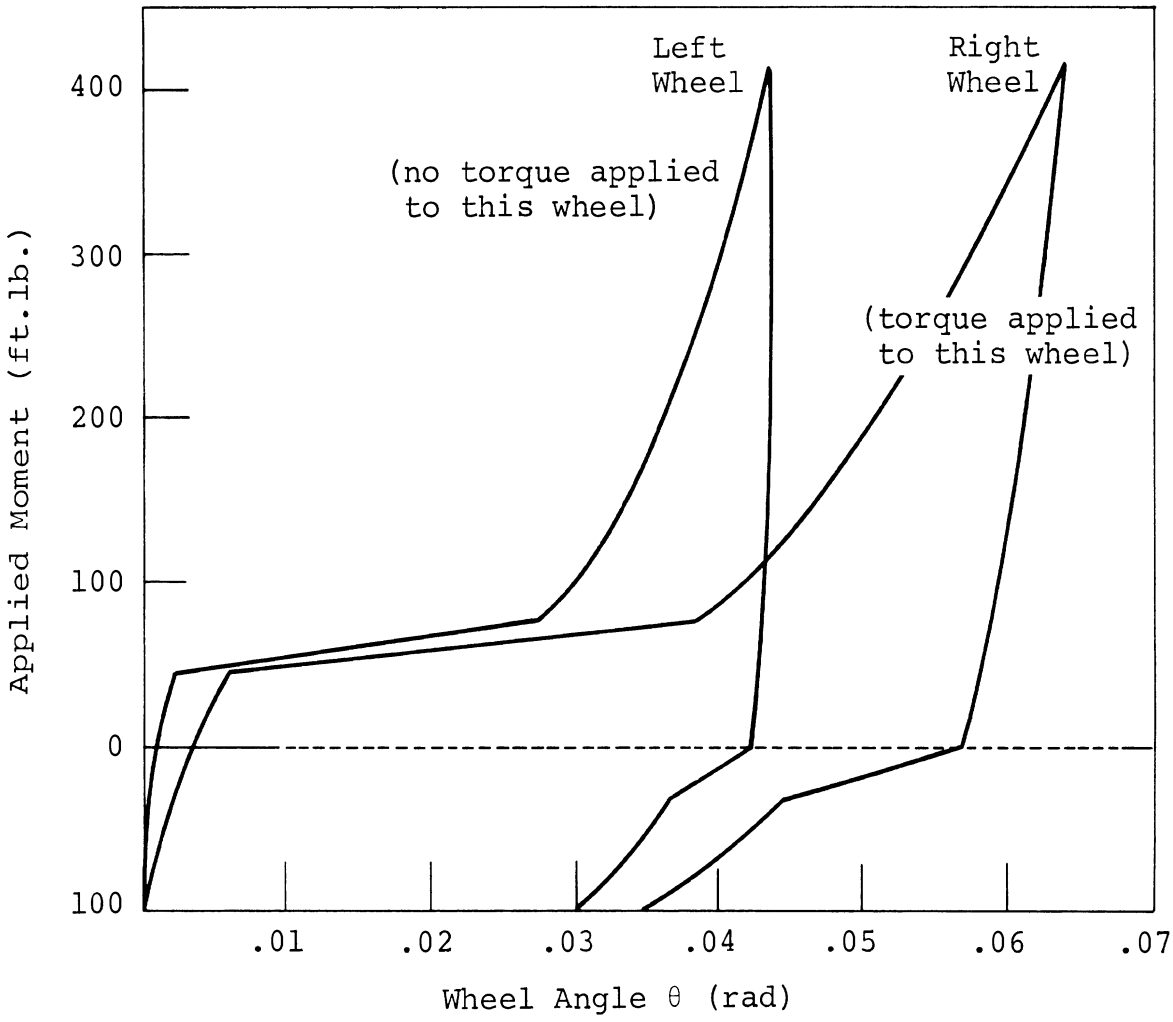

Figure 3.2 Chevrolet, degraded steering gear box

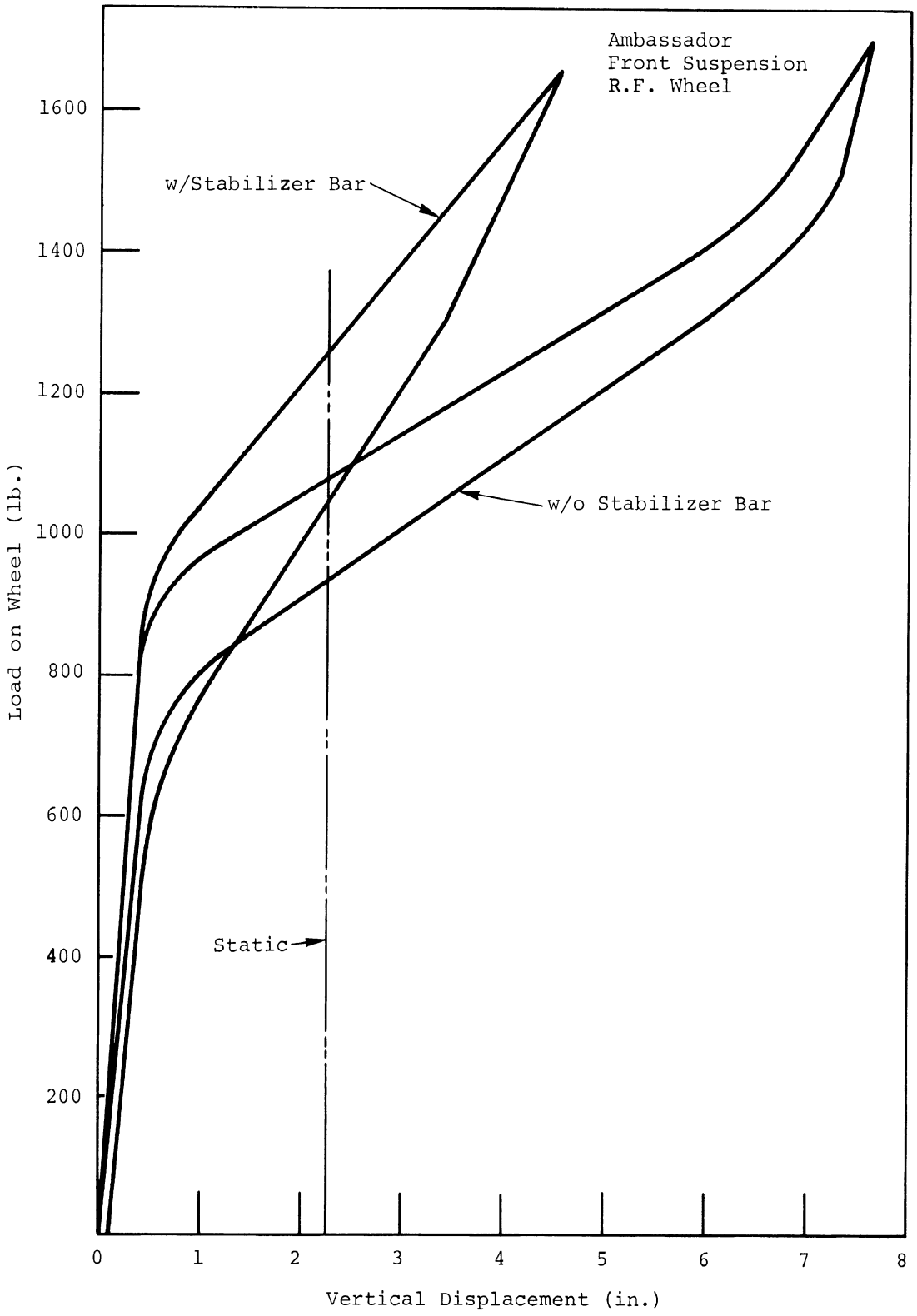

Figure 3.3 Suspension spring rates

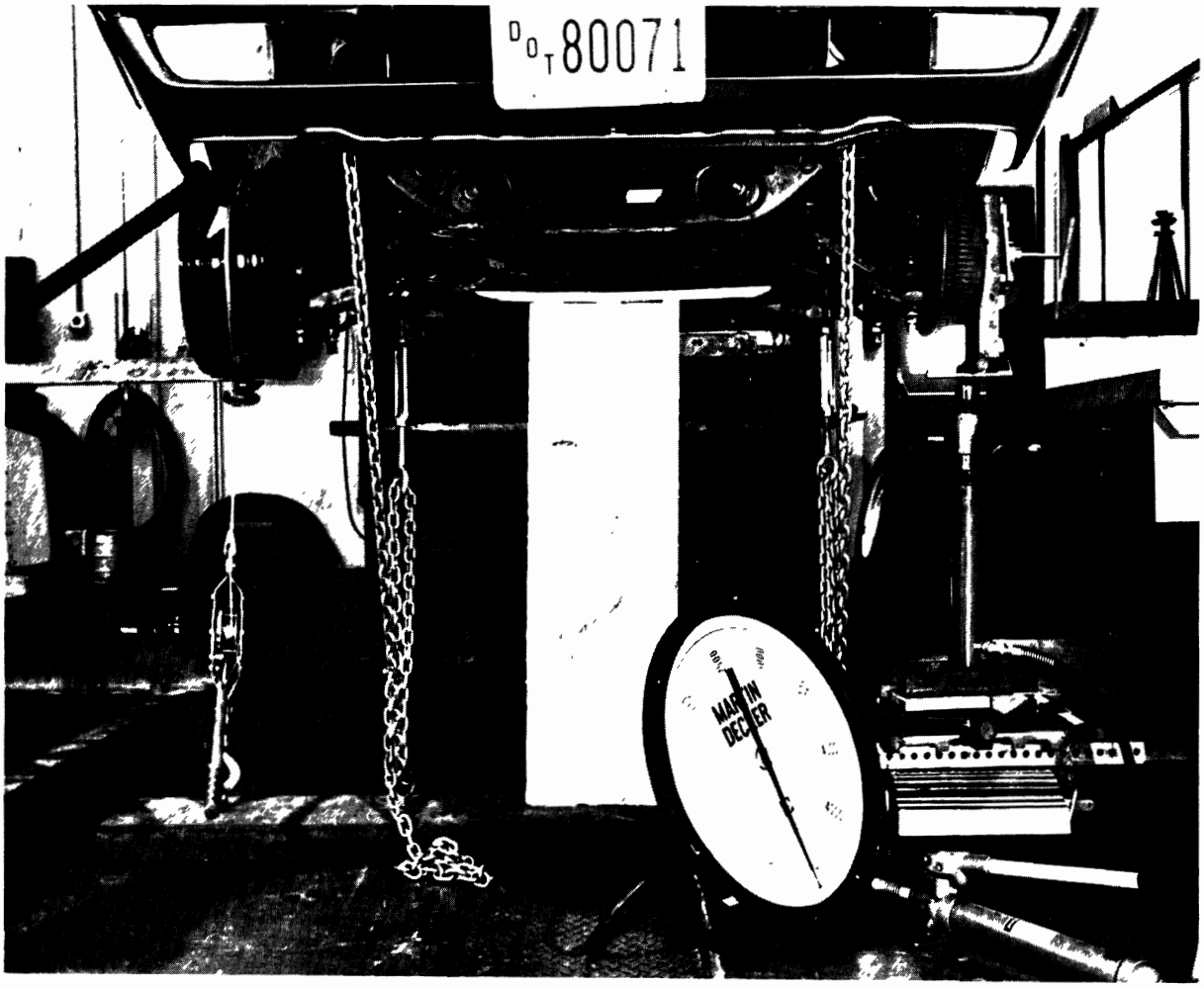

Figure 3.4. Setup for measurement of suspension properties

cables and supports. It should be noted that considerable ingenuity was required to get the job done with equipment that should be considered primitive in comparison with the very versatile device which has recently been developed for measurement of suspension properties [9].

3.2.3 SHOCK ABSORBER MEASUREMENTS. The shock absorbers on each of the eight study vehicles were tested in the laboratory by mounting them in a high-frequency, tensile-testing machine. Each shock absorber was tested by stroking at frequencies of 1 hz, 5 hz, and 10 hz. A representative set of data produced by the adopted procedure is given in Figure 3.5. Due to power limitations of the test equipment, the largest velocity inputs which could be applied to the shock absorber were obtained at 5 hz with a 3-inch amplitude displacement.

Figure 3.6 presents test results for a shock absorber in both an O.E.M and degraded state. These are typical findings and in this example degradation consisting of heavy wear of the piston and rod guide plus a broken valve cover causes the damping force to be reduced to about 5/8 of the damping exhibited by this absorber in its O.E. state. The hysteresis loop observed in the compression half of the new shock absorber is typical of the behavior exhibited by many shock absorbers. This hysteresis loop makes it difficult to simulate the shock absorber in a simple manner. For purposes of this study, the shock absorber was treated as a nonlinear damper and hysteresis loops were replaced by a curve representing the average damping force. Since the force characteristics are somewhat sensitive to stroke amplitude and frequency, an average curve of force versus velocity was adopted to simplify the task of representing an actual shock absorber in the simulation.

Ambassador Rear

Frequency 1 Hz
Amplitude 4 in.

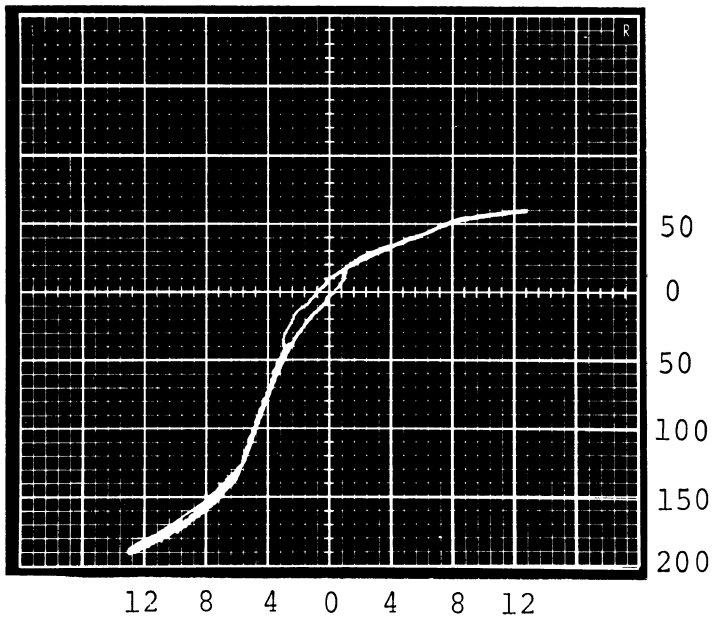

Frequency 5 Hz
Amplitude 3 in.

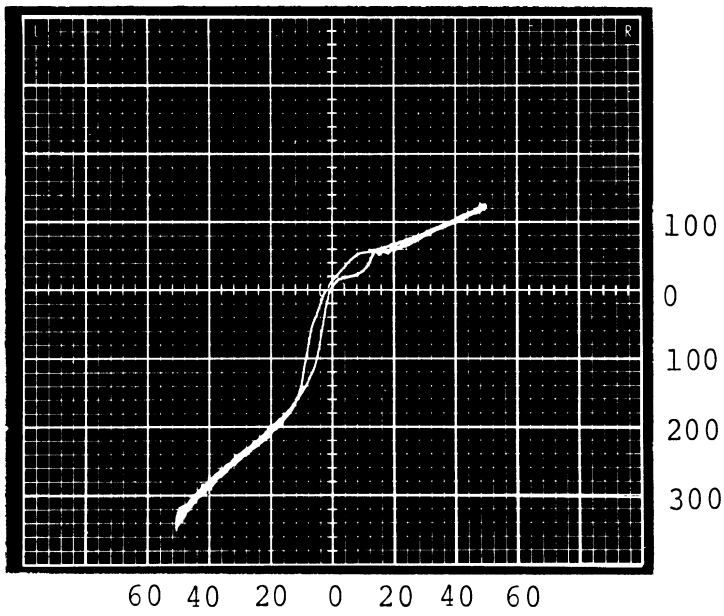

Frequency 10 Hz

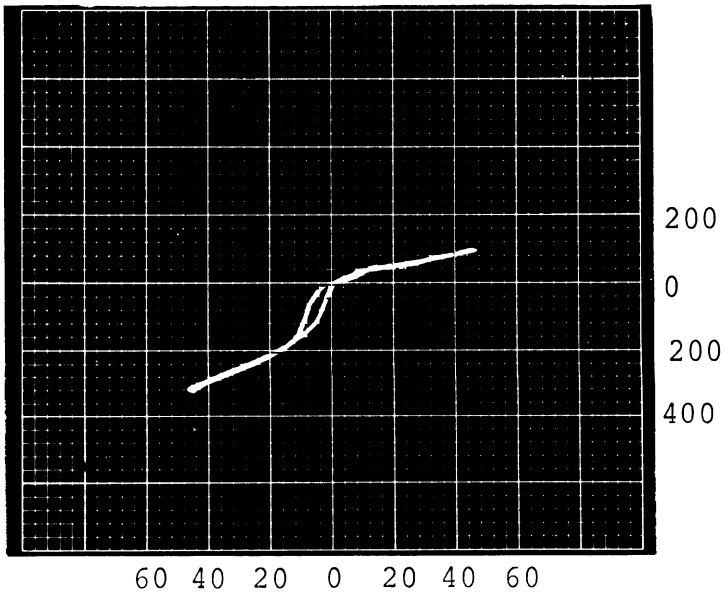

Figure 3.5 Ambassador rear shock absorbers

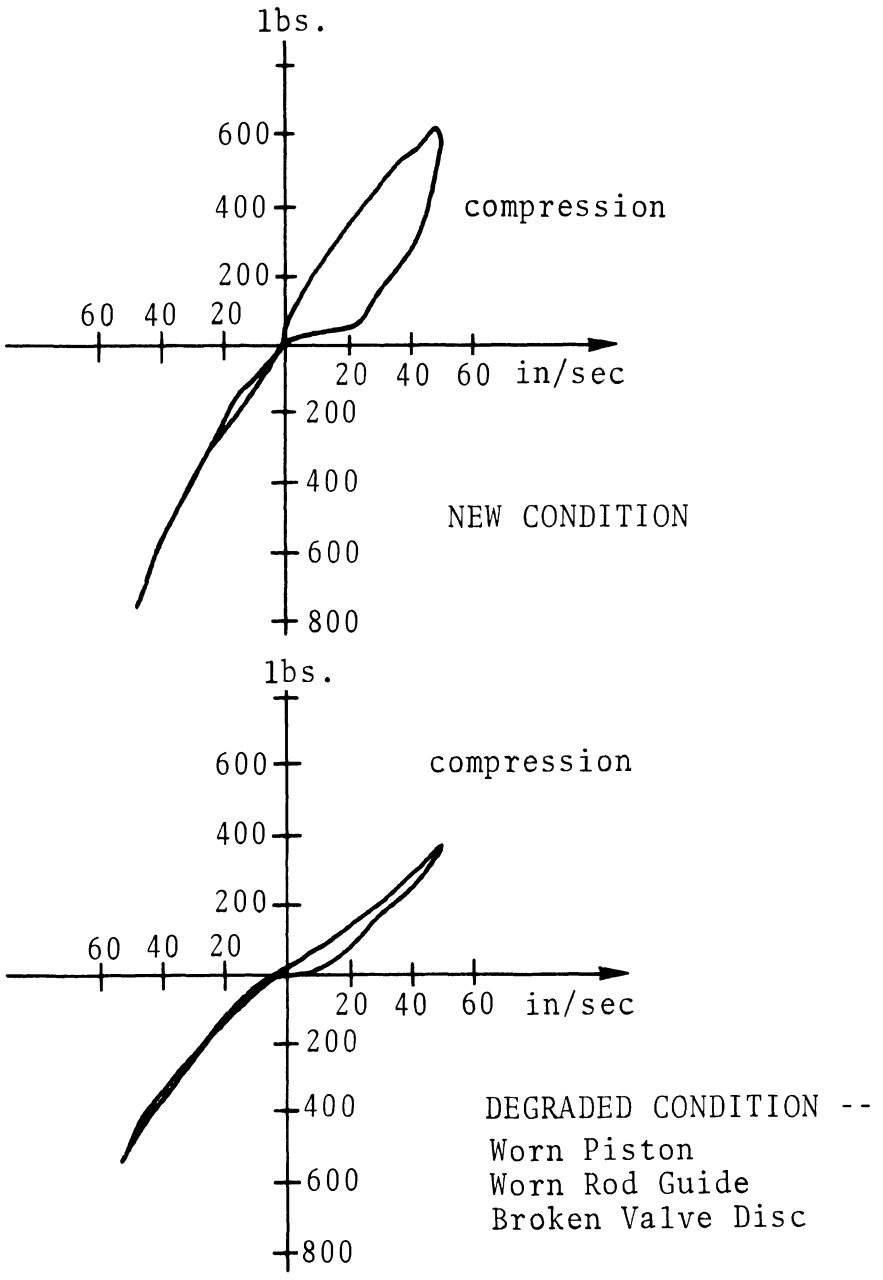

Figure 3.6. Comparison of new and degraded shock absorber. 1971 Dodge Coronet rear; tested at 5Hz, 3 inch amplitude.

3.3 SUMMARY OF SIMULATION RESULTS AND FINDINGS

The simulation studies performed in this program were conducted in two parts. The first portion of the effort was designed to produce findings applicable to two vehicles that were to be tested in the pilot test phase, namely, the Ford Mustang and the Dodge Coronet. The second portion of the simulation study was designed to determine the extent to which the general conclusions derived from this pilot-test planning effort are modified by design differences existing in the eight-vehicle sample study. The findings of these two supplementary studies are discussed separately below.

3.3.1 SIMULATION FINDINGS: MUSTANG AND CORONET. The behavior of the Ford Mustang, in the neighborhood of limit performance, was examined for each of the following steering and suspension degradation categories:

(a) steering gear play

(b) tie-rod and ball joint play

(c) roll-bar bushing play

(d) wheel bearing play

(e) front wheel imbalance

(f) front brake imbalance

(g) rear brake imbalance

(h) wheel alignment variations

(i) introduction of long shackles on the rear spring

(j) shock absorber variations

(k) combined a, b, and d

(l) combined a, b, d, and j

(m) combined a, b, d, and h

(n) combined a, b, d, and e

(o) combined a, b, d, and f

(p) combined a, b, d, e, and f

(q) combined p and j

(r) combined p and h

(s) combined p, h, and j

Measurements of Mustang components degraded in accordance with the concept of virtual maximum rational wear (VMRW) (see Section 2) provided the maximum levels of steering-gear, roll-bar-bushing, wheel-bearing, and tie-rod-end play that were used in the simulation.

The study indicated that

(1) Wheel alignment variations can have a small effect on limit-maneuver performance but no one arrangement of wheel misalignments proved to be consistently bad in all of the limit maneuvers [1] serving as the performance criterion in this investigation.

(2) Brake imbalance is important in all braking maneuvers with or without other degradations.

(3) Ball-joint play, wheel-bearing play, tie-rod-end play and steering-gear play have very little effect.

(4) Degraded shock absorbers in the rear suspension and all four shock absorbers in a degraded state produce noticeable effects.

(5) Wheel imbalance has little influence.

(6) The trapezoidal steer maneuver is very insensitive to all degradations.

Specifically, the simulation study showed that the influence of steering and suspension system degradations did not markedly change the performance of the Mustang from its O.E. performance in the straight-line-braking, braking-in-a-turn, and roadholding maneuvers. Degraded shock absorbers on the rear axle or all four shock absorbers degraded were found to influence the vehicle sideslip angle to a small degree in the roadholding maneuver.

The influence of three levels of brake imbalance on limit maneuver performance were studied by reducing the brake torque on one wheel to 0.7, 0.4, and 0.1 of the O.E. value. It follows that the reduced braking capacity increased the time to decelerate from 5 mph below initial velocity down to 10 mph (the measure of average deceleration chosen for the braking maneuvers). Of more importance, the simulation indicated that an imbalance in brake torque resulting from a sixty percent reduction in the non-degraded brake torque level is required to make a significant change in performance.

The simulation runs performed for the Dodge showed that, in general, this vehicle had a greater tendency to roll than the Mustang and that, in particular, when the shock absorbers were degraded to .25 and .1 times their O.E. condition, the vehicle would roll over in the drastic steer-brake maneuver. When shock absorbers were degraded to a fifty percent level, the simulation predicted a maximum roll angle of 18.3 degrees, which value indicates that the outrigger used for restraining the test vehicle would probably just touch the ground. It was also observed that the Dodge Coronet, on being simulated with degraded shock absorbers, developed a rolling oscillation of the rear axle (axle tramp) in the sinusoidal steer maneuver. In all other respects, steering and suspension degradations appeared to have very little influence on the Dodge when performing the six limit maneuvers.

The tendency for the Dodge, with degraded shock absorbers, to roll over in the drastic steer and brake maneuver, as predicted from simulation runs, was confirmed in the subsequent pilot tests (see Section 4). However, a close examination of time histories produced by test and simulation shows that the roll rate signals are not the same. This lack of exact correspondence is not surprising since the tire properties used in the simulation were obtained by extrapolating a set of force data applicable to a tire with a cross-bias carcass construction, as measured previously with the HSRI mobile tire tester. Since the tires are probably the single most important vehicle component in determining how the vehicle responds in extreme steering and braking maneuvers, the simulation results should not be expected to agree exactly with test results.

3.3.2 SIMULATION FINDINGS: OTHER VEHICLES. The second portion of the simulation study examined the response of the Olds F-85, the American Motors Ambassador, the Chevrolet station wagon, and the Ford pickup truck in executing vehicle handling test procedures, both in the O.E. and degraded states.

The study was expedited by first simulating these vehicles in the O.E. condition to determine the levels of input signals (i.e., steering or braking commands) that produce limit or near-limit response in each of the vehicle handling test procedures. These control input levels were then used to examine limit responses as influenced by the following five categories of degradation:

1. "combined play" from all sources
2. wheel imbalance
3. brake imbalance
4. wheel misalignment
5. degraded shock absorbers

Different levels of degradation were simulated only for brake imbalance and degraded shock absorbers. A total level of "combined play" was assumed on the basis of applying the VMRW concept to the ball-joint, tie-rod-end, wheel-bearing and steering-gear-box designs employed by each of these vehicles. The assumed level of wheel imbalance corresponded to 10 ounces of lead on the rim of one front wheel. The front wheels were assumed to be misaligned in a manner that results in a larger turning capability (see Appendix V). The following values of front-end geometry were specified:

toe—wheels toed in to a 4° included angle

change in caster from O.E.—left wheel: -2°,
right wheel: -2°

change in camber from O.E.—left wheel: 0°,
right wheel: -2°

In the above-defined five categories of degradation, there are 31 distinct combinations of degradations to consider. Each of these 31 possibilities were reviewed in connection with each of the six limit maneuvers and judgments were made that reduced the total simulation matrix to that specified in Table IV-9, Appendix IV.

A comparison of the results obtained in the first portion of the simulation study with the results obtained in the pilot tests indicated that the simulation (in its current state) could only be used to predict trends. Consequently, an extensive set of simulation results will not be presented here. Rather, the findings produced by these simulation efforts have been carefully examined, permitting the following observations:

(a) One vehicle (the Ambassador) appears to have a tendency to spin out in the roadholding test. This tendency is greatly enhanced with degraded shock absorbers.

(b) In the trapezoidal maneuver, little or no change in vehicle performance was indicated between the O.E. and degraded states for the Ambassador, F-85, Chevy wagon or Ford pickup truck.

(c) In the sinusoidal steer maneuver, the F-85, Ford pickup, Chevy wagon and Ambassador directional responses were characterized by an overcorrection in the heading angle (as defined in Section 4). Degraded shock absorbers resulted in the Ambassador exibiting a significant increase in the heading angle.

(d) In the drastic brake and steer maneuver, the degraded Ambassador showed rollover tendencies when the wheels were misaligned in combination with some other degradation. The Ford pickup, F-85, and Chevy wagon did not exhibit a rollover tendency. However, degraded shock absorbers did produce an increase (20 to 30%) in the peak roll-angle exhibited by these three vehicles.

In the aggregate, these simulation findings suggested that the Ambassador will perform very poorly when its steering and suspension system components are degraded. However, the test results, which are discussed in Section 5, indicate that the Ambassador did not perform as poorly as predicted.

4. PROCEDURAL DEFINITIONS AND PILOT TEST FINDINGS

In Section 3, reference was made repeatedly to "limit maneuvers" and "Vehicle Handling Test Procedures" in discussing the structure and findings of the simulation program without explicitly defining what is meant by these terms. It is, of course, true that "limit maneuver performance" and "Vehicle Handling Test Procedures" are the criterion measures by which the influence of wear and degradation on "pre-crash safety performance" (or "accident avoidance performance") is ultimately to be judged. Notwithstanding the importance of defining the criteria by which evaluative comments have already been made, the report, up to this point, has only referred to an earlier publication [1] which does, in fact, document the meaning of these terms. This practice, namely, reference to another publication rather than proceeding to define the criterion measures, was followed primarily to avoid clogging the presentation with an inordinate amount of detail.

To discuss the findings of the pilot test program, however, it is essential that a whole host of terms dealing with vehicle behavior and mechanisms occurring during limit maneuvers be defined and explained. Accordingly, this section of the report contains a description of each of the six test procedures which were developed in an earlier program [1] and which were extended and refined in a research and test program performed jointly with this study [7]. The intention is to give the reader an understanding of (1) the objective of each test procedure, namely, the performance quality being assessed, (2) the basic format of each test, and (3) the different categories of vehicle response and behavior that commonly occur. Additional documentation of the detailed test practice employed in the final full-scale test program will be presented in the next section.

Following this summary of the basic test procedures that have been developed to assess the limit maneuvering performance of passenger vehicles, the scope and findings of the pilot test activity are reviewed. Specifically, the various degradation modes that were imposed, both individually and in combination, on the two test vehicles are both defined and coded, facilitating a discussion of test findings on a maneuver-by-maneuver basis. In addition, the findings of a tire-surface friction study are summarized, which study can be viewed as a portion of the pilot test effort and, further, as having been demanded by the preliminary findings produced by the pilot testing activities.

4.1 VEHICLE HANDLING TEST PROCEDURES: AN OVERVIEW

The Vehicle Handling Test Procedures (VHTP) are open-loop measures of the steering and braking performance which is exhibited by a motor vehicle operated in the vicinity of its performance envelope. They were originally conceived as providing measures of performance which were hypothesized to have first-order relevance to pre-crash safety quality. All six basic test procedures, as used in the pilot test program, are outlined below.

In view of the open-loop character of these test procedures, a requirement for certain test apparatus is imposed to assure precise control inputs without appreciable driver influence. The first three tests to be outlined are executed by a driver with passive limiter mechanisms constraining both steer and brake levels. The second three procedures involve complex control inputs which are provided by a programmable automatic controller. In this system, servo mechanisms replace the driver and provide precise steer, brake, and accelerator controls (Fig. 4.1) (as stored in programmed

Figure 4.1
Servo actuators installed in a van-type vehicle

circuits) upon command from the test operator. A complete description of this system* will be found in Appendix VI.

4.1.1 VHTP #1 - STRAIGHT LINE BRAKING.

Objective: To quantify the vehicle's efficiency in utilizing the prevailing surface friction prior to wheel lockup while stopping in a straight line.

Procedure: A sequence of increasing brake level inputs are applied, from an initially straight course at 40 mph, up to the point of lockup at two front or rear wheels.

Response Features: Two categories of limit response are commonly observed in this maneuver, distinguished by the order with which wheel lockup occurs at the limit:

a) front wheels lock first, thereby degrading the steerability of the vehicle

b) rear wheels lock first, thereby degrading the directional stability of the vehicle which tends to spin out.

Typical time histories of the response to braking inputs are shown in Figure 4.2. Braking performance is viewed as being degraded in this maneuver if wheel locking is experienced at a lower level of longitudinal acceleration than was achieved in some reference or baseline condition.

*Three of these systems have been built, one of them being financed by a portion of the funds allocated to this study.

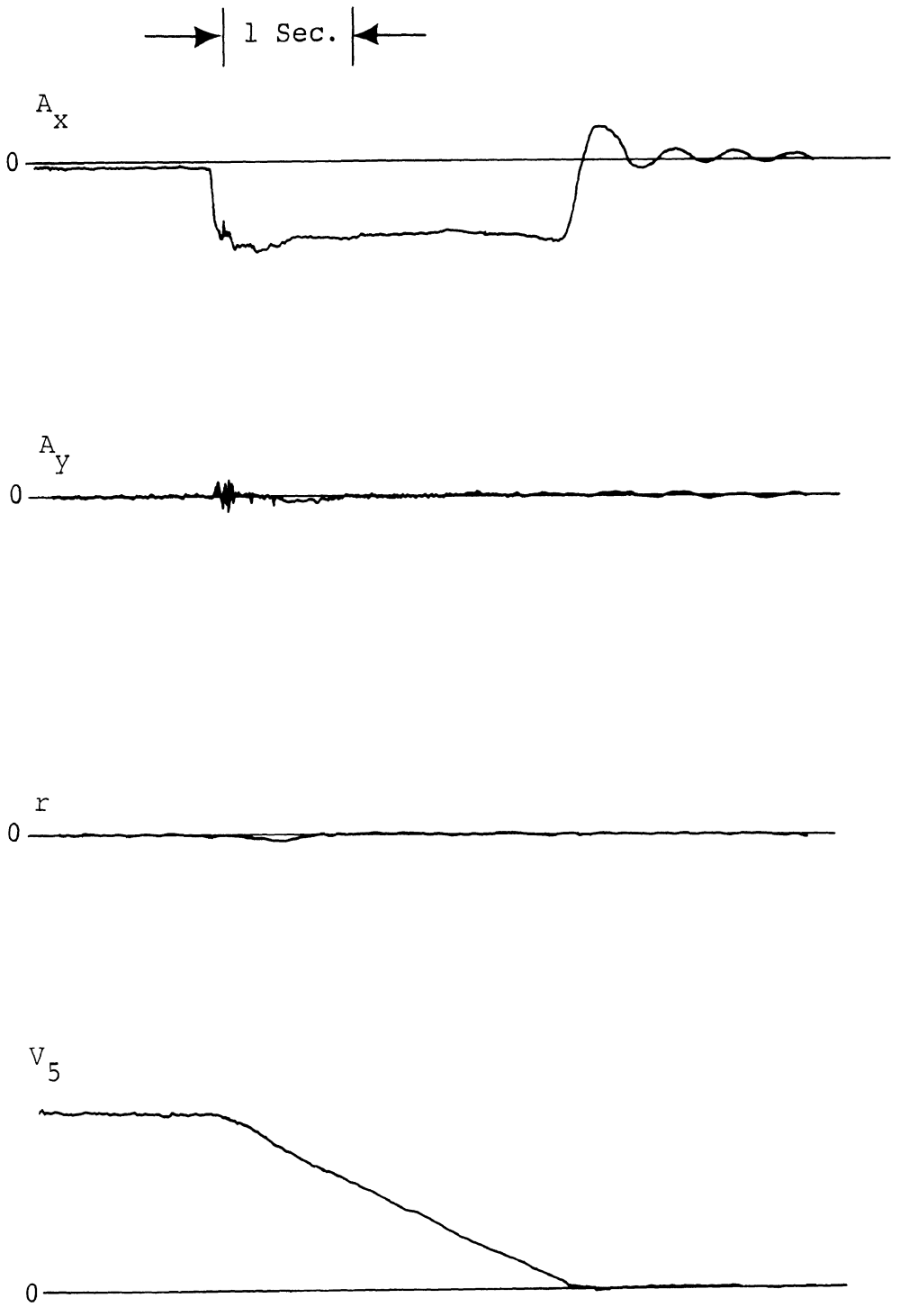

FIGURE 4.2

Straight Line Braking Raw Data Time Histories

4.1.2 VHTP #2 - BRAKING-IN-A-TURN.

Objective: To characterize the vehicle's ability to attain large braking levels in a turn without degrading path curvature and without exhibiting excessive sideslip.

Procedure: A sequence of increasing brake level inputs are applied, in a steady turn at 40 mph (lateral acceleration is 0.3 g) until lockup is encountered at two front or two rear wheels.

Response Features: For all test runs which are "sub-limit", i.e., with no wheels locking, vehicle responses are typified by the time histories shown in Figure 4.3. Wheel locking defines limit response because of the "drift" and "spin" responses which accompany front- and rear-wheel lock-up, respectively. Front-wheel lockup causes path curvature to drop quickly to zero (Figure 4.4), while lockup of both rear wheels (with at least one front wheel still rolling) will result in a classical directional instability, as manifested by the high sideslip rate and a divergent sideslip angle seen in Figure 4.5.

It will be noted that Figures 4.3, 4.4, and 4.5 show both sideslip, β, and path curvature, 1/R, as these response variables vary during the maneuver. (See Figure 4.6 for their definitions.) The sideslip response, β, is felt to be of major safety significance. It can be argued that excessive sideslip responses, as occur under limit maneuvering conditions, disorient the driver with respect to the normal view of his vehicle's path, and cause the vehicle to project a larger target for collision in the roadway. The path-curvature response, 1/R, permits the evaluation of turning response, without introducing any ambiguities in the measure due to a simultaneous sideslip response.

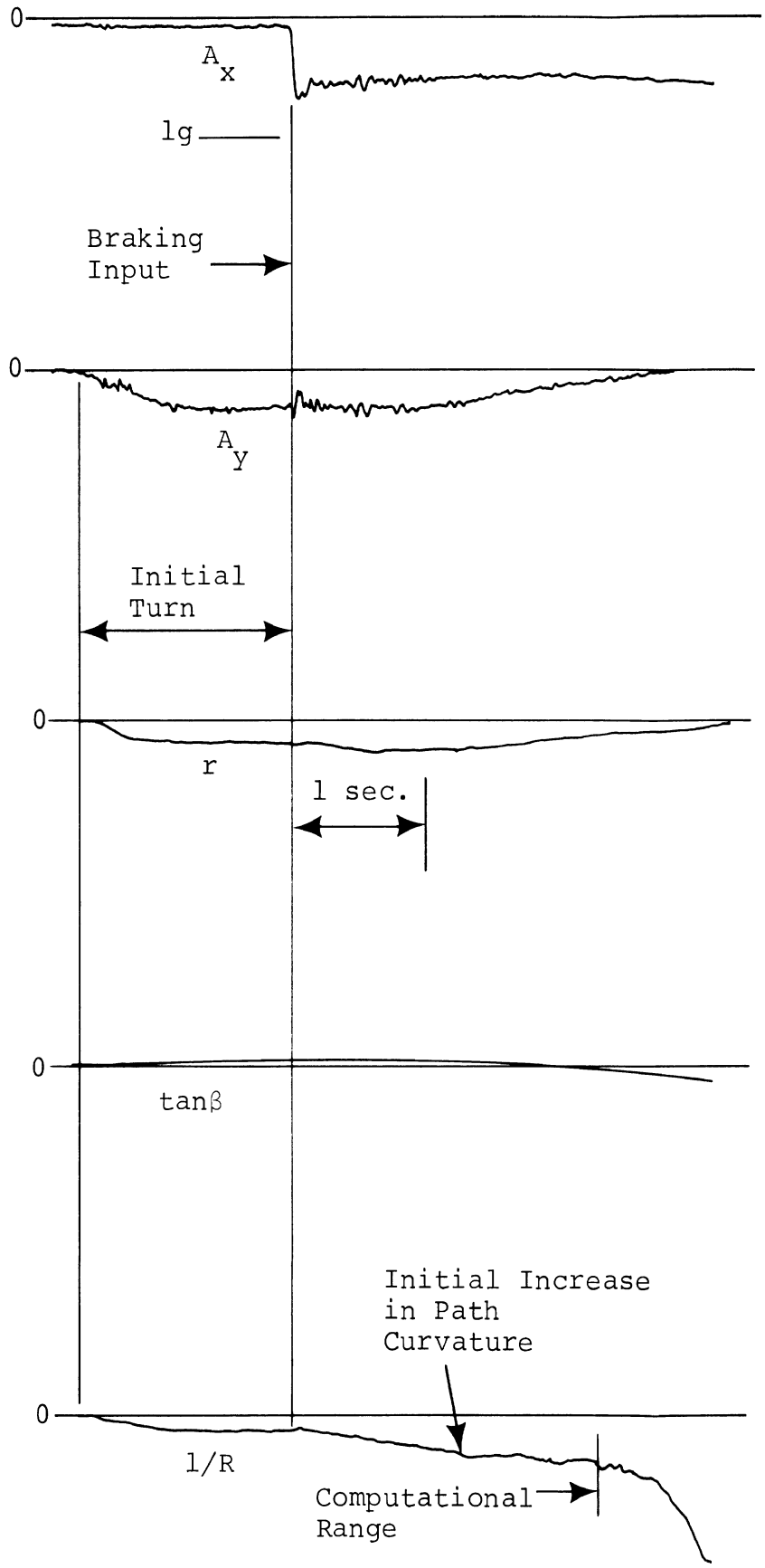

Figure 4.3
Braking In A Turn - No Wheels Locked

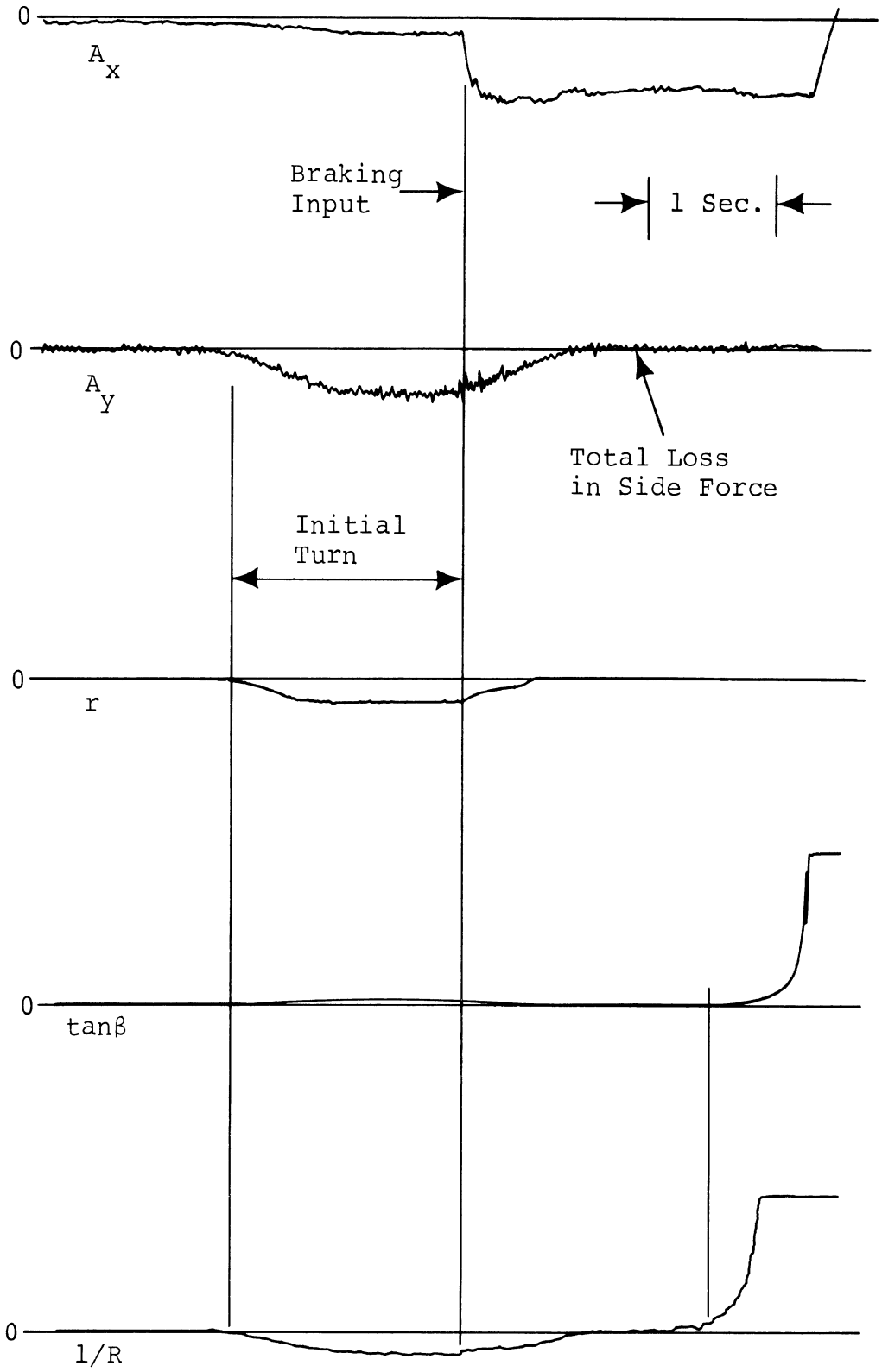

FIGURE 4.4

Braking In A Turn - Front Wheels Lockup

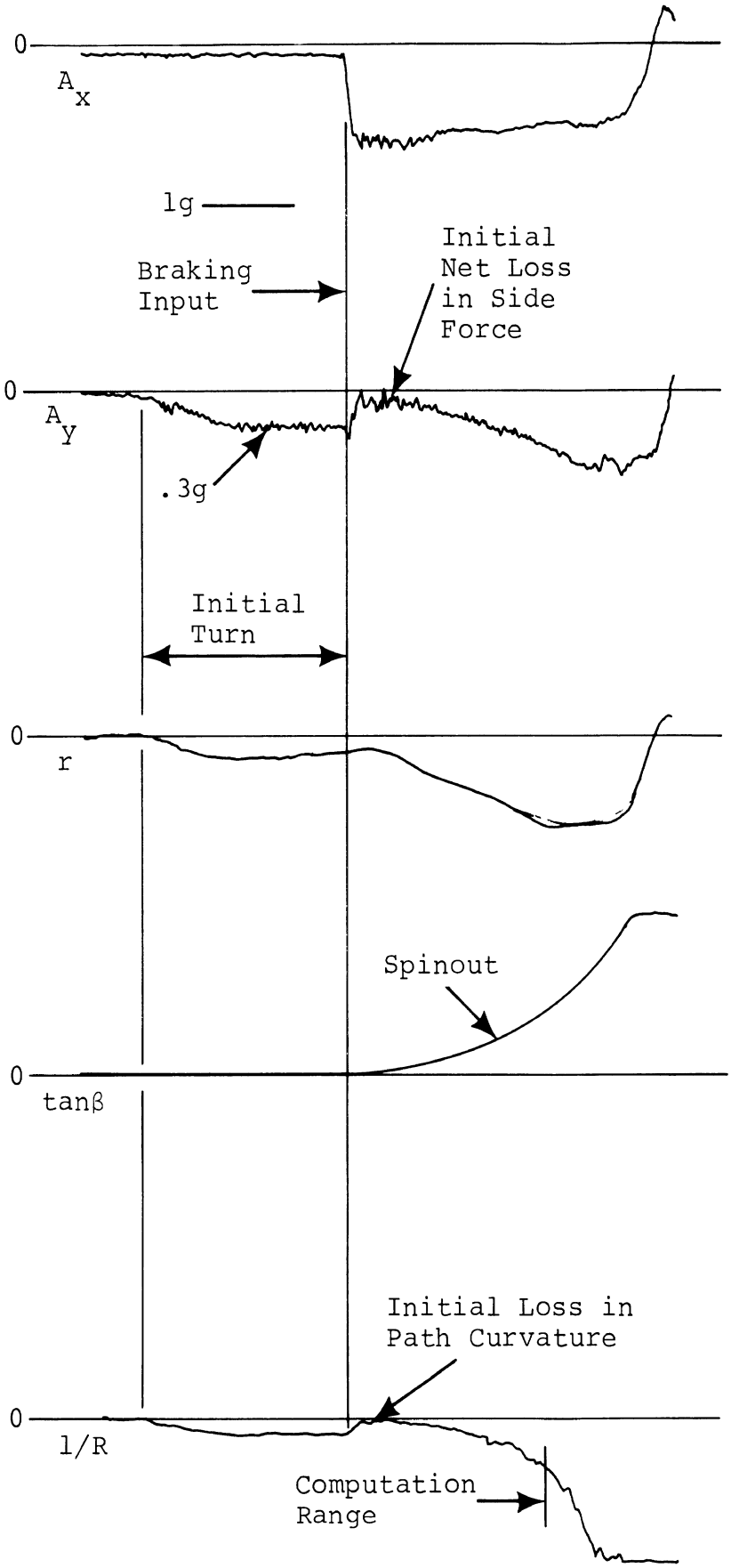

Figure 4.5

Braking In A Turn - Rear Wheels Lockup

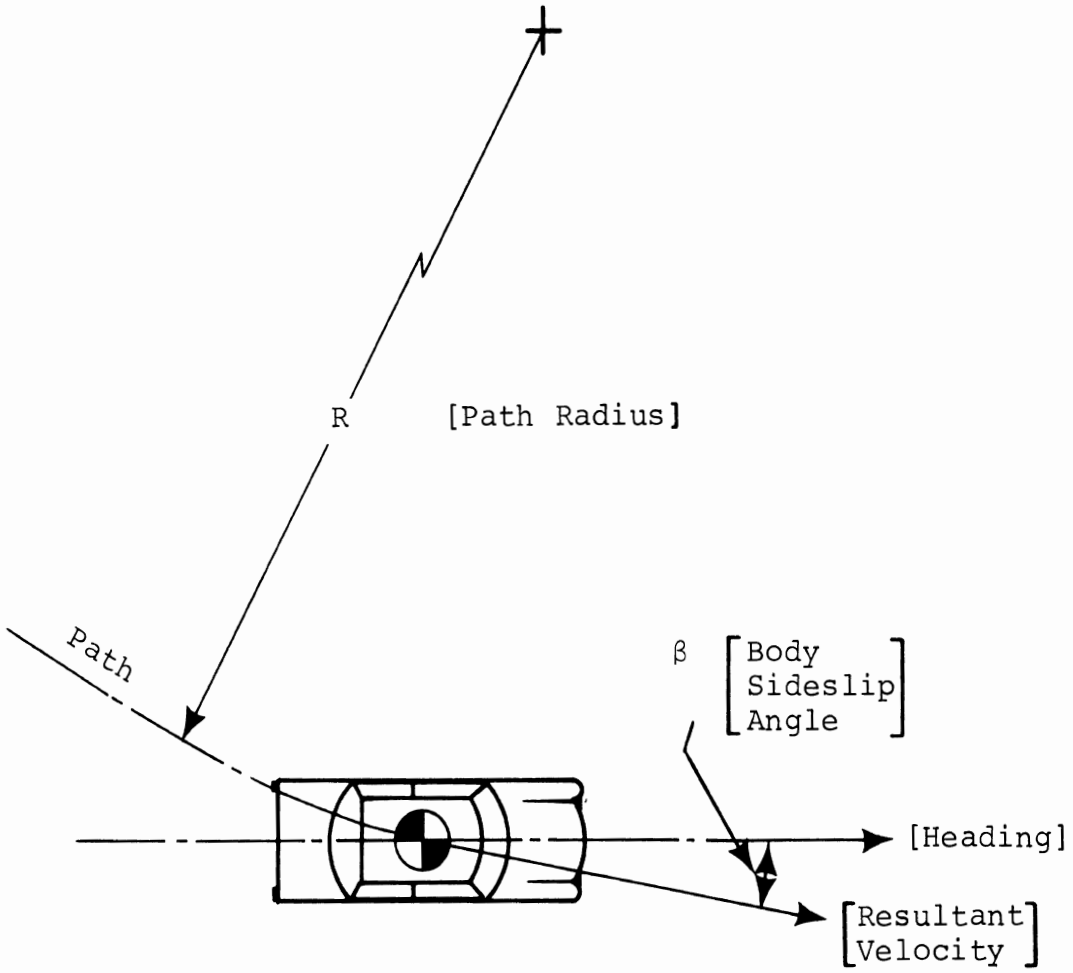

FIGURE 4.6
The Sideslipping Vehicle in a Curved Path

The brake level incrementing procedure is continued up to the point where both wheels on an axle lock up since experience shows that the lockup of a single wheel does not necessarily result in a significant degradation of the initial turn. (Note that in a relatively low level turn of 0.3 g, substantial side force potential resides in the non-locking tire on a given axle and equilibrium can generally be re-established without a major perturbation in yaw response.) Of course, the first wheels to lock are the inside wheels which have a decreased vertical load in a turn.

Vehicle performance in this maneuver is viewed as being degraded if, with respect to some reference condition, it exhibited an excessive loss in path curvature or an increase in sideslip response at a level of longitudinal acceleration which was lower than that achieved in the baseline condition.

4.1.3 VHTP #3 - ROADHOLDING IN A TURN.

Objective: To evaluate the vehicle's ability to track a curve in the presence of periodic road roughness whose fundamental frequencies in successive tests span the range of wheel hop frequencies.

Procedure: The test is performed on a circular course on which rubber strips have been positioned at selected intervals. The strips, made of truck tire tread stock, are glued to a paved surface at three sites with spacings designed to provide vertical disturbances of 9, 11, and 14 Hz, respectively when encountered by the running gear of a vehicle traveling at 30 mph. The vehicle initially contacts the grid from a steady (0.4 g A_y) turn which is nominally at right angles to the first grid element (see Figure 4.7). The test is open-loop in character since the test driver holds the steering input against a stop throughout the curved approach and the traverse of the grid.

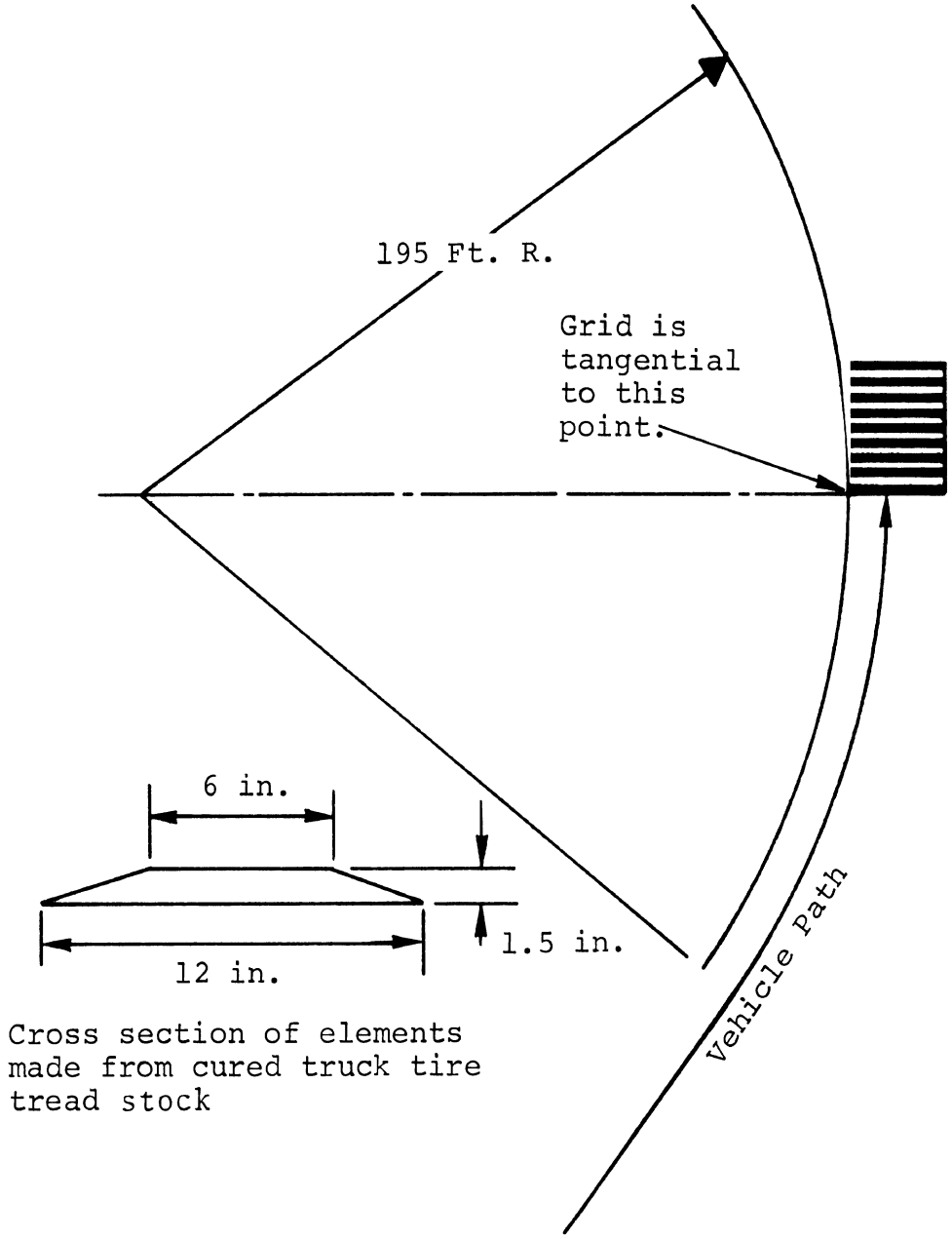

Figure 4.7 Roadholding course layout

Response Features: The grid frequencies, 9, 11, and 14 Hz were selected to span the range of wheel-hop frequencies existing in the vehicle population. Thus, limit performance is determined by the presence of a resonant oscillation in the wheel hop mode, by which a net loss in tire side force accrues. Responses can be grouped into two categories:

1. Predominate loss of front tire side forces due to resonance in the wheel hop mode of the front suspension. Vehicle path curvature decreases but no significant sideslip response occurs. Time histories typifying this behavior are shown in Figure 4.8.

2. Predominant loss of rear tire side forces due to wheel hop resonance of the rear suspension. Dramatic sideslip response can occur while the path curvature response may either increase or decrease. Example time histories are shown in Figure 4.9.

Vehicle performance is viewed as being degraded in this test if either the loss in path curvature or the increase in sideslip response was greater than those levels which had been exhibited by a baseline or reference vehicle. Since the three disturbance arrays are designed to provide merely a frequency sweep, no significance is attached to the particular course upon which the greatest loss in roadholding is observed.

4.1.4 VHTP #4 - TRAPEZOIDAL STEER.

Objective: To characterize the limit cornering capability of the vehicle described in terms of maximum path curvature attainable without excessive sideslipping.

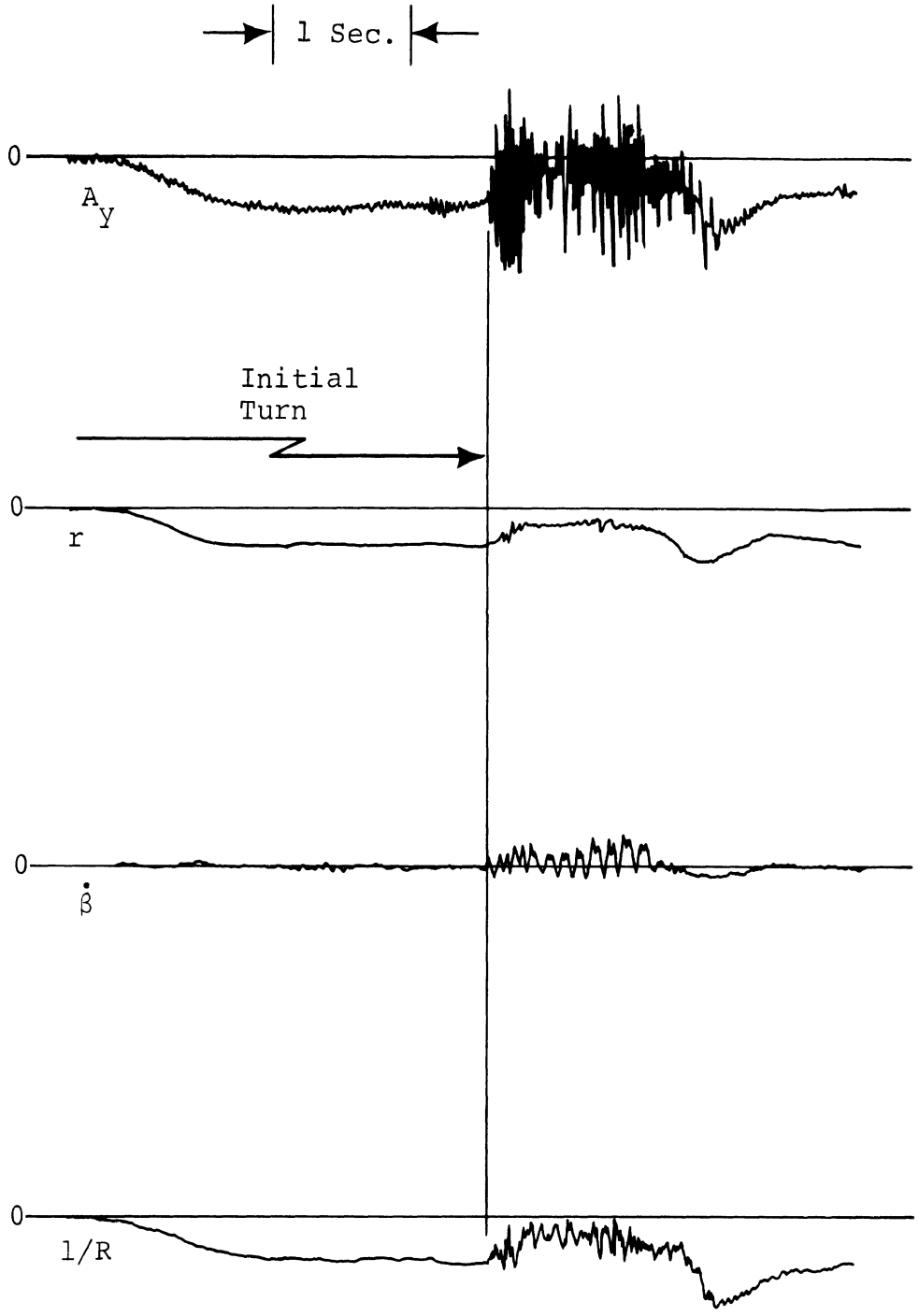

Figure 4.8

Roadholding In A Turn -
Dominant Front Wheel Resonance

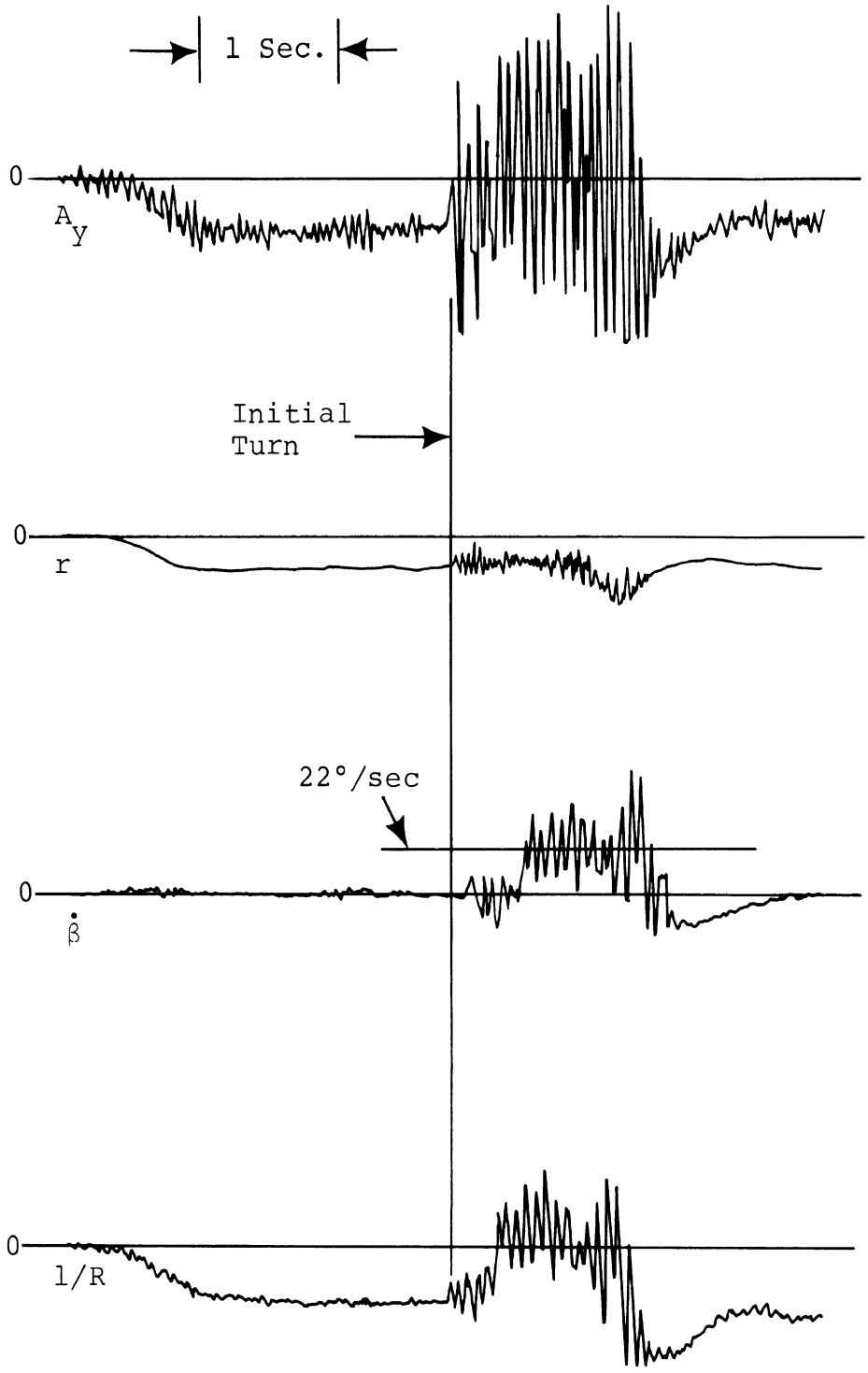

Figure 4.9

Roadholding In A Turn -
Dominant Rear Wheel Resonance

Procedure: This maneuver is conducted by application of a ramp fronted step input of steering displacement while coasting from a 40 mph initial velocity. The test sequence is defined by a set of prescribed steering levels, chosen to sweep from low accelerations to levels sufficiently beyond limit turning performance to assure inclusion of the limit response regime.

Response Features: The J-turn type response, though not representative of any realistic highway maneuver, does provide the conditions appropriate for examination of the transition from straight line to limit turn, such as would occur in the initial phase of an obstacle avoidance maneuver. Typical limit responses exhibited in this test are as follows:

1. Spinout, in which a dramatic yaw divergence is experienced as a result of rear tire side force saturation being incurred at an input level which still leaves considerable side force capability on the front tires. Example time histories are shown in Figure 4.10.

2. Driftout, in which the front tires saturate in side force prior to the rear tires, resulting in residual unrealized side force capability on the rear tires such that any perturbations of vehicle sideslip beyond this nominal trim condition result in increased rear tire side forces. Example time histories produced by this condition are shown in Figure 4.11.

3. Rollover, possibly aggravated by wheel rim contact.

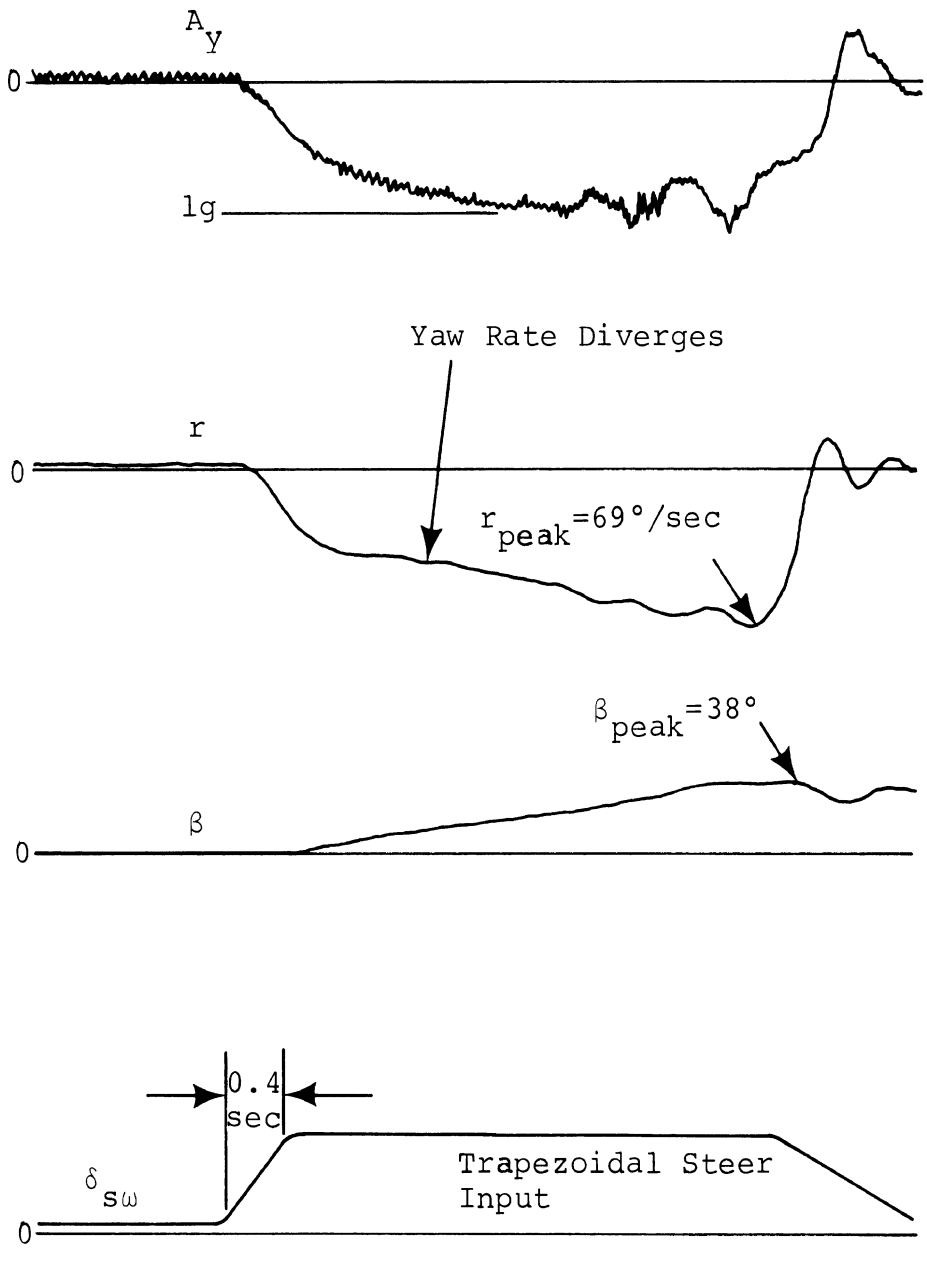

FIGURE 4.10

Trapezoidal Steer Rear Tire
Saturation - Spinout

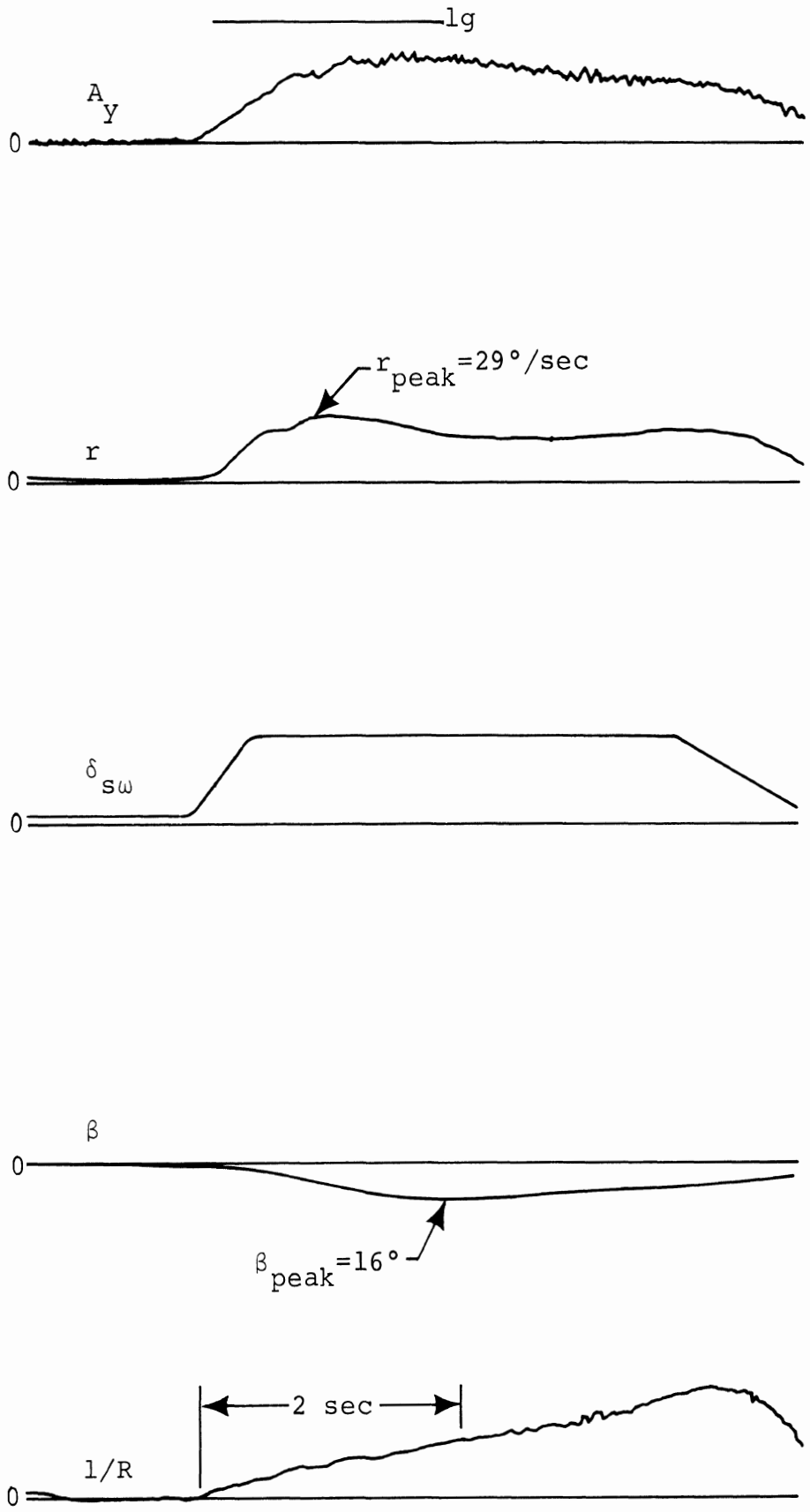

FIGURE 4.11

Trapezoidal Steer Front Tire
Saturation - Driftout

The maximum path curvature attainable by a vehicle is thus constrained by one of the three limiting mechanisms. Vehicle performance would be viewed as being degraded if, in this maneuver, it exhibited a lower maximum path curvature than was achieved by the reference or baseline vehicle. Additionally, it might be argued (although further research is needed to support the argument) that a rollover response at the same level of path curvature represents a degradation in performance from a spin or drift-limited condition. Likewise, spinout may be argued to be representative of a degradation in performance with respect to driftout at the same level of path curvature performance.

4.1.5 VHTP #5 - SINUSOIDAL STEER.

Objective: To evaluate the vehicle's ability to perform a rapid lane change in response to a symmetric sine wave input of steering displacement.

Procedure: This maneuver is executed by applying a single cycle of a sine wave of steering to a vehicle which is initially moving in a straight line path. The input is applied at a selected initial velocity following throttle release. The test procedure involves the execution of a large number of runs, performed at increasing steering amplitudes from each of two velocities, 45 mph and 60 mph. Steer amplitudes are selected such that trajectories cover the full range of emergency lane change performance.

Response Features: In this maneuver, vehicles can exhibit a wide range of responses which are patently unlike a lane change. Most commonly, increasing the steer amplitude simply results in lateral displacements which are in excess of the nominal dimensions of the roadway. Thus, with regard to lateral displacement response, the concept of a definable limit would not seem to apply.

Two categories of yaw response limit have been identified, however, which can be characterized as asymmetries of directional gain in response to the leading and trailing half-waves of the sinusoidal steer input. These limit responses can be categorized as "undercorrective" and "over-corrective" yawing motions in which the second half of the sine wave is viewed as the corrective or recovery stage, during which the driver is attempting to re-establish his initial heading.

In the undercorrective response, the vehicle accumulates a large sideslip angle early in the maneuver, such that the recovery half of the steer input is essentially nullified. Response time histories typical of this condition are shown in Figure 4.12. The front tires, during the second half wave of steering input, experience an insufficient sideslip angle of the recovery polarity to produce a restoring yaw moment of sufficient magnitude. Carried to the extreme, a spinout is initiated with the first half wave of steering, which spinout the second half of the symmetric steer input is incapable of arresting.

The overcorrective response, as typified by the time histories shown in Figure 4.13, results in a terminal heading which is directed back toward the original lane from which the maneuver began—the recovery half of the steering input being more effective than the initial steering input. The physical mechanism underlying this phenomenon remains to be fully identified.

Vehicle performance would be judged as being degraded in this test if it were to exhibit exaggerated undercorrective or overcorrective responses at levels of steer amplitude which were lower than those levels producing similar responses on the reference vehicle.

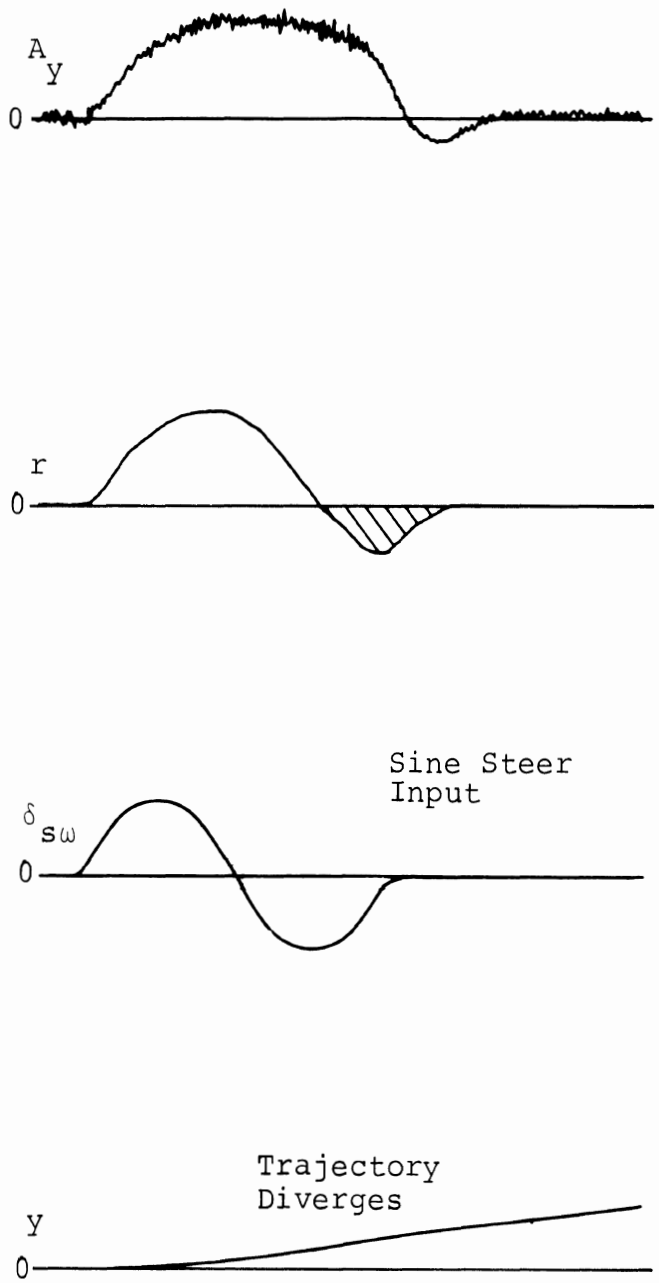

FIGURE 4.12

Sinusoidal Steer
"Undercorrective" Response

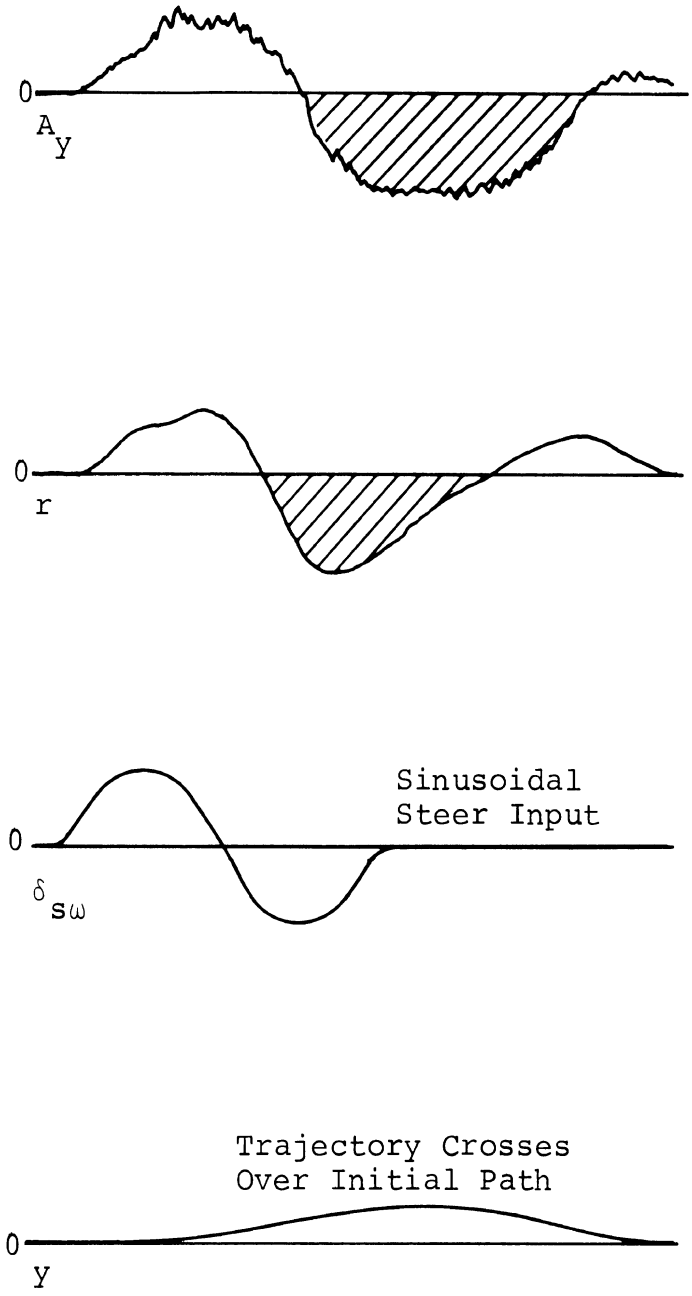

FIGURE 4.13

Sinusoidal Steer
"Overcorrective" Response

4.1.6 VHTP #6 - DRASTIC STEER/BRAKE.

Objective: To impose the maximum challenge to the vehicle's roll stability that can be derived solely from tire/road shear forces and thereby obtain a binary characterization of roll potential under the defined conditions.

Procedure: A half sine wave of steering is applied, with no braking, with the vehicle coasting at an initial velocity of either 50 or 60 mph. A perusal of the response data from that run is made and the time is determined at which yaw rate attains 95% of its maximum value. Next, a run is made with the same velocity and steer input, but a brake input is initiated (such that all wheels lock) at the time at which 95% of peak yaw rate is attained, with braking maintained for two seconds. In this second run, the free transient roll response is examined, such that the precise time for brake release in the following run can be determined. In the next run, the brake release time is set to coincide with the peak in roll rate response of the proper polarity to contribute to the roll over process.

Response Features: The steering input, lasting for one second, provides sufficiently large yaw moments to cause the vehicle to achieve a significant angular momentum in yaw by the time wheels are locked (somewhere between 0.5 and 0.75 seconds). When all wheels attain 100% slip, the vehicle exhibits negligible directional sensitivity, and it slews in yaw, accumulating body sideslip at nearly constant rate (see time histories shown in Figure 4.14). The sprung mass, of course, has responded to the initial roll moment, by rolling clockwise, say, for a counterclockwise steering input. Since wheel lockup results in a loss in tire side force, the roll moment drops to near zero with brake application, and the sprung mass rebounds counterclockwise in roll. Being

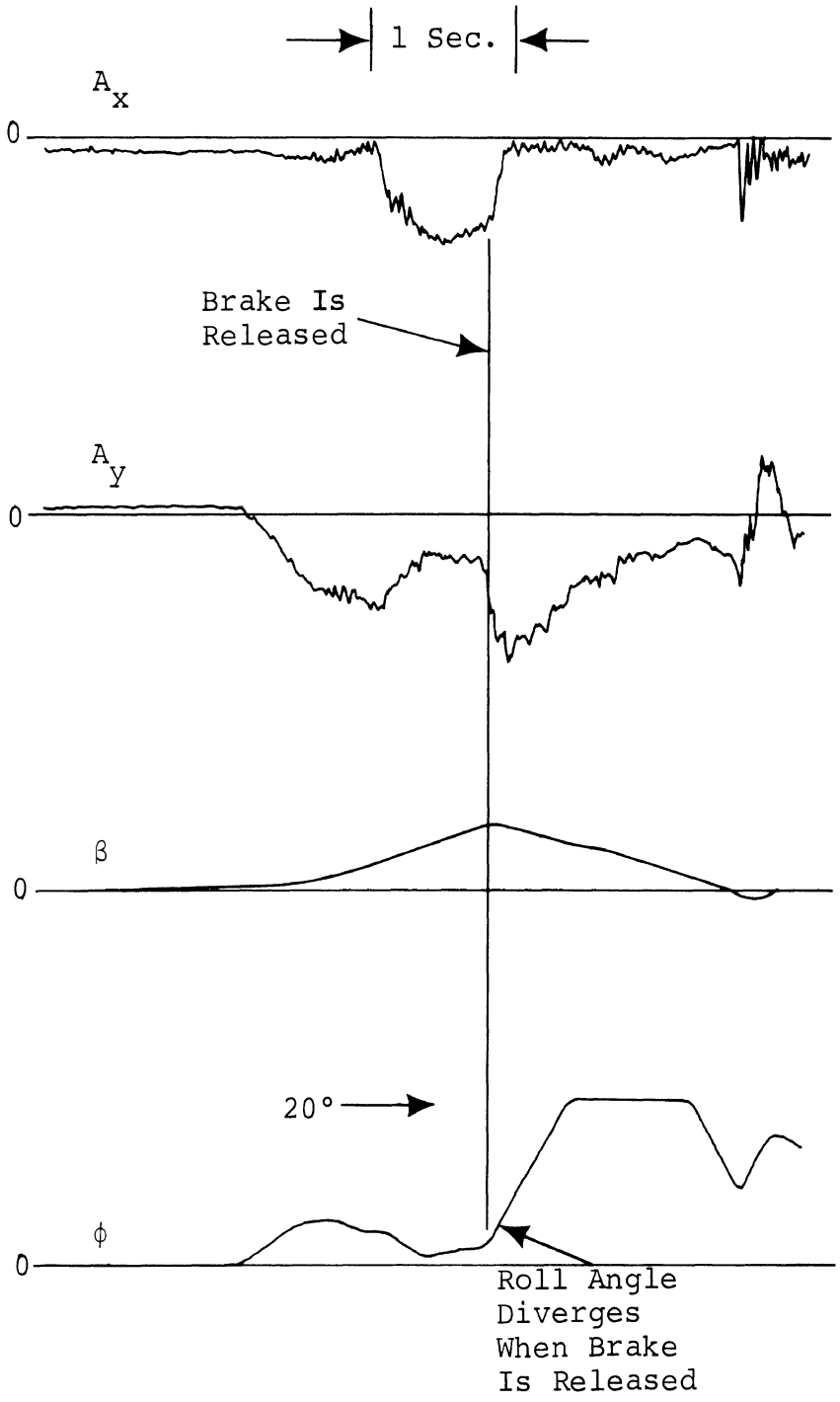

FIGURE 4.14

Drastic Steer and Brake
Divergent Roll Response

an underdamped mode of response, the sprung mass overshoots in roll and rebounds again, now rolling clockwise. Upon brake release, the wheels spin up toward freely rolling under a condition of high slip angle at all four tires (between 10° and 30°, generally). The step-like quality of the side force buildup which follows is crucial to the determination of roll overshoot, because of the requirement to provide maximum net roll moment while the sprung mass is passing through zero roll angle, with peak roll rate.

On most passenger vehicles, sufficient roll energy is accumulated to carry the roll motion into the region of bump stop contact, at which time the roll moment can be further increased as the roll momentum of the sprung mass is reacted with an impulse that immediately increases the vertical tire load on the outside wheels. At this time, the summation of vertical loads will actually be greater than the vehicle static weight and a commensurate increase in side force is realized. If the total overturning moment in roll at this juncture exceeds the gravity moment, the vehicle will lift its inside wheels; if not, the vehicle will not roll over in this maneuver.

Vehicle performance would be judged as being degraded in comparison with a nonrollover baseline performance, if it exhibited roll over in response to the indicated steer and brake inputs.

4.2 PILOT TEST FINDINGS

4.2.1 TEST CONDITIONS. As indicated earlier, two of the total sample of eight vehicles were used in a pilot testing activity to obtain direct experimental evidence relating component degradation to limit maneuver performance. By means of the findings produced in the simulation study, it became possible to examine a reduced matrix of degradations, and still obtain meaningful information. The degraded conditions selected for testing included both "positive" and "negative" sensitivity categories, in terms of their predicted influence on limit maneuver performance.

In order to expedite the testing, the Ford Mustang was equipped to perform the vehicle handling test procedures that are executed by a driver (VHTP #'s 1, 2, and 3), with the Dodge Coronet being equipped with the automatic controller that is needed to perform VHTP #'s 4, 5, and 6. A variety of mechanical devices and vehicle modifications were used to introduce controllable degradations into these two test vehicles and also into the vehicles that were subsequently tested in the full-scale test program. The schemes used for artificially introducing degradation modes into the test vehicles are described in detail in Appendix V.

The following wear and degradation modes were introduced into the driver test series:

(1) Degradation Code 1 - Front End Misalignment

Toe: 15/16" out (2° included angle)

Camber: left wheel 0°, right wheel 3/4° negative

Caster: left wheel 3-1/2° positive, right wheel 4-1/4° positive

(2) Degradation Code 2 - Front Wheel Lash (combined tie-rod end, ball joint, wheel bearing, and steering gear box)—approximately ±2° free play at the front wheels with no load on the wheels. When the elements are loaded, a sizeable moment is needed to reach this amount of play. (The details of introducing play are fully described in Appendix V.)

(3) Degradation Code 50 - Front Wheel Lash Without Wheel Bearing Looseness - Same as (2) without wheel bearing play.

(4) Degradation Code 51 - Front Wheel Lash Plus Wheel Imbalance - Same as (2) with 10 ounces of lead added on the rim of the right-front wheel.

(5) Degradation Code 52 - Removed Roll-Bar Bushings

All four rubber bushings removed from both vertical strut links at the connection of the roll bar to each lower control arm.

(6) Degradation Code 53 - Long Shackles—used in replacement of original equipment rear leaf spring shackles.

(7) Degradation Code 54 - Front Wheel Lash Plus Brake Imbalance

(Code 54-1) Same as (2), with brake pressure imbalance on front brakes of the proportion, 1.0 left, 0.7 right.

(Code 54-2) Same as 54-1, but with front brake pressure imbalanced by the proportion, 1.0 left, 0.4 right.

(8) Degradation Code 55 - 90%-Oil-Loss Shock Absorbers on the Rear.

(9) Degradation Code 56 - 90%-Oil-Loss Shock Absorbers—at all four wheels.

(10) Degradation Code 57 - Shock Absorbers with Worn Rod Guides and Broken Valve Discs on the Rear.

(11) Degradation Code 58 - Worn Rod Guide and Broken Valve Disc Shock Absorbers—at all four wheels.

(12) Degradation Code 61 - Combined Degradations

Play as in (2)
Shock Absorbers as in (10)
0.4 brake imbalance as in (7)

(13) Degradation Code 62 - Dry Surface-Loaded Capacity; Wet Surface

Code 62-1 - as in (12) with no brake imbalance
surface dry
vehicle loaded to capacity

Code 62-2 - as in (12)
surface dry
vehicle loaded to capacity

Code 62-3 - as in (12) with no brake imbalance
surface wet
normal loading

Code 62-4 - as in (12)
surface wet
normal loading

(Note that straight-line-braking tests were not run for degradations with brake imbalance.)

The degradations examined in the automatic controller test series include most of those conditions which were used in the driver test series, with the notable exception of brake imbalance. This latter condition was excluded with the recognition that the one automatic series test involving braking, VHTP #6, was intended to examine roll response following wheel locking. Brake imbalance would merely have rendered the test procedure less effective in challenging the rollover propensity by preventing certain wheels from locking. The wear and degradation modes introduced into the automatic controller test series were:

(1) Degradation Code 100 - Front-End Misalignment

Toe: in, 1-3/16" (4° included angle)

Caster: left wheel - 2°, right wheel - 1°

Camber: left wheel 0°, right wheel -1°

(2) Degradation Code 101 - Front Wheel Lash Plus Wheel Imbalance

Combined tie-rod end, ball joint, wheel bearing, and steering gear play—approximately ±1.1° at the front wheels with no load on the wheels. Wheel imbalance - 10 ounces of lead on the right front wheel.

(3) Degradation Code 102 - 90%-Oil-Loss Shock Absorbers On All Four Wheels

(4) Degradation Code 103 - Worn Rod Guide and Broken Valve Disc Shock Absorbers On All Four Wheels

(5) Degradation Code 104 - Worn Rod Guide and Broken Valve Disc Shock Absorbers Plus Front Wheel Lash Plus Wheel Imbalance (no ball joint lash due to failure of the degradation mechanism) Plus Wheel Imbalance

(6) Degradation Code 105 - Worn Rod Guide and Broken Valve Disc Shock Absorbers Plus Wheel Imbalance

(7) Degradation Code 106 - Worn Rod Guide and Broken Valve Disc Shock Absorbers Plus Front-End Misalignment

4.2.2 FINDINGS RELATED TO THE DEGRADATION STUDY.

4.2.2.1 Straight Line Braking. Examination of straight line braking results for each of the degraded conditions as compared with each of three sets of original equipment condition tests, indicated a general insensitivity of peak (non-two-wheels-locked) acceleration performance to all of the degradations considered. This observation of "insensitivity" reflects that the degraded condition data falls within the scatter of the baseline data. This finding was anticipated in that it is recognized that peak non-wheels locked braking depends primarily upon the longitudinal force capability of tires, the brake-torque distribution, and the location of the vehicle's center of mass.

4.2.2.2 Braking-In-A-Turn. Data gathered for this maneuver, as in VHTP #1, was found to indicate generally negative sensitivities, except for conditions of steering and suspension system degradations combined with brake imbalance. Clearly, data indicated a sensitivity of response deriving from the induced moments accompanying brake imbalance, as well as the expected loss in overall braking due to a decreased effectiveness at one front brake. Nevertheless, this sensitivity was felt to be merely indicative of the importance of brake imbalance, and was not representative of a performance change deriving from degradation of steering and suspension system components.

4.2.2.3 Roadholding In A Turn. The performance of the Mustang was found to be markedly altered only in those test conditions in which there was a heavy reduction in shock absorber effectiveness. In the test corresponding to degradation Code 55 (both rear shock absorbers degraded by removal of 90% of the hydraulic fluid) an apparent spinout tendency was noted, while in the test corresponding to degradation Code 56 (90%-oil-loss in all four shock absorbers) substantial side force loss occurred at all four wheels. Interestingly, however, the shock absorbers which had been altered mechanically (with worn rod guides and broken valve discs) did not appear to cause any perceptible change in performance.

4.2.2.4 Automatic Controller Test Series. Pilot tests were run with the Dodge Coronet, covering the full list of degradations for the trapezoidal steer, sinusoidal steer, and drastic steer/brake maneuvers. Over a three-week period, tests were conducted which yielded data with a very large degree of variability. Responses to trapezoidal steer tests, for example, were seen to indicate peak lateral accelerations which varied over a 0.5 g range. Repeated runs of the Dodge in the O.E. condition showed a 0.2 g range. Sinusoidal steer results were likewise seen to vary widely, indicating apparent sensitivities to component degradation which could not be reconciled with basic principles of vehicle mechanics. It was felt that these variances completely invalidated the pilot test data relating component degradation to vehicle performance for VHTP maneuvers #4 and 5.

In maneuver #6, Drastic Steer and Brake, a single pronounced sensitivity was observed which was felt to be indicative of a fundamental relationship between component degradation and roll over potential. While conducting drastic steer/brake runs with degradation Code 106, (shock

absorbers with worn rod guide and broken valve disc in combination with severe front end misalignment) the Dodge Coronet rolled over with sufficient severity as to collapse the outrigger assembly, with the vehicle coming to rest on its roof (Figure 4.15).

The above findings indicated that a research effort was needed to determine the cause of the observed variability, both to permit meaningful assessments of degradation sensitivity to be made and also to establish baseline, or O.E., performance as a representative characterization of the vehicle.

4.2.3 FINDINGS RELATED TO THE TIRE-SURFACE FRICTION STUDY. Following review of the data gathered in the automatic test series, it was hypothesized that the observed variability could only be attributable to variation in friction properties at the tire/road interface. A "crash" investigation was initiated that concentrated on tire properties felt to be the factors responsible for the observed variabilities. The findings resulting from this investigation are presented in detail in Appendix IX, and are summarized in this section.

By conducting vehicle tests and tire tests, the latter with the HSRI mobile tire tester, the influence of four test condition variables on the peak side force capability of tires was examined. These four variables were:

1. Tire tread wear, as derives from the conduct of limit turning tests.
2. Drying time, as it affects the recovery of "dry pavement" friction properties following a rainfall.

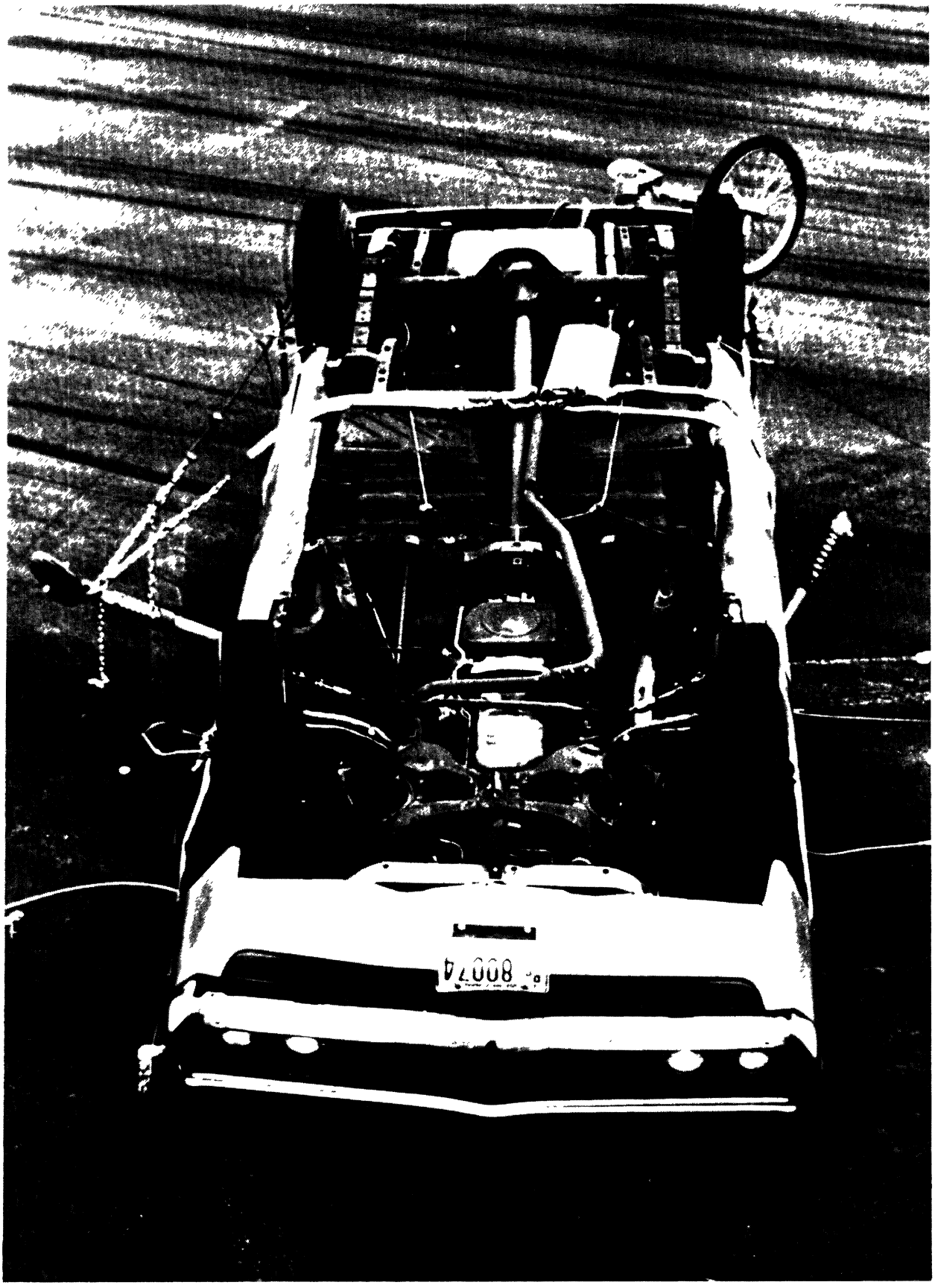

Figure 4.15. This vehicle rolled over in response to drastic steer/brake input while being tested with combined degradations. (Note the large degree of toe-in)

3. Test surface temperature.

4. Test surface material.

A remarkable finding related to the influence of tire shoulder, or buttress, wear on peak side force capability derived from the mobile tire tester experiments and correlated with vehicle experiments. On certain tires it was found that side force improves dramatically as the buttress first begins to wear and eventually achieves steady-state at a normalized force level that can be as much as 40% higher than in the unworn state (see Fig. 4.16). Figure 4.17 shows the results of tire-wearing tests performed with the mobile tire tester on tires constituting original equipment on the twelve vehicles tested in the companion (Vehicle Handling Performance) program. The ranges of normalized side force measurements shown on this figure were yielded by tests in which each tire was loaded to approximate the respective vehicle-imposed loads on the outside tires in a limit turn. All tires were operated at 20° slip angle and subjected to a sequence of test runs to obtain the performance bands indicated. These data clearly reveal that the side force capability of the tire used by the Dodge Coronet is markedly sensitive to shoulder wear, and coincidentally, is substantially more sensitive to shoulder wear than many other tires.

Additional data are given in Appendix IX to indicate the degree to which this wear sensitivity is correlated by vehicle test, in addition to providing measurements that indicate the yaw-destabilizing influence of the higher wear rates on front tires that is experienced during limit-turning experiments.

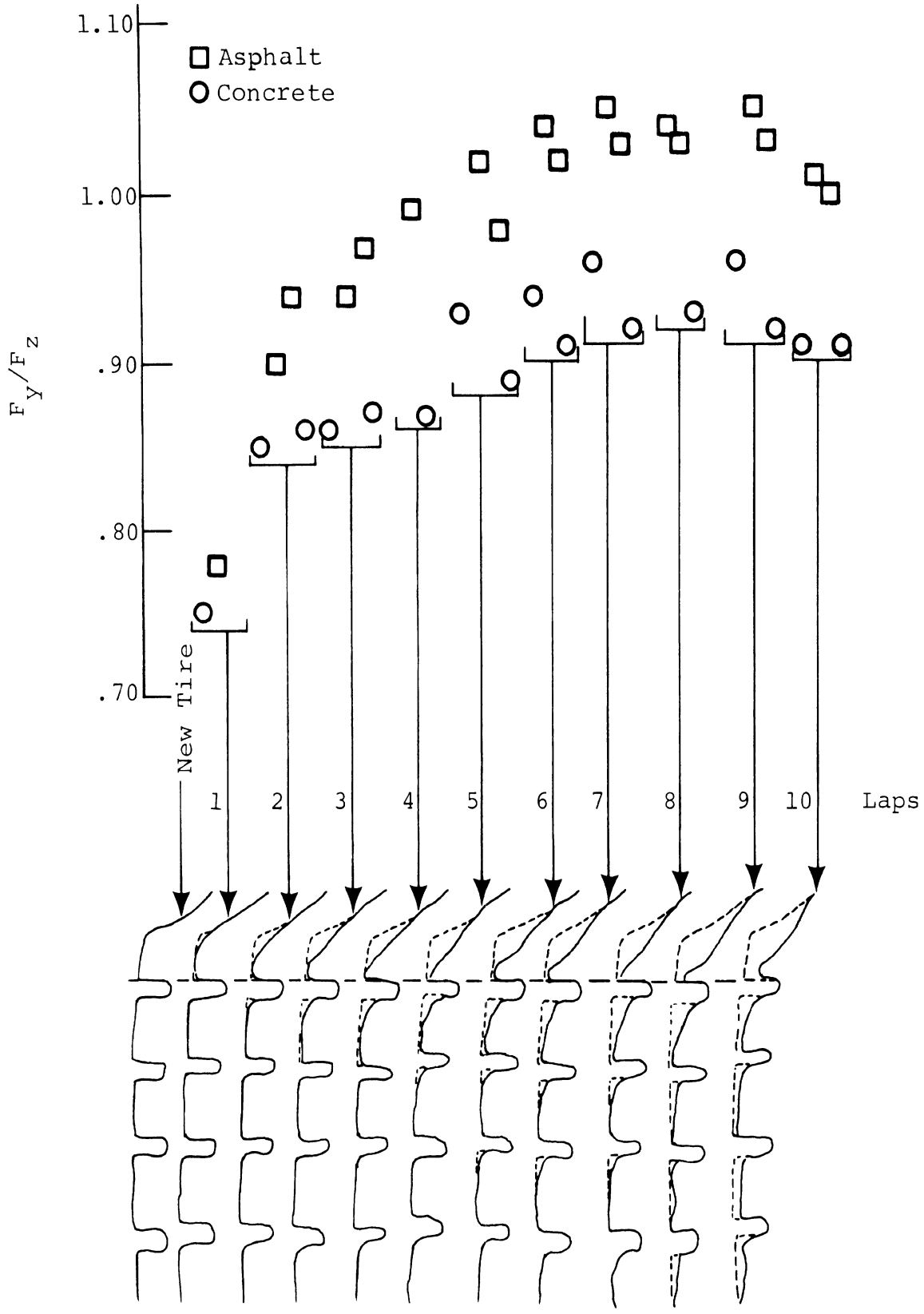

Tread Profile - Outside Shoulder

α=20° F_z=1550 Uniroyal L78-15 Fastrak

Tire Sample No. 1

Figure 4.16

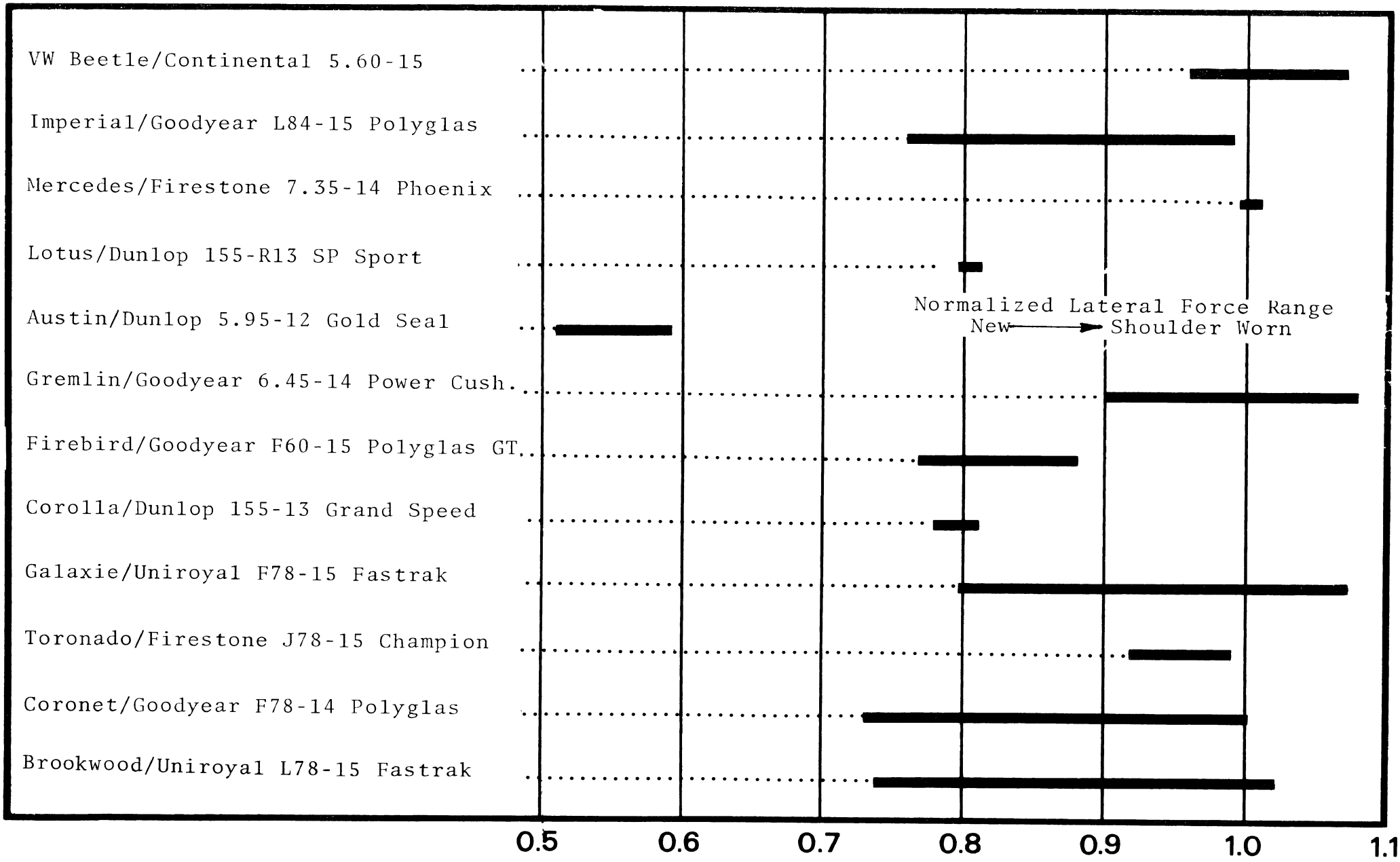

FIGURE 4.17
Normalized Lateral Force Range - Tires were run on a mobile tire test device gathering side force data as shoulder wear accumulated.

The principle conclusions derived from these findings was that further refinement of test practice is necessary to minimize the otherwise inevitable degradation of cornering test results with non-steady tire side force output. A process was outlined by which sets of test tires would be worn in by preliminary limit cornering tests of sufficient number as to assure the achievement of steady-state performance. Although this procedure is clearly an artificial alteration of tire properties, it was deemed to be the only recourse for the purposes of obtaining consistent vehicle performance for this study. An obvious philosophical conflict arises, however, in attempting to label the nominal condition of the baseline experiments. They do not literally represent original equipment performance, nor do they necessarily represent a condition of usage which vehicles would be expected to exhibit in any normal driving mission. It suffices here to summarize that a first-order source of vehicle turning response variability was identified, and that a compensating test practice was adopted, in an attempt to assure data consistency.

With regard to the three other potential sources of variability, data is presented in Appendix IX indicating that

a) "dry pavement" friction properties were recovered following wetting of the asphalt test pad, as soon as the surface "appeared dry," that is, no perceptible darkening was noticeable in comparison to the dry "control surface,

b) no monotonic effect on tire side force or vehicle limit turning capability is seen to derive from large changes in test surface temperature, over the range investigated,

c) no specific repeatability advantages were identified for a concrete surface compared to asphalt, in any of the experiments regarding tire wear or surface temperature.

Thus, no refinements in test practice were found necessary in relation to the temperature, drying time, and surface material factors.

5. FULL-SCALE TEST PROGRAM: EXECUTION AND FINDINGS

This section of the report is concerned primarily with presenting the experimental findings that were produced in the major test program mandated by the requirements of this study. Specifically, the objective was that of applying six open-loop, limit maneuver measures, discussed in Section 4, to a two-vehicle sample. As in the pilot tests, vehicle performance was measured for both the O.E. and component-degraded conditions.

The test practice which was observed in preparing and testing each vehicle is outlined below. Additionally, the matrix of degraded test conditions is presented, together with an itemization of the mechanical characteristics of each degradation that was introduced into each of the test vehicles. The two vehicles selected for full-scale testing were the AMC Ambassador and the Dodge Coronet which had served as one of the pilot test vehicles (see Figure 5.1).

The response data generated in this test program was processed from analog magnetic tapes by a computerized data handling system, fully described in Appendix VII. This computerized processing procedure provided response numerics in digital form which were then plotted for each vehicle, using a presentation format which was identical to that used in the companion Vehicle Handling Performance study [7]. This commonality of test data presentation, as well as test practice, makes possible the comparison of the performance variations that arise due to component degradation with the performance variations that derive from design differences in the new car population. Thus, the full-scale test data for the Dodge and Ambassador are presented in the form of summary plots, along with corresponding summary plots of new

1971 American Motors Ambassador

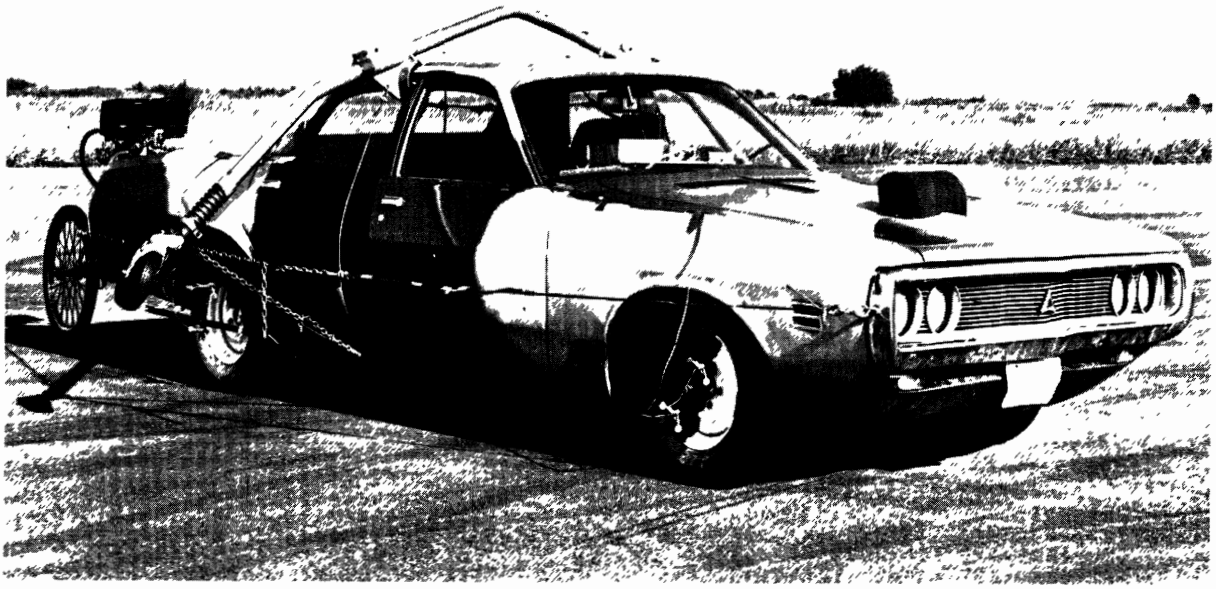

1971 Dodge Coronet

Figure 5.1. Vehicles used in full scale test program.

car performance. By means of such a comparison, it is felt that a necessary perspective is provided for assessing the influence of component degradation on vehicle handling, by way of the vehicle response measures that have been recently developed, given that no general scheme has been established for interpreting these measures in a safety context.

The individual data plots deriving from testing both vehicles in the O.E. and degraded states are presented in Appendix X.

5.1 GENERAL TEST PRACTICE EMPLOYED IN THE FULL-SCALE TEST PROGRAM

Vehicle test progress was facilitated by conducting two parallel series of experiments, with the equipment required to perform the driver and automatic series of tests being sequentially installed and utilized in each of the test vehicles. To facilitate the installation of the test equipment in the field, a number of vehicle modifications were made. These modifications included the following permanent installations fitted to each vehicle:

1. a fifth wheel mount bracket
2. brake lining thermocouples at left front and right rear wheels
3. a plywood platform for mounting test instrumentation
4. a steering limiter mount bracket
5. brake limiter connection tubing
6. painted black/white masks on each wheel
7. front-wheel spindle mounts for front-wheel rotation detectors

8. rear-wheel rotation detector mounts
9. outrigger-tie-cable bolts in the front and rear bumpers
10. hydraulic pump mount and drive pulley on the engine
11. 12-volt fuse block and terminal

As a standard procedural practice prior to test, each vehicle was subjected to the SAE brake burnishing procedure (J843a) and was driven a minimum of 500 miles in a normal traffic environment. Tires for both vehicles were purchased directly from the manufacturers such that all experiments on either vehicle were run with tires obtained from a common lot. Tires were "broken in" on each vehicle by subjecting them to normal driving over 100 to 200 miles.

Prior to initiating either the driver or automatic series tests on each vehicle, the following practices were observed:

1. The vehicle was weighed prior to installation of the instrumentation package.
2. While the vehicle remained in its empty state, the front-end alignment was adjusted to be within the original equipment manufacturer's specification.
3. A physical calibration was performed on all data transducers.
4. The instrument package was installed and functional checks were made.
5. The instrument-laden vehicle was weighed.

6. Measurements of wheel alignment were made on the instrument-laden vehicle.

7. The steering ratio, N_G, was measured statically. This ratio was determined as the average ratio for both wheels turned 12° left and right:

$$N_G = \frac{\delta_{sw_1} + \delta_{sw_2} + \delta_{sw_3} + \delta_{sw_4}}{48}$$

where: δ_{sw_1} = steering wheel angle for 12° left turn on left front wheel

δ_{sw_2} = steering wheel angle for 12° right turn on left front wheel

δ_{sw_3} = steering wheel angle for 12° left turn on right front wheel

δ_{sw_4} = steering wheel angle for 12° right turn on right front wheel.

The value of N_G was used to compute the control input levels of steering per the procedures outlined in Appendix VII.

8. Next, trial runs were conducted, with sample data taken and checked.

9. New tires which had been "broken in" by at least 100 miles of driving were installed prior to conducting the side-force stabilization tests.

10. During these stabilization tests, tire inflation pressures were maintained at the manufacturer's recommended cold inflation pressure and the fuel tank was maintained between half-full and full.

11. The tire side-force stabilization tests were stopped after 20 runs and the tires were transferred to an opposite diagonal position. Further runs were conducted as dictated by the wear-in scheme outlined in Appendix IX.

12. Prior to all data-taking sequences, the vehicle was driven over a 3-mile paved course, and inflation pressure was adjusted as necessary. An electrical calibration sequence was conducted as outlined in Appendix VIII.

13. Test procedures were conducted, with electrical calibrations repeated whenever a run sequence exceeded 25 samples. A sample number was assigned to each test run and to each mode of the electrical zero and gain-set calibration sequence. Each sample was recorded in a data log book as well as being identified on the voice channel of the tape recorder.

14. Following all tests in a series (driver or automatic) a post-calibration sequence was conducted and the physical gains of all transducers compared with the values taken prior to the series. If any of the critical response variables were seen to have varied more than the amounts indicated below, the entire test series was repeated.

Variable	Allowed Calibration Variation
A_x	1 1/2%
A_y	1 1/2%
r	2%
ϕ	2%
V_5	1 1/2%

15. Front-end alignment was measured following each test series to record the alteration in static wheel positions resulting from testing.

16. Recordings were obtained of environmental conditions throughout the test program, even though it was recognized that no basis currently exists for utilizing these data to apply corrections to the test results.

17. The test pad was swept periodically with a scrubbing sweeper to minimize the deterioriation of friction properties caused by surface contamination.

18. Skid trailer measurements were made on the test surface, indicating average dry pavement ASTM skid numbers of 76-82.

19. All response data gathered during the test program was stored and transported in magnetically shielded containers. When tape data canisters were manually carried onto commercial airline flights, the airlines were requested to deactivate whatever high gauss metal detectors may have been operational.

Height of the installed instruments in the automatic test series were measured on each vehicle to enable estimates to be made of the elevation of the center of mass of the installed load. The installed gear weighed 515 pounds. In each vehicle, however, seats were removed, such that the net load compares favorably with a nominal two passenger-no luggage condition. In comparing estimated c.g. heights of a vehicle loaded with two passengers and no luggage, it would appear that neither vehicle suffered a net c.g. height relocation as large as one inch.

5.2 DEGRADED VEHICLE TEST CONDITIONS

A limited matrix of degradation conditions was selected for the full-scale test program, as outlined in Table 5-1, which was structured to pursue both positive and negative sensitivities as indicated from the pilot tests and simulation. In the case of positive sensitivities, the limited matrix included conditions to provide data on:

(1) the effect of shock absorbers on straight-line braking (with limited matrix degradation code D2)

(2) the effect of shock absorbers on turning on a rough road (code D1 and D2)

(3) the effect of shock absorber/front-end misalignment combination on drastic steer/brake performance (code A4)

(4) the effect of front-end misalignment alone on trapezoidal steer and sinusoidal steer (code A3)

To be able to interpret the results of shock absorbers and front-end misalignment in combination, it was necessary that both modes be tested alone. Thus, another set of runs was done in the automatic series under Code A1, shock absorbers alone.

In addition to selecting tests which are expected to provide further data toward positive findings, it was determined that tests be made incorporating degradation modes for which insufficient evidence existed to make solidly negative findings, although there was reason to believe that data can be obtained supporting such findings.

TABLE 5-1

DEGRADATION CODES—FULL-SCALE TESTS

Degradation Code	Description	Applicable Tests
D1	Shock absorber degradation-both rear wheels	VHTP #3
D2	Shock absorber degradation-all four wheels	1, 2, 3
D3	2 steering system elements degraded (ball joints and tie-rod ends)	1, 2, 3
D4	4 steering system elements degraded (ball joints, tie-rod ends, steering gear box, and wheel bearings)	1, 2, 3
D5	Front end misalignment	1, 2, 3
A1	Shock absorber degradation-all four wheels	VHTP #4, 5, 6
A2	4 steering system elements degraded (ball joints, tie-rod ends, steering gear box, and wheel bearings)	4, 5, 6
A3	Front end misalignment	4, 5, 6
A4	Front end misalignment combined with shock absorber degradation at all four wheels	4, 5, 6

Test Procedure Identification

VHTP #1 - Straight Line Braking

VHTP #2 - Braking In A Turn

VHTP #3 - Roadholding In A Turn

VHTP #4 - Trapezoidal Steer

VHTP #5 - Sinusoidal Steer

VHTP #6 - Drastic Steer and Brake

Negative findings were expected to be forthcoming from test data documenting:

(1) the effect of all four steering system indeterminacies on all of the six procedures (with codes D4 and A2)

(2) the effect of ball joint and tie-rod end play on the driver series experiments (with code D3) and,

(3) the effect of front-end misalignment on the driver series experiments (code D5)

On both the Dodge and the Ambassador, components were modified, as per the rationale and discussion given in Appendix V, to provide the various degradations indicated by test condition codes D1 through A4. The mechanical characteristics of these modified components, as determined in the laboratory, are presented below. Of interest are those properties that influence steering and braking performance. For example, degraded shock absorber performance is defined in terms of a force-velocity diagram, which diagram provides a generalized description of this highly nonlinear device that can be contrasted with the force-velocity performance of the original equipment shock absorber. The O.E. and degraded performance of the front and rear shock absorbers on both test vehicles are shown in Figures 5.2 and 5.3.

Likewise, the pertinent mechanical characteristics of steering system degradations are defined by the aligning moment/steer deflection diagrams presented in Figures 5.4 and 5.5. It appears that the diagrammed moment/deflection relationship constitutes a generic characterization of a variety of steering-system degradations. These figures clearly illustrate the load-lash properties of the system while providing a description of the test condition which is helpful in interpreting test results. To produce the results plotted

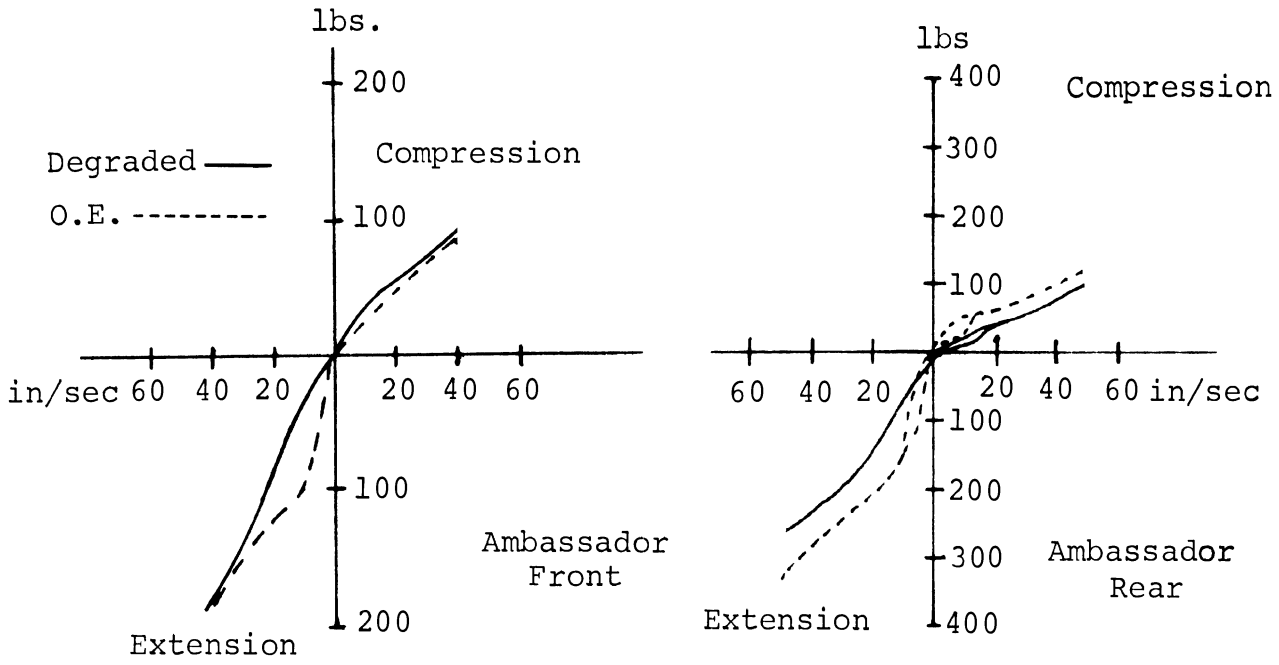

Figure 5.2 O.E. and degraded Ambassador shock absorber characteristics

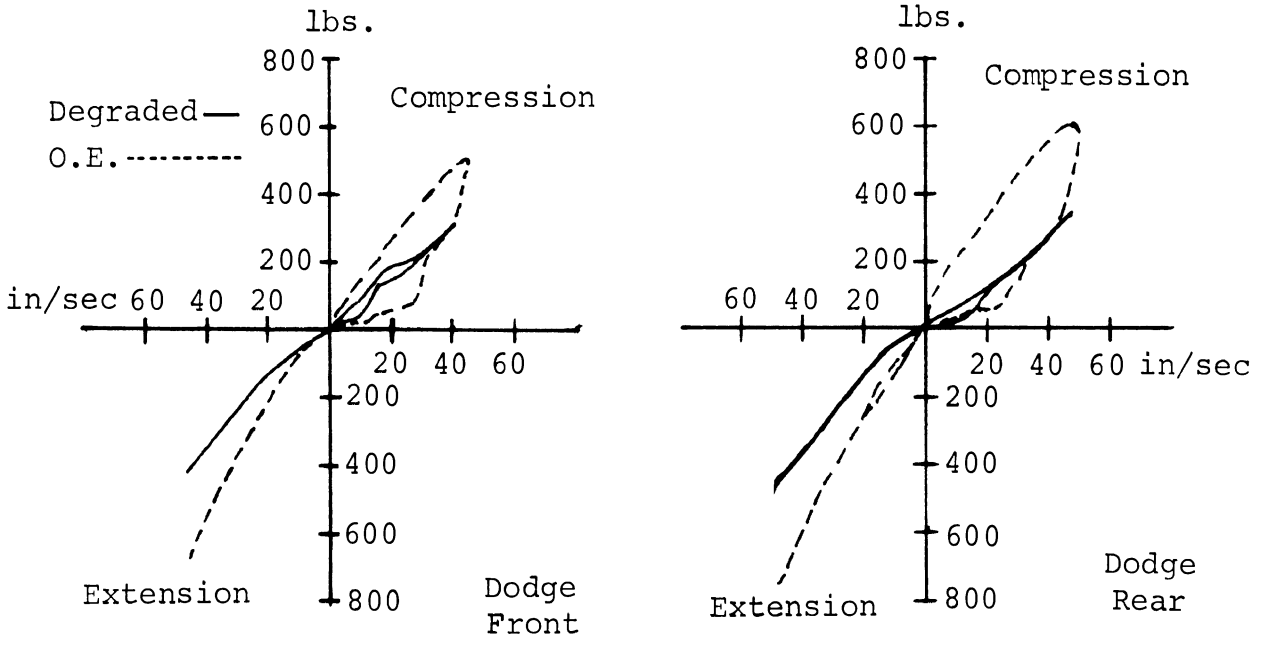

Figure 5.3 O.E. and degraded Dodge shock absorber characteristics

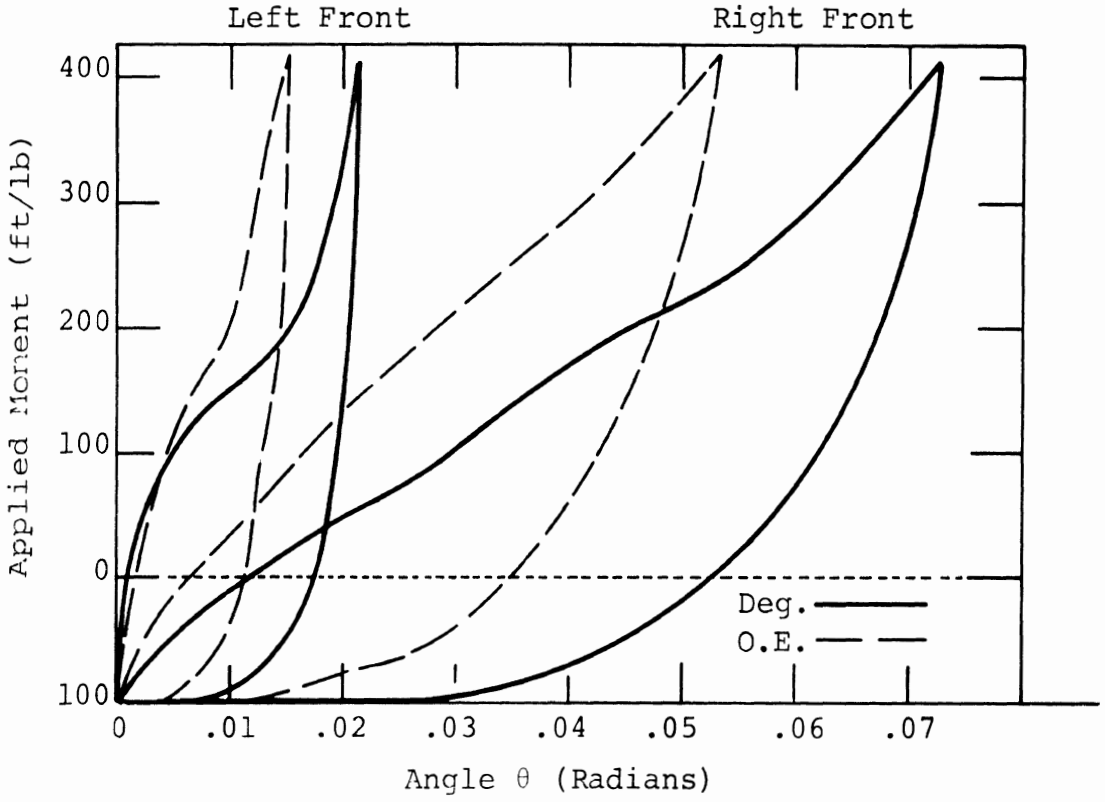

Degraded: Ball Joint, Tie Rod End, Steering Gear, and Wheel Bearing

Figure 5.4 Ambassador steering system measurements; degradation codes D4 and A2

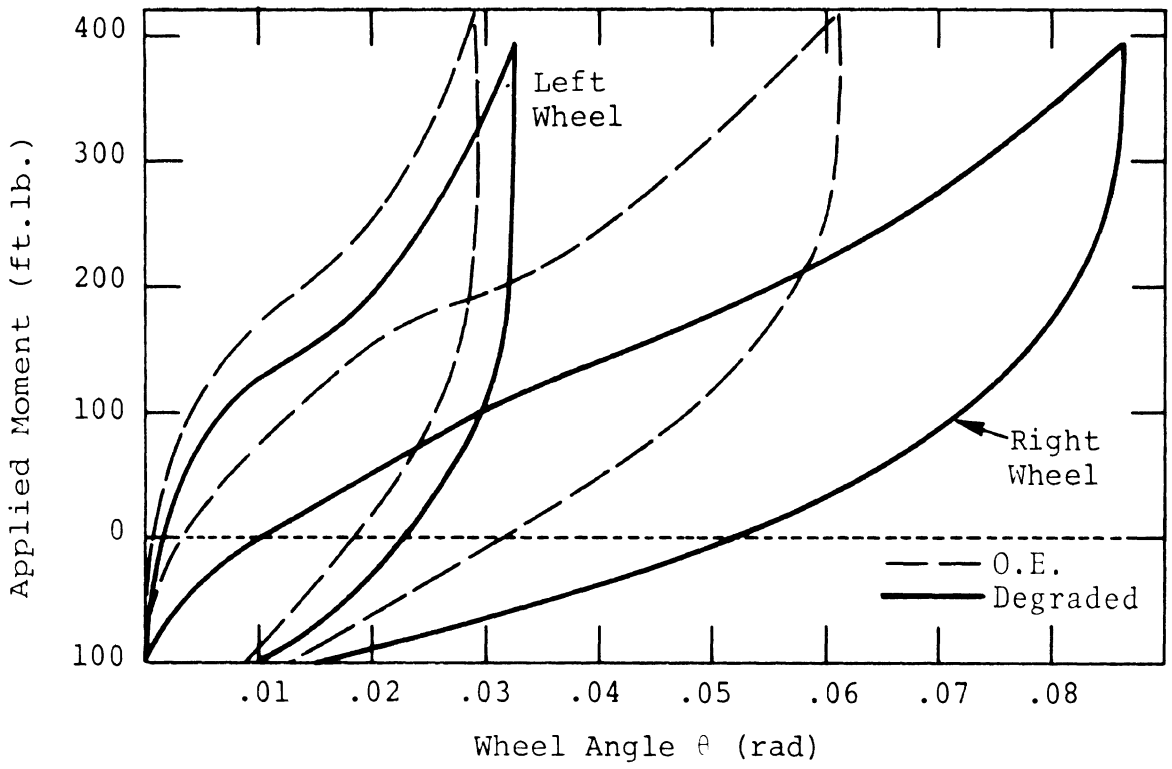

Degraded: Ball Joint, Tie Rod End, Steering Gear, and Wheel Bearing

Figure 5.5. Dodge steering system measurements: Degradation Codes D4 and A2

in Figures 5.4 and 5.5, an external moment was applied to the right front wheel, while measuring the steer deflection of both front wheels. With the steering wheel held fixed, the motion of the right wheel indicates compliant, friction, and lash functions deriving from the series of system components between the front wheel and steering wheel, while motion of the nonrestrained left wheel indicates compliant, frictional, and lash functions existing between the pitman arm and the steering wheel.

(Recall that the methods used to measure shock absorber and steering system properties were discussed in Section 3.3.)

The data obtained for the Dodge and Ambassador shock absorbers indicate a moderate level of force reduction, as a result of the virtually maximum wear and deterioration of the shock absorber assembly assumed to occur in service, without fluid loss.

The degradation of steering system components, taken collectively in test codes D4 and A2, represent a load-related lash of front wheel position on the order of ±1 to 2 degrees maximum indeterminacy. Although this level of play represents the virtually maximum level of degradation which is achievable without jeopardizing structural integrity, the steer angles involved are small in comparison to the large inputs used in limit maneuvering. Conversely, a 1 to 2 degree steer indeterminacy is recognized as representing a tremendous variation in comparison with the steer levels encountered in normal driving.

Three degraded condition tests involved misalignment of the front wheels. In those tests defined by codes D5, A3, and A4, combined caster, camber and toe adjustments were made on both the Dodge and the Ambassador, as specified in

Table 5-2. The rationale for the selected combination of misalignments, as intended to represent a maximum degradation in static wheel orientations, is presented in Appendix V.

TABLE 5-2

FRONT END MISALIGNMENT SPECIFICATIONS EXPRESSING CHANGES, RELATIVE TO THE O.E. CONDITION AS PROVIDED FOR TEST CODES D5, A3, AND A4

	Dodge Coronet	AMC Ambassador
Toe In (Included Angle)	4 1/2°	4 1/2°
Left Wheel Camber	0°	0°
Right Wheel Camber	-1 1/2°	-1 1/4°
Left Wheel Caster	-2 3/4°	-3°
Right Wheel Caster	-2°	-3°

5.3 FINDINGS OF THE FULL-SCALE TEST PROGRAM

The results of the full-scale test program will be reviewed by considering each maneuver category individually. Summary plots are presented which consider all degraded system data collectively in contrast with the performance of the baseline vehicle, namely, the performance of the O.E. vehicle with "stabilized" tires. These plots were constructed by graphical overlay, and are intended to illustrate the distribution and range of the data. In addition, boundaries are shown that define the range of performance in the new car population, as established in the companion Vehicle Handling Performance program [7]. Thus, the findings relating component degradation to limit handling will be an evaluation of

a) the respective vehicle's departure from its O.E. performance as caused by the introduction of degraded steering and suspension system components

b) the relative change in performance, O.E. to degraded, as compared with the distribution of new car performance.

5.3.1 STRAIGHT LINE BRAKING. Summary plots for the O.E. and degraded system performance of the Dodge and Ambassador are presented in Figures 5.6 and 5.7. These figures also include plots summarizing the straight-line-braking performance of the 12-car vehicle sample. The plots represent the average value of longitudinal acceleration which the vehicles achieved in slowing from 35 mph to 10 mph following application of the indicated level of brake pressure. Clearly, the Ambassador and Dodge both represent the "high gain" portion of the braking effectiveness spectrum in terms of the A_x/P_b gradient.

Although both of these plots show that degraded system data cluster very tightly about the respective baseline data, a positive sensitivity to component degradation was observed in the test data produced by the Dodge. Figure 5.8 presents raw data time histories indicating that the Dodge suffers a rear wheel lockup and subsequent spinout during the degradation code D2 (four shock absorbers degraded) test sequence. This behavior, which limited peak deceleration (prior to locking of two wheels on one axle) to 0.59 g as compared with 0.73 g in the O.E. case, apparently resulted from a rear-axle oscillation commonly referred to as "brake hop." This wheel-hop mode, coincident with brake application, clearly became unstable at the prevailing level of damping (as

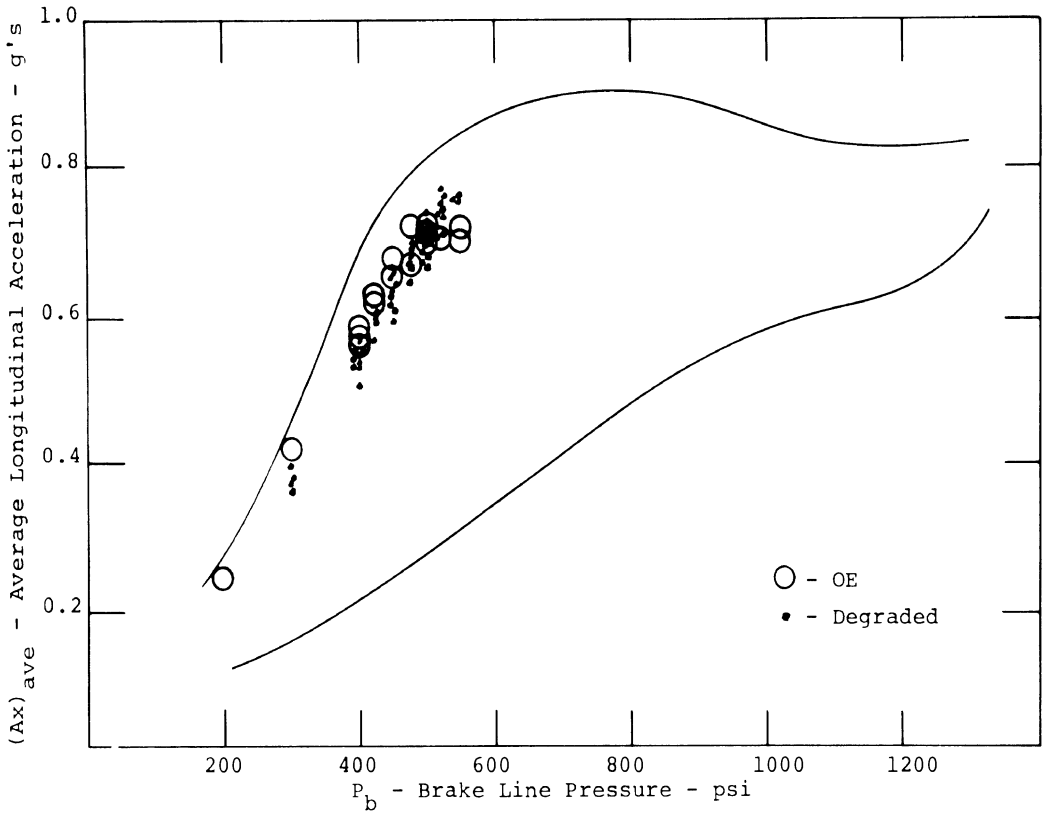

Ambassador O.E./Degraded

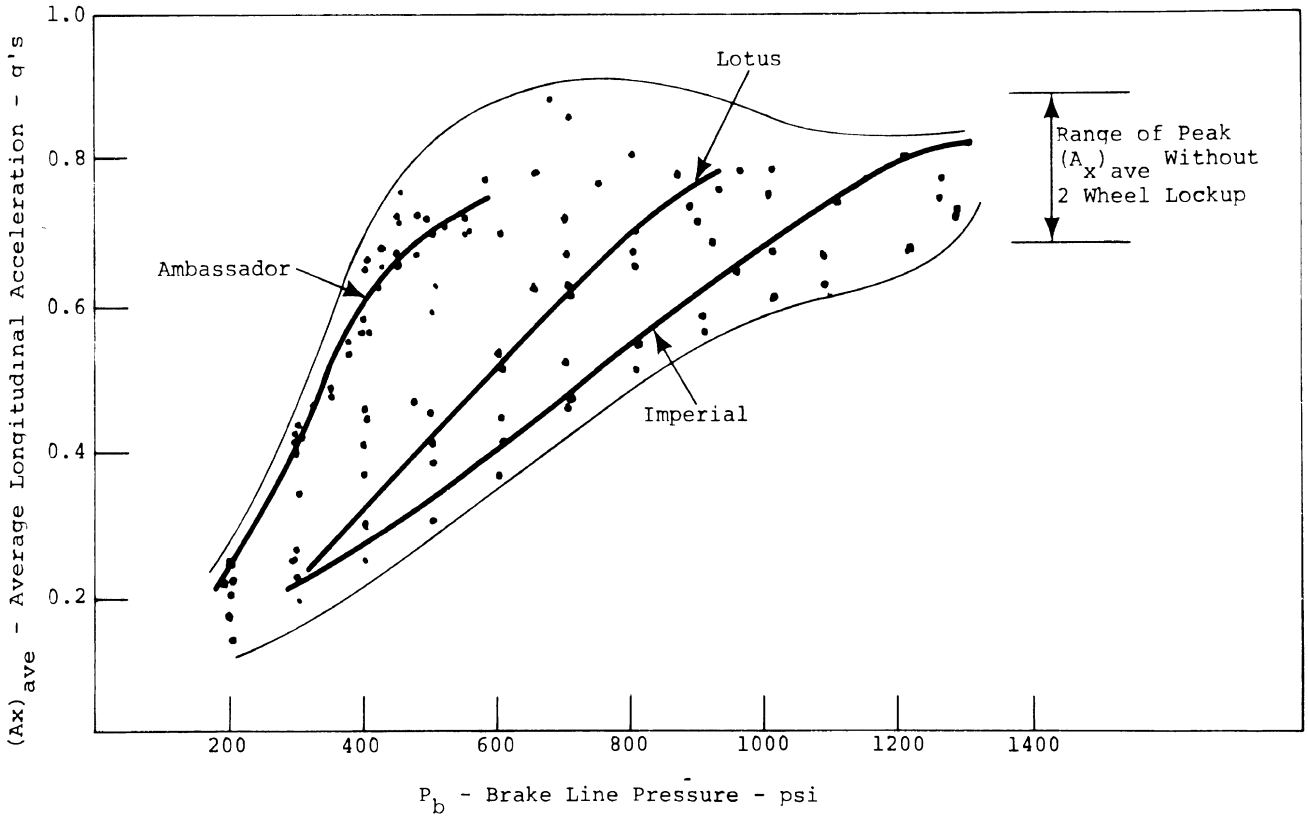

New Car Performance

Figure 5.6. Summary plot - straight line braking

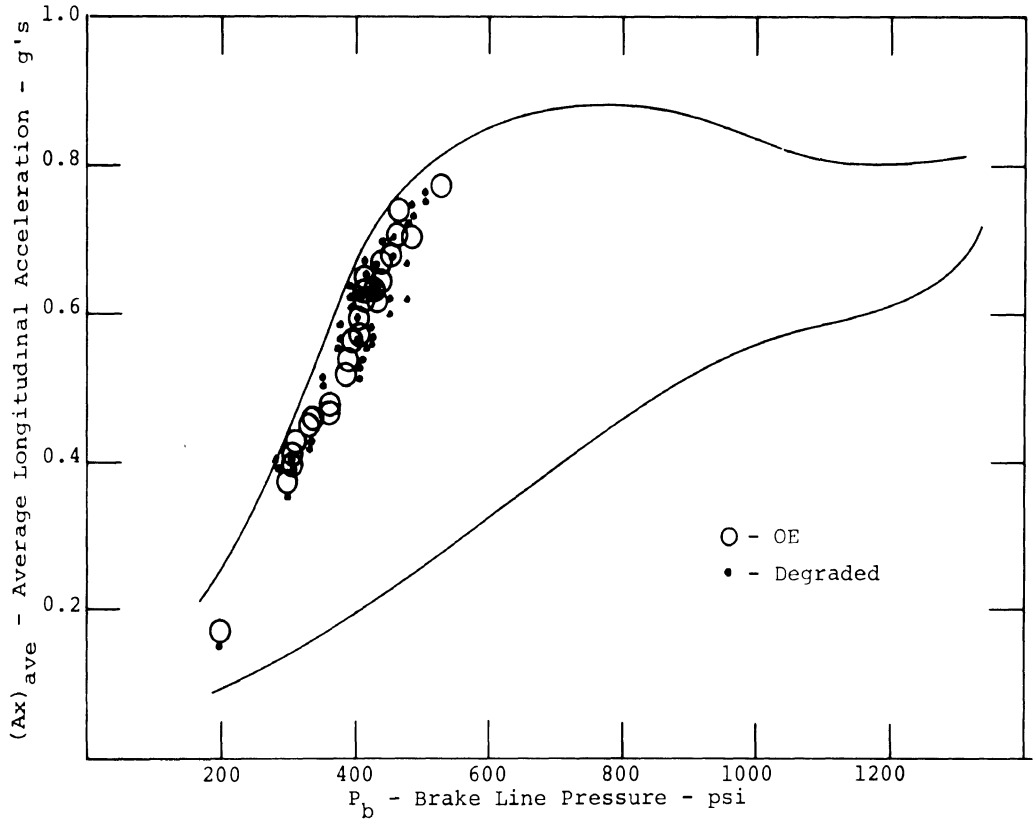

Dodge O.E./Degraded

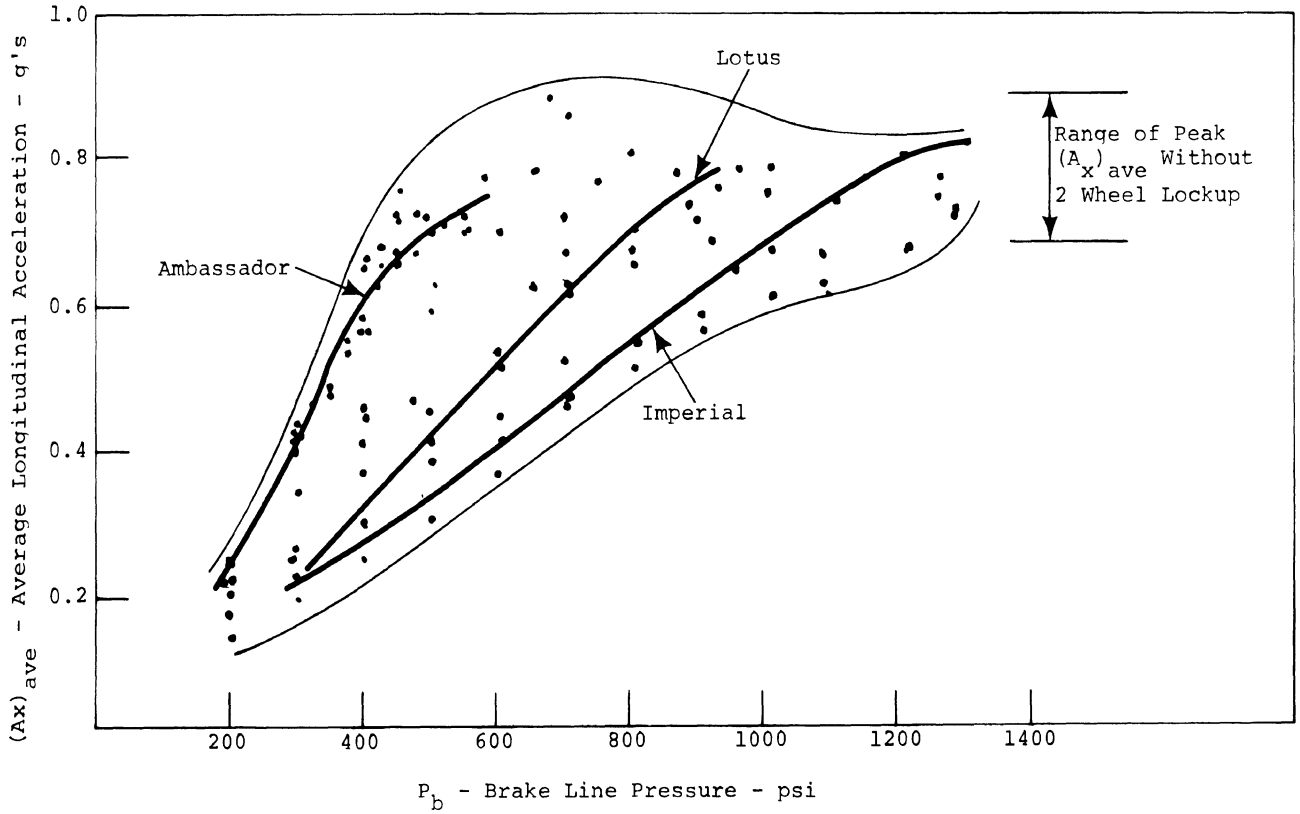

New Car Performance

Figure 5.7. Summary plot - straight line braking

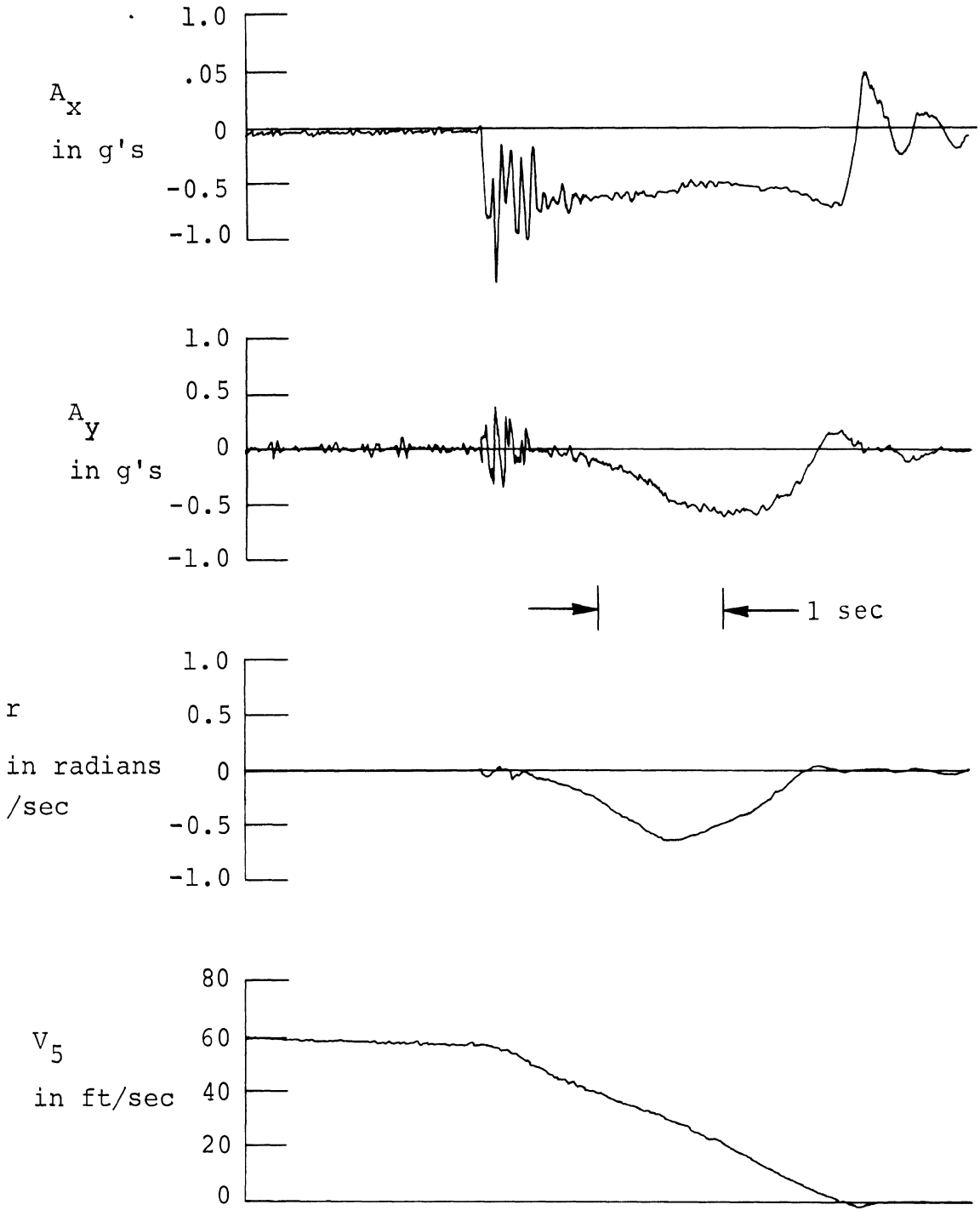

Figure 5.8 Dodge D-2
VHTP #1
sample 1668

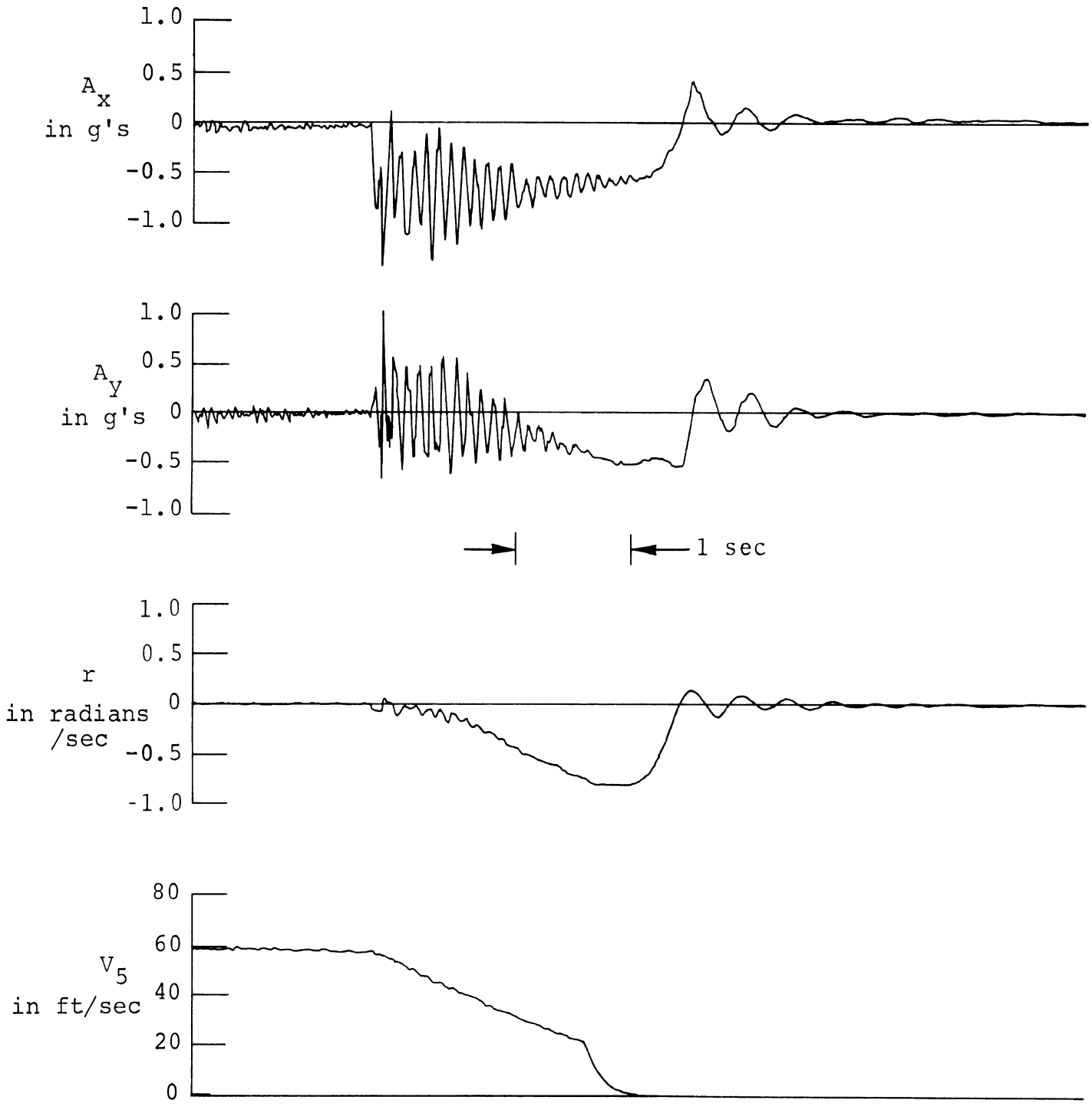

Figure 5.9 Dodge D-2
VHTP #1
sample 1674

provided by the degraded shock absorbers), amplifying at higher braking levels to the violent oscillations appearing in the raw data shown in Figure 5.9.

The net loss in braking efficiency that derived from degraded shock absorbers being installed on the Dodge should be viewed as a finding of positive sensitivity to this degraded condition. The change in braking efficiency caused by all other conditions tested is seen as negligible in comparison with the sizeable spread in the limit-braking performance exhibited by the new car population.

5.3.2 BRAKING IN A TURN. Response to a step brake input applied to a vehicle that is initially in a steady turn can be evaluated in terms of the peak braking attained without an excessive penalty occurring in the directional or path response. The two response variables chosen to characterize directional response are the peak sideslip rate, $\dot{\beta}_p$, and normalized path curvature ratio, $R_o(1/R)$. A large sideslip rate response, $\dot{\beta}_p$, is postulated to constitute a dynamic challenge to controllability such as arises under conditions of rear-wheel lockup—with spinout imminent. Clearly, no significant degradation in sideslip response was observed for either of the test vehicles, as indicated by the summary plots in Figures 5.10 and 5.11, which present all those data runs for which less than two wheels locked on any axle. Both vehicles are seen to achieve approximately 0.7 g longitudinal acceleration in all degraded conditions, without suffering $\dot{\beta}_p$ "penalties" which are significantly different from O.E. values.

The path curvature response in this test is seen as representing a driver challenge factor which increases as the average value of 1/R deviates further from the initial value

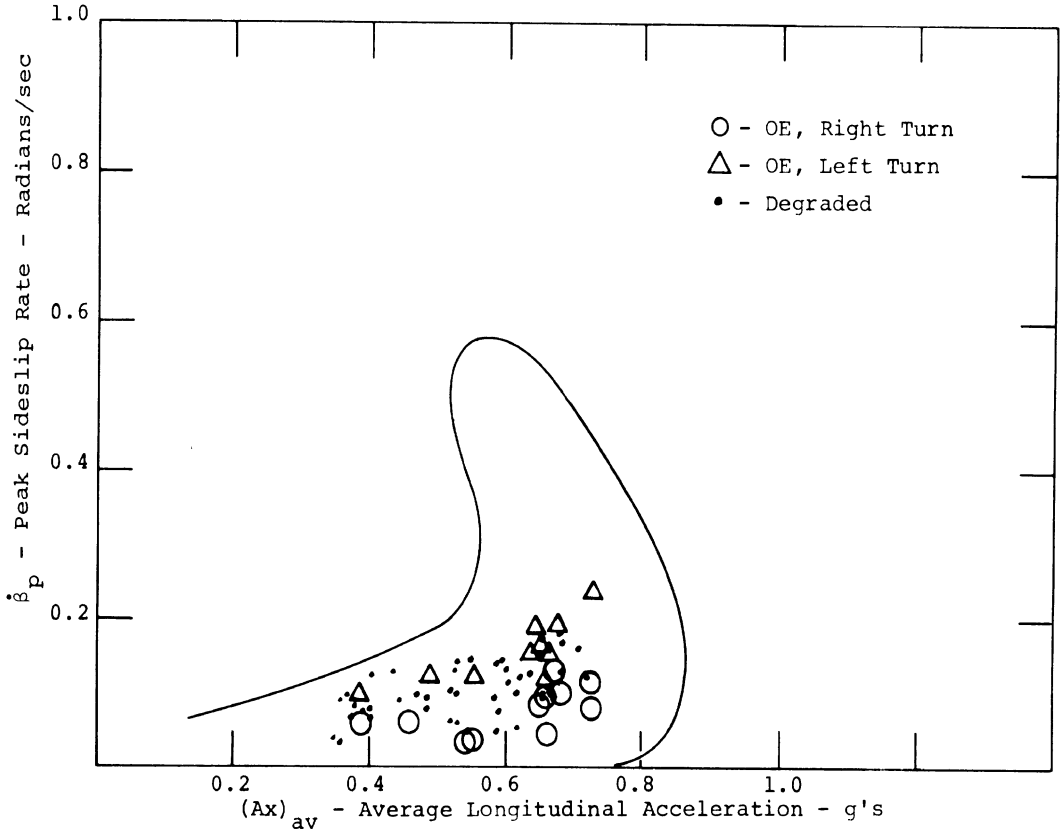

Ambassador O.E./Degraded

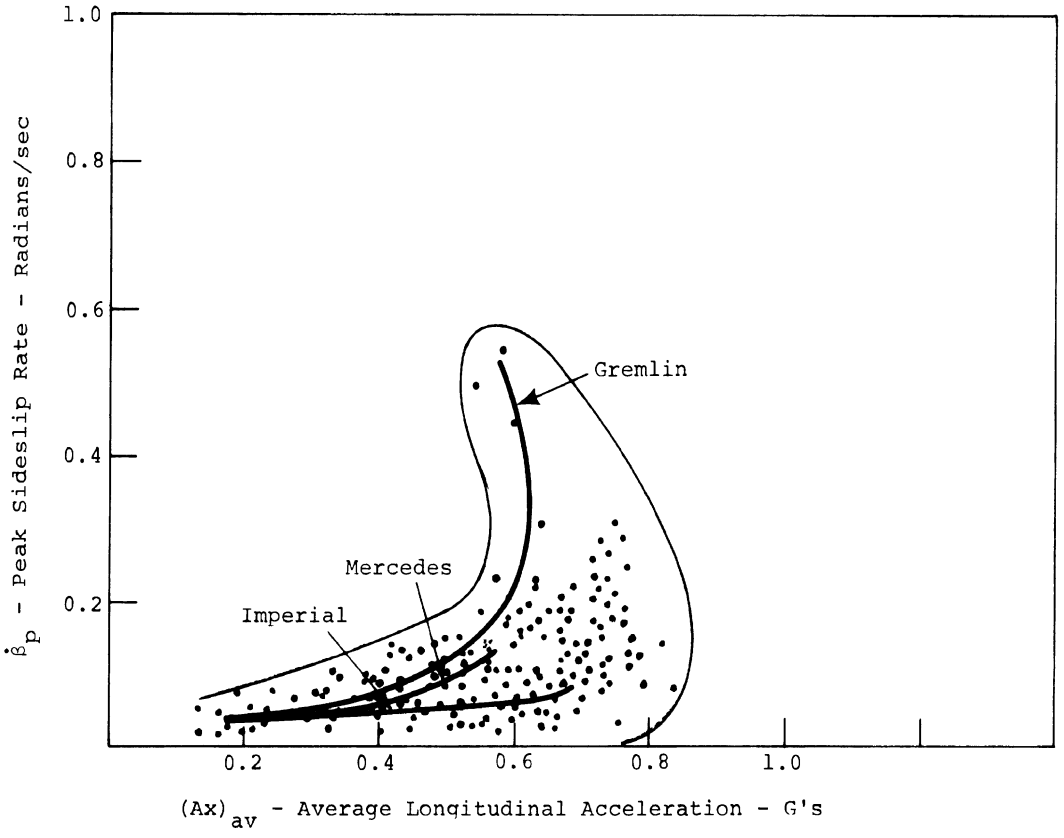

New Car Performance

Figure 5.10. Summary plot - braking in a turn

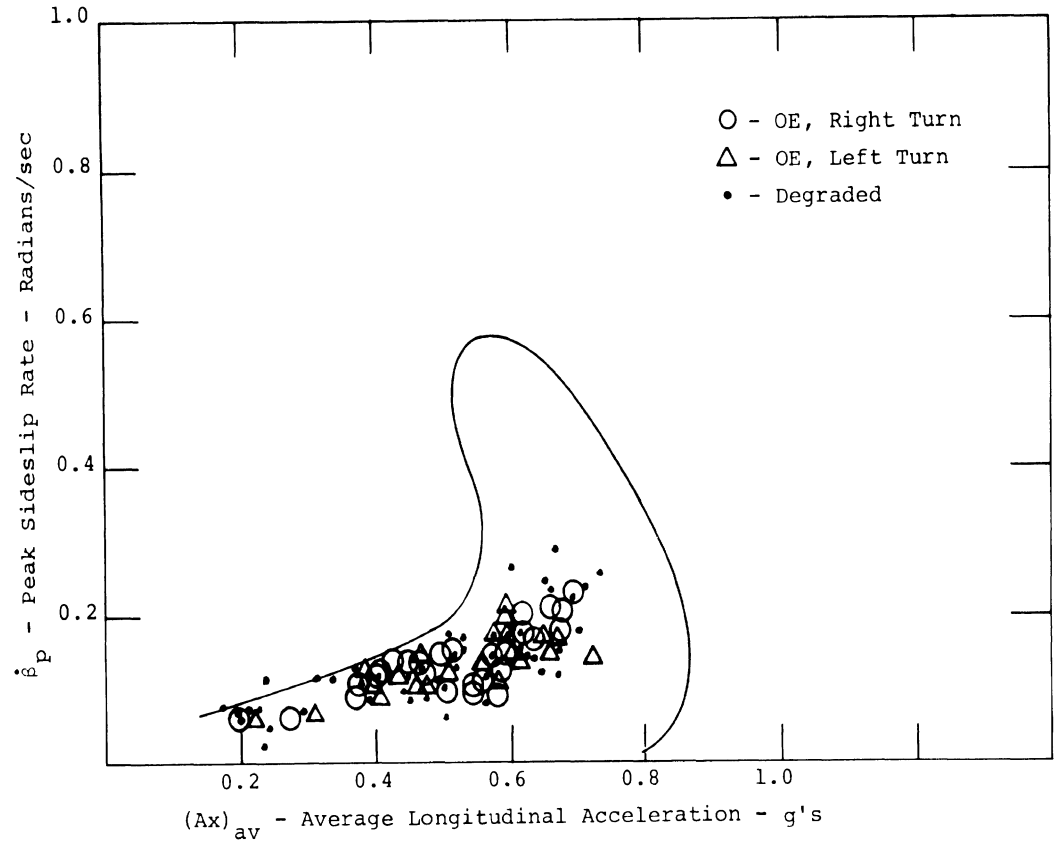

Dodge O.E./Degraded

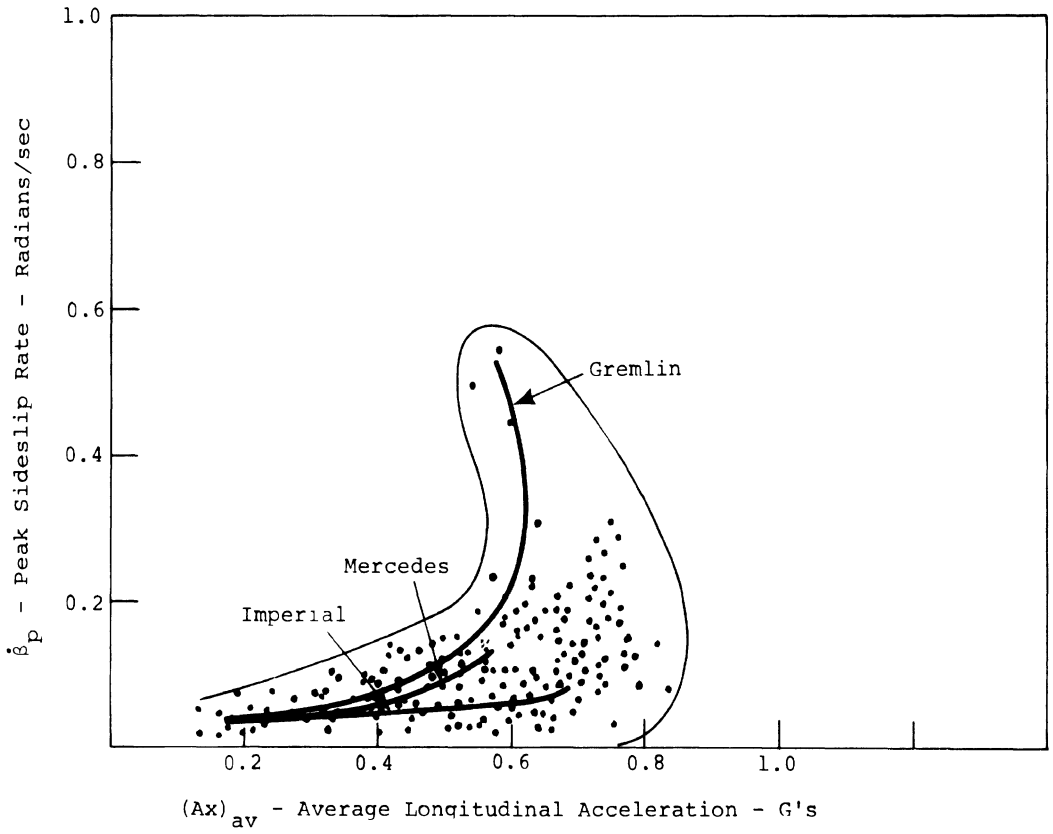

New Car Performance

Figure 5.11. Summary plot - braking in a turn

of path curvature ($1/R_o$) as was present at the initiation of braking. It is argued that drivers do not apply braking for purposes of eliciting changes in path. Thus the normalized term, $R_o(1/R)$, can be interpreted to indicate a larger "penalty" as it deviates further from the initial value of unity.

As indicated by the results plotted in Figures 5.12 and 5.13 for the Ambassador and Dodge, respectively, certain small sensitivities in path curvature response are evident. With respect to the Dodge data, Figure 5.13, it is clear that this vehicle represents an extreme within the range of new car performance, as measured by the $R_o(1/R)$ numeric. A somewhat confounding factor in these data concerns the gathering of a second set of O.E. data with the Dodge, as found necessary following a mid-sequence tire change. (In Appendix X, the baseline data are referred to as O.E.-A and O.E.-B.) Since the O.E.-B data was intended as the baseline reference for the degraded conditions (D3, 4, and 5) which followed it, the performance review must merely apply the proper bookkeeping by evaluating condition D2 in comparison to O.E.-A and conditions D3, 4, and 5 in comparison to O.E.-B.

Data points in Figure 5.13 falling outside of the indicated new car envelope (in the vicinity of $R_o(1/R) = 2.0$), represents a performance degradation produced by condition D2. As in straight-line braking, the "brake hop" phenomenon was elicited when braking in a turn with degraded shock absorbers, resulting in premature lockup of an inside rear wheel. Although the relevant response mechanism is not clearly understood, this condition did cause an increase in path curvature, thus registering the elevated levels of $R_o(1/R)$ as indicated. A sample time history of this response is shown in Figure 5.14, indicating an oscillation in longitudinal and lateral acceleration (A_x and A_y, respectively) followed by a divergent yaw response.

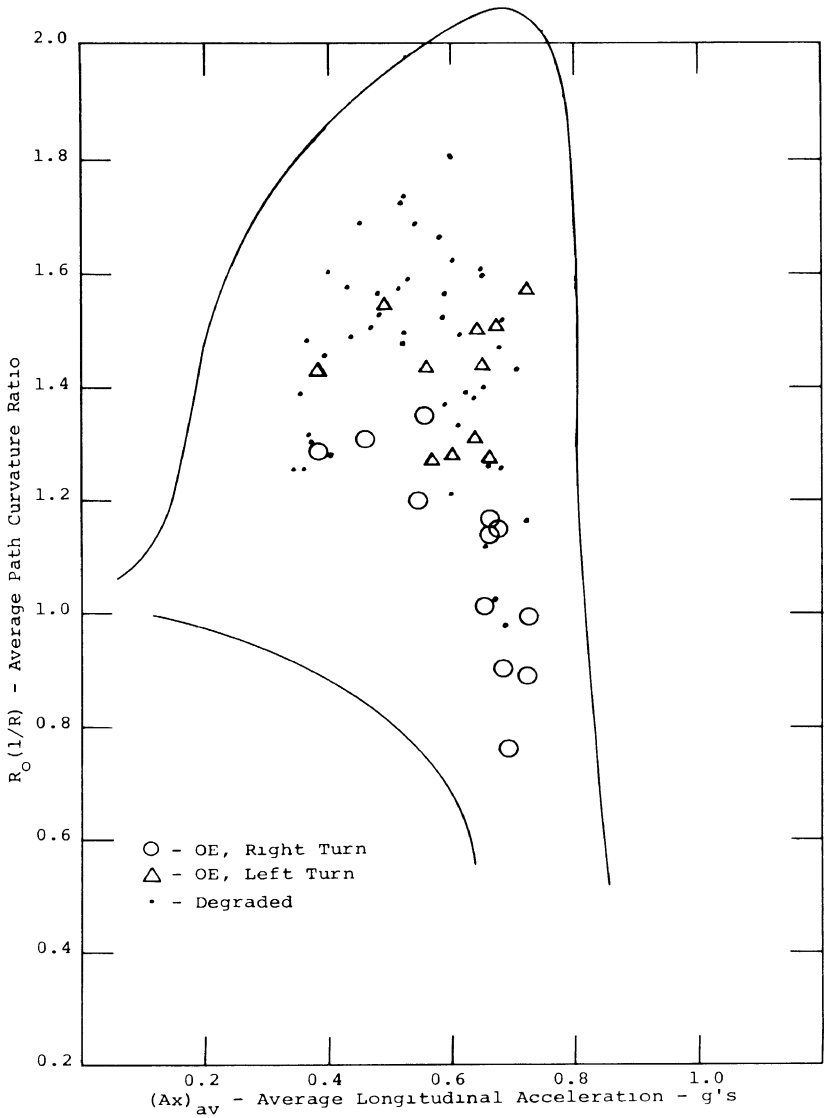

Ambassador O.E./Degraded

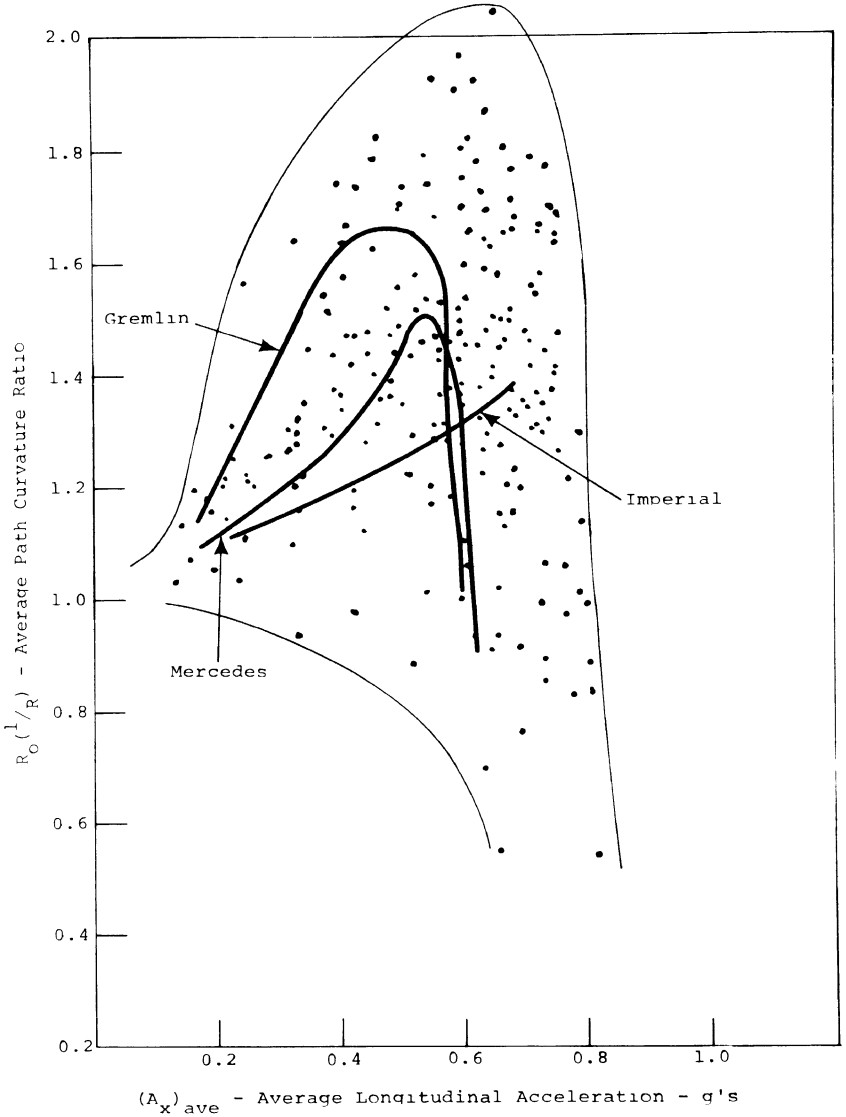

New Car Performance

Figure 5.12. Summary plot - braking in a turn

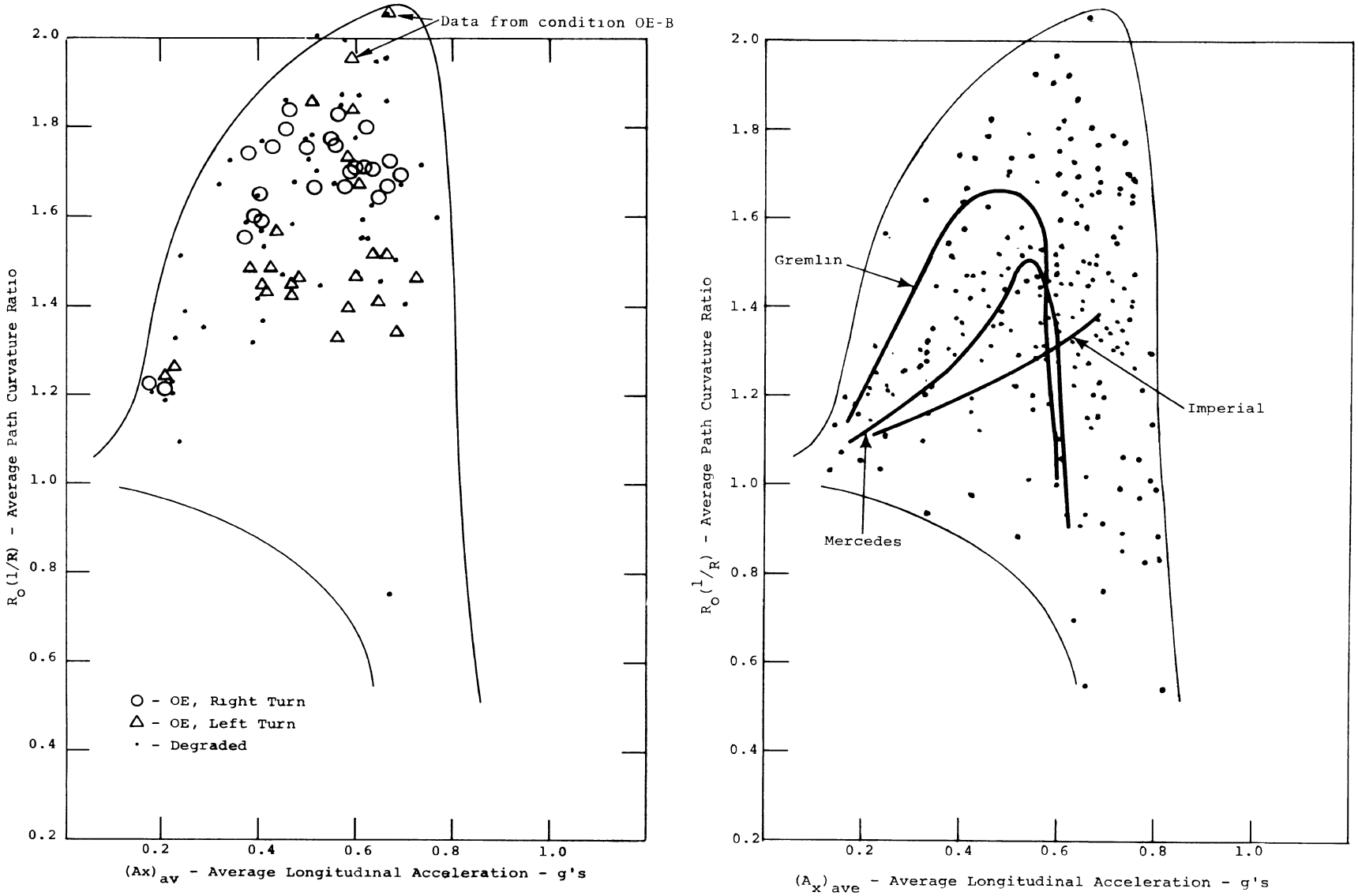

Figure 5.13. Summary plot - braking in a turn

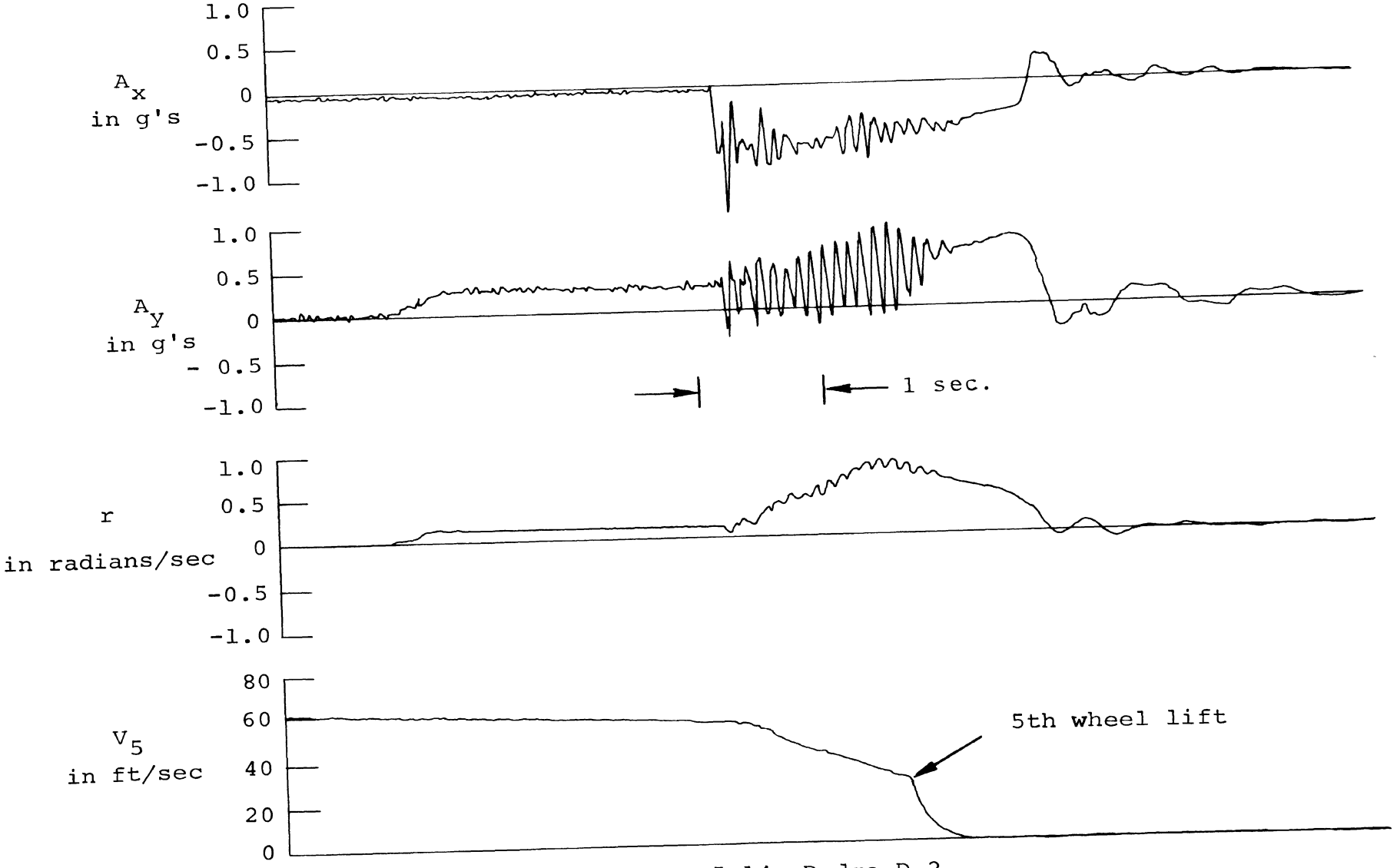

Figure 5.14 Dodge D-2
VHTP #2

No significant sensitivities to component degradation conditions D3, 4, and 5 are identified, as gauged against the Dodge O.E.-B performance, which is seen to yield two data points falling at the top of the new car envelope in Figure 5.13.

The path-curvature response of the Ambassador is summarized in Figure 5.12. Note that all of the O.E. and degraded condition data fall well within the new car performance range, although a certain positive sensitivity is indicated by a set of degraded system data above $R_o(1/R) = 1.6$. These latter data were gathered under degradation code D3, constituting lash in ball joints and tie-rod ends. These measured sensitivities appear to be spurious, however, given the insensitivity of performance to degradation code D4, which combined the ball-joint and tie-rod-end degradations with looseness in the steering gear and in the wheel bearings. Laboratory measurements have shown the latter two lash conditions to contribute a total level of steer-angle indeterminacy that is comparable to the sum of the ball-joint and tie-rod-end contributions. Thus, the small increase in normalized path curvature noted in the condition D3 data is viewed as an artifact of the test process, which artifact is, firstly, of small proportions, secondly, not rationalizable with the other data produced by the Ambassador, and thirdly, not in concurrence with the responses exhibited by the Dodge.

5.3.3 ROADHOLDING IN A TURN. The directional response of a vehicle to the traversal of the road roughness course, with the vehicle being initially in a steady turn, is evaluated in terms similar to those which are applied to the braking-in-a-turn data. The path curvature response of the vehicle is examined by means of a normalized numeric, $R_o(1/R)_{ave}$, which indicates the relative deviation in path curvature (with respect to the initial steady-state value) exhibited

during the one-second traversal of the disturbance grid. Whereas this measure is sensitive to loss in tire side forces (as derives from wheel-hop oscillations imposed by contact with the fixed disturbances) being predominant at the front wheels, another measure is provided to indicate the sideslip response that arises when losses dominate on the rear tire. This second measure, peak sideslip rate, $\dot{\beta}_p$, is interpreted also, in this maneuver, to represent a driver challenge factor, characterizing directional instability and an imminent disorientation of the driver and his vehicle with respect to the direction of travel.

Path-curvature response data obtained for the Dodge and Ambassador are summarized in Figures 5.16 and 5.17. Both of these plots indicate a general insensitivity of path-curvature performance to the degradation modes considered, as evidenced by the path curvature measure, $R_o(1/R)_{ave}$, where a value of unity represents perfect path retention. The reductions in path curvature observed for the Dodge, at excitation frequencies of 9 and 11 Hz, indicate a somewhat degraded performance for condition D2 (i.e., four shock absorbers are degraded). Likewise the decreased performance levels exhibited by the Ambassador at 9 and 14 Hz (see Fig. 5.16) indicate a certain sensitivity to the D2 condition. Additionally, responses produced by the Ambassador in condition D3 (i.e., degraded ball joints and tie-rod ends), show a small reduction in $R_o(1/R)_{ave}$, on the order of 0.05 below the O.E. baseline data.

To place these findings in perspective, however, it must be noted that the spread in Dodge baseline and Ambassador baseline data are large, in both cases spanning a range of values which are substantially larger than the relative reductions in performance produced by the above-defined

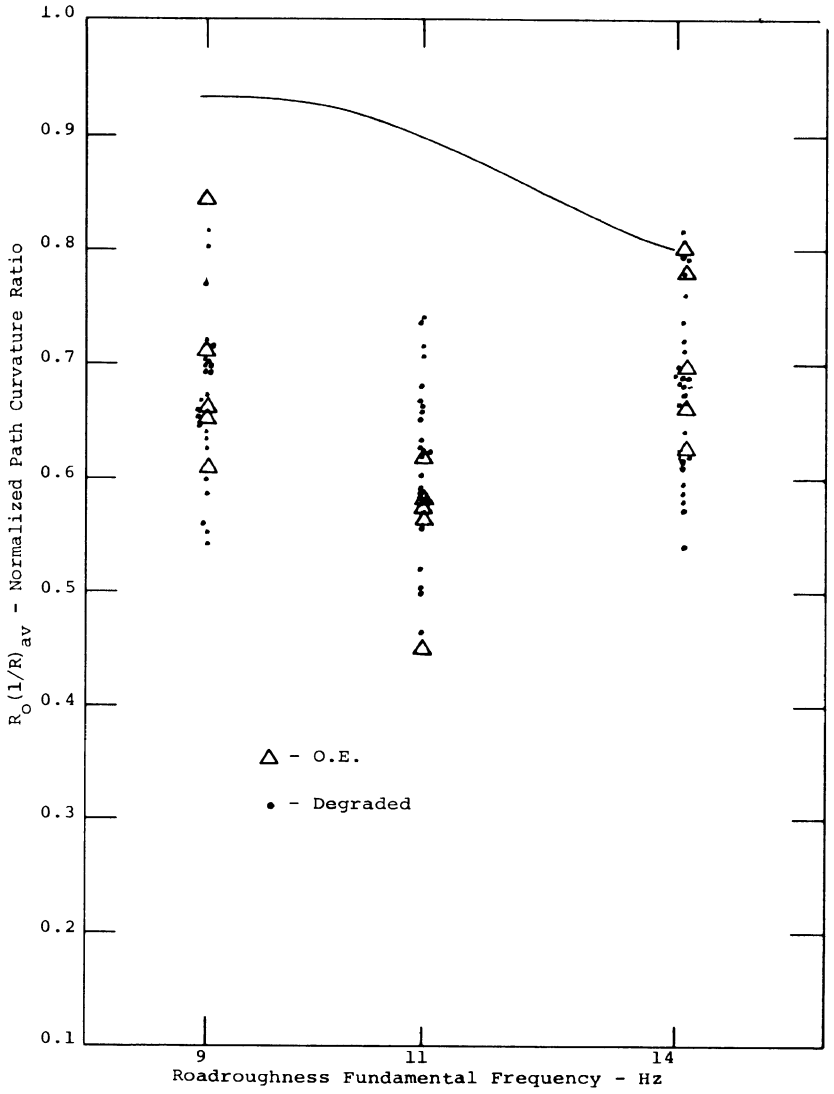

Ambassador O.E./Degraded

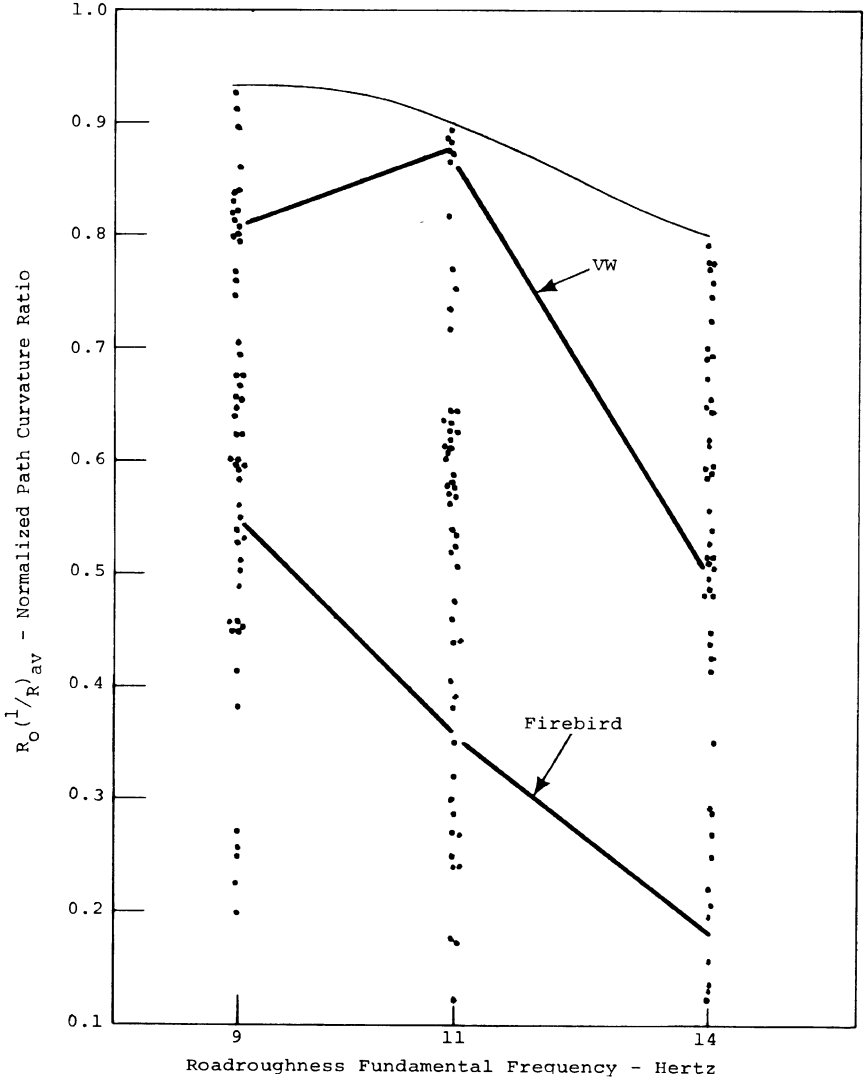

New Car Performance

Figure 5.16. Summary plot - roadholding in a turn

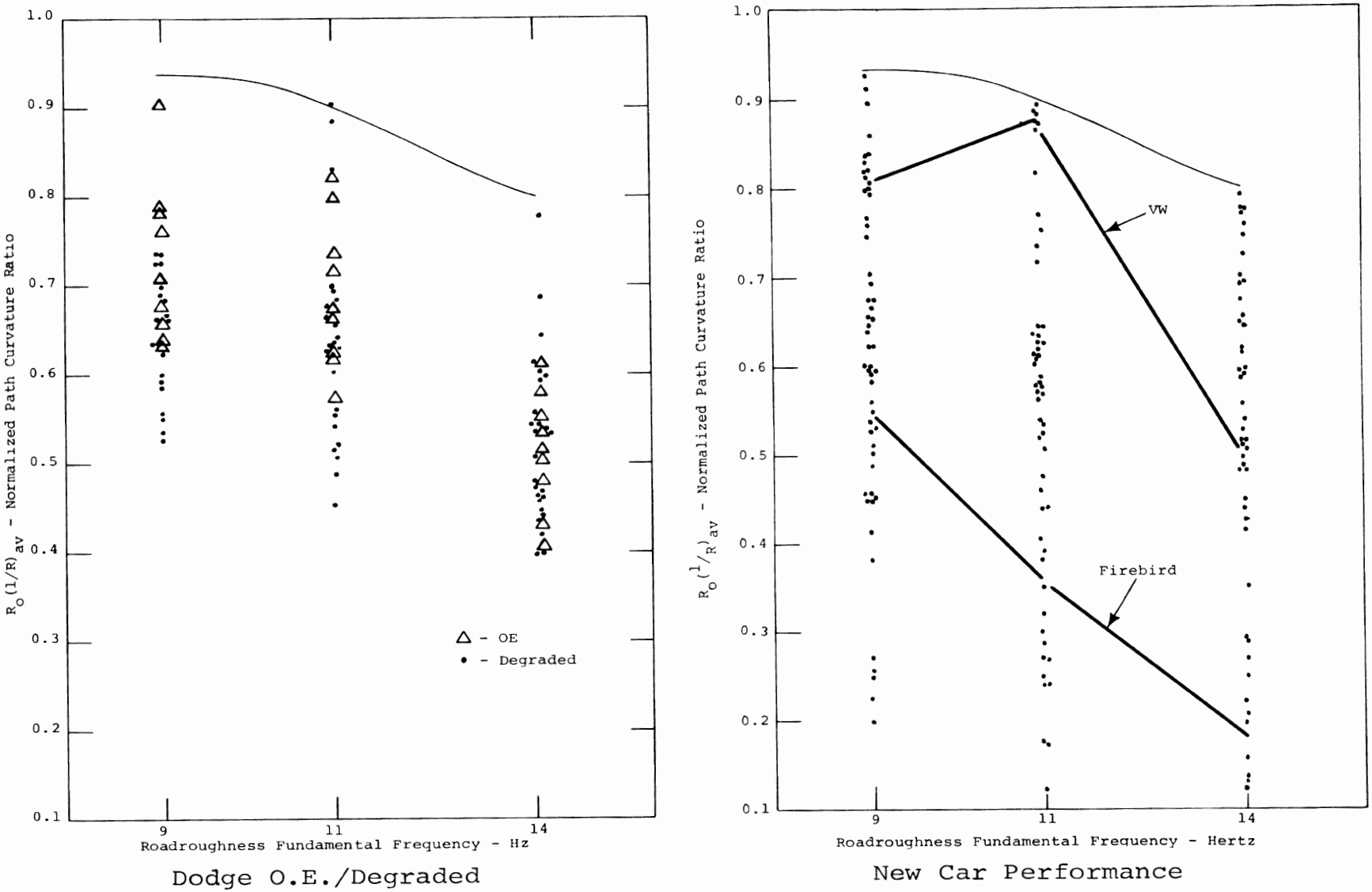

Figure 5.17. Summary plot - roadholding in a turn

degraded conditions. Also, it should be observed that the range of roadholding performance exhibited by new cars is immense and covers almost the entire definable range, with certain new vehicles indicating responses which fall below the 0.1 level of normalized path curvature.

Clearly, however, the roadholding sensitivity to shock absorber degradation is a finding which is solidly supported in vehicle mechanics. The level of the indicated sensitivity is certainly related to the equivalent reduction in damping forces that derived from the mode of shock absorber degradation which was implemented. Thus a degradation in damping forces of substantially greater dimension than was achieved by wearing the rod guide and fracturing the valve disc would be expected to reduce path curvature performance considerably further.

Figures 5.18 and 5.19 summarized the sideslip numerics, produced by the two test vehicles in the roadholding maneuver. These relatively low $\dot{\beta}$ values indicate that neither of these test vehicles was exhibiting dominant loss in tire side force at the rear wheels, in either the O.E. or the degraded conditions. It must be noted, however, that these plots do not indicate as general vehicle property as do the 1/R data. Clearly, the question of whether any degradation mode will influence sideslip response markedly, while encountering road roughness, is related entirely to the distribution of side force losses, and not to the overall side force level which prevails. Thus the dominance in loss of side force at the front tires on both test vehicles merely indicates that no major findings can be obtained from the $\dot{\beta}_p$ measures produced by these vehicles.

Although some increase in $\dot{\beta}_p$ is seen in the 14 Hz data yielded by the Dodge and Ambassador in condition D2, it is felt that these data merely reflect the same shock absorber degradation sensitivity as was exposed in the 1/R measures,

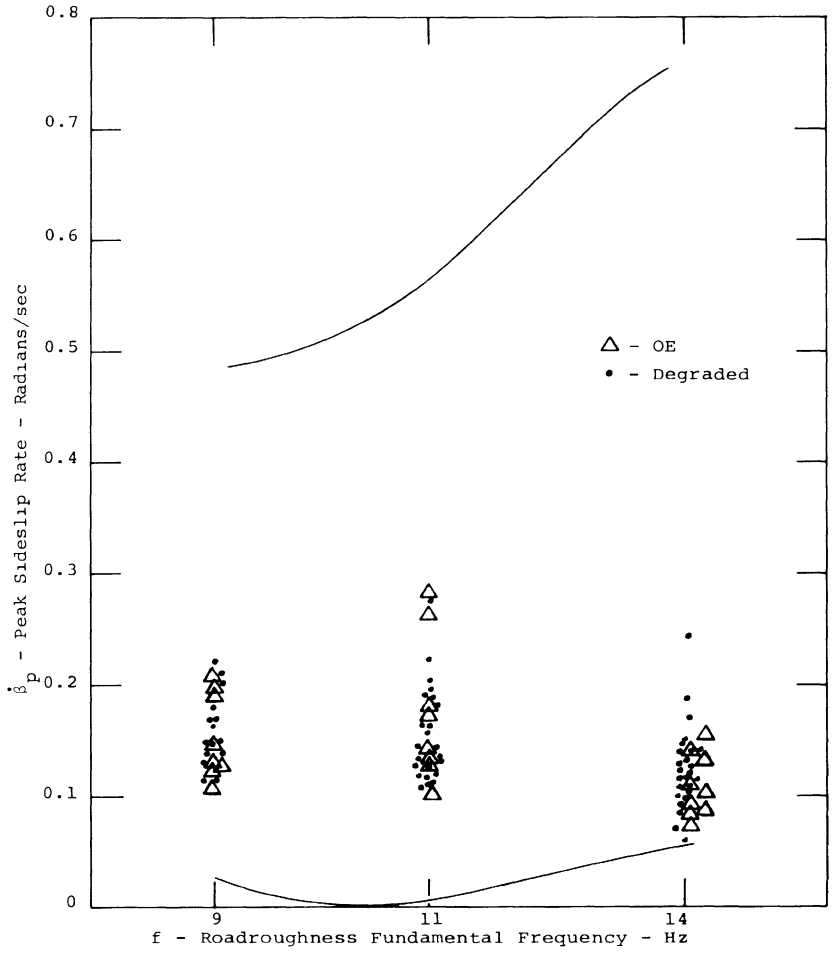

Ambassador O.E./Degraded

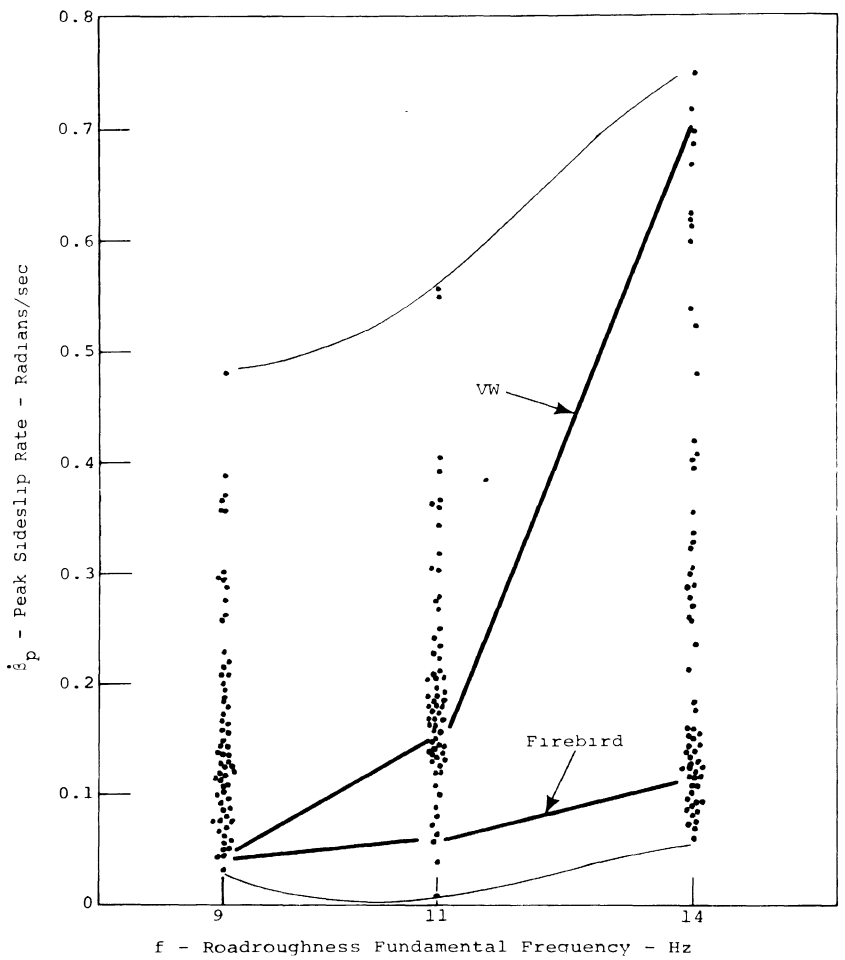

New Car Performance

Figure 5.18. Summary plot - roadholding in a turn

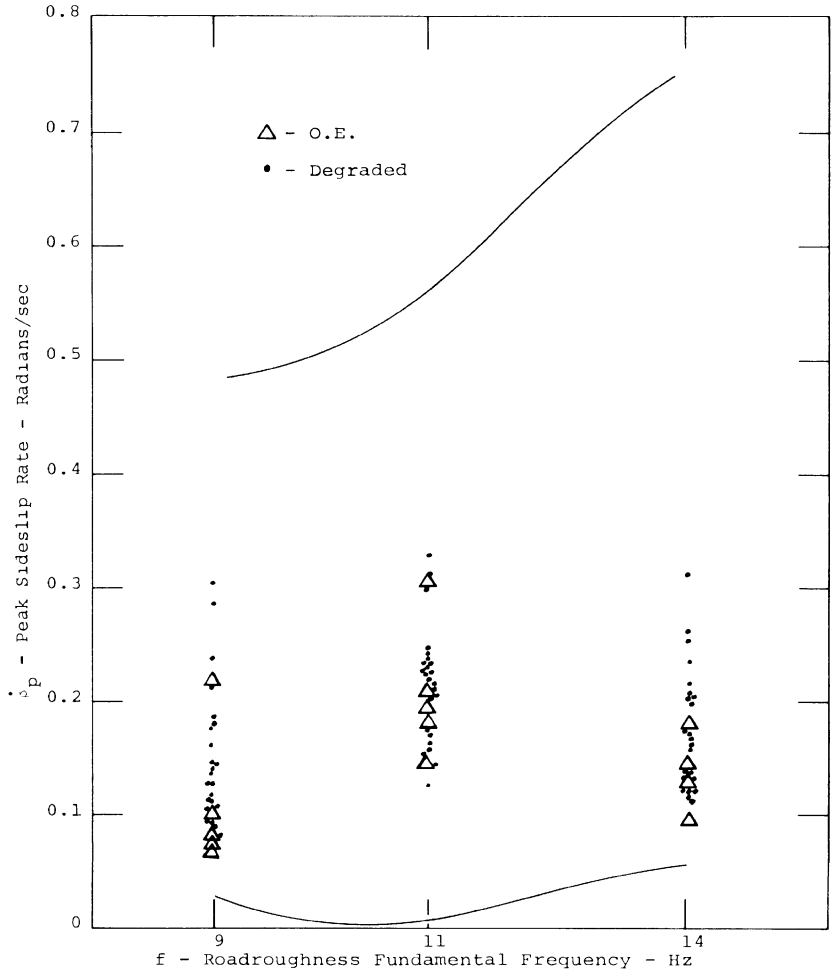

Dodge O.E./Degraded

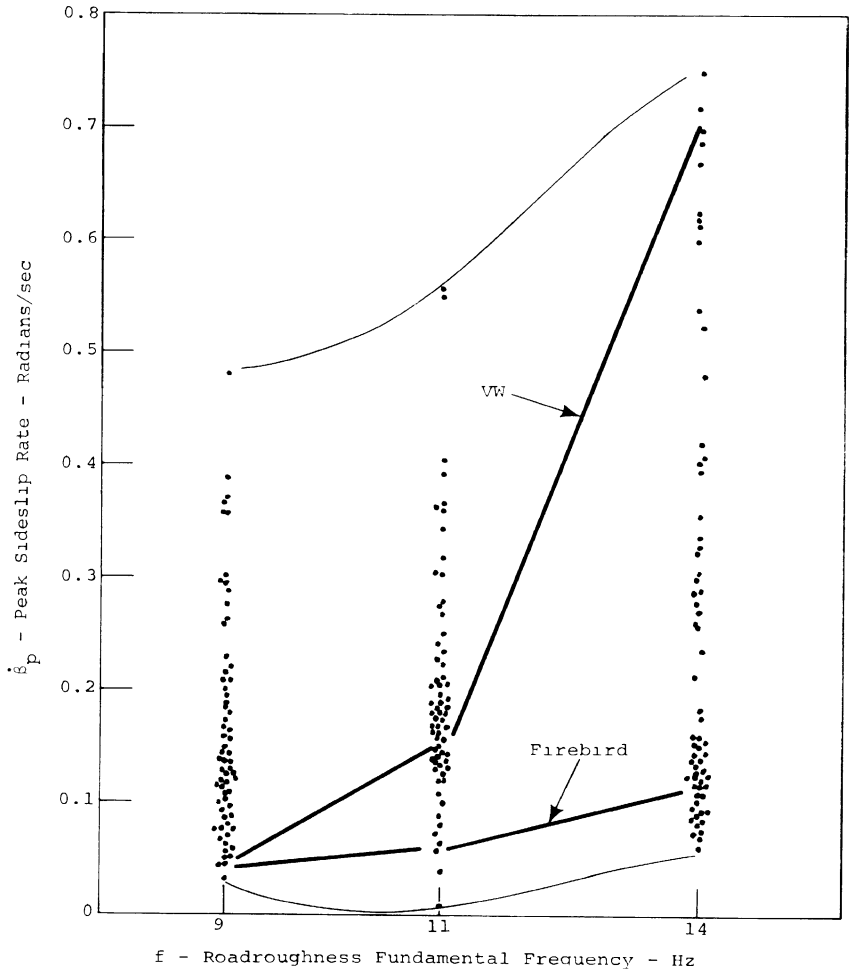

New Car Performance

Figure 5.19. Summary plot - roadholding in a turn

and that the two test vehicles did not happen to provide a very discriminating medium for applying the $\dot{\beta}_p$ measure in the roadholding test.

5.3.4 TRAPEZOIDAL STEER. This test examines limit-turning performance, as characterized by path-curvature and sideslip responses. The path-curvature response in this maneuver is presented as a numeric which averages 1/R over a 2-second period following initiation of steering and ratioes this value to that value of path curvature which would derive from a 1 g steady turn at 40 mph, thereby obtaining a convenient scale. As steering level is increased on successive runs, this measure indicates the gain in vehicle turning performance, consolidating dynamic response with static steering effectiveness by a time-averaging process.

In Figures 5.20 and 5.21, this measure, labelled $R_s(1/R)_{ave}$, is plotted against the steer increment, σ', for both test vehicles. Clearly, the Dodge and Ambassador fall in the middle of the performance spectrum exhibited by other vehicles in this maneuver. Further, their sensitivity to component degradation is negligible according to this presentation. Likewise, Figures 5.22 and 5.23, constituting summary cross plots of the $R_s(1/R)_{ave}$ measure with a $\dot{\beta}_p$ numeric, do not indicate a significant degradation in performance across the matrix of degraded conditions. Rather, substantial reductions in $\dot{\beta}_p$ values are observed on the Dodge at the higher levels of path curvature, suggesting that certain mechanisms have prevailed in balancing front-to-rear tire forces such that lower net sideslip takes place in achieving a limit-turning response.

The insensitivity of vehicle response to component degradation in this maneuver is felt to derive from the "swamping" effects of tire-side-force saturation. When four equally inflated tires are cornering at or near their shear force limits, the forces generated are determined, to first order, simply by vertical load. It follows that the apparent

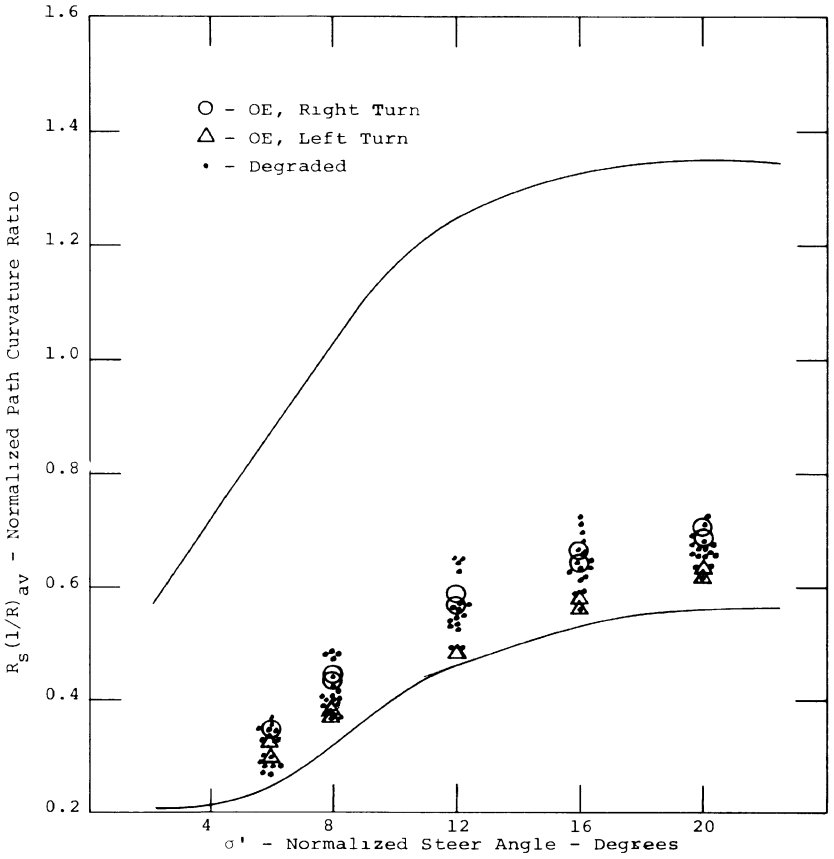

Ambassador O.E./Degraded

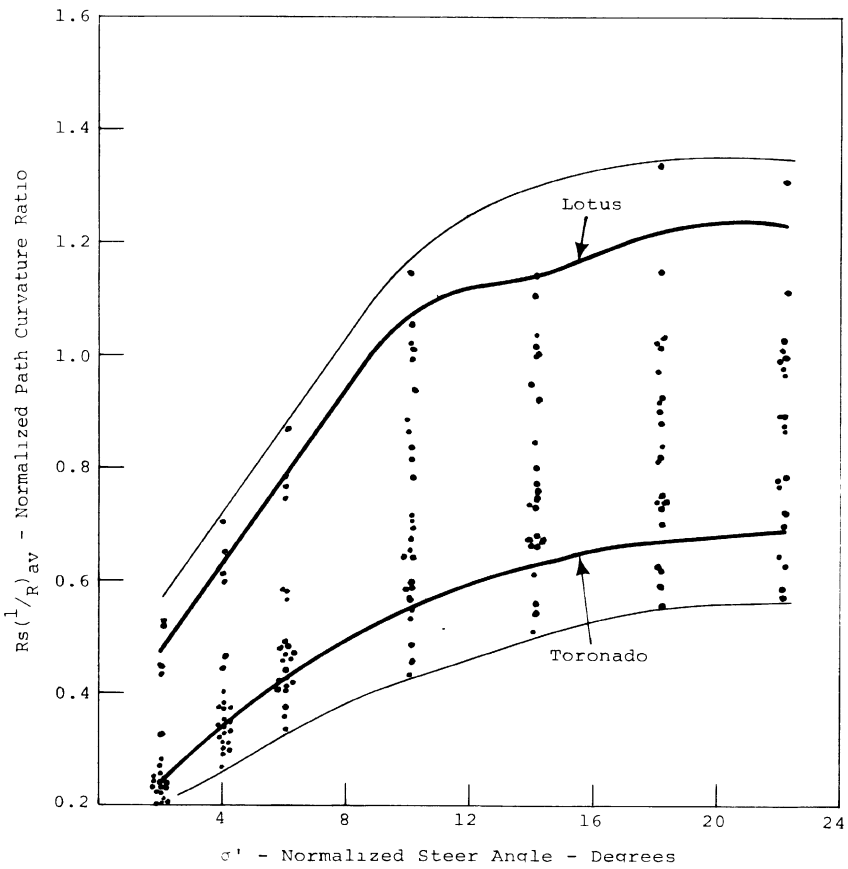

New Car Performance

Figure 5.20. Summary plot - trapezoidal steer

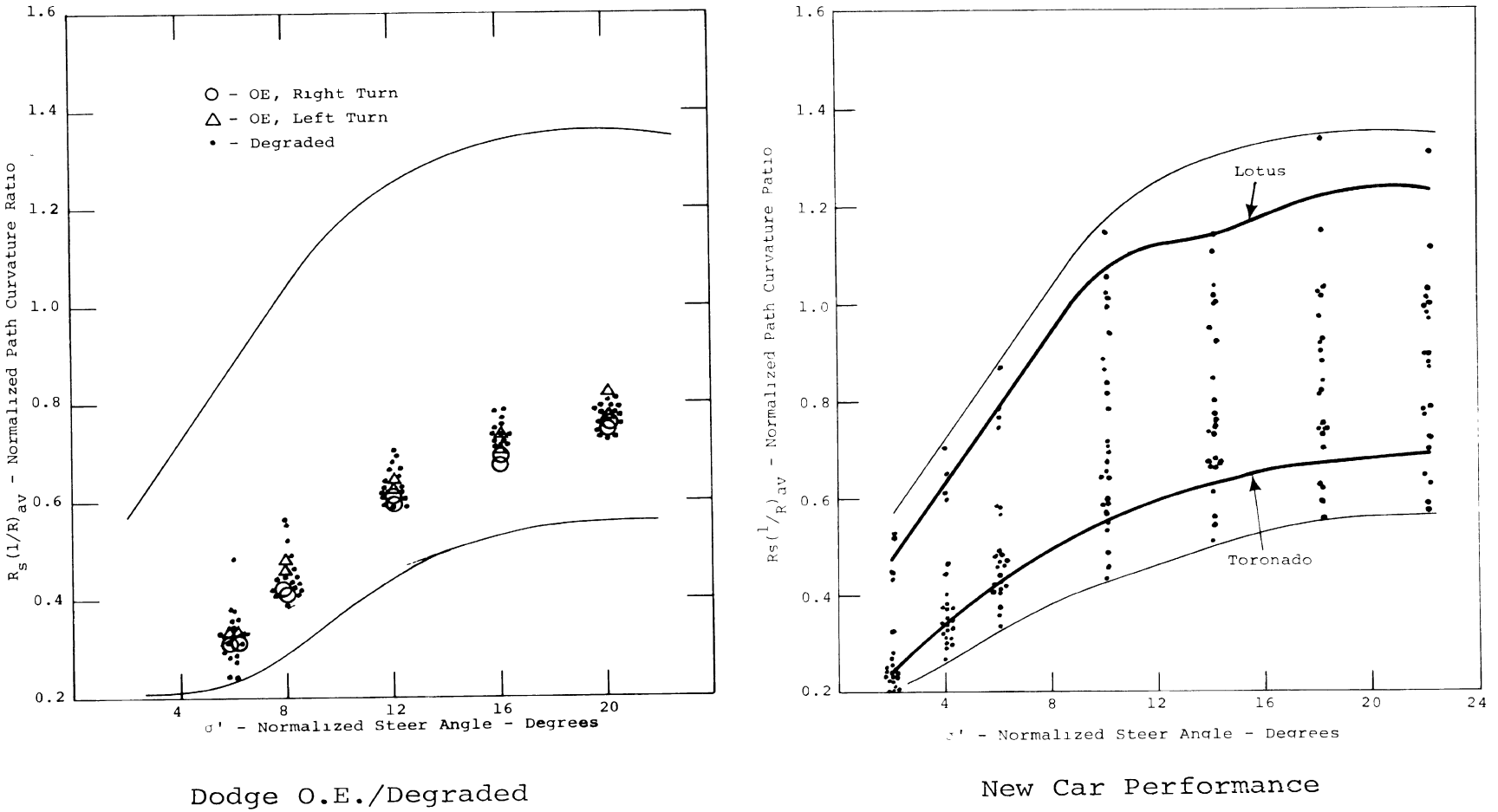

Dodge O.E./Degraded

New Car Performance

Figure 5.21. Summary plot - trapezoidal steer

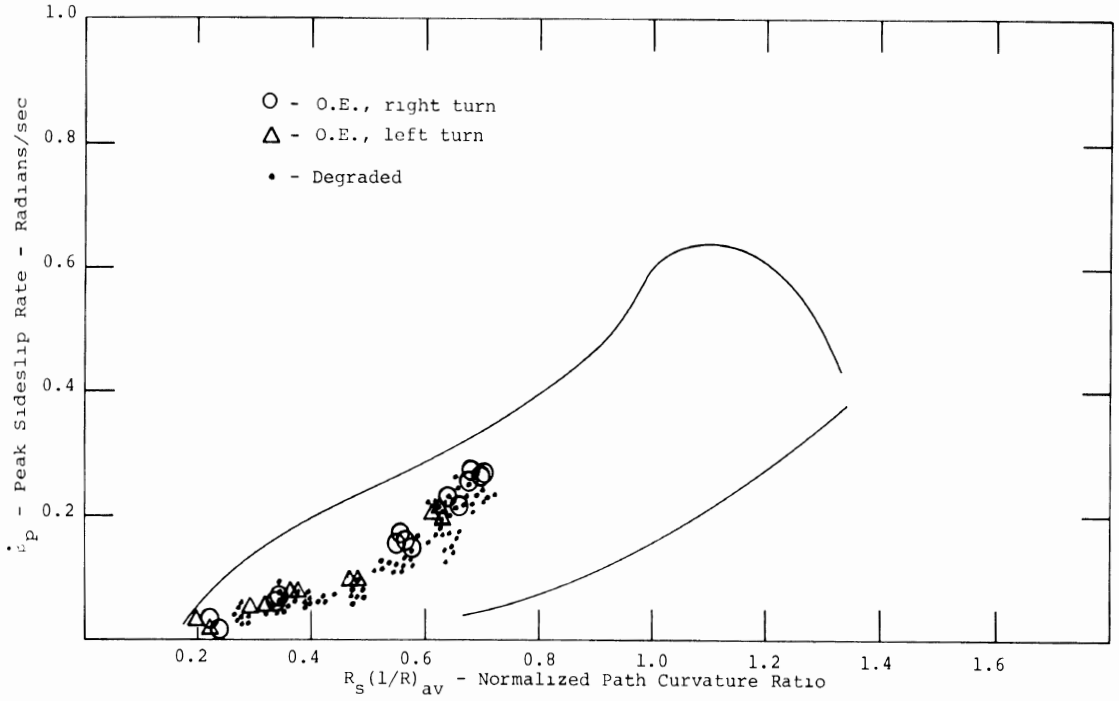

Ambassador O.E./Degraded

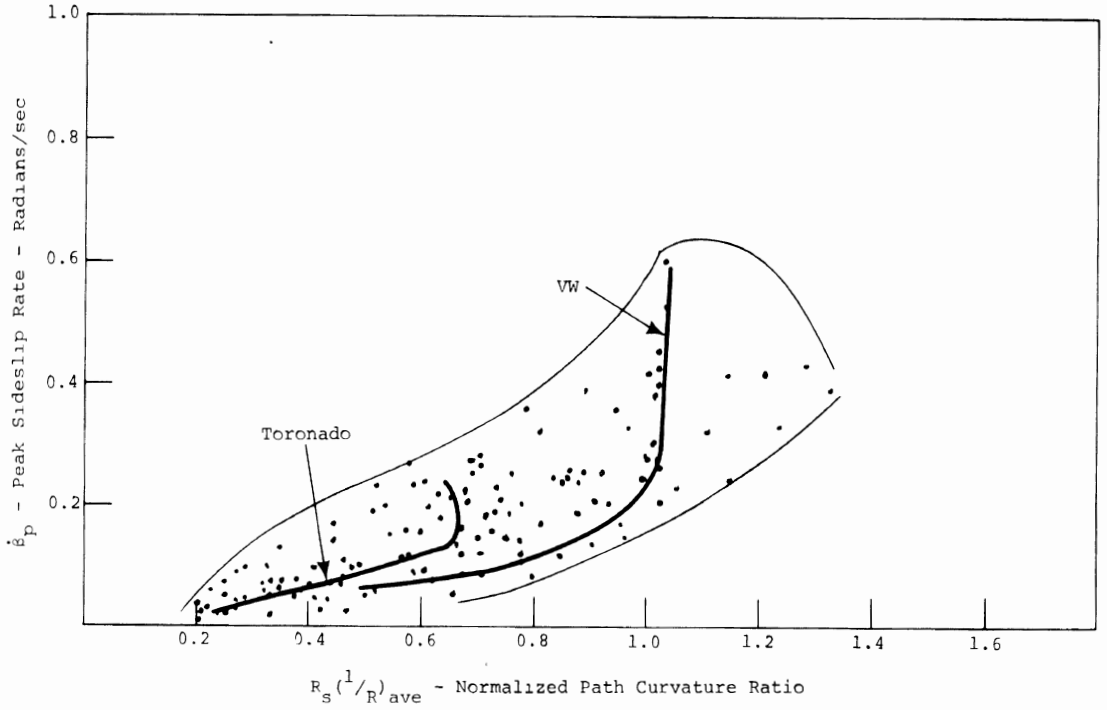

New Car Performance

Figure 5.22. Summary plot - trapezoidal steer

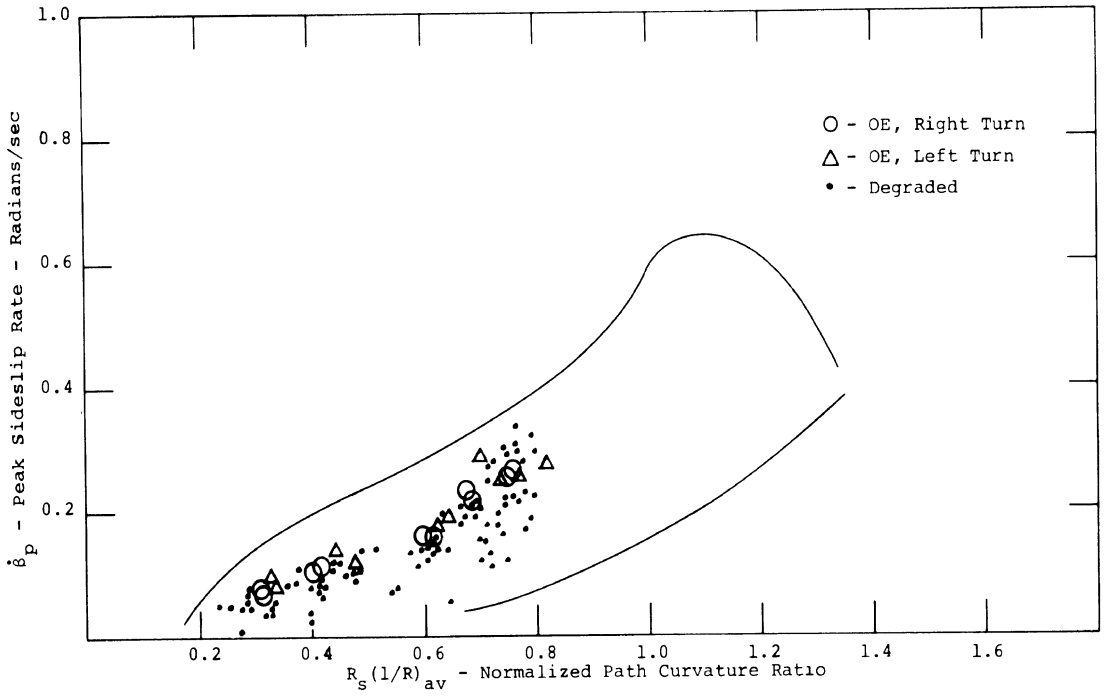

Dodge O.E./Degraded

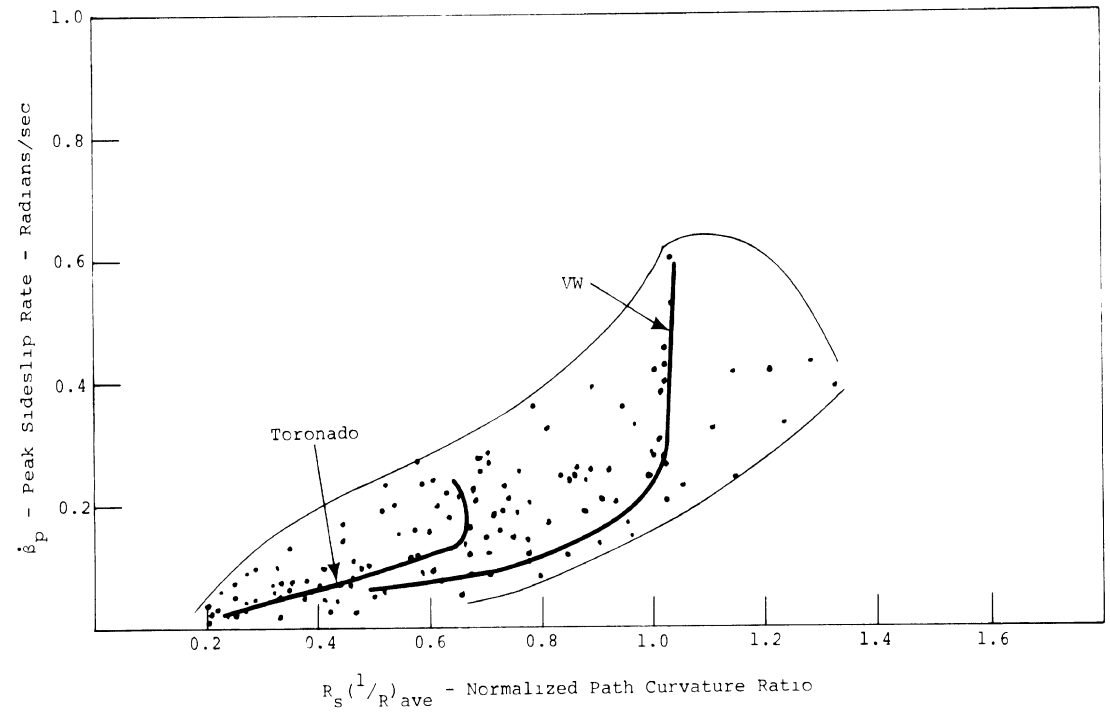

New Car Performance

Figure 5.23. Summary plot - trapezoidal steer

insensitivity of limit turning performance to degradation of steering and suspension components derives from the corresponding insensitivity of tire vertical loads (quasi steady-state) to the degradations which were considered.

5.3.5 SINUSOIDAL STEER. The sinusoidal-steer input elicits a complex array of responses among different vehicles. The lane change-like quality of a vehicle's response to a symmetric sine wave input can be viewed as a lateral-displacement response, in inertial coordinates, in combination with a heading-angle response. The perfect lane change is defined as a 12-foot lateral displacement which is accompanied by zero net deviation in heading angle. The lateral displacement response is evaluated through a computed measure called "lane change deviation," Δ. This measure is defined by an integral error term operating on the lateral displacement time history y(t) (see Fig. 5.24), viz.,

$$\Delta = \frac{\int_0^{3.4} |12-y|\,dt}{3.4}$$

Note that the numeric, Δ, has units of feet, and thus represents an average deviation from the desired 12-foot lateral displacement as determined over a computation time of 3.4 seconds.

Figures 5.25 and 5.26 present the values of Δ which were obtained as steering amplitude, σ, was incremented on both test vehicles in tests covering all degradation conditions. Significant changes are noted in the lane change deviation produced by both vehicles in degradation codes A3 and A4, with the Dodge exhibiting a large change in this measure at a

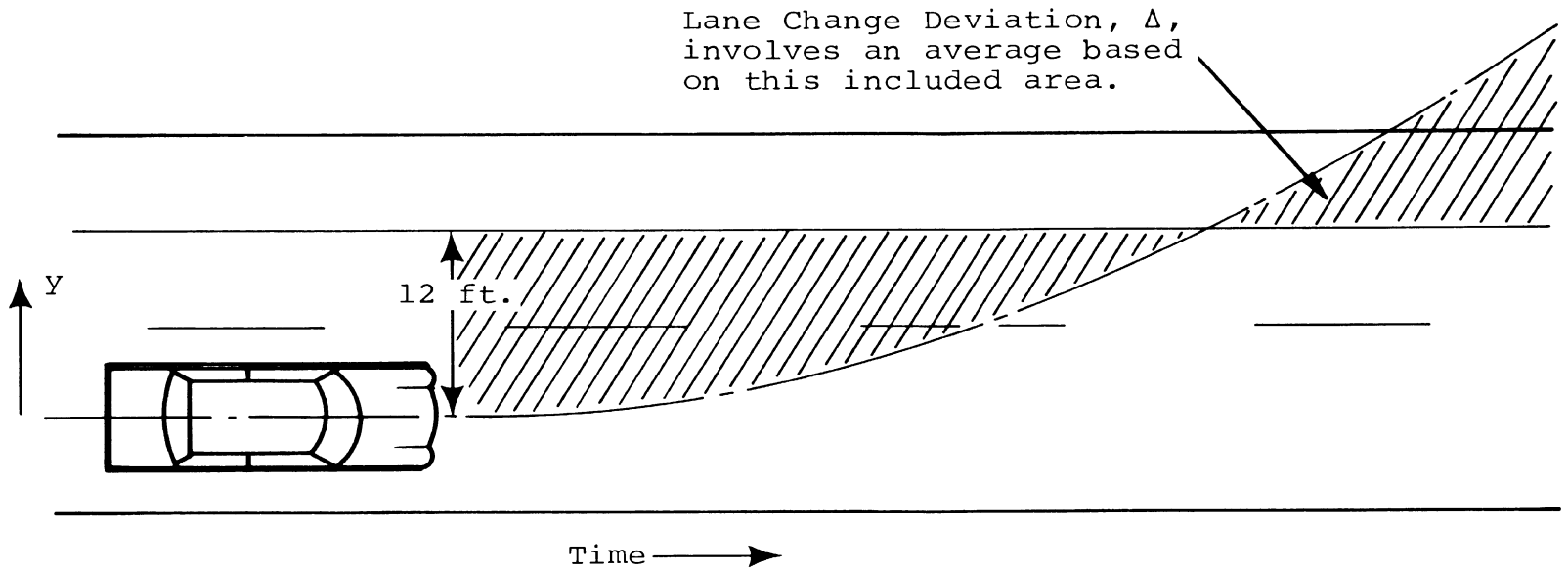

FIGURE 5.24
Open Loop y(t) Time History to Sine Steer Input

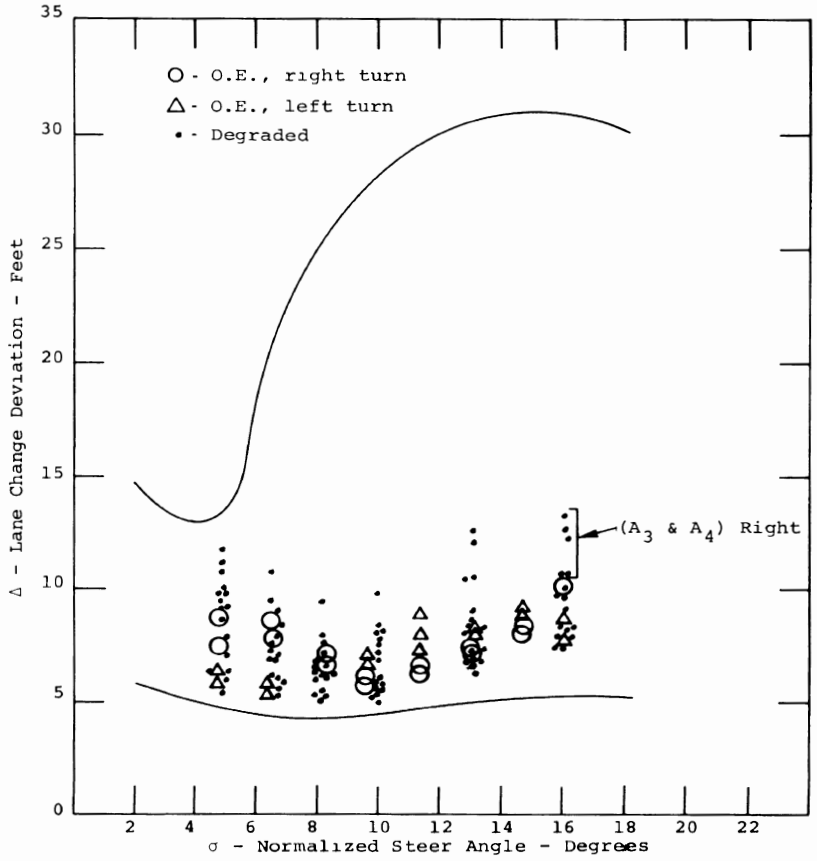

Ambassador O.E./Degraded

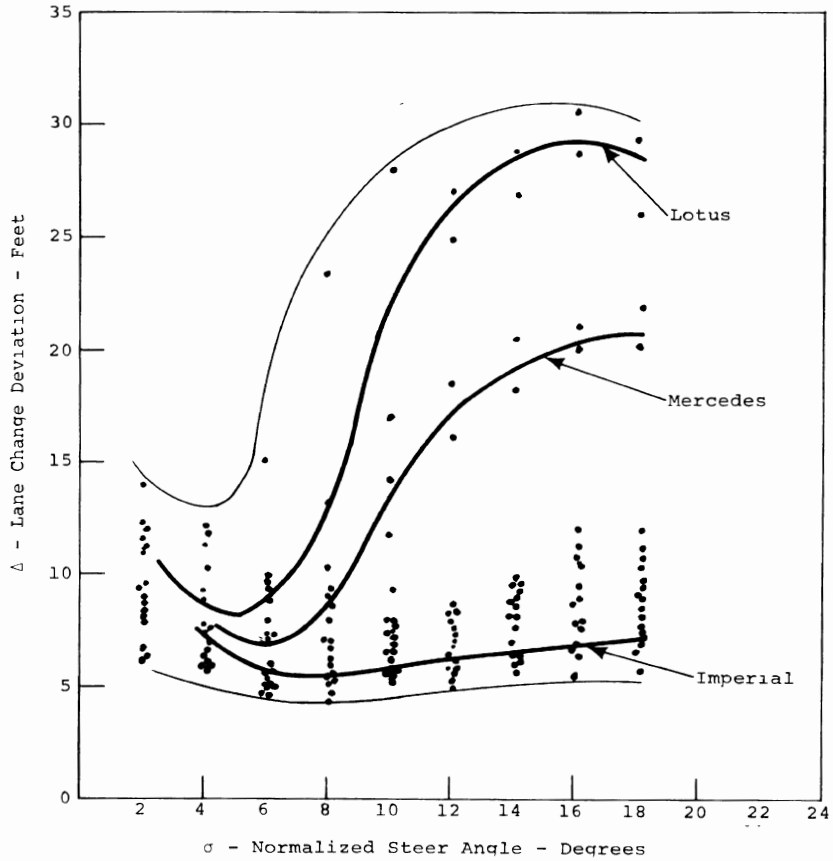

New Car Performance

Figure 5.25. Summary plot - sinusoidal steer - 60 mph

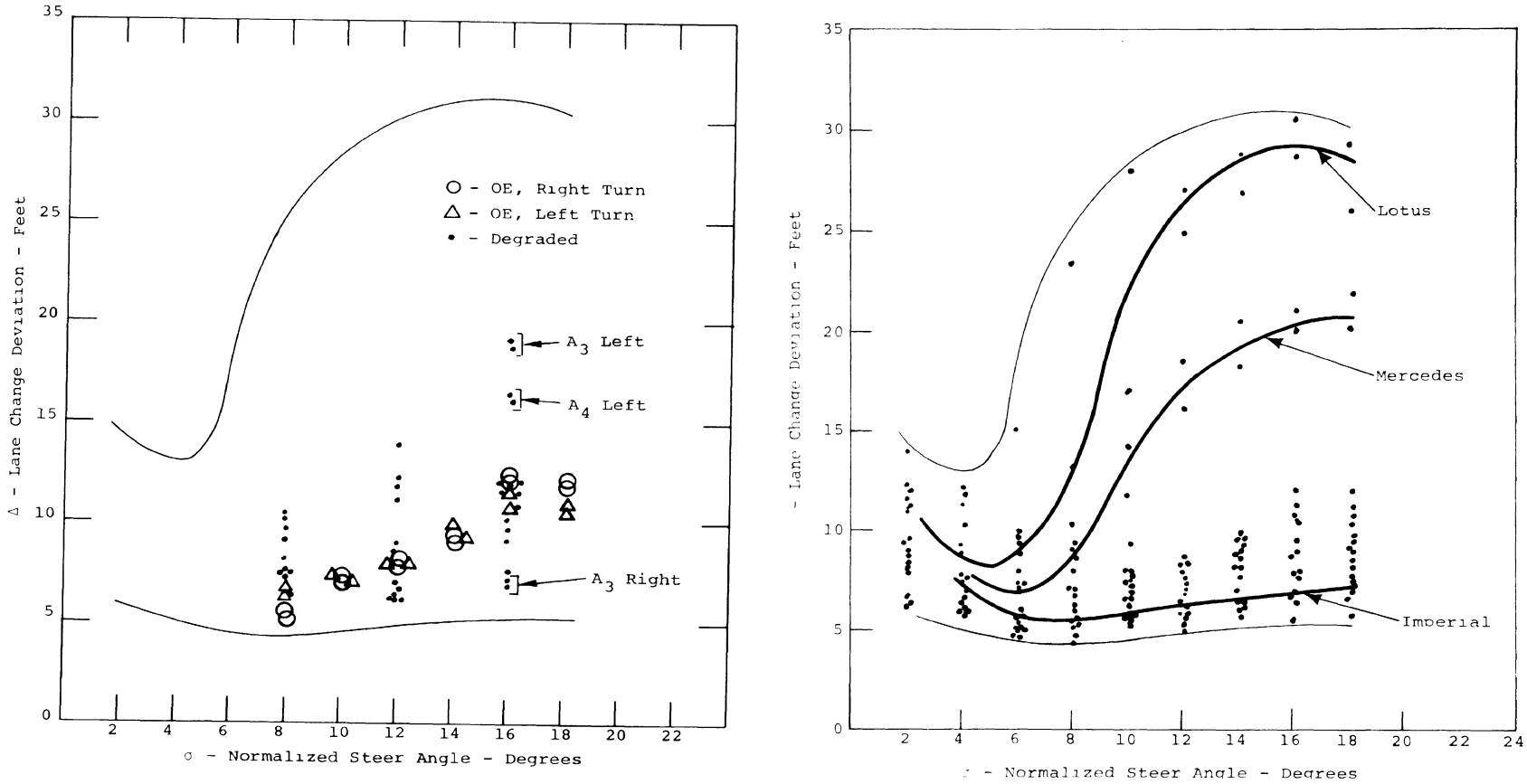

Dodge O.E./Degraded

New Car Performance

Figure 5.26. Summary plot - sinusoidal steer - 60 mph

steer level of σ = 16. Note the designations of "A3 left" and "A3 right" which indicate that a marked asymmetry in performance is caused by the front-wheel-misalignment condition. This asymmetry of response to the sinusoidal steering input which is of the "initially left" variety, as opposed to "initially right" is graphically portrayed by the time histories shown in Figure 5.27. Several points of significance can be drawn from this figure. First, note that run 5081 indicates a sustained turning response long after the steering input has terminated, as evidenced by the terminal portions of the time histories in A_y and r. Conversely, run 5080 indicates a recovery of zero yaw rate response with a net heading angle that is essentially zero. The asymmetry in the lane change deviation measure clearly results from the differences in the time histories of lateral displacement, y, with run 5081 showing the trajectory crossing back over the initial lane, thus registering a relatively low value of Δ, while run 5080 shows a diverging lateral displacement which accounts for the high level of Δ. A similar example of this anomaly, as exhibited by the Ambassador, is shown in Figure 5.28 in which the A3 degradation is seen to emphasize asymmetry in directional response. On the weight of the Δ measure alone, one would be led to conclude that the response to the "initially right" sine input, as shown by the Dodge, is "better" or less demanding on the driver than the response to the "initially left" input which resulted in a high value of Δ. Clearly, this measure is insufficient for characterizing all of the safety relevant properties of the indicated responses, given that a low value of Δ was produced by a response involving a near spinout. Yawing response is characterized in this maneuver by measurement of the peak sideslip angle, β_p, and by the net deviation in heading angle, $\Delta\psi$. Figures 5.29 and 5.30 show summary plots of the β_p numerics produced by both test vehicles. With

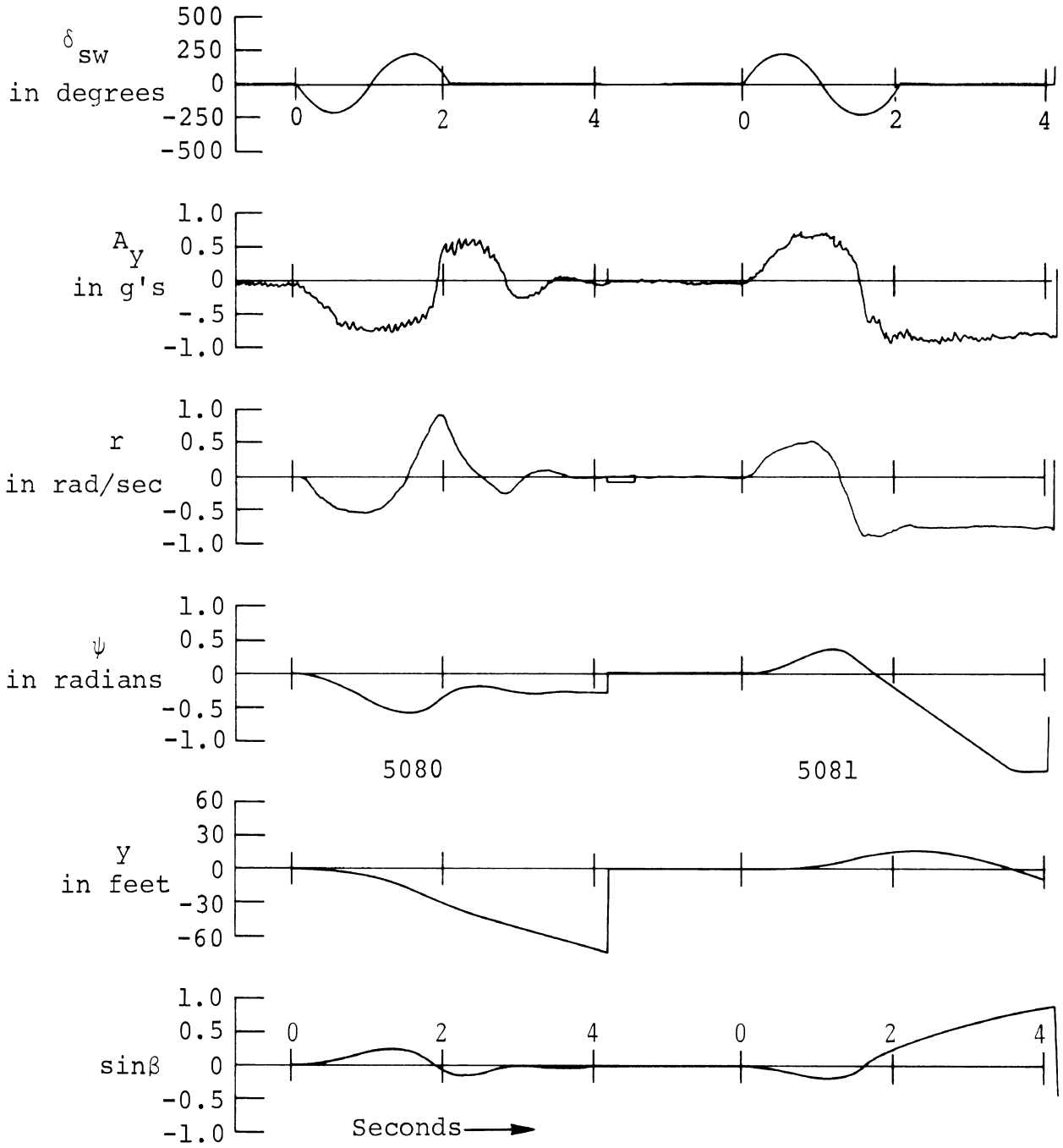

Figure 5.27 Dodge A3
VHTP #5
samples 5080 and 5081

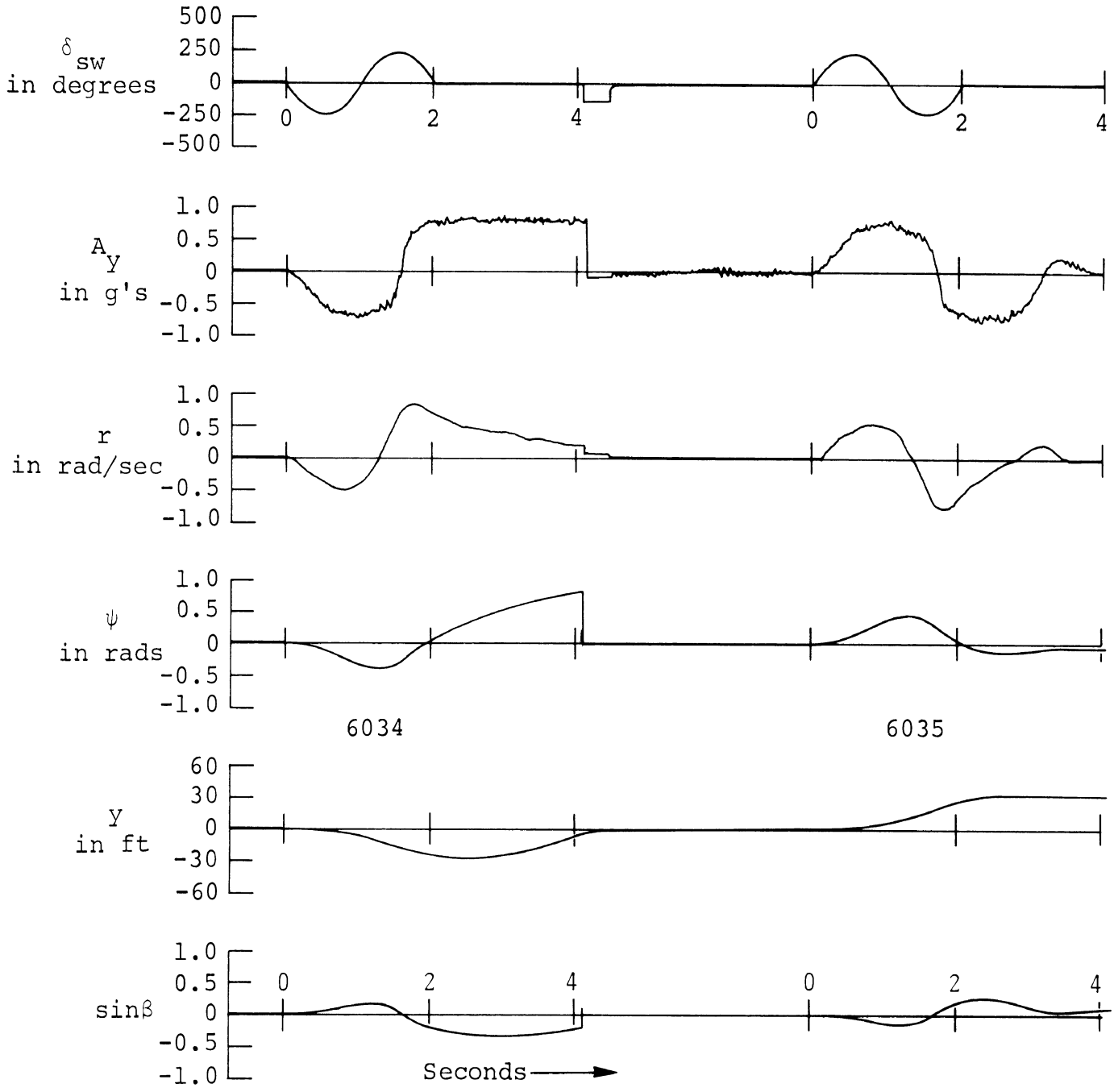

Figure 5.28 Amabssador - A3
VHTP #5
samples 6034 and 6035

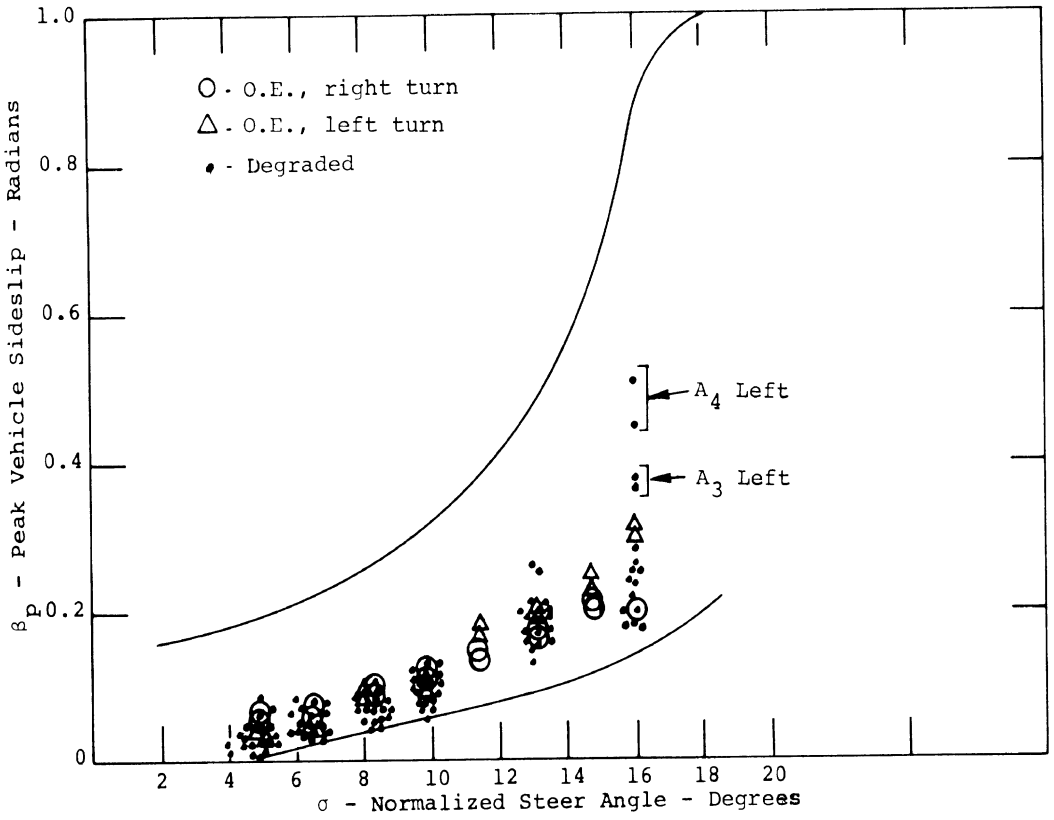

Ambassador O.E./Degraded

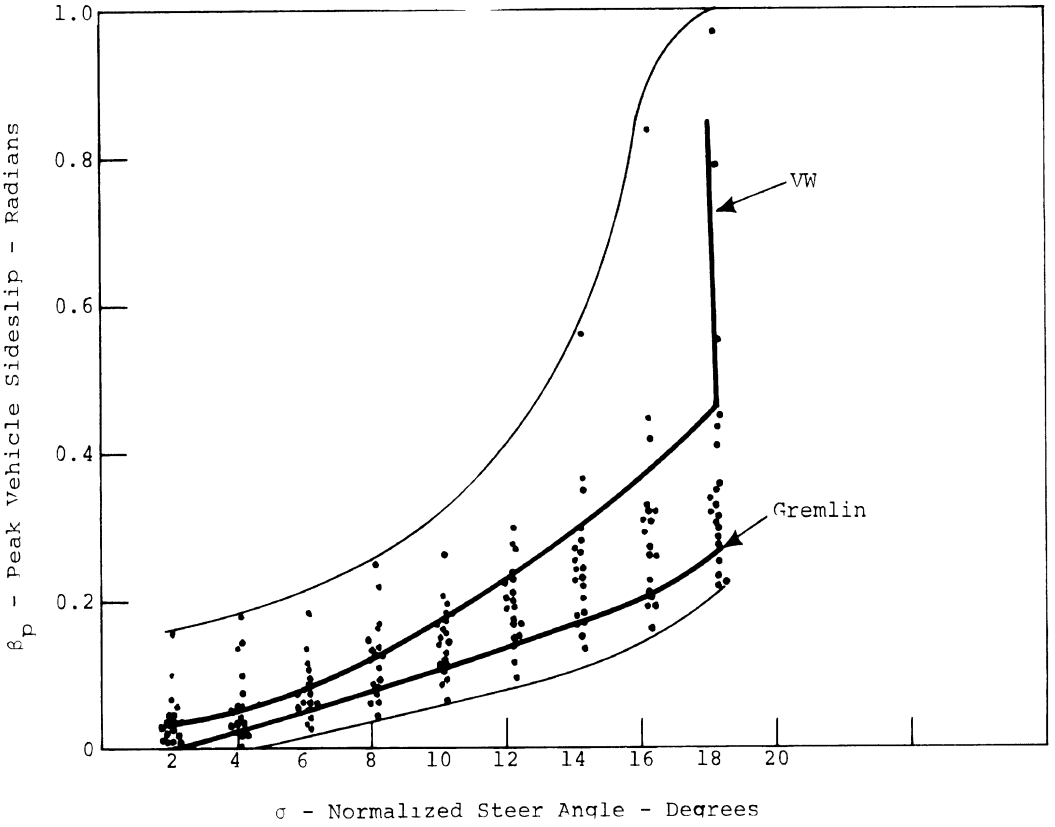

New Car Performance

Figure 5.29. Summary Plot - Sinusoidal Steer, 60mph

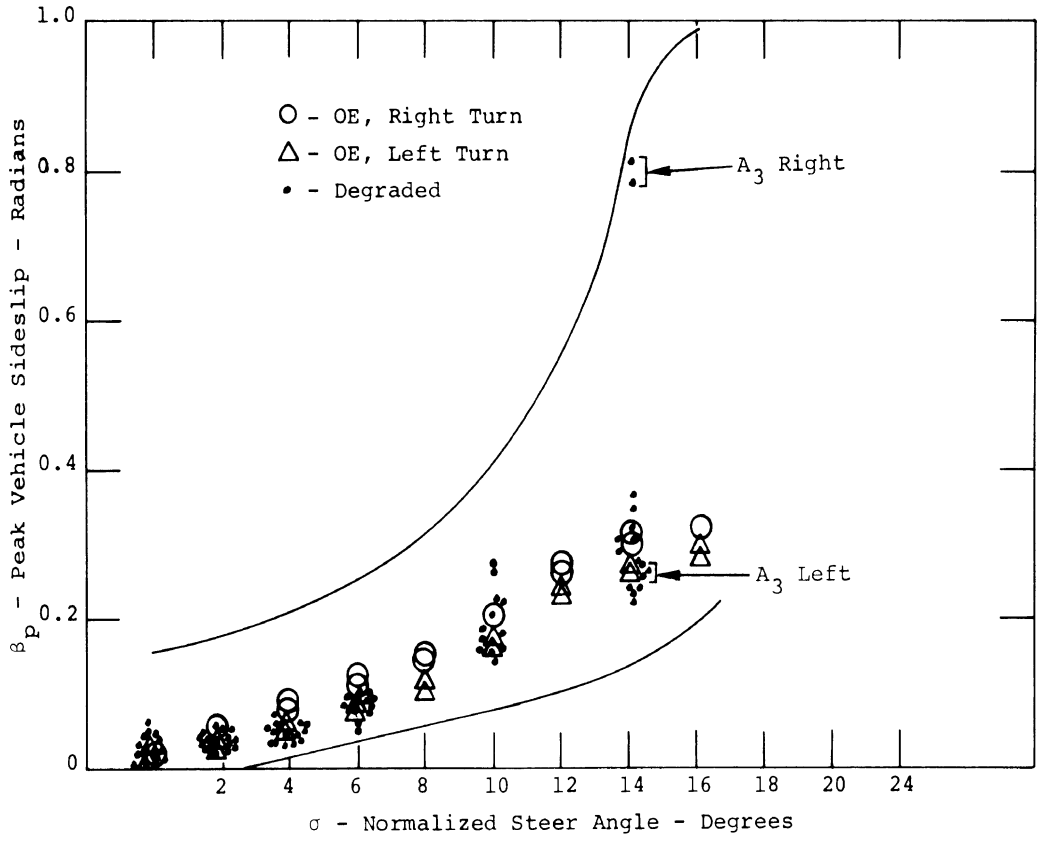

Dodge O.E./Degraded

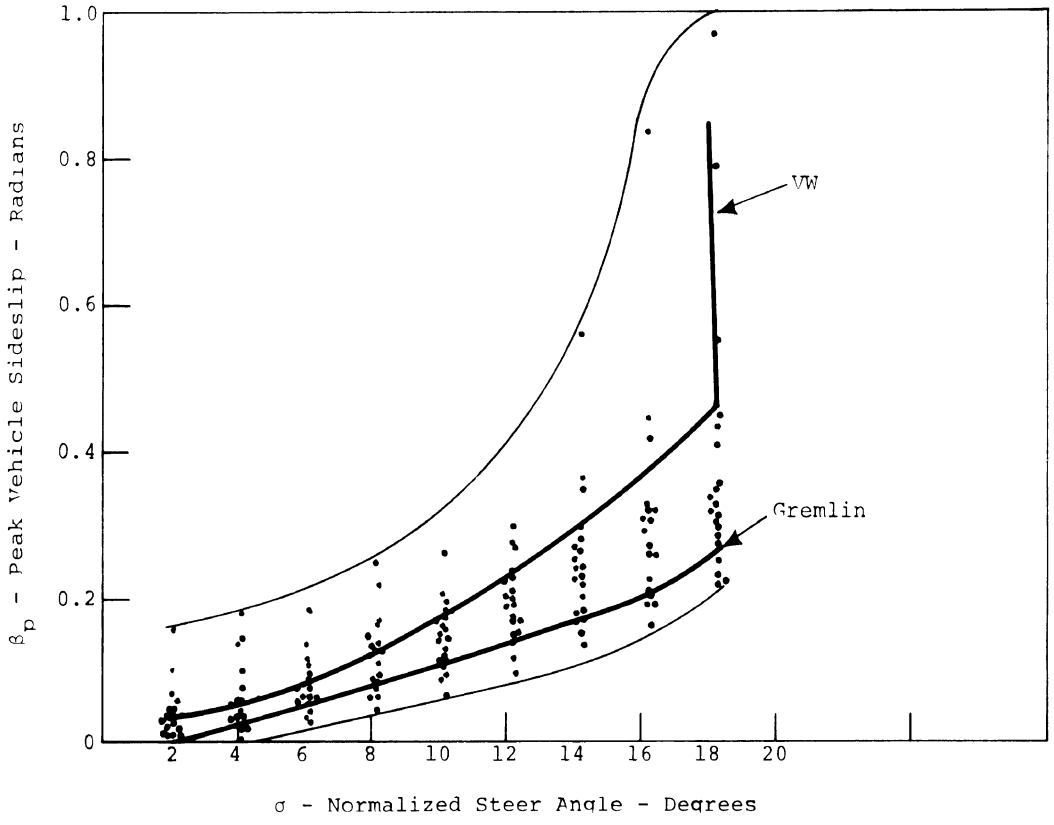

New Car Performance

Figure 5.30. Summary plot - sinusoidal steer - 60 mph

regard to the Dodge data (Figure 5.30), the "A3 right" responses clearly indicate a tremendous degradation in that vehicle's ability to minimize sideslip. On contrasting this latter observation with that noted earlier for the Δ numeric, it is seen that opposite trends in performance are indicated, suggesting a need to determine the relative importance of these measures in determining safety quality.

The third measure, net deviation in heading angle, $\Delta\psi$, is summarized in Figures 5.31 and 5.32, indicating the same basic sensitivities as shown in the β_p measures, but indicating, additionally, a sensitivity to the A4 condition.

The sum of the data gathered in the sinusoidal steer test has indicated that significant alterations in performance are caused by degradation conditions A3 and A4. Since no significant alterations were observed due to condition A1, in which shock absorber degradation was considered alone, it might be concluded that the A4 sensitivities, in which tests shock absorber degradation was combined with front end misalignment, merely indicate a redundant finding on front end misalignment as was derived from the A3 data.

An evaluation of the safety relevance of the above observed sensitivities to degradation appears to be beyond achievement, given the current technology in open-loop measurements. The two vehicles selected for test in the full-scale program happened to exhibit rather unusual directional response asymmetries at the limit, thereby confusing any analysis of their sensitivity to component degradation.

It was observed that both vehicles exhibited a general insensitivity to all degradation conditions at lower levels of steer amplitudes, that is, below σ = 10 (which corresponds to 145° for the Dodge). Performance changes that do occur above that level of steer input, are apparently due to front end misalignment and constitute findings whose value to the vehicle-in-use safety program will be enhanced by further research into the understanding of the relationship between vehicle limit handling behavior and safety.

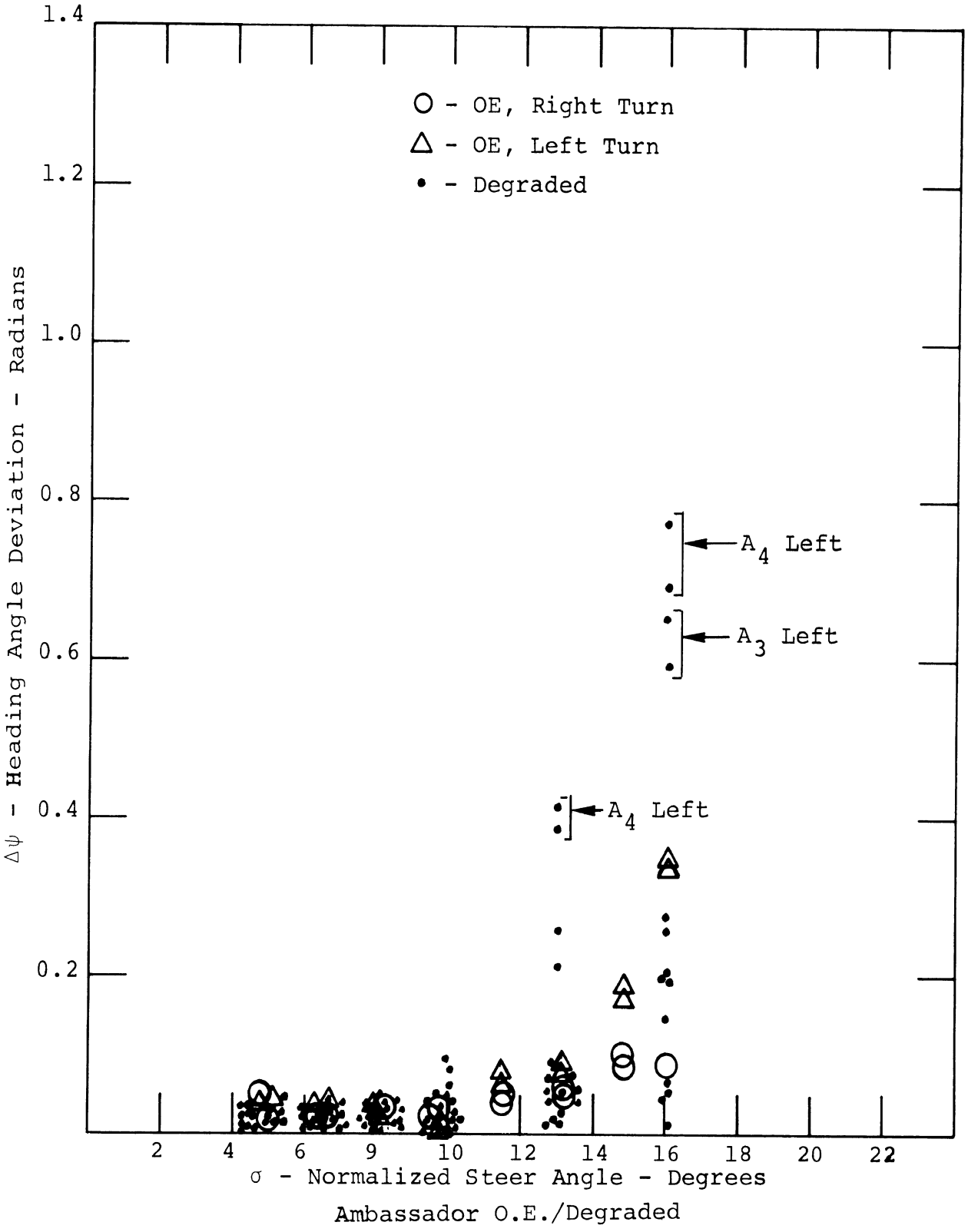

Figure 5.31. Summary plot - sinusoidal steer - 60 mph

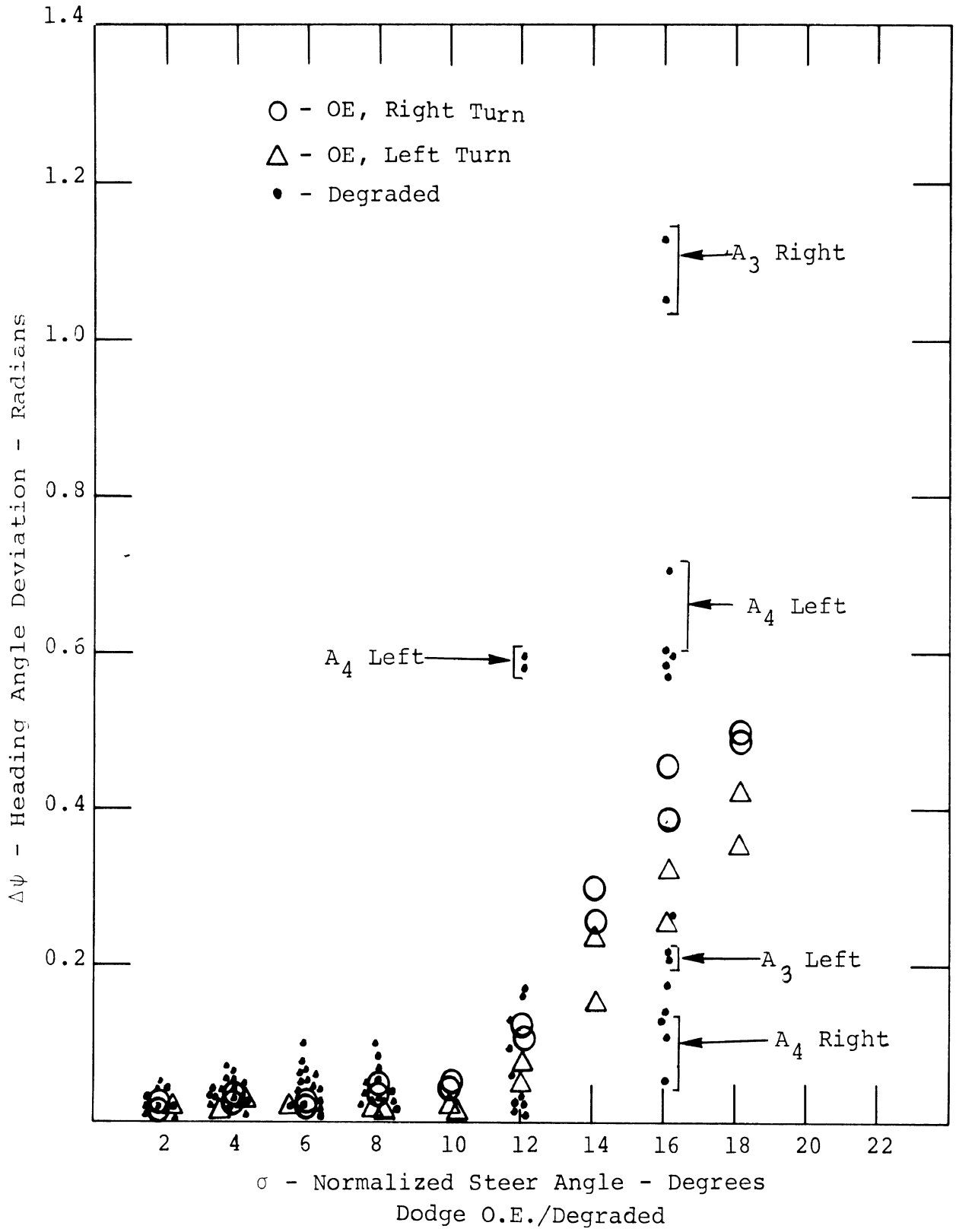

Figure 5.32. Summary plot - sinusoidal steer - 60 mph

5.3.6 DRASTIC STEER AND BRAKE. In this maneuver, the response characteristic of interest is rollover, an event representing a limit of controllability.

In this test, rollover is assumed to occur when the installed outrigger wheels contact the test surface. During the pilot testing activity, the Dodge rolled over completely causing the original outrigger to fail while being tested in a condition identical to A4. During the full-scale tests, none of the degraded conditions elicited rollover or outrigger contact on the Dodge, although significant differences were observed in the induced roll oscillations. No drastic steer and brake tests were run on the Ambassador in the degraded condition following numerous and repeated suspension failures which were experienced during O.E. testing in this maneuver category.

To reconcile the non-repeatability of the Dodge's rollover sensitivity to degradation A4, an explicit measurement of certain test condition variables would be required which are, in fact, unavailable. It is known that wheel rim contact can play a key role in rollover inducement, for example, by causing very large side forces to act on a wheel. Further, this phenomenon can occur in a rather random manner. Additionally, it is suspected that the variations in tire side force, which were found to have confused most of the pilot test data obtained with the Dodge, may have provided a significant difference in test conditions. Recent developments in the understanding of vehicle response to drastic steer/brake inputs have indicated a substantial sensitivity of performance to the timing of brake release—apparently as derives from differences in the instantaneous value of body sideslip that has accured by the time the tires are

freely rolling again. It is quite conceivable that an inadvertant mix in tire shoulder wear distributions around the vehicle during pilot testing could have caused a significantly different sideslip response—leading to rollover.

6. CONCLUSIONS AND RECOMMENDATIONS

Based upon the observations, analyses, computations, and test measurements generating from this study, the following conclusions may be drawn. It must be emphasized that these conclusions relate component degradation to limit handling performance, and not to the sublimit domain in which most normal driving is conducted.

(1) The range of limit handling performance exhibited among new cars, as derives from design differences, is much larger than the in-use changes in performance of individual vehicles deriving from degradation of steering and suspension system components.

(2) The principal suspension component whose likely degradation can be shown to influence limit performance is the shock absorber.

(3) Shock absorber degradation contributes a deterioration in limit performance principally under conditions which excite vertical motions of the unsprung masses; eliciting the "brake hop," "wheel hop," and "axle tramp" phenomena which result in net losses in tire shear force.

(4) Degradation in shock absorber performance can arise from a number of characteristically differing mechanisms. Given that these degradation mechanisms are manifested by coulomb friction, free travel, hysteretic effects, and other complex nonlinearities, it appears inadequate and thus inappropriate that shock absorber condition be represented by such simplistic characterizations as "percent effectiveness."

(5) Indeterminancies of front wheel steer angle which arise due to lash in wheel bearings, ball joints, tie-rod ends, or steering gear box, whether taken singly or in combination, do not exhibit a first-order influence on vehicle limit performance.

(6) Misalignment of front wheels, to the virtually maximum level achievable, has been shown to contribute a significant alteration in limit lane change performance, as measured by an open-loop technique.

(7) Vehicle limit braking performance, both in straight line and curved path conditions, is more severely degraded by the presence of brake imbalance than by any of the steering and suspension component degradations examined. The combination of certain steering and suspension degradations with brake imbalance can possibly further deteriorate limit braking performance beyond the level obtained with brake imbalance alone.

(8) Mass unbalance of the road wheels has been shown to have a negligible influence on limit braking and steering performance.

(9) The limit cornering capability of passenger vehicles has been shown to be insensitive to degradation in steering and suspension systems.

(10) The rollover resistance of passenger vehicles can be reduced through degradation of shock absorbers, and in certain cases may be also influenced by the addition of front end misalignment.

RECOMMENDATIONS

It is felt that this study, as conducted, has provided a sufficiently rigorous examination of the relationship between steering and suspension system degradation and limit handling performance, that the subject can be put to rest. This is not to say that all possible conditions of limit behavior and degradation have been exhausted, but rather that the authors see further research on this relationship as unwarranted. This investigation has clearly shown vehicle limit performance to be insensitive to steering and suspension degradations on a broad scale, and that further, this insensitivity is well supported by consideration of the vehicle mechanics involved. Thus, it is argued that interests of vehicle-in-use safety can best be served by the commitment of resources and effort to the investigation of the influence of steering and suspension degradations on vehicle behavior in the non-limit performance domain.

The many degraded system conditions which contributed relatively inconsequential adjustment to limit behavior are, nevertheless, known to involve factors which impose a challenge to the low level lane-tracking task. A level of driver attention may be required under such circumstances, which, giving rise to driver fatigue, constitute a safety hazard of substantially greater dimension than derives from the marginal deterioration of limit performance properties.

Degradation categories in which limit performance sensitivity is felt to be pronounced, include deterioration of tires and brakes. In this study a tire wear/side force relationship was identified which bears on limit performance to a much exaggerated degree, in comparison with steering and suspension degradation influence. Although the type of wear considered was that which derives from severe cornering,

it is felt that these data and other data clearly indicate the need for an examination of limit maneuvering properties as influenced by the level of normal tire wear and its distribution around the vehicle.

With regard to the implications bearing on vehicle inspection which derive from the findings of this study, it is clear that the inspection for shock absorber degradation is an activity which merits attention. As recommended by the two major preceding studies of steering and suspension system degradation [2, 3], the need for an effective assessment of the degradation in damping of the jounce/rebound motion of the running gear is recognized. Although few systems are currently available for exercising vehicle running gear to evaluate damping level, one such system (contributed by Hartridge Ltd. of England) was examined in the course of this study and shown to provide results which correlated well on a relative basis, with dynamic measurement of shock absorbers alone. A rigorous evaluation of such apparatus should be undertaken, not only for the sake of advancements in periodic motor vehicle inspection practice, but for application by the vehicle maintenance and servicing enterprise as well.

REFERENCES

1. Dugoff, H., Ervin, R.D., and Segel, L., Vehicle Handling Test Procedures. Highway Safety Research Institute, Univ. of Michigan, Ann Arbor, 2 Vol., a Report to NHSB, Nov. 1970.

2. Bird, K.D., Belsdorf, M.R., and Rice, R.S., Effects of Steering and Suspension Component Degradation on Automobile Stability and Control. Cornell Aeronautical Laboratory, Inc., 6 Vol., a Report to NHTSA, Contract No. FH-11-7384, Jan. 1971.

3. Merrill, M.S., Steering Diagnosis: A Study of Degraded Components Affecting In-Use Vehicle Handling. Clayton Mfg. Co., 2 Vol., a Report to NHSB, Contract No. FH-11-6629, Sept. 1969.

4. Hartz, J.R., Computer Simulation of Vehicle Handling. The Bendix Corporation, Research Laboratories, a Report to NHTSA, Contract No. FH-11-7563, Sept. 1972.

5. Howe, R.M. and Gilbert, E.G., "Trigonometric Resolution in Analog Computers by Means of Multiplier Elements." IRE Trans. on Electronic Computers, Vol. EC-6, No. 2, pp. 86-91, June 1957.

6. Rassmussen, R.E., Hill, F.W., and Riede, P.M., "Typical Vehicle Parameters for Dynamics Studies." General Motors Proving Ground Publication, No. A-2542, April 1970.

7. Ervin, R.D., Grote, P., Fancher, P.S., MacAdam, C.C., and Segel, L., Vehicle Handling Performance. Highway Safety Research Inst., Univ. of Michigan, Ann Arbor, 3 Vol., a Report to NHTSA, Nov. 1972.

8. Bendix Research Laboratories, Vehicle Handling. The Bendix Corporation, 2 Vol., a Report to NHSB, Contract No. FH-11-6946, April 1970.

9. Nedley, A.L., and Wilson, W.J., "A New Laboratory Facility for Measuring Vehicle Parameters Affecting Understeer and Brake Steer", SAE paper no.720473, May, 1972.

APPENDIX I

LITERATURE SURVEY

INTRODUCTION

The initial task in this study consisted of an effort "to gather, organize, and synopsize all existing information relative to the objective and performance" of the following project tasks:

- Methodology and Test Plan Development
- Full Scale Test Program
- Data Analysis
- Inspection Requirements

Since the present study constituted an "examination of the effects of steering and suspension component degradation on open-loop measures of vehicle performance", it can be viewed as an extension of the work performed previously for NHTSA under Contract FH-11-7384 [1]*, which investigation focused on the influence of component degradations on closed-loop handling measures.

The earlier study [1] included a very extensive literature review. Consequently, it was only necessary to update the earlier review and to identify pertinent documents that may have been missed previously. Duplication

---

*Numbers in brackets refer to references cited in a Bibliography located at the end of this Appendix.

of effort was thereby avoided and the review presented below should be viewed as a supplement to the excellent literature survey conducted under Contract FH-11-7384.

For the convenience of the reader, we identify, first, the documents deemed to be of first-order significance to this study. The survey of the literature presented in Reference [1] is synopsized, following which we synopsize those reports that have been issued more recently by the various NHTSA contractors which have been involved in "Vehicle-In-Use" safety studies. A bibliographical listing follows remarks serving to summarize and evaluate the state of knowledge on the topic under study.

Although the intent has been to circumvent the necessity for the reader to consult the literature review given in Reference [1], interested readers should certainly do so. Note that a complete listing of the publications cited in Reference [1] is provided in this Bibliography. Additional useful bibliographies can be found in Reference [99] and [101]. Further, many source items, not cited elsewhere, are briefly annotated. In general, these items [102 to 123] are of secondary importance.

LITERATURE OF FIRST-ORDER SIGNIFICANCE

Five documents (see below) are viewed as being of first-order significance to the present study. In each case, these documents are final reports from research projects that were performed under the sponsorship of NHTSA. Each of these documents is summarized and analyzed below.

FH-11-6629, "Steering Diagnosis," [2].

A test program was performed to determine the influence of component degradation on the steering performance of a single American-made vehicle (standard size sedan). Various tests were run at speeds varying from 20 to 60 mph, using a driver to provide a steering function or to hold the steering wheel in a locked position. The following maneuvers were performed:

- Straight course over simulated road obstacles
- Lane change
- Serpentine pylon course
- Straight line braking

During the course of testing, artificial degradation was introduced in the form of:

- Loose steering
- Loose ball joints
- Weak shock absorbers
- Improper wheel alignment
- Brake imbalance
- Loose wheel bearings
- Wheel unbalance

The influence of these degradation modes were studied individually and in various combinations, leading to the following conclusions:

A. Loose Steering

- adversely effects driver work, path deviation, and creates a theoretical exposure to danger

- forty degrees of steering-wheel play represents an apparent critical level of loose steering
- should be checked at the steering wheel as part of periodic motor vehicle inspection (PMVI).

B. Loose Ball Joints

- "degrade the controllability of the vehicle in the Serpentine Course more than any other single component"
- contribute to path deviation under braking
- new techniques for measuring ball joint looseness are needed.

C. Weak Shock Absorbers

- right-left asymmetry in shock strength produced a small adverse effect on handling
- vehicle bounce and pitch increased with weak shocks
- methods of inspecting shocks should be investigated.

D. Front-Wheel Misalignment

- front wheel toe-out and improper camber resulted in detrimental effects on handling
- caster adjustment had little effect on handling
- dynamic wheel alignment is recommended.

E. Brake Imbalance

- had the largest effect on path deviation during braking
- high-speed stopping tests are preferable to slow-speed tests.

The report indicates that a one vehicle test program has limitations and that "extrapolation of the data from this small sample could prove misleading."

Very little discussion is devoted to the question of whether drivers have an important influence on the test results. It is noted that "rate of brake application was found to vary from driver to driver, but was consistent with each driver."

The study appears to have been valuable as a first exercise in the artificial degradation of vehicle components and in the instrumentation of degraded vehicles for test. Lesser levels of significance should be attached to the test procedures and test findings that materialized in this pioneering venture.

FH-11-7384, "Effects of Steering and Suspension Component Degradation on Automobile Stability and Control," [1].

The objectives of this study included determination of

(1) the effects of steering and suspension system component degradation on objective measures of man-vehicle handling performance

(2) cost-effective methods of inspecting these systems.

With respect to objective (1), an experimental approach was taken. "Expert" drivers were used and all tests were closed-loop in nature. Considerable discussion is devoted to the efforts made to insure that vehicles, and not drivers, were being measured.

Six vehicles were put through the following maneuvers:

- Roadholding Test. A straight course over sinusoidal bumps. Test is concerned with measuring the normal forces in the contact patch.
- Severe Avoidance Maneuver. A rapid lane change followed by a second lane change (i.e., passing maneuver) whose execution required violent maneuvering of the test vehicle.
- Avoidance Maneuver. Gradual passing maneuver in a narrowly defined course, thus requiring precise maneuvering of the test vehicle.
- Curb Climbing. A fixed velocity test composed of climbing a 2 1/2 inch curb, which the vehicle initially straddles.
- Straight-Line Running. A narrowly defined, 200-foot, straight path.
- Straight-Line Running with Pavement Irregularities.
- Braking in a Straight Line. A braking maneuver within a narrowly defined straight path.
- Cornering on a Bumpy Surface.
- Braking Tests. Braking in a straight line and in cornering on smooth and irregular roads.
- Ice Patch Traversal. Traversal of an ice patch (simulated by a 24-foot length of wet sheet steel) located on one side of a 170-foot narrow, straight path.

Measurements were made of three performance criteria:

- Driver Inputs (e.g., steering wheel displacement.)
- Maneuver Success/Failure (e.g., did the vehicle successfully negotiate the prescribed course?)
- Vehicle Performance Level (e.g., speed at which the test vehicle was able to follow the prescribed course.)

The study concluded that:

- Shock absorber degradation significantly affects vehicle performance and the levels of driver skill required. About 50% degradation is the critical level.
- Degradation of ball joints short of failure does not affect handling performance.
- Free-play in the steering system causes increased steering work but does not influence the handling performance of the vehicle.
- Front-end misalignment has little effect on vehicle performance.

To fulfill the second objective of the study, inspection procedures currently in use were reviewed and several experienced automotive service managers were interviewed. The following conclusions were drawn:

- No egregious design shortcomings were found in the cars tested.
- Independent service operators find that a large percentage of cars require periodic alignment.
- Brake and tire problems are more serious than steering and suspension faults.

The investigators also concluded that motor vehicle inspection practice should be based on the following principles:

- A reasonably high probability of detecting degraded conditions.
- High cost and time effectiveness.

- Inspection should determine the existence of a faulty condition, not necessarily diagnose that condition.
- Inspection equipment should be inexpensive and easy to operate.

Specific recommendations included the following statements:

- Shock absorbers should be checked for visible signs of leakage and mechanical damage.
- Ball joints should be rejected for loss of boot seal integrity, looseness or wear of taper, 1/8" axial free-play in loaded ball, discernible free-play in unloaded ball joint.
- Present practice of limiting free-play at steering wheel to 2 to 3 inches at rim is reasonable.
- Front-wheel alignment is unsatisfactory if asymmetric tire wear is evident. Toe-in should be within manufacturers' specifications.

This study was comprehensive in scope, with its findings being rather effectively presented. A questionable feature, however, is the influence that the drivers may have had on the results. Expert drivers were allowed to practice and learn the testing procedures, thus introducing a mechanism that could compensate for degradation effects.

FH-11-6746, "Vehicle Handling," [3].

This report describes (1) a 17 degree of freedom, hybrid computer simulation of the automobile, (2) an associated vehicle testing program undertaken for the purpose of verifying the simulation, and (3) a vehicle handling study

intended to investigate the behavior of the vehicle in combined braking and steering maneuvers. The project is categorized as having first-order significance in that it is this computer model of the automobile which was employed in the present study, albeit in a somewhat altered form.

The study demonstrated that it is possible to allocate analog and digital computing tasks such that the simulation can run in real or near-real time with satisfactory accuracy and without the need for excessive nonlinear, analog equipment. Analog tasks included the solution of the equations describing the motions of the vehicle body, the steering and vertical motions of the front wheels, the motions of the rear axle, and the angular rotation of all wheels about their spin axes. Computations related to wheel-road orientation, the forces and moments produced by the tires, and wheel slip and friction coefficients were handled in the digital realm.

The developed simulation was verified by comparing computer predictions with results produced by tests on a standard-size American sedan. Both steady-state and transient maneuvers were conducted. In general, simulation and test results were deemed to be in good agreement.

In the vehicle handling study, two basic investigations were undertaken:

- Vehicle response to several types of simultaneous steering and braking inputs.
- Effects of changes in vehicle parameters (damping, etc.) on response to combined rear wheel drive and steering.

Open-loop maneuvers employing quasi-step inputs to the vehicle were simulated. Of interest to the present study

were the results of simulation runs studying the effects of viscous and coulomb damping on the oscillations of the steering system. Increasing friction was found to reduce the extraneous oscillations of the front wheels. (Friction, however, was only increased above that prevailing on the test vehicle; it was not reduced.)

FH-11-7297, "Vehicle Handling Test Procedures," [4].

This study was conceived as a first effort in defining a set of safety-relevant performance qualities of the passenger car. As such, it was limited to defining and measuring the open-loop behavior of the vehicle in order to eliminate the potentially confusing effects of man-vehicle interactions. As was indicated in the main text of this report, the tests, procedures, and equipment developed in the Vehicle Handling Test Procedure study constitute the framework for the testing program employed in the present study.

Specifically, six limit performance maneuvers were developed to constitute a first-order assessment of safety performance. These limit maneuvers were given the following titles:

- Limit Braking (no steering).
- Response to Rapid, Extreme Steering (no braking).
- Braking in a Turn (fixed, non-zero steer angle).
- Turning on a Rough Surface.
- Rapid Lane Change.
- "Drastic" Steer and Brake.

The test procedures developed to yield a limit maneuver numeric were executed on four automobiles of widely varying design philosophies. The first four maneuvers were executed by drivers and employed passive brake and steering limiters. The lane-change and drastic steer and brake maneuvers employed an automatic controller system providing steering, braking, and accelerator inputs.

The study concluded that "a set of performance characteristics postulated to reflect the pre-crash safety quality of the motor vehicle have been defined....[And] methods of testing and data analysis have been demonstrated which provide objective and discriminating procedures for measuring these safety-related characteristics."

FH-11-7563, "Computer Simulation of Vehicle Handling," [5].

This study constituted an extension of an earlier study entitled "Vehicle Handling" (see above) and embodied (1) improvements in the hybrid simulation and (2) implementation of the testing procedures developed in "Vehicle Handling Test Procedures." In this program, the handling characteristics of a 1967 Ford station wagon and a 1971 Volkswagen Super Beetle were determined by exercising the simulation and by physical testing. The hybrid computer results were compared with subsequent test results to validate the simulation. Established Vehicle Handling Test Procedures were utilized to derive limits of vehicle performance.

The Volkswagen simulation was deemed to have accurately predicted the test results for straight line braking, braking in a turn, sinusoidal steering, and trapezoidal steering. However, roadholding and rollover tests imposed conditions which exceeded the available tire data and violated the assumptions of the suspension model so that quantitative prediction was compromised. It was recommended that the

suspension model be refined and that more extensive tire data be obtained for specific application to roadholding and rollover tests.

SYNOPSIS OF THE LITERATURE REVIEW CONTAINED IN REFERENCE [1]

Part II (Technical Report), Volume 1 (Literature Review) of "Effects of Steering and Suspension Component Degradation on Automobile Stability and Control" contains an annotated bibliography and discussion of some 94 relevant documents. The discussion gives a comprehensive review of the information then available in the literature regarding the effects of wear and degradation in steering and suspension system components. Unfortunately, almost all of this information is of a secondary or background nature, for until the findings developed by the research performed under Contract No. FH-11-7384 [2] were published, very little information related to this problem was available in the open literature.

The following paragraphs constitute a brief outline of the literature review presented in Reference [1]. All references cited under specific topics are listed in the Bibliography.

1.0 GENERAL SOURCES OF INFORMATION

Documents are cited which provide background information on steering and suspension systems, and thus contribute only indirectly to the study.

1.1 Codification and Nomenclature [6, 7]

1.2 Descriptive Information, Design and Test
- Design [8, 35]
- Testing [35-50]

1.3 Computer simulations applicable to steering and suspension system design studies [36, 38, 51].

1.4 Vehicle handling qualities [52, 53, 54].

2.0 BASELINE SOURCE GROUP

This section contains a discussion of the reports resulting from seven major research programs sponsored by NHTSA. The authors of Reference [1] viewed these reports as constituting a baseline for their research.

2.1 FH-11-6629, "Steering Diagnosis," [2].

This document is the only report of the baseline group considered to be directly applicable to the current investigation.

2.2 FH-11-6522, "Used Vehicle Safety Study," [55].

This study constituted an examination of the broad problem of the safety of vehicles in use. Its major contribution was the production of seven mathematical models of various aspects of used vehicle safety.

2.3 FH-11-6921, "Used Car Safety Standards--Safety Index," [6].

This study attempted to obtain data on wear, degradation, and failure of vehicle components and to evaluate the effects of PMVI through the use of simulation models based on probability analysis. Modeling was accomplished, but manufacturers, fleet owners, and government agencies were generally not cooperative in the attempts to obtain data.

2.4 FH-11-6915, "Used Car Safety Standards Vehicle Safety Status," [56].

The AAA Club of Missouri inspected 8543 cars (up to five years old) in order to discover the status of cars in use and to gain knowledge that would help in setting inspection criteria. The toe-in and caster angle of front wheels were alignment variables that were most commonly found to be outside of specification. Several seemingly subjective recommendations were made for inspection procedures.

2.5 FH-11-6538, "Automated Diagnostic Systems--Vehicle Inspection," [57].

This study constituted an investigation of the possible use of automated diagnostic systems for performing vehicle inspection. Three hypothetical inspection systems possessing varying degrees of automation were developed and analyzed on a cost basis. Some hypothetical equipment was discussed.

2.6 FH-11-6938, "Used Car Safety Standards," [58].

An effort was made to determine the significant correlations of various factors (such as age) with the occurrence of out-of-specification conditions on vehicles in use, and to recommend vehicle inspection schedules and techniques. The accounting of inspection techniques is of interest to the present study.

2.7 FH-11-6886, "Alternative Inspection Policies for Collision Damaged Vehicles and Inspection of Special Purpose Vehicles," [59].

This study was aimed at determining appropriate procedures for inspecting collision-damaged vehicles. Seventy-eight vehicles were used for

case studies, and components from eighteen other vehicles (found in junk yards) were also studied. It was concluded that inspection should be tailored to the severity of the accident. Four possible procedures were given.

3.0 SOURCES RELATED TO DEGRADATION OF STEERING AND SUSPENSION SYSTEMS

3.1 Degradation Mechanisms (fatigue, wear, and chemical attack)

fatigue [32, 50, 60, 61].
wear [62, 63].

(Also, impact loading and human error are mentioned [59]).

3.2 Detection of Degraded States

•Regular usage and routine maintenance were seen as the two major means of monitoring vehicle condition. Recall campaigns and PMVI also serve to detect a degraded state.

recall [64].
PMVI review [65].

•Statistical information with respect to the pass/fail records of the existing state inspection programs appears to be plentiful [55, 56, 66-69].

•Similar statistics are available from diagnostic centers. These statistics generally show higher failure rates than those obtained by more conventional methods [55, 58, 70].

•Post accident analysis [59, 71].

3.3 Life Expectancy and Failure Data [6, 40, 55, 72-76].

4.0 SOURCES RELATED TO THE RELATIONSHIP BETWEEN COMPONENT DEGRADATION AND PERFORMANCE

4.1 Techniques for Studying Vehicle Performance

Techniques mentioned for the study of vehicle performance include computer simulation, laboratory simulation, road and proving ground testing, and accident reconstruction. The advantages and disadvantages of each are discussed.

computer simulation [1].
laboratory simulation (See 1.2)
full-scale testing [1, 2, 38, 54, 77, 78, 79].

4.2 Safety Implications of Degraded Systems

A direct connection between degraded systems and safety records is difficult to make. Many statistical studies have been made. Reference is made to a scheme of "criticality" ranking for various component failures [65, 66, 80-86].

5.0 SOURCES DEALING WITH THE PROCEDURAL ASPECTS OF INSPECTION

There are four important aspects to inspection: what, how, and when to inspect, and what is the acceptable level. "What" and "how" has been the subject of much discussion. It is generally accepted that motor vehicle inspection should have a maximum interval of one year [6, 20, 21, 36, 41, 55-59, 68, 83, 87-95].

In reviewing the above-cited documents, the authors of Reference [1] concluded that differences in classification, nomenclature, and methods made correlations between the various studies most difficult. Centralizing steering and suspension system information was found to be necessary (see [1], Volume 5, Part III). It was noted that Eisner [55] and Wells [6] have created an organizational framework for classifying steering and suspension system degradation. However, safe/unsafe limits of degradation in vehicle components have yet to be established in an objective manner. Further, the relationship of motor vehicle inspection and safety has not been objectively established. It was also concluded that simple, inexpensive inspection techniques are needed.

ADDITIONAL NHTSA CONTRACT REPORTS

FH-11-7330, "Vehicles in Use, and State Compulsion Vehicle Inspection," [98] [sic].

This study is essentially an extension of the earlier work done by Oldham [56]. Study objectives included the following tasks:

- Determine status of vehicles in use
- Collect data on reasons for rejection
- Compare results of vehicles which have or have not been previously tested
- Assess the relative worth of platform and high speed roller brake testers

Data was gathered on 12,604 cars and was processed by computer methods.

The study concluded that brake linings and front end alignment constitute the most serious defects. Headlight misalignment was found to be the most common fault. The rejection rate was found to be 50 percent higher for those vehicles which had not been previously inspected. Approximately the same comparison holds for rejections caused by defects in steering and suspension systems only.

The lack of available equipment for ball joint inspection and for on-car shock absorber testing was noted. The relative merits of static and dynamic alignment testing were discussed.

FH-11-7302, "Relationship Between Vehicle Defects and Vehicle Crashes," [99].

Fifty accidents known to be influenced by mechanical failure were studied. The following classification resulted:

- There were six accident cases presumably caused by steering defects. Three were classified as "loss of control" accidents. In three of the six cases, service had been recently performed on, or near, the part involved.
- Two accidents were cited as suspension related. Both cases were classified as "design inadequacies."
- Eighteen cases of wheel loss were reported. Two resulted from failures of the drive axle or bearing. Twelve resulted from improper wheel mounting in recent servicing. One truck lost a wheel because the retaining nut did not have a cotter pin installed.

Of great significance with respect to PMVI procedures, is the fact that twenty of the fifty accident cases studied had had some service in the previous month. Of these

twenty, fourteen had accidents directly attributable to faulty repair service. In the other six cases, service personnel "did not notice" faulty parts in close proximity to the work being done.

Volume V of this report is an Annotated Bibliography of the title subject. Sources are reviewed under the headings of:

- Components. (Including general component failure, steering, suspension, tires, and wheels.)
- Inspection, Maintenance, and Repairs.
- Accident Investigation and Analysis.
- Other Information Listings and Sources

A listing of researchers is also included.

FH-11-7216, "Vehicle-In-Use System Safety Analysis," [100].

A systems analysis approach was used to discover and rank, in terms of criticality, the important modes of failure among the major subsystems of the motor vehicle. Rankings were given to several modes of steering system failure. In order of "criticality" these included:

- Wheel or tire imbalance.
- Frozen front-wheel bearing.
- Malfunction of power steering--fluid level.
- Excessive friction at steering gear.
- Malfunction of power steering--drive belt.
- Worn or incorrect shocks.
- Alignment error--toe-in or camber.

The following conclusions were drawn:

- Shock absorber performance is "safety critical," but no adequate means of testing on the vehicle exist. Research should be undertaken to correct this situation.
- Front-end looseness (in ball joints) is "safety important." The relative safety merits of the several ball joint configurations and the effectiveness of inspection procedures should be evaluated.

FH-11-7254, "Multidisciplinary Investigations to Determine Relationship Between Vehicle Defects, Failure, and Vehicle Crashes," [101].

Case summaries are given for post-crash investigations of 34 accidents in Houston, Texas during 1969-70. The objective was to determine the relative causation importance of the driver, the vehicle, and the accident-site environment.

It was found that steering system defects were of a "contributory nature" in 20.5 percent of the study vehicles, but were never "causative."

The study concluded that although vehicles may become mechanically defective, fault generally lies with the driver for neglecting maintainance, knowingly or unknowingly. Also, "if priorities must be established, the steering/suspension system would have to be rated low priority for inspection when compared with brakes."

An annotated bibliography of the title subject is included. Subheadings are:

- Component Systems. (Including steering system, suspension system, tires and wheels)
- Periodic Motor Vehicle Inspection, Maintenance, Quality Control and Warranties.

•Collision Investigation and Analysis.

•Data Centers and Mechanical Defects Libraries.

•Author-Researcher List.

FH-11-7329, "Vehicle Deterioration Accident Investigation," [102].

The objective of the study was to determine the importance of defects, malfunction and maladjustments in vehicle systems and components in causing and/or contributing to accidents. Twenty-seven accidents were investigated in depth and an additional 48 were investigated by using police records. Steering defects were involved in three of the twenty-seven in-depth cases and in five of the 48 "police" cases. Accident involvement due to vehicle defects was generally found to rise with age.

A brief survey of the literature was made and an annotated bibliography with thirty-seven sources is presented.

EVALUATIVE COMMENTS

The majority of work accomplished to date on developing relationships between steering and suspension system degradation, vehicle performance, and safety falls into the category of statistical analysis. Data acquired from accident and vehicle inspection records have been used to define relationships between the various relevant factors, and to develop mathematical models based on probability considerations. Although the volume of this work has been considerable, these activities have not as yet led, nor is it likely that they can lead, to the establishment of standards limiting the levels of component degradation deemed permissible for reasons of safety.

On the other hand, very little information on the physical effects of component degradation on steering and suspension system performance has been published. In fact, the only formal documents on this topic are that of Bird, Belsdorf, and Rice [1] and Merrill [2]. Unfortunately, the results of these two studies often appear to be in direct conflict. In particular, Merrill found that (1) ball joint looseness has an important influence on vehicle handling and (2) degraded shock absorbers to have little effect on handling performance. Bird and his associates, in essence, arrived at the opposite conclusion. Further, the validity of the findings produced by these two studies is clouded by the fact that both groups of investigators used test procedures in which the vehicles were driven by experienced or "expert" drivers that had ample opportunity to adapt to the demands imposed both by the assigned maneuvering task and by the degraded components.

Until the necessary research has been performed and component degradation limits have been established, the basis for discussing inspection equipment requirements remains on shaky ground. Nevertheless, the existing lack of equipment to measure shock absorber performance and ball joint looseness clearly needs to be remedied. Whenever inspection equipment and techniques applying to any vehicle system are developed, however, it would be well to bear in mind the findings of Schmidt [99] which indicated that the human errors made by service personnel can be among the most important factors causing component failure.

Finally, it should be noted more information and data on the phenomenon of component wear and its effects on vehicle performance probably exists than is readily apparent. Wells [6], for example, indicates that manufacturers, in all likelihood, possess a good deal of wear and failure data

but consider this information proprietary. The current authors are aware that, many years ago, a study of the effects of front-end misalignment and other factors on safety performance was made under SAE auspices but unfortunately was not carried through to produce a final published document.

BIBLIOGRAPHY

1. Bird, K.D., Belsdorf, M.R., and Rice, R.S., 'Effects of Steering and Suspension Component Degradation on Automobile Stability and Control. Cornell Aeronautical Laboratory, Inc., 6 Vol., a Report to NHTSA, Contract No. FH-11-7384, Jan. 1971.

2. Merrill, M.S., Steering Diagnosis: A Study of Degraded Components Affecting In-Use Vehicle Handling. Clayton Mfg. Co., 2 Vol., a Report to NHSB, Contract No. FH-11-6629, Sept. 1969.

3. Bendix Research Laboratories, Vehicle Handling. The Bendix Corporation, 2 Vol., a Report to NHSB, Contract No. FH-11-6946, Apr. 1970.

4. Dugoff, H., Ervin, R.D., and Segel, L., Vehicle Handling Test Procedures. Highway Safety Res. Inst., Univ. of Mich., Ann Arbor, 2 Vol., a Report to NHSB, Nov. 1970.

5. Hartz, J.R., Computer Simulation of Vehicle Handling. The Bendix Corporation, Research Laboratories, a Report to NHTSA, Contract No. FH-11-7563, Sept. 1972.

6. Wells, E.N., et al., An Investigation of Used Car Safety Standards - Safety Index. 8 Vol., Operations Research, Inc., Silver Springs, Md., Rept. No. PB-190518, a Report to NHSB, Contract No. FH-11-6921, 12 Sept. 1969.

7. Lovejoy, B.H., et al., A Study of Garage Repair and Dealer Warranty Procedures. Operations Research, Inc., Silver Springs, Md., Sept. 1969.

8. Dillman, O.D. and Collier, E.J., Building Stability into the Modern Automobile. Chrysler Corp., c. 1954.

9. Gough, V.E., "Front Suspension and Tire Wear." G. R. Shearer, Proceedings of the IME, Automobile Division, No. 6, 1955-56, p. 171.

10. Marquis, D.P., "How Fundamentals are Applied to the Design of Safe, Efficient Automotive Steering Systems." General Motors Engineering Journal, Vol. 4, No. 4, Oct.-Nov.-Dec. 1957, p. 2.

11. U. S. Army Materiel Command, Engineering Design Handbook - Automotive Series - The Automotive Assembly. AMCP 706-335, Feb. 1965.

12. U.S. Army Materiel Command, Engineering Design Handbook - Automotive Series - Automotive Suspension. AMCP 706-356, Feb. 1965.

13. Anon., "Sealed-for-Life Ball Joints." Automobile Engineer, Vol. 54, No. 1, Jan. 1964, p. 14.

14. Billiet, W.E. and Alley, W.V., Jr., "Automotive Suspensions, Steering, Alignment, and Brakes." American Technical Society, 4th Ed., 1969.

15. Bloom, F.W., Ball Joint Front Suspension. Ford Motor Company, AMA Presentation to AAMVA Committee on Engineering and Vehicle Inspection, June, 1961.

16. Bond, J.R., "Suspension System Differences in the Compacts are Tremendous." SAE Journal, Vol. 68, No. 5, May 1960, p. 56.

17. Booth, J.H., "Application of Ball Joints to Front Suspensions." SAE (Quarterly) Transactions, Vol. 6, No. 4, Oct. 1952, p. 710.

18. Carrier, H., "Evolution of Rear Suspension." Motor Age, Nov. 1968, p. 83.

19. Love, R.R. and Dillman, O.D., "Chrysler Torsion-Aire Suspension - Across the Board." SAE Preprint 79, Mar. 1957.

20. Automobile Manufacturers Association, Front Suspension System Panel of the AMA D7 Advisory Committee Presentation. AMA Presentation to AAMVA Committee on Engineering and Vehicle Inspection, June 1962.

21. Dwiggins, B.H., Automotive Steering Systems. Delmar Publishers, 1968.

22. Anon., Experimental Safety Car Study, Phase I Final Report. Fairchild-Hiller, Republic Aviation Div., Report FHR 3653, 4 Vol., Aug. 1968.

23. Gschwind, L.D., Ball Joints and Tie Rod Ends. Chrysler Corp., AMA Presentation to AAMVA Committee on Engineering and Vehicle Inspection, 1968.

24. Knightson, C.L. and Marshall, R.J., "Designing Front Suspensions." SAE Journal, Vol. 71, No. 6, June 1963, p. 46. (Abbreviated version of SAE Preprint 627A, Jan. 1963.)

25. Schilling, R., "Flexible or Spring Medium of Suspensions." SAE Transactions, Vol. 54, No. 7, July 1946, p. 366.

26. Schoelfield, C.M., "Rear Suspension Isolation - Its Effect on Ride and Handling." SAE Preprint 627B, Jan. 1962.

27. Tea, C.A., "Secondary Vibrations. Part I - In Front End Suspensions." SAE Journal, Vol. 58, June 1950, p. 55.

28. Polhemus, V.D., "Secondary Vibrations. Part II - In Rear Suspensions." SAE Journal, Vol. 58, July 1950, p. 41. [27].

29. Thomas, P.P., "Service-Free-For-Life Suspension and Steering Systems." SAE Journal, Vol. 69, No. 7, July 1961, p. 78.

30. Kuhn, P.H., "Designing Passenger Cars for Service-Free Operation." (Ford Motor Co.), FISITA , Paper S-1, 1964.

31. Parker, R.C., "Projected Private Vehicles Without After-Sales Service." FISITA, 1964, p. 334.

32. Larson, W.B. and Devers, M.W., "Design of Integral Ductile Iron Steering Knuckles for Disc Brake Vehicles." SAE Paper 690501, May 1969.

33. "Allowable Stress Diagrams Can Help Designers Solve Automotive Strength Problems." SAE Journal, Vol. 71, No. 4, Apr. 1963, p. 70.

34. Schilling, R., "Operational Stresses in Automotive Parts." SAE (Quarterly) Transactions, Vol. 5, No. 2, Apr. 1951, p. 290.

35. Yamamoto, M., "Strength and Rigidity Requirements for the Automobile Structure." SAE Preprint 298B, Jan. 1961.

36. Bollinger, R.H. and Lipkin, L., "Passenger Car Suspension Analysis." SAE Preprint 536, June 1955.

37. Conover, J.C., Jaeckel, H.R., and Kippola, W.J., "Simulation of Field Loading in Fatigue Testing." SAE Paper 660102, Jan. 1966.

38. Kohno, T., Tsuchiya, S., and Komoda, N., "On the Vehicle Dynamic Response to the Steering Control - Experimental Evaluation of the Response and Analytical Approach to the Design of the Performance with Seven Degrees Model." SAE Paper 690488, May 1969.

39. Love, R.J., "Fatigue in Automobiles." Proceedings of the International Conference on Fatigue of Metals, IME, 1956, p. 570.

40. McConnell, W.A., "How Good is Testing? A Correlation of Customer, Laboratory, and Proving Ground Experience." SAE Transactions, Vol. 68, 1960, p. 588.

41. Betz, E.R., "Studying Structure Dynamics with the Cadillac Road Simulator." SAE Paper 660101, Jan. 1966.

42. Brand, B.G., "Accelerated Product Deterioration." Industrial Research, Vol. 10, No. 9, Sept. 1968, p. 70.

43. Fister, L. P., "Moog Improves Automotive Suspension Parts by Revolutionary Laboratory Testing." MTS Closed Loop, The Magazine of Mechanical Testing, Vol. 2, No. 3, 1969, p. 13.

44. Kelly, A.H., Jr., Elder, C.J., and Freas, W.S., "Reliability Testing - Dynamic Safety." General Motors Automotive Safety Seminar, Paper No. 5, July 1969.

45. Gassner, E. and Schultz, W., "Evaluating Vital Vehicle Components by Programmed Fatigue Tests." FISITA , 1962.

46. Geschelin, J., "Ford Reliability Laboratory." Automotive Industries, Vol. 137, No. 10, Nov. 15, 1967, p. 105.

47. Jaeckel, H.R. and Swanson, S.R., Random Load Spectrum Test to Determine Durability of Structural Components of Automotive Vehicles. MTS Systems Corp., TR 900.22-1, 1967. Also Paper 3-02 of FISITA, 1968.

48. LeMense, R.A., "Use of the Weibull Distribution in Analyzing Life Test Data from Vehicle Structural Components." SAE P-2, 1964, p. 628.

49. Scott, T.C.F., "Fatigue Testing of Vehicle Components." Proceedings of the IME, Automobile Div., No. 1, 1958-59, p. 21.

50. Templin, R.J., Hoban, J.T., and Cislo, C. J., "The Cadillac Development of an Integral Ductile Iron Steering Knuckle." SAE Paper 690500, May 1969.

51. McHenry, R.R., "An Analysis of the Dynamics of Automobiles During Simultaneous Cornering and Ride Motions." Inst. of Mech. Eng., 1969.

52. Janeway, R.N., "Vehicle Design Aspect of Safe Handling." Proceedings of a Conference on Research; Passenger Car Design and Highway Safety, Association for the Aid of Crippled Children and Consumers Union of the U.S., 1962, p. 25.

53. Dell'Amico, F., A Program Plan for Developing Safe Handling Standards for Motor Vehicles. Cornell Aeronautical Laboratory, Inc., Rept. No. VJ-2494-V-I, Contract No. FH-11-6529, Sept. 1967.

54. Rice, R.S. and Whitcomb, D.W., "Ground Vehicle Dynamics - Past, Present and Future." ASME, 90th Winter Annual Meeting, Los Angeles, Calif. Nov. 1969.

55. Eisner, H., Kalin, S.R., Wells, E.N., and Williams, P.D., An Investigation of Used Car Safety: Final Report. Operations Research, Inc., 5 Vol., a Report to NHSB, Contract No. FH-11-6522, June 1968.

56. Oldham, F.B., Used Car Safety Standards (Vehicle Safety Status). Automobile Club of Missouri, St. Louis, Mo., 2 Vol., a Report to NHSB, Contract No. FH-11-6915, July 1969.

57. Beraru, J. and Champion, G., Automated Diagnostic Systems - Vehicle Inspection. TRW Systems Group, Rept. No. 09793-6001-R000, 2 Vol., Mar. 1968, and 09793-6001-R001, 2 Vol., Nov. 1968, a Report to NHSB, Contract No. FH-11-6538.

58. Beraru, J., Used Car Safety Standards. TRW Systems Group, Rept. No. TRW-11786-6001-RO, 3 Vol., a Report to NHSB, Contract No. FH-11-6938, Oct. 1969.

59. Hull, B.W., Cromack, J.R. and Ward, R.G., Alternative Inspection Policies for Collision Damaged Vehicles and Inspection of Special Purpose Vehicles. Southwest Research Institute, Proj. 11-2389, 2 Vol., a Report to NHSB, Contract No. FH-11-6886, June 1969.

60. Swanson, S.R., "Evaluating Component Fatigue Performance Under Programmed Random, and Programmed Constant Amplitude Loading." SAE Paper 690050, Jan. 1969.

61. Lipson, C., "Analysis of Failures." SAE Paper 690494, May 1969.

62. Burwell, J.T., Jr., "Survey of Possible Wear Mechanisms." Wear, Vol. 1, 1957/58, p. 119.

63. Bisson, E.E., The Various Modes of Wear and Their Controlling Factors. NASA, TMX-52426, June 1968.

64. Anon., "Motor Vehicle Safety Defect Recall Campaigns." U.S. Dept. of Transportation, Fed. Highway Admin., Nat. Highway Safety Bureau, Quarterly issues and annual cumulative edition.

65. Brenner, R., Bradford, L., and Parker, G., "State-of-the-Art Motor Vehicle Inspection." SAE Paper 700380, May 1970.

66. Anon., Data on Vehicle Inspection Programs for State Appointed Stations (and) State Owned and Operated Stations. American Association of Motor Vehicle Administrators.

67. Anon., Report on an Evaluation of Motor Vehicle Inspection. Coverdale and Colpitts, Apr. 1967.

68. Anon., Report on Recommendations Regarding Motor Vehicle Inspection. Coverdale and Colpitts, May 1967.

69. Reinfurt, D.W. and Pascarella, E.A., Periodic Motor Vehicle Inspection in North Carolina: A Descriptive Study. Univ. of North Carolina, Highway Safety Research Center, Nov. 1969.

70. Klaffky, G.A., "Mobil's Vehicle Diagnostic System." SAE Paper 760c, Oct. 1963.

71. Burnstine, M., "Some Defective Vehicle Conditions in Traffic Death Cases." In Research on Fatal Highway Collisions, (A. L. Moseley, Ed.), Papers 1962-1963, Harvard Medical School, 1964.

72. Knowles, J., "Engineering Reliability Into Today's Automotive Vehicles." IEEE, Annual Symposium on Reliability, 68C, 33-R, Jan. 1968, p. 67.

73. Anon., "Frequency-of-Repair Records." 1964 to 1969 Models, Consumer Reports, 1970.

74. Earles, D.R. and Edins, M.F., Reliability Engineering Data Series. AVCO Corp., Apr. 1962.

75. Fulton, D., Holtz, J.N., and Schafer, R.E., "Non-electronic Reliability Part Data Collection and Analysis." Proceedings of the 1968 Annual Symposium on Reliability, IEEE 68C 33-R, Jan. 1968, p. 114.

76. Pollock, S.E. and Richards, E.T., "Failure Rate Data (FARADA) Program." USN Ordnance Lab., Corona, Calif., SAE Aerospace Reliability and Maintainability Conference, Proceedings, P-2, July 1964, p. 265-72.

77. Milliken, W.F., Jr. and Dell'Amico, F., "Standards for Safe Handling Characteristics of Automobiles." Paper presented at the Joint Symposium on Vehicle and Road Design for Safety, College of Aeronautics, Cranfield, England, July 3-4, 1968.

78. Hildebrandt, T.J. and Poskicil, A.R., "Objective Testing in Handling Research." SAE Automotive Engineering Conference, SAE Paper 680015, 1968.

79. Anon., Development of Task Performance Handling Tests. General Motors Corp., Engineering Publication A-2591, Mar. 1969.

80. Anon., Compulsory Motor Vehicle Inspection Systems in the Various States. Arkansas Legislative Council, Research Dept., Research Rept. No. 106, Nov. 1961.

81. Brenner, R., Some Trends and Views on New Car and Used Car Safety Performance Standards. U.S. Dept. of Transportation, NHSB, Apr. 1968. (Also available as SAE Paper 68-0268.)

82. Cottell, G.A., "Lessons to be Learned from Failures in Services." IME, Proceedings of the International Conference on Fatigue of Metals, 1956, p. 563.

83. Lister, R.D. and Grime, G., "Inspection of Vehicle for Road Worthiness, with Special Reference to Methods and Equipment." Proceedings of the IME, Automobile Div., No. 5, 1957-58, p. 129.

84. Hoffman, E.R. and Joubert, P.N., "Just Noticeable Differences in Some Vehicle Handling Variables." Human Factors, Vol. 10, No. 3, June 1968, p. 263.

85. Anon., Research in Vehicle Handling Properties. McDonnell-Douglas, Rept. No. DAC-66636, Sept. 1967.

86. Schreiber, R.J., "Effects of Aging and Mileage on the Accident Rates of Vehicles: An Example of Methodological Problems in Accident Research." Proceedings of a Conference on Research - Passenger Car Design and Highway Safety, Association for Crippled Children; Consumer Union, 1961.

87. Anon., A Study of Motor Vehicle Inspection. Program performed by V.E. Rothe, J.W. Turnbow, and L.G. Robertson of Arizona State Univ. for the American Automobile Association, July 1967.

88. Anon., American Standard Inspection Requirements for Motor Vehicle, Trailers, and Semitrailers Operated on Public Highways. American Standard Association, D7.1-1963, July 1963. (A)

Anon., American Standard Station Requirements for Inspection of Motor Vehicles, Trailers, and Semitrailers in Stations Owned and Operated by Regulatory Authority. ASA, D7.2-1963, July 1963. (B)

Anon., American Standard Station Requirements for Inspection of Motor Vehicles, Trailers, and Semitrailers in Stations Appointed and Licensed by Regulatory Authority. ASA, D7.3-1963. (C)

89. Anon., The Modern Diagnostic Center. Automotive Center Consultants, May 1966.

90. Cline, E.L., "Development of Techniques and Equipment to Improve Reliability of Automotive Diagnosis." Clayton Mfg. Co., SAE Paper 670517, May 1967.

91. Anon., Inspection Laws Annotated. National Committee on Uniform Traffic Laws and Ordinances, 1969.

92. Anon., An Evaluation of Automotive Safety Test Equipment for PMVI. Research Inst. for Diagnostic Engineering, 1968.

93. Stonex, K.A., "State Vehicle Inspection Techniques." SAE Paper 665A, Mar. 1963.

94. McCutcheon, R.W. and Sherman, H.W., The Influence of Periodic Motor Vehicle Inspection on Mechanical Condition. Highway Safety Res. Inst., Univ. of Michigan, Ann Arbor, July 1968.

95. Buxbaum, R.C. and Colton, T., "Relationship of Motor Vehicle Inspection to Accident Mortality." Journal of the American Medical Assoc., Vol. 197, No. 1, July 4, 1966, p. 101.

96. Anon., "Tires Tell the Tale." Motor Age, Aug. 1968, p. 70.

97. Campbell, K.L., "Determination of Passenger Car Tire Performance Levels - Treadwear." SAE Paper 690507, May 1969.

98. Oldham, F.B., Vehicles in Use, and State Compulsion Vehicle Inspection. Automobile Club of Missouri, 2 Vol., a Report to NHSB, Contract No. FH-11-7330, Aug. 1970.

99. Schmidt, P.N., Relationship Between Vehicle Defects and Vehicle Crashes. Stanford Research Inst., 5 Vol., a Report to NHSB, Contract No. FH-11-7302, July 1970.

100. Anon., Vehicle-In-Use System Safety Analysis. Booz-Allen Applied Research, Inc., 5 Vol., a Report to NHSB, Contract No. FH-11-7316, July 1970.

101. Finch, J.R. and Smith, J.P., Multidisciplinary Investigations to Determine Relationship Between Vehicle Defects, Failure, and Vehicle Crashes. Baylor College of Medicine, a Report to NHTSA, Contract No. FH-11-7254, April 1970.

102. States, J.D. and Balcerek, J.C., Vehicle Deterioration Accident Investigation. Univ. of Rochester, School of Medicine, a Report to NHTSA, Contract No. FH-11-7329, June 1970.

103. Mackey, G.M., Causes and Effects of Road Accidents - Part 3, The Vehicles. Univ. of Birmingham, a Report to the Dept. of Transportation and Environmental Planning.

A post-accident study of 1049 vehicles. Although forward vision and inadequate lighting were found to be most important, steering deficiencies were contributing factors in 3% of the vehicles studied. The author believes that the benefits of PMVI will not be great because vehicle causation of accidents is not great.

104. Anon., Analysis of Motor Carrier Accidents Involving Mechanical Defects. Bureau of Motor Carriers, I.C.C., Washington, D.C., Nov. 1963.

Contains an elaborate statistical breakdown of the factors involved in accidents involving mechanical defects of trucks and buses in 1959 through 1962. During this time period, steering and suspension component failures were involved in about 25% of the bus accidents and 38% of the truck accidents in the sample.

105. Anon., Weak Points of Cars. AB Svensk Bilprouning, Stockholm, Oct. 1969.

A presentation of the data gathered by inspecting 951,215 vehicles during the first half of 1969. Separate accounts of faults in 1966 models are given. This is only one, in a steady stream of publications of similar data for different time periods. Other publications exist under the same title. Other titles are "Motor Vehicles, Points to Watch" and "Control Inspections." Also see, Technical Aspects of Road Safety, Vol. 31, Sept. 1967.

106. Tiffany, N.O., Cornell, G.A., and Code, R.L., "A Hybrid Simulation of Vehicle Dynamics and Subsystems." SAE Paper 700155, Jan. 1970.

107. Hickner, G.B., Elliott, J.G., and Cornell, G.A., "Hybrid Computer Simulation of the Dynamic Response of a Vehicle with Four-Wheel Adaptive Brakes." SAE Paper 710225.

An improved version of the vehicle simulation developed under Contract No. FH-11-6948 [3] is discussed.

108. Gilbert, E.G., "Dynamic - Error Analysis of Digital and Combined Analog-Digital Computer Systems." Simulation, Vol. 6, No. 4, Apr. 1966.

109. McHenry, R.R., "Simulating Car Crashes." Science Journal, Dec. 1969.

110. Anon., Vehicle Dynamics in Single Vehicle Accidents. Technical Report Cal. No. VJ-2251-V-3, Cornell Aeronautical Laboratory, Inc., Dec. 1968.

111. Segel, L., "On the Lateral Stability and Control of the Automobile as Influenced by the Dynamics of the Steering System." Transactions of the ASME, Aug. 1966.

112. Bergman, M., "Effects of Compliance on Vehicle Handling Properties." SAE Paper No. 700369, May 1970.

Discusses the several ways in which compliance effects steering. A method developed for measuring compliance is discussed.

113. Braess, H.H., "Theoretical Investigations of the Directional Behavior of Motor Vehicles." 13th FISITA Congress, Paper No. 17.1.B, June 1970.

This investigation includes and evaluates the influence of the dynamic behavior of the steering gear.

114. Dugoff, H. and Brown, B.J., "Measurement of Tire Shear Forces." SAE Paper 7000923, Jan. 1970.

Provides data for the tire/road interface model used in the simulation by Hickner, Elliott, and Cornell [107].

115. Willumeit, H.P., "Loss in Side-Force of Obliquely Rolling Tire Under Harmonically Variable Wheel Loads and Constant Slip Angle." Auto. Industries, Vol. 15, No. 4, Nov. 1970, p. 79-84.

116. Belsdorf, K.D., Rice, R.S., and Bird, K.D., "Performance Task as Measures of Vehicle Handling Qualities at the Limit of Performance." SAE Paper 710081, Jan. 1971.

Derived from work done for [1].

117. Belsdorf, M.R. and Rice, R.S., "Tests Show that Degradation of Steering, Suspension Systems Doesn't Always Affect Car Safety." SAE Journal of Automotive Engineering, Vol. 79, No. 7, July 1971, pp. 22-24.

Derived from work done for [1].

118. Dugoff, H., Segel, L. and Ervin, R., "Measurement of Vehicle Response to Severe Braking and Steering Maneuvers." SAE Paper 710080, Jan. 1971.

Derived from work done for [4].

119. Ilarionov, V.A., "On the Evaluation of Vehicle Handling and Stability." Auto. Prom., No. 2, Feb. 1971, pp. 19-22.

Discusses the pros and cons of testing vehicles with human or automatic controllers. The author feels that tests of sufficient severity to bring the vehicle to limit behavior will also severely tax a driver psychologically.

120. Gallagher, J.P., "What the Designer Should Know About Fracture Mechanics Fundamentals." SAE Paper 710151, Jan. 1971.

121. Holliday, F.R. and Allmen, C.R., "In-Car Fatigue Data Acquisition." SAE Paper 690172, Jan. 1969.

Discusses techniques for obtaining time varying load data in a car. Two example installations are discussed.

122. Swanson, S.R., "Evaluating Component Fatigue Performance Under Programmed Random and Programmed Constant Amplitude Loading." SAE Paper 690050, Jan. 1969.

Paper gives an assessment of the two major testing techniques for random loading fatigue failure prediction.

123. Jaeckel, H.R., "Simulation, Duplication, and Synthesis of Fatigue Reviews." SAE Paper 700032, Jan. 1970.

Reviews, compares and gives examples of programmed fatigue, service duplication, and constant amplitude fatigue test methods.

APPENDIX II

VEHICLE PARAMETER DATA

GENERAL DISCUSSION

An extensive set of vehicle parameter information is needed to use the Bendix/NHTSA hybrid simulation. In this study, the necessary parameters were obtained for simulating eight vehicles. The acquisition of this data was a costly and time-consuming task.

A variety of techniques were employed to evaluate vehicle parameters:

1. A special test rig was constructed for measuring steering system play and compliances.
2. Shock absorber characteristics were measured in the laboratory using a tensile test machine.
3. An individualized test set-up was implemented for measuring the suspension properties of each vehicle.
4. A system of balances and vertical force application was used to obtain center of gravity location.
5. The moments of inertia, sprung weight and unsprung weights were estimated from suitable empirical relations which apply to passenger cars [6]. These formulas are sufficiently accurate to preclude the necessity for measuring these quantities in a study devoted to the influence of steering and suspension system degradations.
6. The tire parameters for each vehicle were estimated from a complete set of tire data for a single tire. The tire data was scaled up or down to correspond to the tire load for the particular vehicle of interest. Clearly, this is a very

inaccurate method, but it should be noted that the tires on vehicles in use differ greatly in type, wear, and inflation pressure. Thus, the approximate tire parameters were satisfactory for evaluating the influence of changes in steering and suspension system parameters. To have measured and to have simulated a complete set of tire characteristics for each tire at each inflation pressure used in these vehicles would have been beyond the scope of this study.

PARAMETER DATA LISTS

The vehicle parameters used in the simulation study are defined in Table II-1. Values of these parameters for eight vehicles are given in Table II-2. Further information on the simulation study is given in Appendix III.

STEERING SYSTEM MEASUREMENTS

Figures II-2 and II-3 show the measurements made on the degraded steering systems in the Ambassador and Coronet.

TABLE II-1

DEFINITIONS OF PARAMETERS

A. DISTANCES

a	Longitudinal distance between sprung mass center of gravity and front wheels.
b	Longitudinal distance between sprung mass center of gravity and rear wheels.
T_F	Wheel tread width at front.
T_R	Wheel tread width at rear.
T_S	Distance between spring mountings on solid rear axle.
y_{SA}	Distance between wheel center and king pin axis; measured along wheel spin axis.
z_F	Static distance between the center of gravity of the sprung mass and the spin axis of the front wheels; measured along the z-axis.
z_R	Static distance between the center of gravity of the sprung mass and the roll center of the rear suspension; measured along the z-axis.
a_P	Length of Pitman arm.
a_L	Length of steering linkage arm
Ω_{FC}	Maximum suspension deflection for front wheel in compression mode.
Ω_{FT}	Maximum suspension deflection for front wheel in tension mode.
Ω_{RC}	Maximum suspension deflection for rear wheel in compression mode.
Ω_{RT}	Maximum suspension deflection for rear wheel in tension mode.
z_{RO}	Anti-pitch center height.
L_F	Effective anti-pitch arm.
T_{LF}	Tread between anti-pitch arms.

TABLE II-1 (Continued)

C_3	Rear roll center height coefficient.
h_R	Distance from center of rear axle to the roll center of the rear suspension.
h_F	Distance from ground to the roll center of the front suspension.
R_W	Undeflected tire radius.

B. MOMENTS OF INERTIA

I_{xs}	Moment of inertia of sprung mass about the x-axis.
I_{ys}	Moment of inertia of sprung mass about the y-axis.
I_{zs}	Moment of inertia of sprung mass about the z-axis.
I_D	Drive line moment of inertia about its spin axis.
I_{FW}	Moment of inertia of one front wheel about the king pin axis.
I_R	Moment of inertia of rear unsprung mass about an axis through its center of gravity and parallel to the x-axis.
I_{WJ}	Moment of inertia of wheel about spin axis.

C. SPRUNG AND UNSPRUNG MASSES

M_S	Sprung mass.
M_{uF}	Total front unsprung mass.
M_{uR}	Total rear unsprung mass.

D. DIMENSIONLESS PARAMETERS

N_G	Gear ratio of steering gear box.
N_L	Steering linkage gear ratio.

TABLE II-1 (Continued)

λ_F	Spring rate proportionality factor for operation on suspension deflection stops at front.
λ_R	Spring rate proportionality factor for operation on suspension deflection stops at rear.
$\overline{AR}$	Drive axle ratio.

E. SPRING RATES

K_F	Suspension load-deflection rate for a single wheel in the quasi-linear range about the design position; effective at the front wheel.
K_R	Suspension load-deflection rate for a single wheel in the quasi-linear range about the design position; effective at the rear spring.
K_{TF}	Radial spring rate of a single front tire in the quasi-linear range.
K_{TR}	Radial spring rate of a single rear tire in the quasi-linear range.
R_F	Auxiliary roll stiffness of front suspension.
R_R	Auxiliary roll stiffness of rear suspension.

F. ADDITIONAL STEERING AND SUSPENSION SYSTEM PARAMETERS

K_{SC}	Steering column-gear flexibility.
K_{SL}	Steering linkage flexibility between the output of the steering unit and the king pin.
K_{RS}	Roll steer gain of rear wheels relative to the vehicle coordinate system.
C_{CR}	Viscous damping coefficient of steering system connecting rod.
C_{FCR}	Coulomb damping coefficient of steering system connecting rod.
H_D	Front wheel viscous damping derivative.

TABLE II-1 (Continued)

m_C	Mass of steering system connecting rod.
E_{sp}	Free play in the steering gear box.
E_p	Free play in steer of front wheel.
ϕ_{si}	King pin inclination angle; i=1, 2 = right front, left front.
C'_F	Coulomb damping coefficient for a single wheel; effective at the wheel for the front suspension.
C'_R	Coulomb damping coefficient for a single wheel; effective at the wheel for the rear suspension.
θ_{si}	Front wheel caster angle; i=1, 2 = right front, left front.
ε_i	Front wheel toe-in angle; i=1, 2 = right front, left front.
ϕ_i	Front wheel camber angle; i=1, 2 = right front, left front.
ϕ_{pi}	Camber angle due to degradations.
C_F	Viscous damping function for a single wheel; effective at the wheel for the front suspension.
C_R	Viscous damping coefficient for a single wheel; effective at the wheel for the rear suspension.

TABLE II-2

VALUES OF VEHICLE PARAMETERS USED

Symbol	Units	Ambassador	Austin American	Chevrolet Brookwood	Dodge Coronet	Ford F-100	Ford Mustang	Olds F-85	Volkswagen Super Beetle
a	inches	49.2	31.8	66.8	50.8	47.9	42.5	47.5	52.3
b	inches	72.2	61.7	58.2	67.2	83.1	66.5	68.5	43.0
T_F	inches	60.0	51.5	64.1	59.7	64.4	61.5	59.7	54.3
T_R	inches	60.0	50.9	64.1	62.0	60.4	61.0	59.0	53.3
T_S	inches	33.8	N.A.*	45.1	47.1	40.25	43.0	35.5	N.A.
y_{SA}	inches	5.25	2.0	5.25	4.59	4.22	5.1	4.0	3.75
z_F	inches	11.5	11.25	9.5	8.9	15.2	9.35	9.11	10.8
z_R	inches	11.25	11.5	9.5	8.7	14.6	9.35	9.11	10.6
a_P	inches	5.5	0.278#	6		6.12	5.3	4.87	6.06
a_L	inches	6.65	5.5#	6.46		7.65	6.67	5.73	5.53
Ω_{FC}	inches	4.4	3.44	3.375	1.875	2.375	2.5	3.6	2.4
Ω_{FT}	inches	1.4	1.56	2.0	3.0	5.125	3.25	2.0	2.3
Ω_{RC}	inches	2.5	4.5	4.0	1.625	5.7	3.7	3.625	3.1
Ω_{RT}	inches	1.75	2.6	6.0	5.0†	2.3	2.875	1.25	2.2
z_{RO}	inches	0.†	N.A.	0.	N.A.	0.	-2.75	0.	0.
L_F	inches	132.†	N.A.	63.3	N.A.	23.25	66.0	159.	-13.
T_{LF}	inches	24.†	N.A.	20.0	N.A.	44.8	22.0	28.5	27.
C_3	inches		N.A.	0.		0.		-1.5	N.A.
h_R	inches		N.A.	0.		0.		5.25	N.A.
h_F	inches		4.0	3.5		8.05		2.0	7.2

*N.A. means not applicable.
#Austin has rack and pinion steering arrangement.
†Estimates.

TABLE II-2 (Continued)

Symbol	Units	Ambassador	Austin American	Chevrolet Brookwood	Dodge Coronet	Ford F-100	Ford Mustang	Olds F-85	Volkswagen Super Beetle
R_w	inches	14.	12.0	15.0	14.0	15.0	14.0	14.0	12.63
I_{xs}	in.lb.sec^2	3,960	2,275	5,850	3,620	3,910	2,940	3,975	2,565
I_{ys}	in.lb.sec^2	20,350	8,565	36,610	18,510	18,420	11,080	19,770	10,310
I_{zs}	in.lb.sec^2	29,250	8,860	41,650	27,000	28,900	22,500	28,150	10,430
I_D	in.lb.sec^2	0.6	0.3	0.6	0.6	0.6	0.6	0.6	0.3
I_{FW}	in.lb.sec^2	11.0	6.0	8.0	8.0	11.0	8.0	8.0	8.0
I_R	in.lb.sec^2	600.	N.A.	600.	600.	600.	600.	600.	N.A.
I_{WJ}	in.lb.sec^2	17.0	11.0	17.0	16.0	17.0	16.0	16.0	.15.0
M_S	lb.sec^2/in	8.21	4.23	10.49	7.79	8.18	9.98	7.99	4.16
M_{uF}	lb.sec^2/in	0.541	0.372	0.642	0.522	0.539	0.484	0.531	0.359
M_{uR}	lb.sec^2/in	0.889	0.579	1.050	0.847	0.875	0.789	0.864	0.574
N_G	-----	16.0	1.0#	13 to 17	15.7	17.0	17.5	13 to 16	17.53
N_L	-----	1.21	19.8#	1.079	1.19	1.25	1.26	1.176	0.912
λ_F	-----	2.4	4.8	2.7	1.8	1.75	3.66	2.59	5.1
λ_R	-----	2.7	4.0	3.22	1.25	1.78	3.84	5.5	4.0
$\overline{AR}$	-----	2.87	3.76	2.73	2.71	3.25	2.79	2.73	4.125
K_F	lb/in	92.	105.	133.	95.	160.	87.4	100.	52.2
K_R	lb/in	99.	76.5	185.	104.	245.	114.	80.	100.
K_{TF}	lb/in	1,330	1,100	1,350	1,420	1,770	1,295	1,320	812
K_{TR}	lb/in	1,420	920	1,800	1,420	1,770	1,295	1,420	1,192
R_F	in.lb./rad	306,000	0	506,000	0	0	151,000	222,500	81,000
R_R	in.lb./rad	0	0	0	0	0	0	57,500	0

TABLE II-2 (Continued)

Symbol	Units	Ambassador	Austin American	Chevrolet Brookwood	Dodge Coronet	Ford F-100	Ford Mustang	Olds F-85	Volkswagen Super Beetle
K_{SC}	in.lb./rad	1,028	582	1,290	509	510	720	778	610
K_{SL}	in.lb./rad	94,200	205,000	391,000	128,500	226,000	185,000	257,000	117,000
K_{RS}	rad/rad	-0.151	N.A.	0.110	0.073	-0.108	-0.09	-0.12	N.A.
C_{CR}	lb.sec/in	11.0	2.0	11.0		11.0	11.0	10.0	3.75
C_{FCR}	lb.sec/in	235.0	109.	167.		148.	207.	206.	163.
H_D	in.lb.sec/rad	400.	200.	400.	400.	400.	400.	400.	200.
m_C	$lb.sec^2/in$	0.085	0.08	0.085	0.085	0.085	0.085	0.085	0.08
E_{sp}*	deg								
E_p*	deg								
ϕ_{si}	deg	7.25	10.0	10.0	7.5	8.5	6.75	8.0	10.0
C'_F	lb.	70.0	40.0	45.0	43.0	29.0	36.0	40.0	25.0
C'_R	lb.	20.0	18.0	71.0	45.0	87.5	50.0	31.5	45.0
θ_{si}	deg	1.0	5.5	-1.0	0.75	3.5	0.	-1.25	2.0
E_i#	deg	0.25	-0.15(front) 0.(rear)	0.36	0.25	0.24	0.	0.25	0.16(front) 0.(rear)
ϕ_i#	deg	0.	0.75(front) 0.(rear)	0.5	0.5	1.5	0.75	-0.125	1.(front) -1.3(rear)
ϕ_{pi}*	deg								
C_F†	lb.sec/in.		**						
C_R†	lb.sec/in.		**						

* Degraded condition values (ordinarily zero).
\# Static values at normal curb weight (see Table II-4 for data versus suspension deflection).
† See Table II-3 for damping data.
**Hydro elastic suspension.

TABLE II-3

PIECEWISE LINEAR APPROXIMATIONS
TO SHOCK ABSORBER DATA

The entries in this table are the values of the slopes, SLi, of the approximations to the effective damping relationships. The mounting angle and location of the shock absorber in the suspension have been accounted for in this data. The original curves can be reconstructed as illustrated in Figure II-1. The units of the entries are lbs/(in/sec) and V is velocity in (in/sec).

Vehicle	For Shock Absorber Damping Effective At The Front Wheel	For Shock Absorber Damping Effective At The Rear Spring
Ambassador	0.6 for V>0 1.34 for 0<V<3 5.0 for -6<V<0 0.89 for -40<V<-6 3.76 for V<-40	1.2 for V>3.5 4.22 for 0<V<3.5 15.65 for -6<V<0 4.18 for -15<V<-6 2.57 for V<-15
Chevrolet Brookwood	1.9 for V>0 5.66 for V<0	5.0 for V>0 15.0 for V<0
Dodge Coronet	3.66 for V>0 5.3 for V<0	4.0 for V>0 6.67 for V<0
Ford Mustang	1.44 for V>-24 3.55 for V>-24	2.13 for V>0 5.94 for -12<V<0 3.48 for -25.5<V<-12 4.60 for V<-25.5
Ford F-100 Truck	5.5 for V>0 9.76 for V<0	4.43 for V>0 9.74 for V<0
Oldsmobile F-85	.745 for V>17.5 1.34 for 1.5<V<17.5 7.27 for -10<V<1.5 1.82 for -30<V<-10 3.03 for V<-30	1.65 for V>13 3.69 for 0<V<13 15.0 for -8<V<0 3.75 for -30<V<-8 6.5 for V<-30
Volkswagen	3.28 for V>0 5.46 for V<0	1.73 for V>3 10.8 for -14<V<3 5.55 for V<-14

Note: No more than 5 slopes are used.
However, less than 5 are used whenever
it is appropriate.

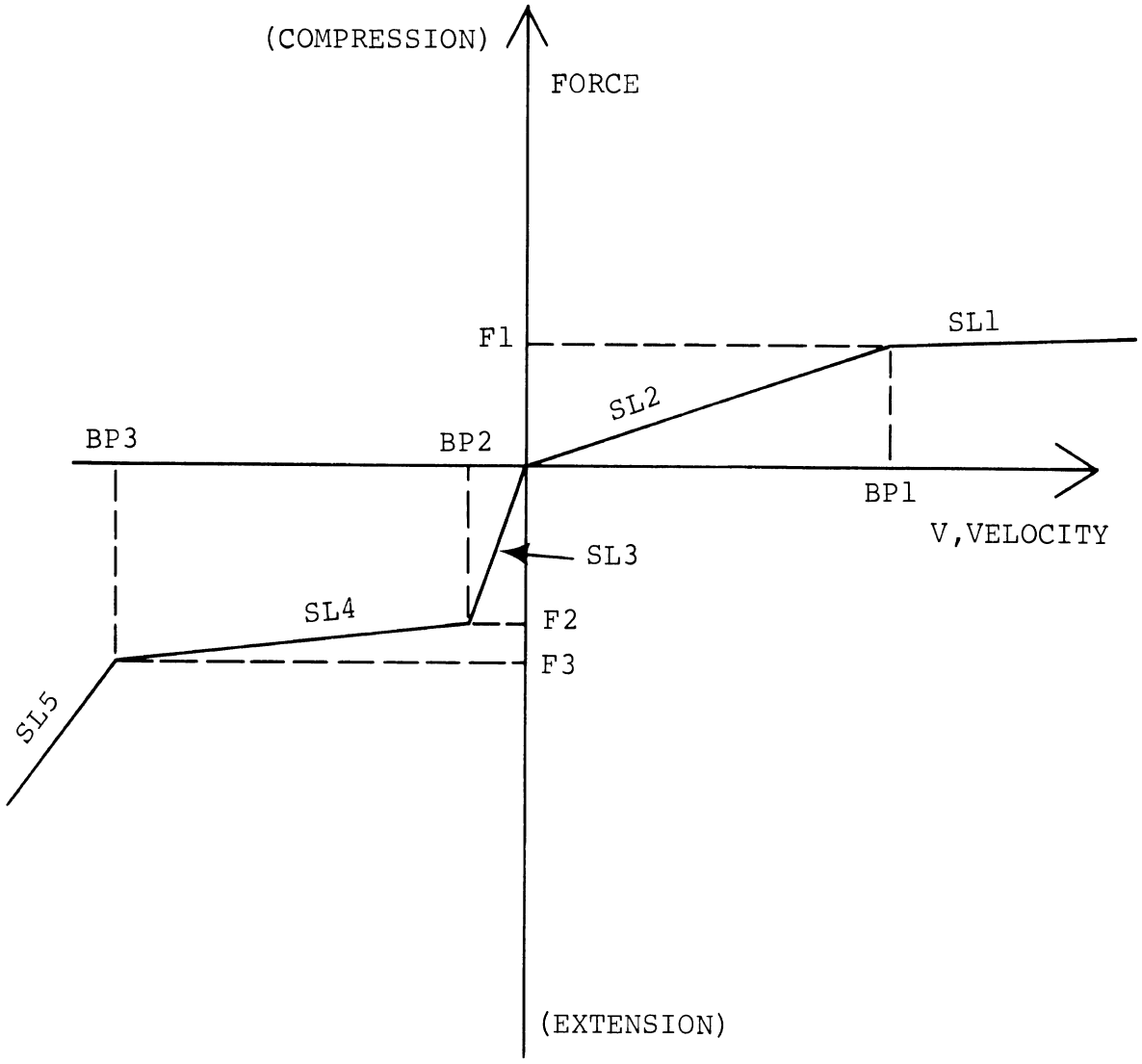

PARAMETERS:	Breakpoints	Slopes
	The Origin	SL1
	BP1	SL2
	BP2	SL3
	BP3	SL4
		SL5

CLEARLY, F1=SL2•BP1
F2=SL3•BP2
F3=F2+SL4•(BP3-BP2)

FIGURE II-1 SHOCK ABSORBER PARAMETERS

TABLE II-4

CAMBER AND TOE MEASUREMENTS

To obtain these data the wheel was moved from resting on the rebound bump stop to compressing the jounce bump stop. The steering wheel was held fixed. In order to use these data in calculations, one must know the values of toe and camber at a reference value of suspension deflection. Naturally, the reference value of suspension deflection (from the full rebound position) depends upon vehicle loading. For this project, the reference values of suspension deflection were measured with the vehicle at curb weight. Then the specified static values of toe and camber (given in Table II-1), combined with the data given here, were employed to compute toe and camber as a function of suspension deflections.

Reference Displacement (inches)	Displacement From Full Rebound Position (inches)	Camber Change From Full Rebound Value (degrees)	Toe Change From Full Rebound Value (degrees)
AMBASSADOR, Left Front Wheel			
2.25	0	0	0
	1	-0.7	0.92
	2	-1.63	1.89
	3	-2.35	2.61
	4	-2.55	3.29
	5	-2.30	3.90
	6	-1.77	4.42
	7	-1.0	4.86
AUSTIN, Left Front Wheel			
2.31	0	0	0
	1	0.6	-2.80
	2	1.45	-3.54
	3	2.35	-3.80
	4	3.30	-3.70
	5	4.35	-2.85
	6	5.75	-1.35
AUSTIN, Right Rear Wheel			
3.0	0	2.50	0
	1	1.80	0.16
	2	1.49	0.32
	3	1.24	0.48
	4	1.14	0.65
	5	1.10	0.81
	6	1.08	0.90
	7	0.92	0.90

TABLE II-4 (Continued)

Reference Displacement (inches)	Displacement From Full Rebound Position (inches)	Camber Change From Full Rebound Value (degrees)	Toe Change From Full Rebound Value (degrees)
CHEVROLET, Left Front Wheel			
2.70	0	0	0
	1	0.75	0.60
	2	2.02	1.19
	3	2.48	1.50
	4	2.56	1.74
	5	2.25	1.94
	6	2.02	2.10
DODGE, Left Front Wheel			
3.9	0	0	0
	1	-0.28	0.58
	2	-0.66	0.88
	3	-0.72	1.11
	4	-0.60	1.29
	5	-0.28	1.37
	6	0.31	1.24
	7	1.42	0.40
MUSTANG, Left Front Wheel			
4.18	0	0	0
	1	0.77	0.59
	2	0.38	0.90
	3	0.42	1.15
	4	0.85	1.37
	5	1.42	1.55
	6	2.15	1.64
	7	2.97	1.74
FORD F-100, Left Front Wheel			
5.0	0	0	0
	1	1.10	0.16
	2	2.20	0.29
	3	3.35	0.40
	4	4.50	0.49
	5	5.70	0.56
	6	6.90	0.60
	7	8.10	0.61
	8	9.30	0.58
	9	10.50	0.45

TABLE II-4 (Continued)

Reference Displacement (inches)	Displacement From Full Rebound Position (inches)	Camber Change From Full Rebound Value (degrees)	Toe Change From Full Rebound Value (degrees)
OLDS F-85, Left Front Wheel			
3.25	0	0	0
	1	0.92	-0.75
	2	2.11	-1.30
	3	2.78	-1.64
	4	2.85	-1.80
	5	2.85	-1.89
	6	2.80	-1.94
	7	2.29	-2.16
VOLKSWAGEN, Left Front Wheel			
2.9	0	0	0
	1	0.92	0.30
	2	1.66	0.57
	3	2.25	0.82
	4	2.79	1.04
	5	3.29	1.21
	6	3.92	1.35
VOLKSWAGEN, Right Rear Wheel			
2.75	0	-0.55	0
	1	-1.35	0.03
	2	-2.10	0.06
	3	-3.10	0.08
	4	-3.90	0.11
	5	-4.75	0.19
	6	-5.60	0.34

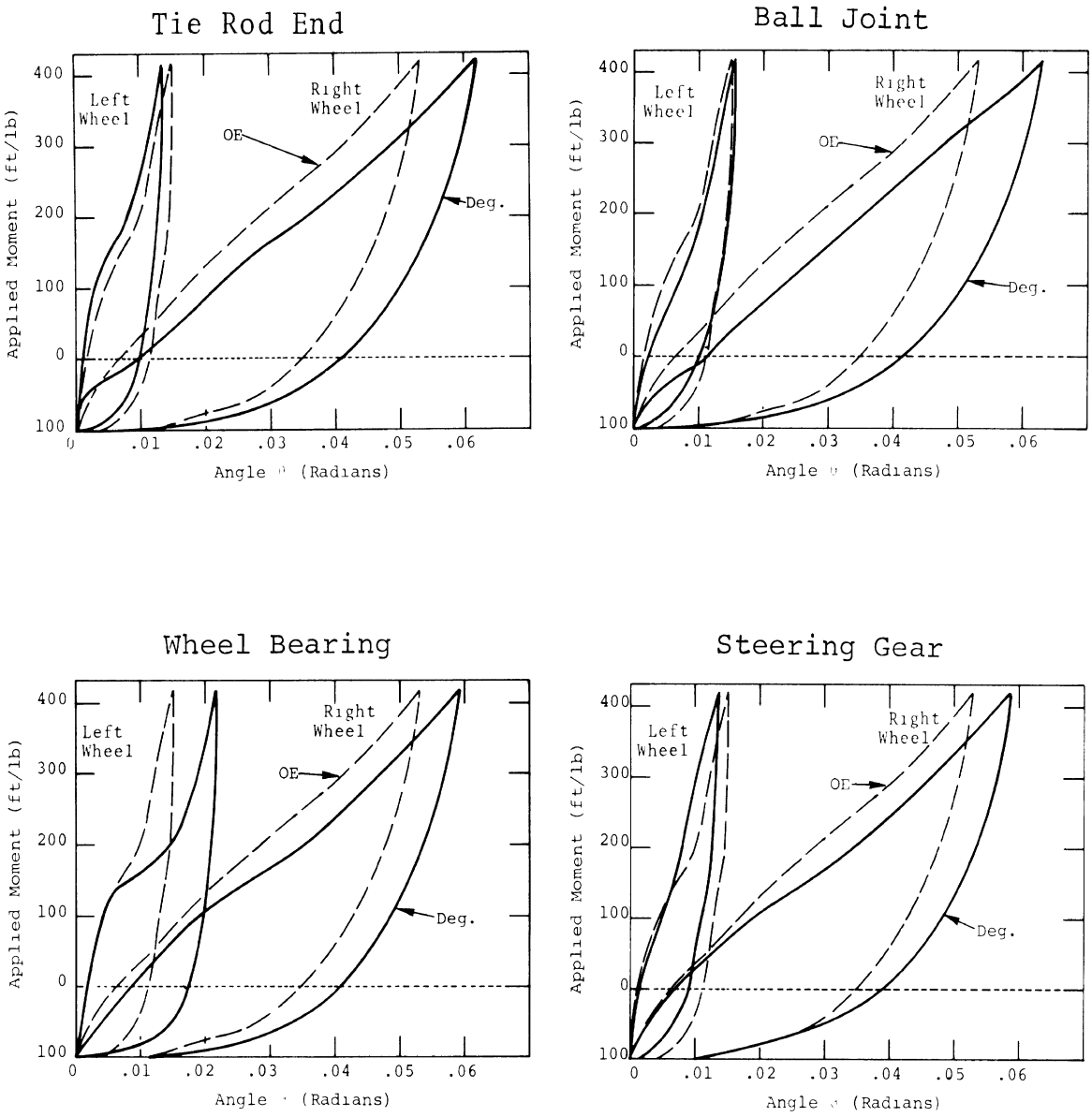

Figure II-2. Degraded steering gear measurements for the Ambassador

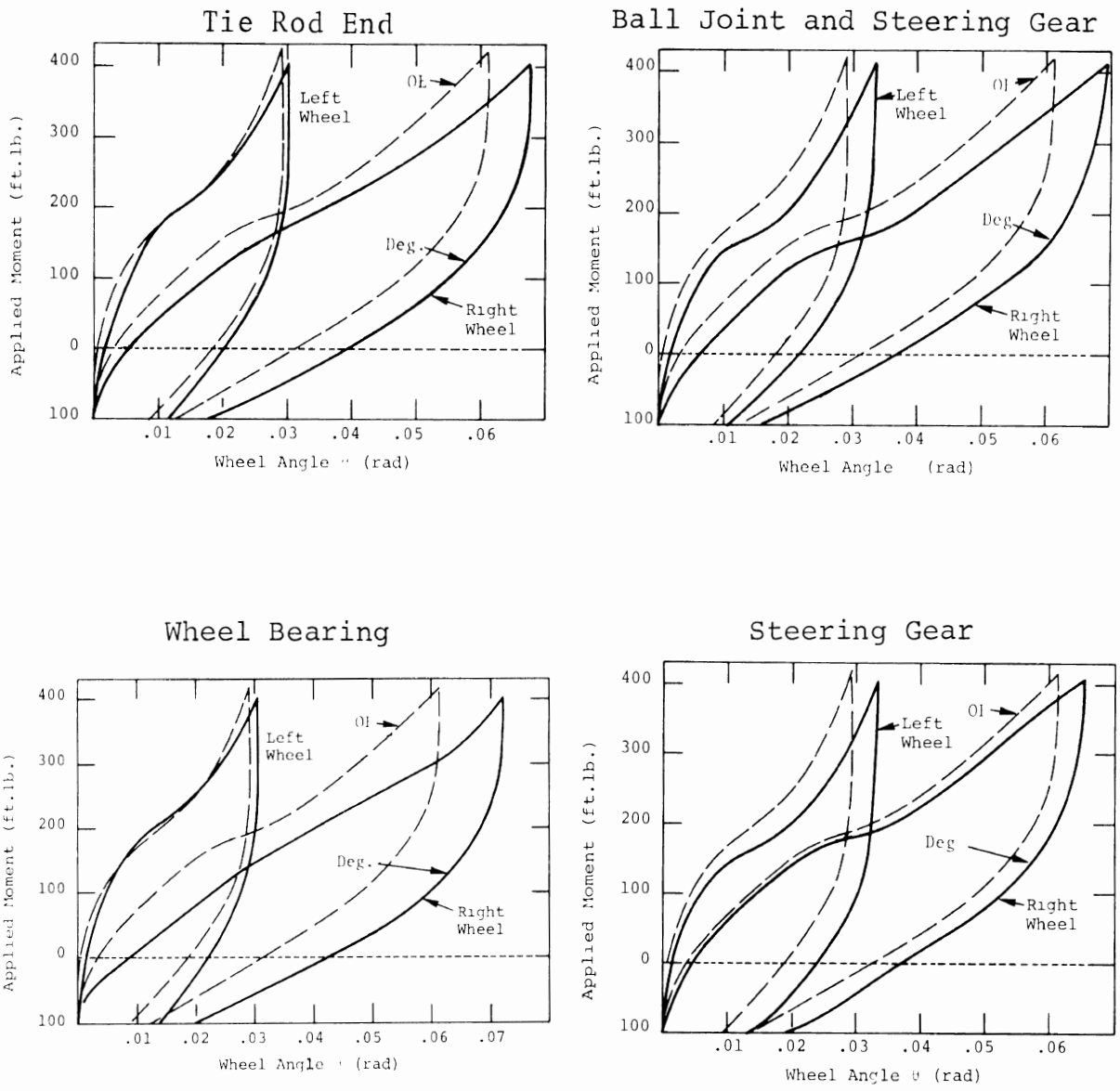

Figure II-3. Degraded steering gear measurements for the Dodge Coronet

APPENDIX III

SIMULATION DESCRIPTION

GENERAL DISCUSSION

The Bendix Research Laboratories were engaged to use their simulation to perform calculations for this study. For several years, Bendix personnel have been developing a hybrid computer vehicle dynamics simulation for NHTSA under Contracts FH-11-6946 and FH-11-7563 [8, 4].

The simulation is a seventeen-degree-of-freedom model of a four-wheeled highway vehicle. In the simulation, tire data is fitted with empirical relations. Changes in wheel caster, camber, and toe are programmed as functions of wheel center motion. The shock absorbers are treated as nonlinear dampers using piecewise linear functions of suspension velocity. The effects of bump stop location and steering system friction and compliance are included. Provisions for simulating either a solid rear axle or independent rear suspensions are available.

For the purpose of studying the influence of steering and suspension system degradations on vehicle performance, the simulation was refined and augmented to include:

(1) a more detailed model of the steering system,

(2) a more extensive representation of shock absorber characteristics,

(3) provision for representing steer and camber angle play due to wheel bearing and ball joint looseness,

(4) provision for representing steer angle play due to tie-rod end and steering gear box looseness,

(5) wheel imbalance

(6) roll bar bushing degradation, and

(7) unbalanced brake torque (side-to-side on an axle).

In addition, for the purpose of trying to improve the representation of the eight subject vehicles, the simulation was modified to allow:

(1) Different tire characteristics, front and rear (required for vehicles employing different front and rear tire pressures).

(2) A variety of front and rear roll center locations.

(3) Representation of anti-pitch effects in the suspension.

(4) Representation of "jacking forces" in swing axle rear suspensions.

(5) Different magnitudes of static caster, camber, and toe for each front wheel.

Since the extensive set of equations for the entire seventeen-degree-of-freedom simulation have been recently documented in [4], the reader, who is interested in the details of the entire simulation, is referred to Appendix B of Reference [4].

The remainder of this appendix contains a discussion of the various changes which were made in the simulation for the purpose of representing steering and suspension system degradations. Special emphasis is placed on the steering system model which was developed for this program.

STEERING SYSTEM MODEL

The steering system was modeled in considerable detail in order to be able to represent free play in worn or degraded components. Definitions of the parameters and variables used in this model are given in Table III-1 and the equations are given in Table III-2. A schematic diagram of the steering system model is shown in Figure III-1. The model is intended for fixed control applications in which the steering wheel angle is given as a prescribed function of time.

The model contains three degrees of freedom:

(1) δ_{FW_1}, rotational motion of the right front wheel about its steering pivot.

(2) δ_{FW_2}, rotational motion of the left front wheel about its steering pivot (δ_{FW_2})

(3) Y_{CR}, translational motion of the connecting rod and associated mass elements.

Clearly, this is a lumped parameter model of a continuous system. The degree of freedom associated with the connecting rod is included for two reasons: first, to provide a convenient mechanism for introducing coulomb friction in the steering gear computations and second, to provide a means of dynamically computing the influence of the free plays (E_{sp}, E_{p1}, and E_{p2}).

TABLE III-1

STEERING SYSTEM PARAMETERS AND VARIABLES

Parameters

K_{SC}	steering column and power steering "stiffness"
E_{sp}	play in steering gear
C_{CR}	viscous friction in steering gear (effective at connecting rod)
C_{FCR}	coulomb friction in steering gear (effective at connecting rod)
K_{SL_1}	right front linkage compliance
K_{SL_2}	left front linkage compliance
E_{p1}	right front play from tie-rod end, ball joints, and wheel bearing
E_{p2}	left front play
H_{D_1}	right front wheel viscous friction
H_{D_2}	left front wheel viscous friction
M_C	effective mass of connecting rod
a_p	pitman arm length
a_1	forward distance from connecting rod to wheel center, right side
a_2	same as a_1 except for left side
N_G	gear ratio of gear box
N_L	linkage gear ratio, $\frac{a_1}{a_p}$

Variables

M_{T_1}	torque about steering pivot, right wheel
M_{T_2}	torque about steering pivot, left wheel
δ_{SW}	steering wheel angle
δ_p	pitman arm angle
y_{CR}	connecting rod position
δ_{FW_1}	right front wheel angle
δ_{FW_2}	left front wheel angle

TABLE III-2

STEERING SYSTEM EQUATIONS

$$I_{FW_1}(\ddot{\delta}_{FW_1} + \dot{r}) = - H_{D_1}\dot{\delta}_{FW_1} + M_{T_1} - M_{SS_1}$$

where M_{SS_1} is as shown below with i=1

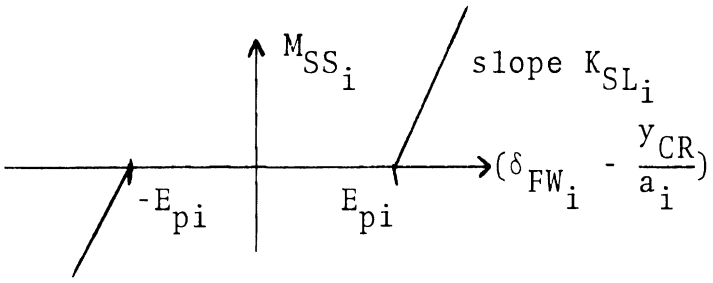

$$I_{FW_2}(\ddot{\delta}_{FW_2} + \dot{r}) = - H_{D_2}\dot{\delta}_{FW_2} + M_{T_2} - M_{SS_2}$$

where M_{SS_2} is as shown above with i=2.

$$M_C\ddot{y}_{CR} + C_{FCR}\,\mathrm{sgn}(\dot{y}_{CR}) + C_{CR}\dot{y}_{CR} = \frac{T_p}{a_p} + \frac{M_{SS_2}}{a_2} + \frac{M_{SS_1}}{a_1}$$

where T_p is as shown below: $(\delta_p = \frac{y_{CR}}{a_p})$

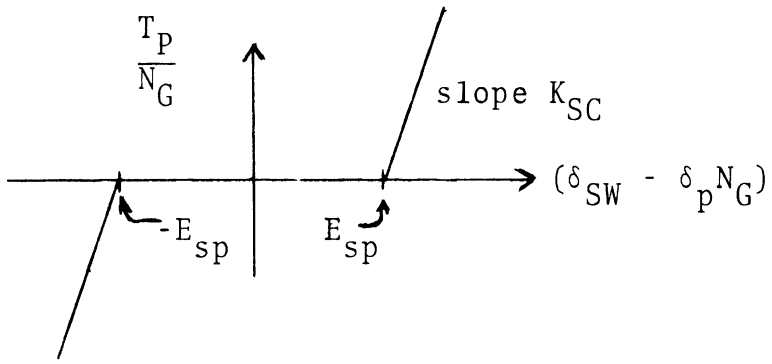

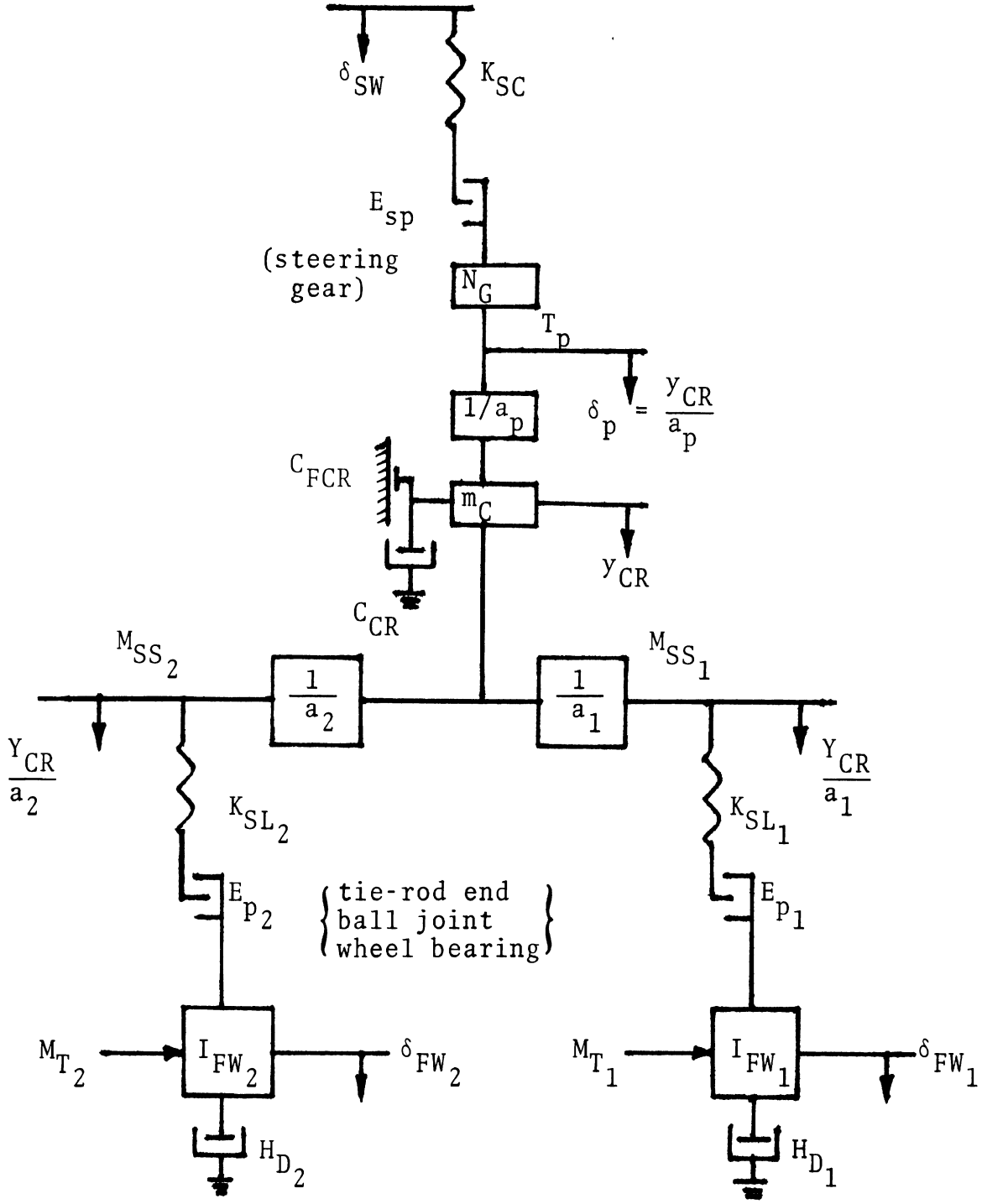

Figure III-1. Simplified steering system model

The value of the quantity E_{pi} (i=1,2) is selected to correspond to the steering free play at the front wheel due to ball joint, tie-rod end, and wheel bearing looseness. The value of E_{sp} is chosen to describe the amount of free play in the steering gear box.

CAMBER FREE PLAY

The amount of free play in front wheel camber angle, due to ball joint and wheel bearing looseness, is described by the value of the parameter ϕ_{pi}. For the degraded condition, camber angle, ϕ_{Di}, is given by

$$\phi_{Di} = \phi_i - \phi_{pi}$$

where ϕ_{pi} is positive if the tire side force is positive and ϕ_{pi} is negative if the tire side force is negative. (The symbol ϕ_i represents the non-degraded camber angle.)

WHEEL IMBALANCE

Wheel imbalance was modeled as 10 ounces of lead on the outside edge of the wheel rim. The main influence of this degradation is to produce a rotating force whose magnitude is given by

$$F = m R_{rim} \omega^2$$

where

m = 0.0194 slugs

R_{rim} = radius of the rim

ω = tire rotation rate

This force produces an oscillating moment about the steering pivot. The magnitude of this moment is given by:

$$T = F \cdot (Y_{SA} + \frac{R_{WR}}{2})$$

where R_{WR} is the rim width and Y_{SA} is the king pin offset measured at the wheel center.

SHOCK ABSORBER REPRESENTATION

The shock absorber forces were represented by piece-wise linear functions of suspension velocity. Up to 5 slopes (and 4 break-points) were allowed. These slopes and break-points were selected to provide a good fit to the shock absorber test data.

APPENDIX IV
SIMULATION STUDY RESULTS

FORD MUSTANG

An extensive simulation study of the Mustang was used to survey a large number of levels of degradation and combinations of degradation modes.

Control inputs (steering and braking functions) which caused limit performance or near limit performance were found by simulating the original equipment vehicle for each step of the test procedure for each maneuver. Then the vehicle was simulated in degraded state while operating at or near limit performance as determined for the O.E. vehicle. The set of control inputs selected for the Mustang are given in Table IV-1. Three values of control inputs were used for each of the 6 maneuvers.

Table IV- 2 contains a list of the various levels of single degradations which were used to make a thorough examination of the influence of degradation level on limit performance in the 6 open-loop vehicle handling maneuvers.

In straight line braking the minimum wheels unlocked deceleration time period to slow down from 25 mph to 10 mph* was not changed by any steering or suspension system degradation. (Obviously, reduced brake torque on one wheel increased the stopping time.) Brake imbalance wherein the braking effort on the front wheel was reduced to 0.4 or 0.1 of its normal value was shown to produce a sizeable directional response. However, a reduction to 0.7 the normal braking effort on one front wheel had a small effect upon directional response. Front brake imbalance caused more of a directional response than rear brake imbalance.

*Note that the simulation study was performed before the refinements in the test procedures were developed. Thus the old test procedures (Contract FH-11-7297 [1]) were used.

TABLE IV-1

MUSTANG O.E. RUNS SELECTED FOR DEGRADATIONS

VHTP #1	650 psi	30 mph
Straight Line Braking	675 psi	
	700 psi	
VHTP #2	625 psi	30 mph
Braking In A Turn	700 psi	
	800 psi	
VHTP #3	Run the 3 road roughness grids	
Roadholding	30 mph	
VHTP #4	δ_{sw} = -241°	30 mph
Trapezoidal Steer	= -281°	
	= -321°	
VHTP #5	δ_{sw} = -305°	60 mph
Sinusoidal Steer	= -324°	
	= -343°	
VHTP #6	Same as #5	
Drastic Steer/Brake		

TABLE IV-2

1971 FORD MUSTANG

Run	Single Degradation	
1	E_{sp} = 1.0°	Steering gear play
2	E_{sp} = 5.0°	
3	E_{pl} = 0.6°	Ball joint play
4	E_{pl} = 0.3°	
5	E_{RR} = 0.6"	Roll bar bushing play
6	E_{RR} = 1.2"	
7	$\Delta\phi_{pl}$ = 0.25°, E_{pl} = 0.25°	Wheel bearing play
8	$\Delta\phi_{pl}$ = 0.5° , E_{pl} = 0.5°	
9	.7 times OEM	Right front brake imbalance
10	.4 times OEM	
11	.1 times OEM	
12	.7 times OEM	Left front brake imbalance
13	.4 times OEM	
14	.1 times OEM	
15	.7 times OEM	Right rear brake imbalance
16	.4 times OEM	
17	.1 times OEM	
18	.7 times OEM	Left rear brake imbalance
19	.4 times OEM	
20	.1 times OEM	
21	Ek2 = -0.5, Ek1 = 0.5	Wheel alignment, TOE
22	Ek2 = -1.0, Ek1 = +1.0	
23	Ek2 = -2.0, Ek1 = +2.0	
24	Ek2 = 2.0, Ek1 = -2.0	
25	THE2 = 2, THE1 = 0	Caster
26	THE2 = -2, THE1 = 0	
27	THE2 = 4, THE1 = 0	
28	THE2 = 0, THE1 = 2	
29	THE2 = 0, THE1 = -2	

TABLE IV-2 (Continued)

Run	Single Degradation	
30	FEE2 = 0, ϕ_{s2} = 6.75, FEE1 = -1, ϕ_{s1} = -7.75	Camber and Kingpin
31	FEE2 = 0, ϕ_{s2} = 6.75, FEE1 = -2, ϕ_{s1} = =8.75	Inclination
32	FEE2 = -1, ϕ_{s2} = 5.75, FEE1 = 0, ϕ_{s1} = -6.75	
33	FEE2 = -2, ϕ_{s2} = 4.75, FEE1 = 0, ϕ_{s1} = -6.75	
34	FEE2 = 2, ϕ_{s2} = 8.75, FEE1 = 0, ϕ_{s1} = -6.75	
35	FEE2 = 0, ϕ_{s2} = 6.75, FEE1 = 2, ϕ_{s1} = -4.75	
36	K_{RS} = -.145 Z_R = 11.35	Long shackles
37	K_{RS} = -.145 Z_R = 13.35	
38	BOTH REAR = .5 times OEM	Shock Absorbers
39	BOTH REAR = .25 times OEM	
40	BOTH REAR = .1 times OEM	
41	BOTH FRONT = .5 times OEM	
42	BOTH FRONT = .25 times OEM	
43	BOTH FRONT = .1 times OEM	
44	All 4 = .5 times OEM	
45	All 4 = .25 times OEM	
46	All 4 = .1 times OEM	
47	KSL_1 = 140,000 in lb/rad	Steering linkage compliance
48	KSL_1 = 230,000 in lb/rad	

In the trapezoidal steer maneuver the simulated Mustang performance was not influenced by any steering or suspension system degradation. A typical set of computer results is shown in Table IV-3. (The run key is given in Table IV-2.) For the total set of O.E. and degraded vehicle performance studied, examinations of Table IV-3 shows that maximum lateral acceleration had a spread of only 0.021 g's and maximum yaw rate had a spread of 0.8 degrees/sec. The maximum vehicle sideslip angle changed by no more than 0.2 degrees. Apparently in these calculations the tire side forces have saturated to the point where further changes in slip angle, as may be caused by realistic levels of steering or suspension system degradation, have no effect on side force. And, thus, limit vehicle performance is not changed in the trapezoidal steer maneuver.

In the braking-in-a-turn maneuver, steering and suspension system degradations did not cause any noticeable change in average deceleration. Loss of brake torque on the front wheel on the outside of the turn had a large influence on the yaw rate and lateral acceleration response of the vehicle. At 625 psi brake line pressure, the maximum yaw rate, obtained for a brake imbalance resulting from 0.1 normal brake effort on the outside front wheel, was 28.4 deg/sec, while the original equipment vehicle obtained a maximum yaw rate of 17.5 deg/sec. The maximum yaw rate resulting from steering or suspension system degradations was from 15.7 to 18.3 deg/sec. Clearly, these results indicate that large amounts of brake imbalance have a greater influence on vehicle limit performance than large amounts of steering or suspension system degradation in braking-in-a-turn.

Simulation of the roadholding maneuver requires representation of the tire forces generated when the tires contact the road roughness grid. This phenomenon was treated in an approximate manner in the simulation. The tires were modeled as a single radial spring passing over bumps of the

TABLE IV-3

TRAPEZOIDAL STEER
321°
MUSTANG SINGLE DEGRADATIONS

RUN	DSW	AYMAX	RMAX	DELPHI	BTVMAX
OEM	321.	0.744	36.4	6.6	2.4
1	321.	0.742	35.8	7.0	2.3
2	321.	0.736	35.8	6.8	2.3
3	321.	0.743	35.4	6.8	2.3
4	321.	0.745	35.8	6.7	2.3
5	321.	0.747	36.0	6.6	2.4
6	321.	0.751	36.1	6.7	2.3
7	321.	0.757	36.0	6.7	2.3
8	321.	0.757	36.0	6.6	2.4
21	321.	0.749	36.3	6.6	2.4
22	321.	0.751	36.1	6.6	2.4
23	321.	0.753	36.2	6.6	2.4
24	321.	0.746	36.2	6.6	2.4
25	321.	0.749	36.0	6.6	2.4
26	321.	0.753	36.1	6.7	2.4
27	321.	0.749	35.6	6.6	2.3
28	321.	0.749	36.0	6.5	2.4
29	321.	0.748	36.2	6.7	2.4
30	321.	0.749	36.0	6.7	2.4
31	321.	0.748	36.2	6.7	2.4
32	321.	0.748	35.9	6.6	2.4
33	321.	0.749	35.8	6.6	2.4
34	321.	0.739	35.9	6.9	2.4
35	321.	0.745	35.7	6.9	2.3
36	321.	0.743	35.7	7.1	2.2
37	321.	0.756	35.7	7.7	2.3
38	321.	0.752	35.7	6.9	2.4
39	321.	0.740	35.8	6.8	2.3
40	321.	0.744	35.6	6.8	2.3

TABLE IV-3 (Continued)

RUN	DSW	AYMAX	RMAX	DELPHI	BTVMAX
41	321.	0.743	35.7	6.9	2.3
42	321.	0.739	35.7	6.9	2.3
43	321.	0.739	35.7	6.9	2.3
44	321.	0.741	35.6	6.9	2.3
45	321.	0.747	35.7	6.9	2.4
46	321.	0.736	35.7	6.9	2.3
47	321.	0.754	35.5	6.8	2.3
48	321.	0.740	35.9	6.9	2.3

height of the road roughness grid. Experimental runs on the simulation showed that higher or lower bump heights give less acceptable results. However, the simulation results, even though they were adjusted to appear like the test results, may not be very accurate [4].

In the roadholding maneuver, the simulation results show that heavily degraded shock absorbers can cause an increase in maximum vehicle sideslip angle. Not much change is observed when the shock absorbers are reduced to 0.5 times their O.E. value. However, when all shock absorber damping characteristics are reduced to 0.1 times their O.E. value, the simulation predicts a 4.5° increase in maximum sideslip angle in the roadholding maneuver.

For the lane change maneuver, the simulation shows that a slight change in performance was obtained with long shackles. In this case the vehicle attained a higher lateral acceleration than it did in O.E. condition without suffering an increase in peak sideslip angle. (See Table IV-4; run key in Table IV-2.) For the longer long shackle case (run 37) the sideslip was less than the sideslip angle value obtained in the other cases.

The heading angle at 5 seconds after the initiation of steering in the sinusoidal steer maneuver was increased for heavily degraded shock absorbers and for the left front wheel cambered in 2° more than O.E. Cambering out of the left front wheel results in a small reduction of final heading angle. These results indicate that wheel alignment and shock absorber degradation have an effect on final heading angle but maximum yaw rate and lateral acceleration are not greatly influenced by steering and suspension system degradations in the sinusoidal steer maneuver.

In the drastic steer/brake maneuver, the Mustang rolls to approximately 9 or 10 degrees in the O.E. or degraded state. For a steer input of 324° amplitude at 60 mph the maximum

TABLE IV-4

SINUSOIDAL STEER
VHTP #5 - 324° - 60 mph
MUSTANG SINGLE DEGRADATIONS

RUN	DSW	AYMAX	RMAX	DELPSI	DELPHI	BTVMAX
OEM	324.	0.777	43.1	*	7.0	16.2
1	324.	0.786	43.5	54.	6.9	17.1
2	324.	0.788	43.8	56.	6.9	17.6
3	324.	0.796	43.9	56.	6.9	17.7
4	324.	0.808	43.8	56.	6.8	18.0
5	324.	0.799	44.0	57.	7.0	18.3
6	324.	0.788	43.4	55.	7.1	17.7
7	324.	0.785	43.8	55.	6.9	17.4
8	324.	0.799	44.4	58.	6.9	18.4
21	324.	0.805	43.7	56.	6.9	17.6
22	324.	0.796	43.7	55.	6.9	17.4
23	324.	0.784	44.4	55.	6.9	17.8
24	324.	0.790	43.6	56.	7.0	17.8
25	324.	0.789	44.2	58.	6.9	18.3
26	324.	0.787	44.0	56.	6.9	17.7
27	324.	0.795	44.0	55.	6.9	17.4
28	324.	0.787	43.4	52.	6.9	16.3
29	324.	0.798	43.7	56.	6.9	17.8
30	324.	0.789	43.7	54.	7.0	17.2
31	324.	0.780	43.3	54.	6.9	17.1
32	324.	0.784	42.8	50.	6.9	15.9
33	324.	0.775	43.1	51.	6.9	16.2
34	324.	0.803	44.7	63.	6.9	19.5
35	324.	0.796	44.4	58.	6.9	18.6
36	324.	0.791	40.5	--	7.9	14.4
37**	324.	0.859	39.3	--	8.3	12.8
38	324.	0.793	44.2	56.	7.0	18.0
39	324.	0.784	44.5	57.	7.1	18.2
40	324.	0.796	45.3	60.	7.1	19.4

* OEM, $\Delta\psi$ = 22° at 4 sec
**Long Shackles

TABLE IV-4 (Continued)

RUN	DSW	AYMAX	RMAX	DELPSI	DELPHI	BTVMAX
41	324.	0.808	44.7	57.	7.2	18.6
42	324.	0.801	44.4	57.	7.2	18.2
43	324.	0.800	44.5	57.	7.3	18.3
44	324.	0.790	44.2	55.	7.1	17.9
45	324.	0.792	44.9	58.	7.3	18.9
46	324.	0.811	46.0	61.	7.4	20.3
47	324.	0.789	44.0	56.	6.9	17.8
48	324.	0.788	43.4	54.	6.9	17.1

roll angle reached for any degradation was 12.6°. This roll angle was obtained with all shock absorber forces reduced to 0.25 times their O.E. value. It is concluded that heavily degraded shock absorbers will increase the roll tendency of the Mustang but the simulation results indicate that the Mustang does not tend to roll over.

In addition to the single degradations listed in Table IV-2, a set of calculations were made to evaluate the influence of wheel imbalance on limit performance in all 6 maneuvers. The results show that wheel imbalance has a negligible effect in these maneuvers.

Combinations of degradation modes were studied for the Ford Mustang. Since the Mustang was the first vehicle simulated, a great variety of combinations of degradation modes were used to explore the possibility that combinations of degradations would produce larger effects than single degradations. The combinations of degradations which were used in the simulation study are given in Table IV-5. The combinations selected to be used for maneuvers with braking were different than the combinations selected for the other 3 maneuvers. Since play in tie rod ends, ball joints, wheel bearings, or the steering gear box did not prove to be important in the single degradation calculations, all four types of play were used together at a maximum reasonable level for the combined degradation simulation runs. Three different sets of front end misalignment were used. However, later in the study (after the Mustang calculations were finished), a rationale for selecting a "worst" case misalignment was developed by analyzing the influence of caster, camber, and toe in rapid turning maneuvers. The influence of level and location of shock absorber degradation was included in the calculations.

The simulation results for straight line braking show that brake imbalance is far more important than any of the

TABLE IV-5

STEERING AND SUSPENSION COMPONENT
DEGRADATION PROGRAM - 1971 FORD MUSTANG

Simulation Run Key for Combined Degradation Runs:
Straight Line Braking, Braking In A Turn, Drastic Steer/Brake

RUN NUMBER	RUN CONDITION
1	Play
2	Play + brake imbalance (0.4)
3	Play + brake imbalance (0.1)
4	Play + wheel imbalance
5	Play + wheel imbalance + brake imbalance (0.4)
6	Play + wheel imbalance + brake imbalance (0.1)
7	Play + wheel alignment - 1
8	Play + wheel alignment - 1 + wheel imbalance
9	Play + wheel alignment - 2
10	Play + wheel alignment - 2 + wheel imbalance
11	Play + wheel alignment - 3
12	Play + wheel alignment - 3 + wheel imbalance
13	Play + SArr (0.1)
14	Play + SArr (0.1) + wheel imbalance
15	Play + SAfr (0.25)
16	Play + SAfr (0.25) + wheel imbalance
17	Play + SAfr (0.25) + wheel imbalance + brake imbalance (0.4)
18	Play + SAfr (0.1)
19	Play + SAfr (0.1) + wheel imbalance
20	Play + SAfr (0.1) + wheel imbalance + brake imbalance (0.1)
21	Play + SAfr (0.1) + wheel imbalance + wheel alignment - 3 + brake imbalance (0.1)

TABLE IV-5 (Continued)

Simulation Run Key for Combined Degradation Runs: Roadholding, Trapezoidal Steer, Sinusoidal Steer

RUN NUMBER	RUN CONDITION
1	Play
2	Play + wheel imbalance
3	Play + wheel alignment - 1
4	Play + wheel alignment - 1 + wheel imbalance
5	Play + wheel alignment - 2
6	Play + wheel alignment - 2 + wheel imbalance
7	Play + wheel alignment - 3
8	Play + wheel alignment - 3 + wheel imbalance
9	Play + SArr (0.1)
10	Play + SArr (0.1) + wheel imbalance
11	Play + SAr (0.25)
12	Play + SAr (0.25) + wheel imbalance
13	Play + SAr (0.1)
14	Play + SAr (0.1) + wheel imbalance
15	Play + SAf (0.25)
16	Play + SAf (0.25) + wheel imbalance
17	Play + SAf (0.1)
18	Play + SAf (0.1) + wheel imbalance
19	Play + SAfr (0.25)
20	Play + SAfr (0.25) + wheel imbalance
21	Play + SAfr (0.1)
22	Play + SAfr (0.1) + wheel imbalance
23	Play + SAfr (0.1) + wheel imbalance + wheel alignment - 3

TABLE IV-5 (Continued)

Notes:

Brake reduction is on the right front wheel.

Wheel imbalance means: 10 oz. on rim of right front wheel

Wheel alignment - 1: EK1 = 1, EK2 = -2, THE1 = 0, THE2 = 4, FEE1 = 2, FEE2 = 0, ϕ_{s1} = -4.75, ϕ_{s2} = 6.75

Wheel alignment - 2: EK1 = 2, EK2 = -2, THE1 = 0, THE2 = -4, FEE1 = 0, FEE2 = 0, ϕ_{s1} = -6.75, ϕ_{s2} = 6.75

Wheel alignment - 3: EK1 = -2, EK2 = -2, THE1 = 0, THE2 = -4, FEE1 = 0, FEE2 = -2, ϕ_{s1} = -6.75, ϕ_{s2} = 4.75

SArr means right rear shock only.

SAr means both rear shocks.

SAf means both front shocks.

SAfr means all four shocks.

combinations of steering and suspension system degradations which were studied. Just as in the case of single degradations, combined degradations had almost no influence on the vehicle's peak yaw rate or lateral acceleration in the trapezoidal steer maneuver.

In the braking-in-a-turn maneuver any combination of degradations which included brake imbalance produced a large change in vehicle directional response. Inspection of the typical results given in Table IV-6 indicate that brake imbalance will completely mask any vehicle response changes due to the steering and suspension system degradations in a braking-in-a-turn maneuver.

For the roadholding maneuver, the simulation results indicate that degraded shock absorbers combined with front end play will usually produce an increase in yaw rate and vehicle sideslip angle. In some cases, the results show that wheel imbalance, in addition to shock absorber degradation and play, will aggravate the situation and cause even greater changes in yaw rate and sideslip angle. However, the degraded shock absorbers by themselves caused nearly the same level of change as these combined degradations. Therefore, it is concluded that shock absorber degradation alone is the most important effect in this maneuver.

The predicted limit performance in the sinusoidal steer maneuver was not greatly influenced by any of the combined steering and suspension system degradations.

The drastic steer/brake maneuver is not intended to be run with unbalanced brakes. The maneuver is defined to be run with sufficient braking to lock all 4 wheels. Nevertheless, simulation runs were made for the Mustang with large amounts (0.4 and 0.1) of brake imbalance in combination with steering and suspension degradations. The effect of brake imbalance was to cause the vehicle to develop a large yaw rate and sideslip angle. In cases with heavily degraded

TABLE IV-6

BRAKING IN A TURN
625 psi
MUSTANG COMBINED DEGRADATIONS

RUN	DSW	TQBF	TQBR	TBRAKE	AYMAX	RMAX	DELPSI	DELPHI	BTVMAX	BRAKE IMBALANCE*
OEM	90.	843.	494.	1.17	0.336	18.0	-59.	3.0	2.2	1.0
1	90.	843.	494.	1.17	0.314	17.4	-57.	2.9	2.1	1.0
2	90.	843.	494.	1.40	0.456	28.5	-77.	3.9	2.8	0.4
3	90.	843.	494.	1.51	0.547	39.0	-98.	4.6	5.5	0.1
4	90.	843.	494.	1.17	0.319	17.2	-57.	2.9	2.2	1.0
5	90.	843.	494.	1.40	0.455	28.7	-77.	3.8	2.8	0.4
6	90.	843.	494.	1.50	0.561	41.6	-101.	4.8	6.4	0.1
7	90.	843.	494.	1.15	0.280	13.6	-48.	2.5	2.3	1.0
8	90.	843.	494.	1.17	0.280	13.9	-48.	2.5	1.9	1.0
9	90.	843.	494.	1.17	0.317	18.2	-58.	3.1	2.2	1.0
10	90.	843.	494.	1.17	0.316	18.2	-58.	3.1	2.2	1.0
11	90.	843.	494.	1.17	0.329	18.5	-59.	3.1	2.2	1.0
12	90.	843.	494.	1.17	0.329	18.5	-60.	3.1	2.2	1.0
13	90.	843.	494.	1.17	0.315	17.2	-57.	2.8	2.1	1.0
14	90.	843.	494.	1.17	0.316	17.3	-57.	2.8	2.1	1.0
15	90.	843.	494.	1.18	0.319	17.5	-57.	2.9	2.2	1.0
16	90.	843.	494.	1.17	0.316	17.5	-57.	2.9	2.2	1.0
17	90.	843.	494.	1.40	0.463	28.6	-78.	4.0	2.9	0.4
18	90.	843.	494.	1.18	0.314	17.5	-57.	2.9	2.2	1.0
19	90.	843.	494.	1.17	0.316	17.6	-57.	2.9	2.2	1.0
20	90.	843.	494.	1.51	0.567	42.9	-102.	4.7	6.8	0.1
21	90.	843.	494.	1.52	0.532	37.3	-92.	4.5	5.3	0.1

*Note: 1.0 means no brake imbalance.
0.4 means a right front brake pressure reduction to 0.4 the left front brake pressure.
0.1 means a right front brake pressure reduction to 0.1 the left front brake pressure.

shock absorbers, play, wheel misalignment, wheel imbalance, and brake imbalance combined, the simulation showed that the vehicle would roll over.

For the cases without brake imbalance, the Mustang did not show a roll-over response in the drastic steer/brake maneuver.

DODGE CORONET

The Dodge Coronet and Ford Mustang simulation results were used to plan the pilot test program. Due to the experience gained in simulating the Mustang, it was possible to greatly reduce the Dodge simulation study in order to get useful results before the pilot test program started. Approximately 1260 separate vehicle maneuvers were simulated in the Ford Mustang study (not counting preliminary runs) while about 400 maneuvers were simulated for the Dodge Coronet.

The single degradations selected for the Coronet simulation study are given in Table IV-7. (Obviously, the brake imbalance cases were not run in maneuvers with no braking.) For straight line braking and trapezoidal steer the simulated vehicle responses were insensitive to steering and suspension system degradations. The change in lateral accelerations from the highest to the lowest value achieved in degraded or O.E. state for trapezoidal steer was 0.03 g's and the yaw rate peak did not vary more than 2 deg/sec from its lowest to its highest value. The vehicle response is insensitive to steering and suspension system degradations in these two maneuvers. Thus, it was decided not to make any combined degradation calculations for these maneuvers.

For the braking-in-a-turn maneuver simulation runs were made with 675 psi brake line pressure. With the brake torque reduced on the right front wheel, the vehicle developed a larger yaw rate and lateral acceleration than it had in its initial left turn. The left front and the left rear wheels

TABLE IV-7

STEERING AND SUSPENSION COMPONENT DEGRADATION PROGRAM

Run Key for Single Component Degradations - 1971 Dodge Coronet

RUN NUMBER	SIMULATION CONDITION
1	OEM
2	Steering gear play - 1, E_{sp} = 4°
3	Steering gear play - 2, E_{sp} = 8°
4	Ball joint play, E_{p1} = 0.6°, E_{p2} = 0.6°
5	Camber play, ϕ_{p1} = 0.5°, E_{p1} = 0.5°, ϕ_{p2} = 0.5°, E_{p2} = 0.5°
6	Wheel imbalance, right front (10 oz. on the rim)
7	Brake imbalance, right front (0.4)
8	Brake imbalance, right front (0.1)
9	Brake imbalance, left front (0.4)
10	Brake imbalance, left front (0.1)
11	Brake imbalance, right rear (0.4)
12	Brake imbalance, right rear (0.1)
13	Brake imbalance, left rear (0.4)
14	Brake imbalance, left rear (0.1)
15	Toe - 1, EK1 = +2.0°, EK2 = -2.0°
16	Toe - 2, EK1 = -2.0°, EK2 = +2.0°
17	Caster offset - 1, THE1 = 2.0°, THE2 = 2.0°
18	Caster offset - 2, THE1 = -2.0°, THE2 = -2.0°
19	Camber offset - 1, FEE1 = 0, ϕ_{s1} = -7.5°, FEE2 = -2°, ϕ_{s2} = 5.5°
20	Camber offset - 2, FEE1 = 0, ϕ_{s1} = -7.5°, FEE2 = 2°, ϕ_{s2} = 9.5°
21	Camber offset - 3, FEE1 = -2°, ϕ_{s1} = -9.5°, FEE2 = 0, ϕ_{s2} = 7.5°
22	Camber offset - 4, FEE1 = 2°, ϕ_{s1} = -5.5°, FEE2 = 0, ϕ_{s2} = 7.5°
23	Rear shock absorbers, 0.1
24	Rear shock absorbers, 0.25

TABLE IV-7 (Continued)

RUN NUMBER	SIMULATION CONDITION
25	Rear shock absorbers, 0.5
26	Front and rear shock absorbers, 0.5
27	Front and rear shock absorbers, 0.25
28	Front and rear shock absorbers, 0.1

locked up due to the increased lateral load transfer which was caused by the higher lateral acceleration rate.

A 10 "bump" grid was selected for the roadholding study. No single degradation produced a large change in vehicle response for this maneuver. Degraded shock absorbers did cause about a 1° increase in vehicle sideslip angle.

For the sinusoidal steer maneuver, the simulation predicted a roll oscillation of the rear axle (axle tramp) when the shock absorbers were degraded to 0.25 or 0.1 times their O.E. value. The result of this oscillation was to obtain less rear side force from the rear tires and thus, greater yaw rate and sideslip angle than the O.E. vehicle.

In the drastic steer/brake maneuver, the simulation predicted that the Coronet would roll over with all shock absorbers being 0.25 or 0.1 times as effective as the O.E. shock absorbers.

Table IV-8 lists the combinations of degradations studied for the Dodge Coronet in braking-in-a-turn, roadholding, sinusoidal steer and drastic steer/brake. Clearly, the cases with the least damping (0.1 shock absorbers in the rear or front and rear) produced the greatest changes from O.E. performance. With degraded shocks, the simulation predicted roll over in drastic steer/brake and axle tramp in the sinusoidal steer maneuver. The combined degradations did not produce appreciably worse results than the single degradations.

SIMULATION PHASE 2 - THE OTHER SIX VEHICLES

The following five categories of degradation were considered in the simulation of the Ambassador, Austin, Chevrolet Brookwood, Ford F-100 pickup truck, Oldsmobile F-85, and VW Super Beetle:

1. Play with $E_{sp} = 8°$ (from the steering gear box)

   $E_{p1} = E_{p2} = 1.2°$ (from ball joints, tie rod ends, and wheel bearings)

TABLE IV-8

STEERING AND SUSPENSION COMPONENT DEGRADATION PROGRAM

Run Key for Combined Degradation Effects: 1971 Dodge Coronet

RUN NUMBER	DEGRADATION CONDITION
X00	OEM
1	Combined play + LF wheel imbalance
2	Play + RF brake imbalance (0.4)
3	Play + RF brake imbalance (0.1)
4	Play + LF wheel imbalance + wheel alignment
5	Play + LF wheel imbalance + wheel alignment + SA-rear (0.1)
6	Play + LF wheel imbalance + wheel alignment + SA-rear (0.5)
7	Play + LF wheel imbalance + wheel alignment + SA-front, rear (0.5)
8	Play + LF wheel imbalance + wheel alignment + SA-front, rear (0.1)

NOTE:

Play means: $E_{sp} = 8°$, $E_{p1} = E_{p2} = 1.1°$, and $\phi_1 = \phi_{p2} = 0.5°$

Wheel imbalance means: 10 oz. on the rim of the left front wheel

Wheel alignment means: EK1 = 2°, EK2 = -2°
THE1 = -2°, THE2 = -2°
FEE1 = -2°, FEE2 = 0
$\phi_{s1} = -9.5°$, $\phi_{s2} = 7.5°$

$\phi_{p1} = \phi_{p2} = 0.5°$ (from ball joints and wheel bearings)

2. Wheel imbalance - 10 oz. of lead on the outer rim of the left front wheel

3. Brake imbalance - right front brake pressure 0.7 times O.E. and 0.4 times O.E.

4. Wheel alignment changes from O.E.

	Left Wheel	Right Wheel
Toe:	EK2 = +2°	EK1 = -2°
Caster:	THE2 = -2°	THE1 = -2°
Camber:	FEE2 = 0	FEE1 = -2°

5. Shock absorber force - 0.5, 0.25, and 0.1 times O.E.

The levels of play parameters (E_{sp}, E_{p1}, E_{p2}, ϕ_{p1}, and ϕ_{p2}) were selected to correspond to the maximum reasonable levels of degradation which could be obtained without structural failure of ball joints, tie rod ends, wheel bearings and steering gear box. A very large amount of wheel imbalance was selected. (Normally, the maximum lead weight, used in passenger car tire balancing, is 5 ounces.) Reduced braking was applied on the right front wheel in order to obtain a large influence in a left turn. The wheel alignment changes were selected to cause a tendency for more extreme left turns while minimizing the driver's ability to correct for the misalignment by re-centering the steering wheel. Both wheels are toed in 2° more than the original equipment values. The side force on the heavily loaded wheel in a drastic turn is increased and is in the direction of the turn. The caster of the wheels is selected to reduce the mechanical trail and thereby reduce the moment tending to align the wheels with their direction of travel. The magnitude of the camber angle on the heavily loaded wheel in a left turn is increased in a direction which will produce

more force to the left. Clearly, the intention of the selection of degradations is to cause the vehicle to turn left more rapidly and accentuate any spin-out or roll-over tendencies.

In order to make the simulation study as cost-effective as possible, degradations and combinations of degradations were selected for each maneuver. The conditions used in the simulation of each car are listed in Table IV-9.

In straight line braking, brake imbalance was the only important degradation mode for any of these vehicles. The simulation indicated that there is a wide range of maximum wheels unlocked braking performance for these vehicles in O.E. condition.

In turning maneuvers, the Austin and VW simulation results appear to be in error. In a recently published report [4], it is shown that the simulation does not predict the correct roll angle for the VW. For the work in [4], a rear roll center concept was used. In this case, independent swing axle equations were employed, but they did not provide reasonable answers. Accordingly, in the remainder of this section, the Ambassador, F-100, F-85, and Brookwood results will be discussed.

Table IV-10 contains a summary of the trapezoidal steer results for the degradation conditions given in Table IV-9. Examination of the table indicates that these steering and suspension system degradations have negligible influence on trapezoidal steer results.

Brake imbalance causes a greater change in vehicle response in the braking-in-a-turn maneuver than any of the steering and suspension degradations for the Ambassador, Olds F-85, Ford pickup, and Chevrolet Brookwood. This same type of result was obtained for the Dodge Coronet and the Mustang. It is clear that a brake imbalance, which is 0.4 times the O.E. value for a front wheel, is a more serious degradation than any of the other degradations studied.

TABLE IV-9

DEGRADATIONS SELECTED FOR SIMULATION

Notation: 1, combined play
2, wheel imbalance
$3_{(x)}$, brake imbalance (x=fraction of OEM)
4, wheel alignment
$5_{(x)}$, shock absorber (x=fraction of OEM)

Straight Line Braking	Braking In A Turn	Roadholding	Trapezoidal Steer
$3_{(.4)}$	1	1	2
$3_{(.7)}$	2	2	1
$3_{(.7)}+2$	$3_{(.4)}$	4	4
$3_{(.7)}+1$	4	1+2	1+2
$3_{(.7)}+1+2$	1+2	1+4	1+4
$5_{(.5)}+3_{(.7)}+1$	$1+3_{(.7)}$	2+4	1+2+4
$5_{(.5)}+3_{(.7)}+2$	1+4	1+2+4	$5_{(.5)}$
$5_{(.1)}+1+2+4$	$1+2+3_{(.7)}$	$5_{(.5)}$	$5_{(.5)}+2$
$5_{(.1)}+1+2+3_{(.7)}+4$	1+2+4	$5_{(.5)}+1$	$5_{(.5)}+4$
	$2+3_{(.7)}+4$	$5_{(.5)}+2$	$5_{(.5)}+1+2$
	$1+2+3_{(.7)}+4$	$5_{(.5)}+4$	$5_{(.5)}+1+4$
	$5_{(.5)}+3_{(.7)}$	$5_{(.5)}+1+2$	$5_{(.5)}+1+2+4$
	$5_{(.5)}+3_{(.7)}+2$	$5_{(.5)}+1+2+4$	
	$5_{(.5)}+3_{(.7)}+4$	$5_{(.25)}$	
	$5_{(.5)}+1+2+3_{(.7)}$	$5_{(.25)}+1+2+4$	
	$5_{(.5)}+1+3_{(.7)}$	$5_{(.1)}+1+2+4$	
	$5_{(.5)}+1+4$		
	$5_{(.5)}+1+2+4$		

TABLE IV-9 (Continued)

Straight Line Braking	Braking In A Turn	Roadholding	Trapezoidal Steer
	$^{5}_{(.5)}{}^{+1+3}_{(.7)}{}^{+4}$		
	$^{5}_{(.5)}{}^{+1+2+3}_{(.7)}{}^{+4}$		
	$^{5}_{(.25)}{}^{+1+2+3}_{(.17)}{}^{+4}$		

NOTE: Sinusoidal Steer is the same as Roadholding.
Drastic Brake/Steer is the same as Roadholding.

TABLE IV-10

SUMMARY OF TRAPEZOIDAL STEER RESULTS

Vehicle	Input	O.E. Result	Range of Degradation Results
Ambassador	393°	A_{ymax} = .74g	.732g $\leq A_y \leq$ .759g
		r_{max} = 39.4 deg/sec	38.3 deg/sec $\leq r \leq$ 39.6 deg/sec
		β_{max} = 4.4°	3.8° $\leq \beta \leq$ 4.4°
Olds F-85	326°	A_{ymax} = .808g	0.797 $\leq A_y \leq$ 0.816g
		r_{max} = 45.2 deg/sec	44.0 deg/sec $\leq r \leq$ 45.5 deg/sec
		β_{max} = 6.2°	5.6° $\leq \beta \leq$ 6.2°
Chevrolet Station Wagon	349°	A_{ymax} = .863g	.858g $\leq A_y \leq$ .914g
		r_{max} = 49.8 deg/sec	48.6 deg/sec $\leq r \leq$ 50.1 deg/sec
		β_{max} = 6.3°	5.9° $\leq \beta \leq$ 6.3°
F-100 Truck	462°	A_{ymax} = .907g	.891g $\leq A_y \leq$ .928g
		r_{max} = 47.0 deg/sec	45.4 deg/sec $\leq r \leq$ 47.1 deg/sec
		β_{max} = 8.5°	7.8° $\leq \beta \leq$ 8.5°

In the roadholding maneuver, the simulation shows that in degraded condition one vehicle, the Ambassador, will develop a very large sideslip angle (spin out) while passing over the roadholding grid. It is felt that this may be an artifact of the simulation because the other three vehicles do not tend to spin out. A summary of the results for the Ford pickup, Chevrolet Brookwood, and Olds F-85 is given in Table IV-11. The largest sideslip angle is obtained for the combined degradation case consisting of 0.1 shock absorber forces, combined play, wheel imbalance, and wheel misalignment. Of these degradations, the 0.1 shock absorber force is the most significant contributor to the increase in sideslip angle.

The sinusoidal steer results are summarized in Table IV-12. Examination of Table IV-12 shows that the Ambassador is sensitive to steering and suspension system degradations and the other three vehicles are not. With degraded shock absorbers (0.5, 0.25, or 0.1), alone or combined with other degradations, the Ambassador obtains changes in heading angle from 21° to 44°. Thus, the level of shock absorber force was shown to be important for the Ambassador in the sinusoidal steer maneuver.

In the drastic steer/brake maneuver, the simulation predicted that the degraded Ambassador would spin out and roll over. The roll-over prediction was made for degradation combinations with shock absorber force levels reduced to 0.25 and 0.1 times their O.E. value. For the other vehicles, the maximum roll angle was predicted for the heavily degraded shock absorber condition but the roll angle was not near to the critical angle for roll over instability. The peak O.E. and degraded roll angles are as follows:

Vehicle	O.E.	Degraded
Olds F-85	9.2°	12.1°
Chevrolet Station Wagon	7.5°	8.6°
Ford Pickup	7.1°	10.7°

TABLE IV-11

SUMMARY OF ROADHOLDING RESULTS

Vehicle	Grid	β_{max} O.E.	Range of β_{max} for Degradation
Ford Pickup	9 hz (8 bumps)	0.8°	$0.7° < \beta_{max} < 2.7°$
Chevrolet Brookwood	9 hz (8 bumps)	2.6°	$1.5° < \beta_{max} < 4.8°$
Olds F-85	11 hz (10 bumps)	1.2°	$0.8° \leq \beta_{max} \leq 1.6°$

TABLE IV-12

SUMMARY OF SINUSOIDAL STEER RESULTS

Vehicle	Steer Level and Velocity	O.E. Responses	Range of Degradation Responses
Ambassador	60 mph $\delta_{sw} = 319°$	$\Delta\psi = 12°$	$11° \leq \Delta\psi \leq 44°$
Olds F-85	60 mph $\delta_{sw} = 198°$	$\Delta\psi = 35°$	$27° \leq \Delta\psi \leq 40°$
Chevrolet Brookwood	50 mph $\delta_{sw} = 160°$	$\Delta\psi = 32°$	$30° \leq \Delta\psi \leq 35°$
Ford Pickup	60 mph $\delta_{sw} = 264°$	$\Delta\psi = 33°$	$25° \leq \Delta\psi \leq 41°$

By careful selection of conditions and inputs for each maneuver, it was possible to obtain useful results with about 130 computer runs per vehicle. Thus, about 800 computer runs were made to complete Phase II of the simulation study.

APPENDIX V

MECHANICAL SIMULATION OF DEGRADATION MODES

A study of vehicle sensitivity to degraded components requires that degradations be introduced sufficient to point out such sensitivity. Previous study had indicated that the change in handling characteristics due to some of the proposed degradations is small. With this in mind, it was decided to develop means for introducing as large a degradation as possible, it being assumed that if the vehicle is insensitive to a large degradation, it certainly will be insensitive to a smaller one. In general, degraded components were prepared to represent the Virtual Maximum Rational Wear (VMRW) that would be found among in-service components. An amount of wear or degradation larger than that defined as the VMRW value would be unrealistic or jeopardize the structural integrity of the component under load. It follows that an amount of wear or degradation smaller than the VMRW value would be less likely to show vehicle sensitivity to the degraded component.

The degradations introduced into the test vehicles are grouped into five categories. They are front-end lash, wheel imbalance, brake imbalance, wheel alignment, and shock absorbers. In keeping with the VMRW concept mentioned above, it became necessary to provide degradations in each category which were as large as possible and yet not compromise any of the mechanical constraints of the components. It was also desired that the degradations be relatively simple to introduce and that they not prevent returning the vehicle to an undegraded condition.

FRONT-END LASH

Front-end lash consists of looseness in ball joints, tie-rod ends, steering gear and wheel bearings. These elements provide two classes of steering tightness degradations. There are those degradations which allow the position of both front wheels to be indeterminate from steering wheel position even though the position of one wheel relative to the other is known. Such would be the case when the gear box is worn or loose on the vehicle, with all parts from the pitman arm to the wheels in good condition. Secondly, there are those degradations which allow one wheel to move independently of the other and/or the steering wheel. This behavior results when tie-rod ends or idler-arm bushings become worn. Each of these conditions was provided physically by a different mechanism. These separate means are thus described below.

The first degradation category, that of both wheels operating together but independently of the steering wheel, can be produced by introducing lash in the steering gear box. The procedure for tightening a loose steering gear box is well spelled out in the service manual for each vehicle where this adjustment is possible. Reversing this procedure produces a loose steering system by introducing clearance between the sector gear and the worm.

The second degradation category is produced by either loose ball joints or loose tie-rod ends. A decision was made to introduce ball joint play by modifying the original equipment ball joints themselves. In much of the earlier work comparable to this study, attention was confined to the loaded ball joint because it normally shows the greatest wear. The wear that occurs, however, is in an axial direction parallel to the ball stud. Thus, with the vehicle weight supported by the ball joint, the ball stud is forced deeper

into its socket to take up virtually all lateral play that accompanies wear in the axial direction. In order to limit the number of ball joints to be modified and yet obtain meaningful insight into the relationship between ball joint wear and vehicle performance, it was decided to confine our attention to the follower or unloaded ball joint. Lateral play on this unit is much more likely to result in wheel position indeterminancies because of the absence of a large axial load to force the ball stud and socket together.

Making a rational selection of the maximum degradation to be simulated in tie-rod ends and ball joints is very difficult. No data bank exists on the amount of wear that is typically found on these components of in-service vehicles. In fact, the methods of determining the extent of component wear vary widely among service facilities. This is to say nothing about the maximum wear permitted before the part is to be replaced. In some cases, manufacturers have listed tolerances in their service manuals. All too frequently, the service manuals omit the inspection procedure or merely say that the component should be replaced if wear is excessive.

No two sets of tie-rod ends or ball joints are identical. However, the same maximum lateral freedom was provided in all ball joints and tie-rod ends and an adjustment mechanism was incorporated, permitting reduction of the radial play to zero, for representing the baseline condition.

The tie-rod ends on the Mustang were the first to be modified. Consequently, these modifications became a model for all later modifications. Disassembly of this unit revealed a spherical wear shim placed between the ball stud and the outer socket. The thickness of this shim is about

.040". If the shim were completely worn out, the ball stud would separate from the socket. Therefore, the maximum lateral freedom was chosen to be twice the thickness of the wear shim (because it is on both sides of the ball stud) or .080". "Virtually maximum wear" was achieved by grinding about .050" from the diameter of the ball stud, leaving sufficient material to prevent separation. In all subsequent modifications to tie-rod ends, these dimensions served as a target. It was not possible to produce the desired amount of lateral freedom in all cases because of construction details.

Similar procedures were followed in arriving at the maximum amount of lateral movement in ball joints. The typical ball joint modification which was implemented is shown in Figure V-1.

Disassembly of several different units indicated a spherical wear bushing over the ball stud with lubrication grooves .025" deep. These grooves provided a convenient reference such that their elimination by grinding resulted in a .050" reduction of the diameter of the wear bushing. Actual measurements on the resulting sample of degraded ball joints indicated maximum lateral play ranging from .050" to .075".

Another point considered in modifying ball joints and tie-rod ends to represent the worn state was the necessity to preserve authenticity of the load-lash relationship. Due to the construction of modern ball joints and tie-rod ends, introducing axial play in a new unit does not necessarily result in radial play. On the other hand, once radial play is introduced by grinding the ball, it is not possible to simulate the non-degraded condition without providing an artificial axial constraint to prevent radial play from being realized. Thus it was decided to modify the ball joints and tie-rod ends to produce two conditions.

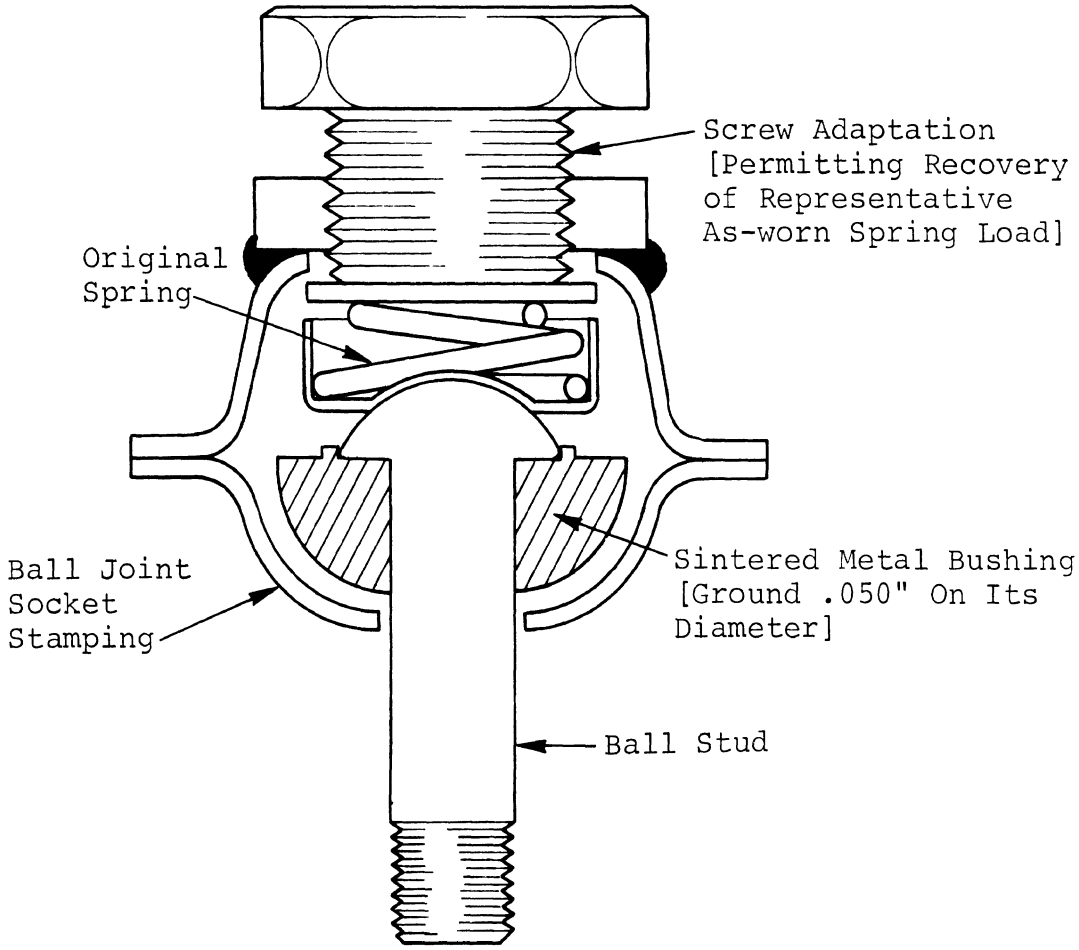

Figure V.1. Modified Ball Joint Assembly. (This modification also typifies the alterations to tie rod ends.)

The first condition represents a new unit with virtually no radial or lateral movement. This condition is achieved by providing a hard stop which can be placed against the ball to prevent axial and thus radial movement of the ground ball stud.

The second condition is that of a hypothetically worn unit which, even though worn, has spring pressure on the ball resulting in some load/deflection relationship. In order to preserve this relationship, some estimate of the amount of spring pressure on the ball, when worn, had to be made. This estimate was produced by making measurements on the new and degraded units. The amount of spring deflection in a new unit and the amount of axial movement resulting from grinding the ball were determined. From these measurements the amount of spring deflection required in the worn unit was calculated. Knowing the lead on the adjusting screw that was incorporated into the ball joint assembly, the number of turns required to produce this deflection was found. It was not necessary that the actual load in pounds ever be known.

The other contributor to front wheel indeterminacy, wheel bearing play, was simulated simply by backing off on the spindle nut. In achieving the VMRW level of wheel bearing play the spindle nut was loosened to the furthest position which would still permit attachment of the cotter pin, within a maximum of two full turns beyond the zero lash condition.

WHEEL ALIGNMENT

In attempting to create a worst case wheel alignment in accordance with the VMRW concept, it was necessary to consider the character of the maneuvers performed and the

effect of misalignment on the directional behavior of a vehicle. A cambered wheel, if unrestrained, tends to follow a curved path whose radius is equal to the distance between the point of intersection of the axle (if extended) with the ground and the tire contact point. This then is a steer effect. A right wheel cambered in at the top will tend to steer the vehicle to the left.

Caster relates to directional behavior in that it affects the aligning moment of the front wheels, resulting in steering displacements in the presence of either compliance or lash. If caster is positive, the aligning moment tends to return the wheels to a straight ahead position and if negative, tends to cause the wheels to turn more sharply.

Toe is, in effect, a bias setting of the steered wheels. If the wheels are toed in, the outside wheel in a turn (more heavily loaded) has a greater steer angle than if the wheels are toed out. The nonlinear mechanics of the pneumatic tire indicate that the more heavily loaded wheel has the greater influence on the directional response of the vehicle in a limit turn. The above reasoning taken with the fact that most test maneuvers required turns to the left, lead to a worst case alignment condition.

In general, degraded alignment corresponding to the VMRW condition was defined as maximum negative camber of the right wheel, maximum negative caster of both wheels, and not over 2" of toe in. Note that both wheels are not cambered because such a setting would produce a neutral condition if both wheels were cambered in (or out) or would produce a steer offset if one wheel were cambered in and the other out at the top. Accordingly, the left wheel is set to the O.E. camber value while the right is set to the maximum negative value possible.

WHEEL IMBALANCE

The largest wheel imbalance likely to be found in service is somewhat larger than the largest weight that can be used to correct it. A 5-ounce weight is the largest weight commonly used to balance a wheel. Therefore, it was decided that 10 ounces of weight located on one side of a wheel would create a virtually maximum level of wheel imbalance. In fact, it is difficult to place much more weight than this on one side of a wheel without covering more than half the circumference of the rim.

BRAKE IMBALANCE

Brake imbalance was created by differential brake pressures among the four wheels during braking. This method of providing brake imbalance was chosen rather than modifying brake shoes, drums or wheel cylinders because it permits rapid and precise adjustment of individual wheel braking effort.

A pressure limiting device was built to control hydraulic pressures during braking. As shown in Figure V-2, lines from the right-front, left-front brake, both rear brakes, front piston of the master cylinder and rear piston of the master cylinder lead to a valve manifold where each can be connected to either of two accumulators. The accumulators can be set independently to any desired level of nitrogen precharge pressure which then becomes the limiting value of brake pressure for any lines connected to it. For normal undegraded braking, the valves are set such that all lines lead to one accumulator. The precharge on that accumulator would be the maximum pressure that could be generated in any part of the brake system.

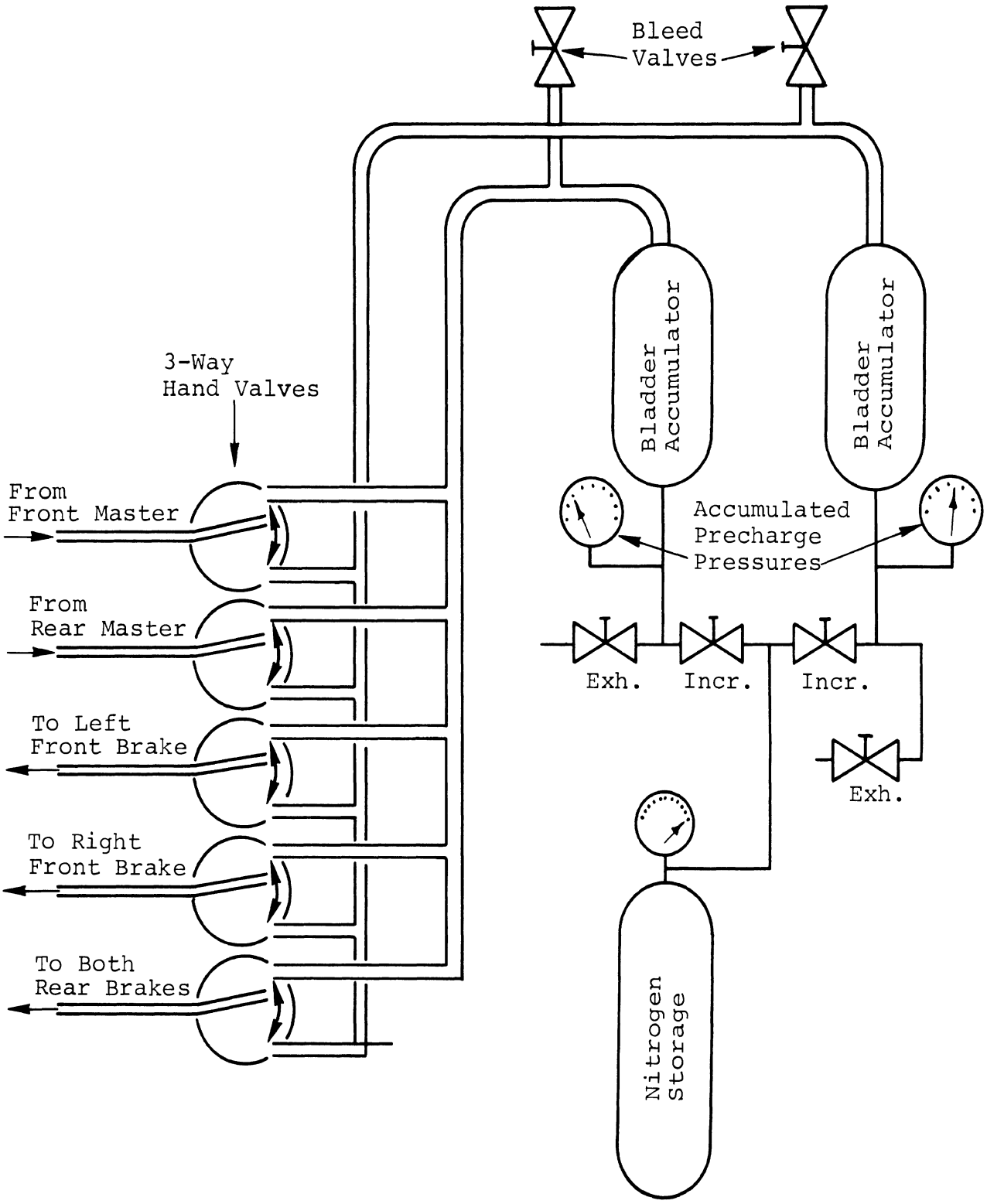

Figure V-2. Brake limiter assembly

The limiter is operated merely by depressing the brake pedal fully, dispensing fluid from the master cylinder at increasing pressure up to the precharge level. Additional fluid displaced from the master cylinder flows into the bladder accumulator at essentially constant pressure.

SHOCK ABSORBER DEGRADATION

The application of the VMRW concept to shock absorber degradation resulted in the more or less obvious selection of large fluid loss as a degradation mechanism. In addition, however, due to the conviction that near total loss of wheel damping would yield decidedly positive sensitivity findings, it was decided to also construct shock absorbers which simulated a "non-maximum degradation" but did incorporate alteration of dimensional clearances as large as might be found in service.

The Monroe Auto Equipment Company provided two shock absorber variations to meet these performance degradation conditions:

1. Shock absorber with 90% of its fluid removed, which was used only in pilot testing, and
2. Shock absorber upon which (a) machining of the rod guides and piston and (b) fracturing of the orifice disc provided an intermediate performance degradation.

Force velocity measurements made in the laboratory indicated that a small amount of coulomb friction (about ±10 lbs) was the only damping force remaining in shock absorbers with 90% fluid removed. Measurements made on shock absorbers with heavily worn rod guides and pistons, however, showed that certain models had lost almost 50% of their original equipment force while others indicated less than 25% loss in equivalent damping force at high actuation velocities.

APPENDIX VI

AUTOMATIC VEHICLE CONTROLLER

THE REQUIREMENT FOR AN AUTOMATIC CONTROLLER

Open-loop test procedures are designed to evaluate the properties of a vehicle minus the driver. Consequently, a requirement exists for minimizing driver influence in test execution. Despite the ability of many test drivers to apply control inputs in an open-loop manner without regard for vehicle response, there reside certain limitations on input fidelity which the driver is incapable of improving.

Driver control is, in general, deemed to be an acceptable method in those test procedures in which the observed lack of driver precision is known to have a negligible effect on vehicle response or in which the influence of imprecise inputs are significant but can be tolerated by virtue of data interpretation schemes which focus on specific aspects of the overall response.

In certain open-loop limit performance test procedures, however, control input functions are required which place unreasonable demands upon a test driver for their adequate application. Imprecision of driver control input poses problems in the provision of:

1. initial velocity
2. steering function shape
3. braking function shape
4. phase relationship between steering, braking and accelerator inputs.

In the sinusoidal steer procedure, for example, the requirement for accuracy of the steering function shape, as well as level, automatically eliminates the unaided driver as a viable controller. Certain mechanical measures can be employed as aids in executing simple inputs, such that the driver is enabled to act simply as a power element (such as the application of a quasi-constant rotational rate of steering displacement until contacting a mechanical stop, for provision of a trapezoidal steer function). Where feasible, simple devices are generally desirable to insure control input fidelity without requiring an excessive hardware burden.

In test maneuvers involving complex inputs, e.g., combined applications of steering and braking, servo actuation becomes attractive. Moreover, in the research context, the versatility and precision of a programmable automatic control system is required. Only by the use of such a system can a vast regime of potential test procedures be considered in an efficient manner. Further, by virtue of the precision that an automatic controller provides, the effects of imprecision can be systematically studied to determine the extent to which simplified methods might be acceptable.

THE HSRI AUTOMATIC VEHICLE CONTROLLER

An Automatic Vehicle Controller has been developed at HSRI which replaces the driver with servomechanisms that provide control actuation to the steering shaft, brake and accelerator pedals. By way of a radio control transmitter (Figure VI-1), operated from a "chase" vehicle, continuous control of steering, braking and acceleration is achieved

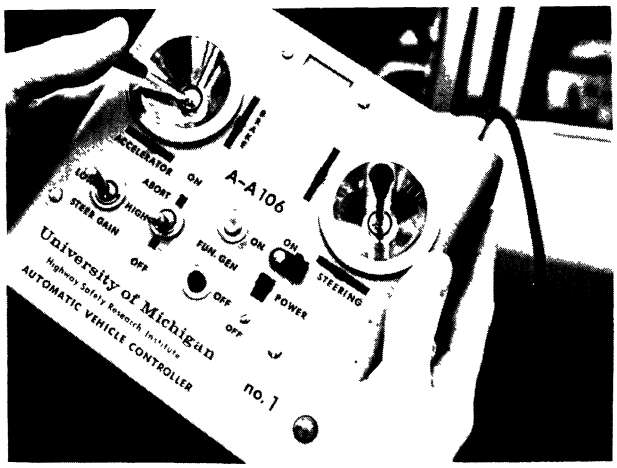

Figure VI-1.
Radio control transmitter.

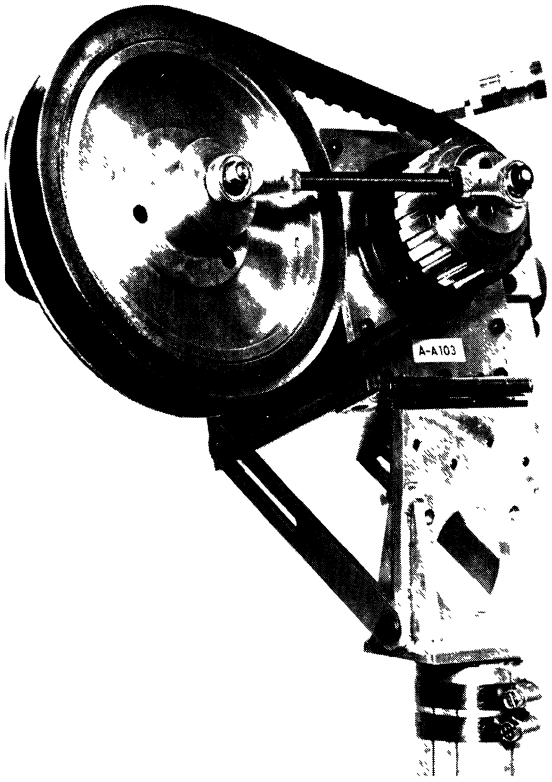

Figure VI-2.
Steering servo.

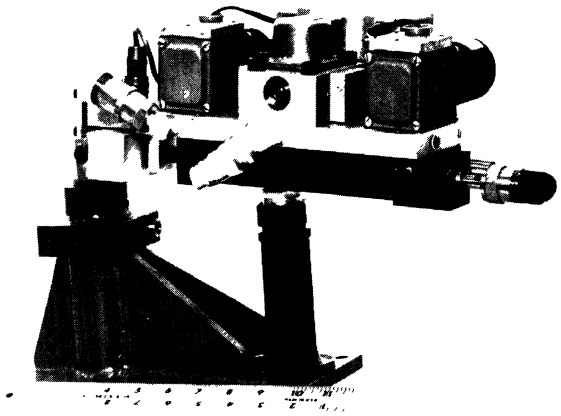

Figure VI-3.
Brake servo.

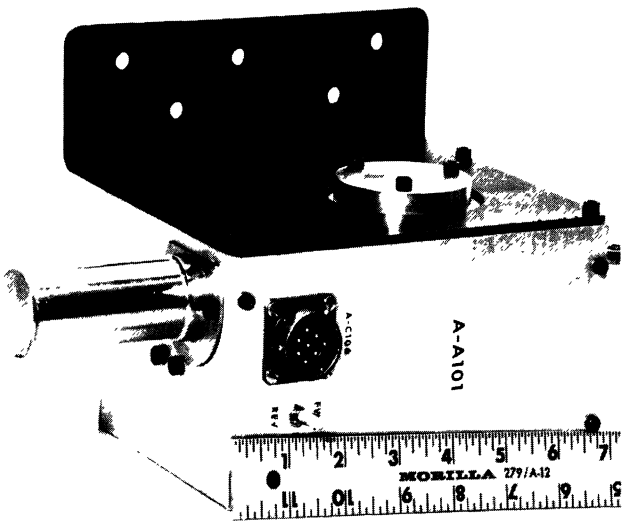

Figure VI-4.
Accelerator servo.

while the test vehicle is being guided as a drone. Upon command from the transmitter operator, the drone mode is interrupted to permit a pre-programmed set of control input time histories to be generated by the installed servos. The desired program of control inputs is generated from circuitry constituting an on-board function generator.

The time at which the stored program is initiated is determined by a circuit which compares the actual velocity of the vehicle with the programmed level, thereby providing precise control of the initial velocity desired for a given test.

It is desirable that the performance of the steer and brake servomechanisms have a relatively broad bandwidth compared to the low frequency content of possible control inputs in order to assure a high level of precision in input time histories. Steer and brake servos have been designed to provide linear operation over a bandwidth in excess of 30 Hz. The steer servo (Figure VI-2) has a torque capability of 50 ft/lbs at the steering shaft which torque can be achieved at its design rotational velocity, 1300 deg/sec. The brake servo (Figure VI-3) has a peak force capability of 400 lbs, which force can be achieved at its peak translational rate, 130 in/sec.

The accelerator actuator (Figure VI-4) is a relatively low performance servo, with a 12 Hz bandwidth, and a 16 lb force capability.

The function generator (Figure VI-5) operates with a single master clock which controls the timing of the program events over a maximum program term of 10 seconds.

Steer function inputs can assume either a sinusoidal or trapezoidal waveshape, or any superposition of the two. Single sine waves are initiated at a time, t_1, and if

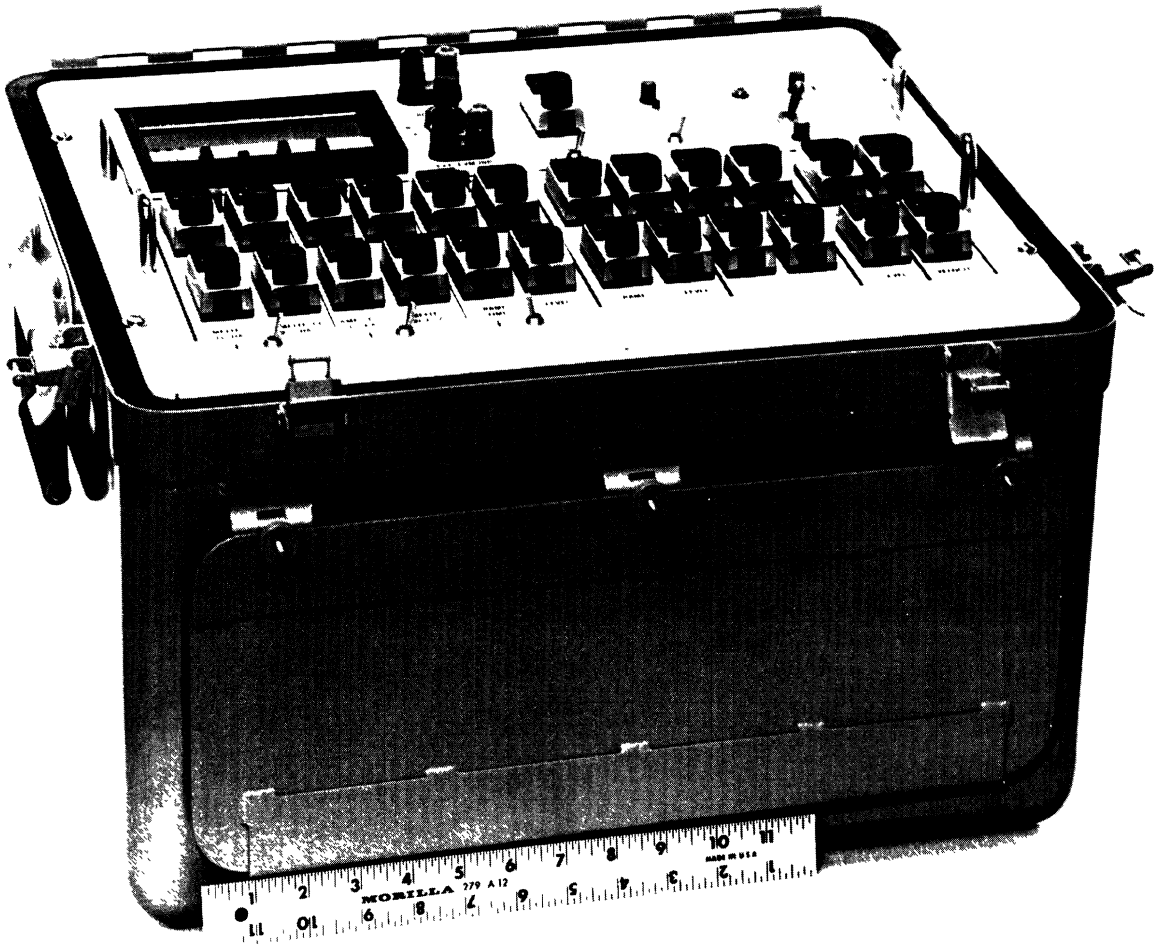

Figure VI-5a.
Programmed function generator.

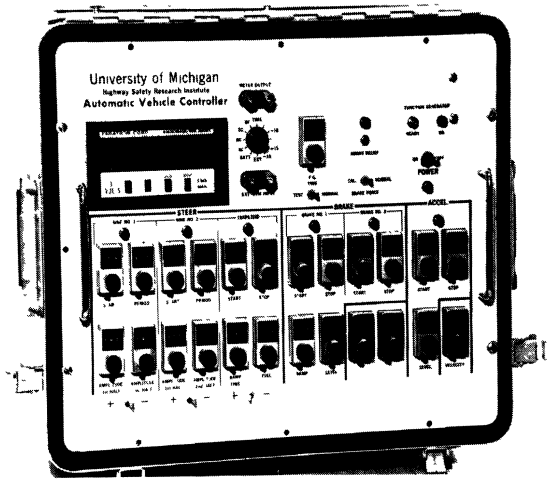

Figure VI-5b.
Function generator control panel.

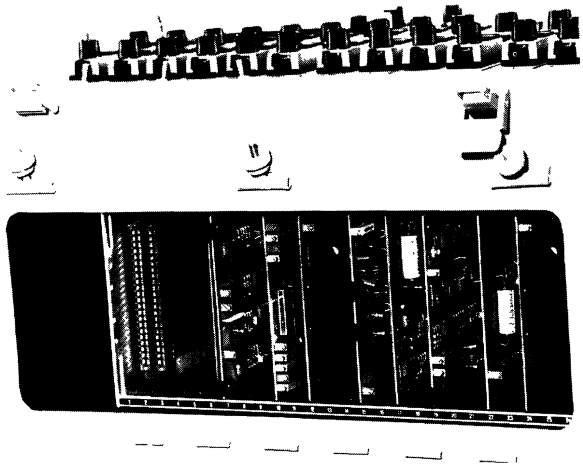

Figure VI-5c.
Function generator circuit cards.

desired, a second sine wave can be initiated in the same program at t_2 (see Figure VI-6). The period, T_1 and T_2, of each wave is adjustable, as is the amplitude of each "half wave," A_1, A_2, A_3, and A_4. Either wave may be inverted independently of the other. A half sine wave is obtained merely by selecting a single wave whose A_2 amplitude is set to zero.

Steering trapezoids can be produced having the general configuration shown in Figure VI-7, with adjustable parameters, t_3, t_4, A_5, and S_1. This wave shape can also be inverted.

Braking inputs can be generated with trapezoidal wave shapes as in Figure VI-8. Two successive trapezoids are available with selectable parameters, t_5, t_6, t_7, t_8, S_3, and A_6. A brake application or release can be selected to occur at any time in the program, but the obvious logical conflicts must be avoided (t_6 must be greater than t_5, etc.).

Accelerator inputs can be programmed into a maneuver as step functions only. Both the on/off times and level are adjustable.

The power requirements for the controller are provided by the test vehicle's engine. A pressure compensated variable displacement pump is driven by the engine through a V belt, Figure VI-9. The pump draws fluid from a reservoir, Figure VI-10, delivering a maximum of 5 gpm at 1500 psi to a circuit package, Figure VI-11, which stores fluid for use during the peak flow requirements of the steer and brake servos, and for application of the abort brake.

Electrical power is derived from the vehicle's 12 volt charging system, driving a 115 volt square wave inverter, Figure VI-12, which in turn powers DC supply modules. The

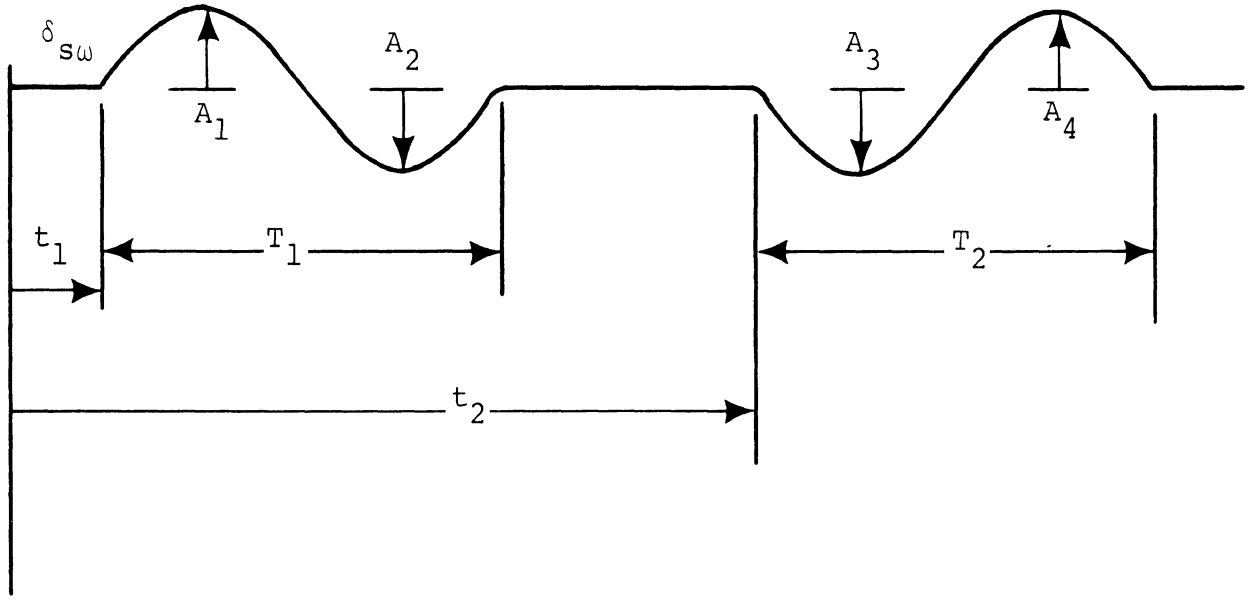

Figure VI-6

Programmable Steering Command
One or Two Sine Waves of Steering Displacement

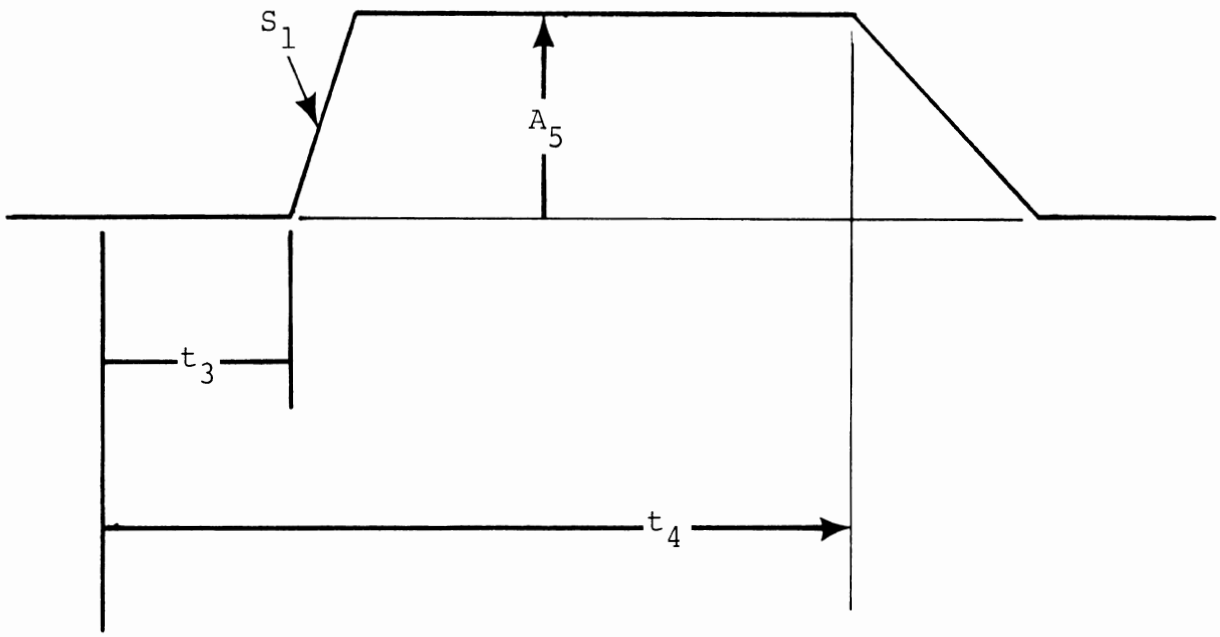

Figure VI-7

Programmable Steering Command
One Trapezoid of Steering Displacement

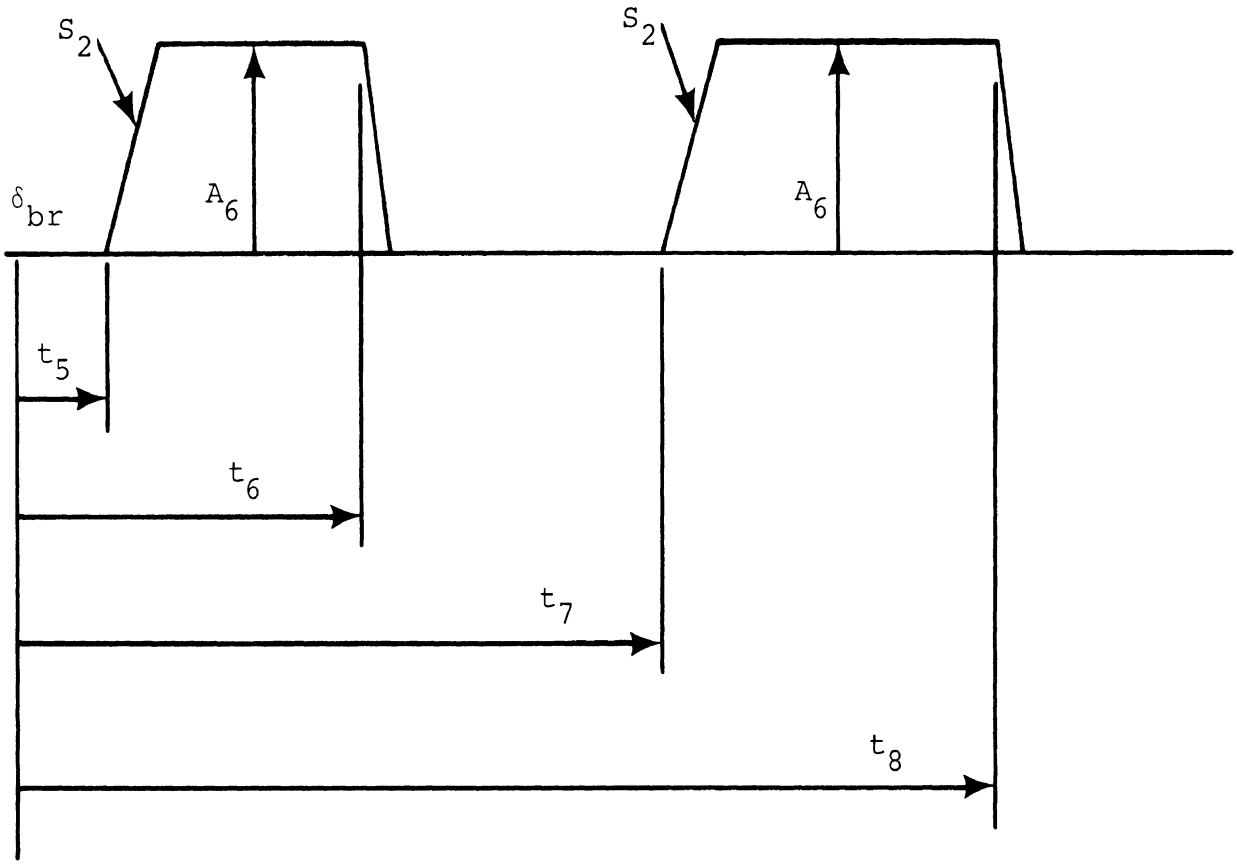

Figure VI-8.

Programmable Brake Commands
One or Two Trapezoids of Pedal Displacement
(or Force)

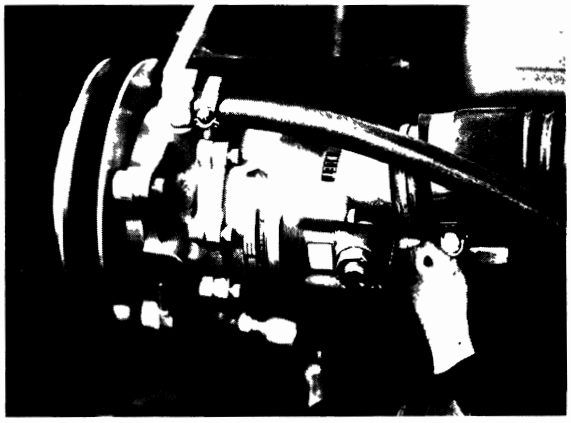

Figure VI-9.
Hydraulic pump.

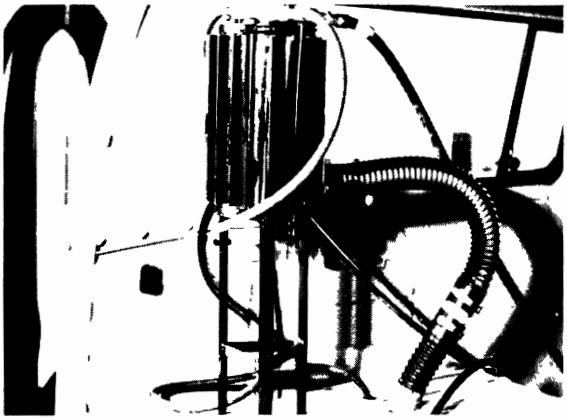

Figure VI-10.
Hydraulic system reservoir.

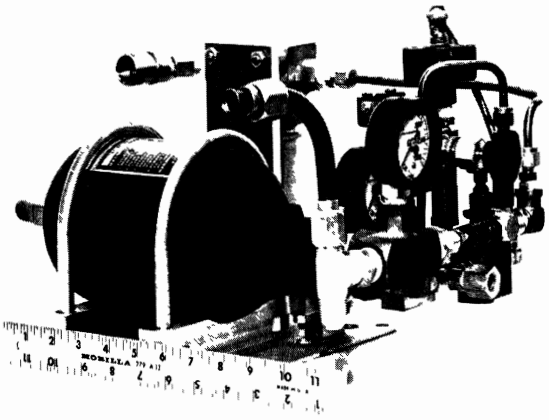

Figure VI-11.
Hydraulic circuit assembly.

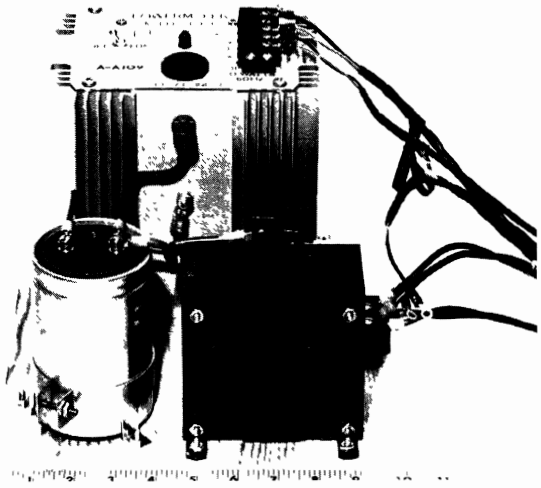

Figure VI-12.
Power inverter with filter.

electrical power consumption is less than 150 watts, while at times of peak hydraulic flow requirement, the pump draws 6 Hp from the engine.

The total automatic vehicle controller system weighs 257 lbs.

The operation of this system in manual transmission vehicles has been accomplished for the simple case of one selected gear. A clutch actuator is provided to apply or release the clutch pedal in response to a transmitted command. With the vehicle initially at rest, the clutch is depressed and the proper gear is selected manually, with the engine running. The vehicle is pushed by the chase vehicle (Figure VI-13) until a velocity of 20 mph is achieved. The chase vehicle is then backed away and the clutch released. Over 400 test runs were executed on the Lotus test vehicle by this procedure.

Approximately 6000 test runs were executed with three automatic vehicle controllers in twelve automobiles, over the course of this study.

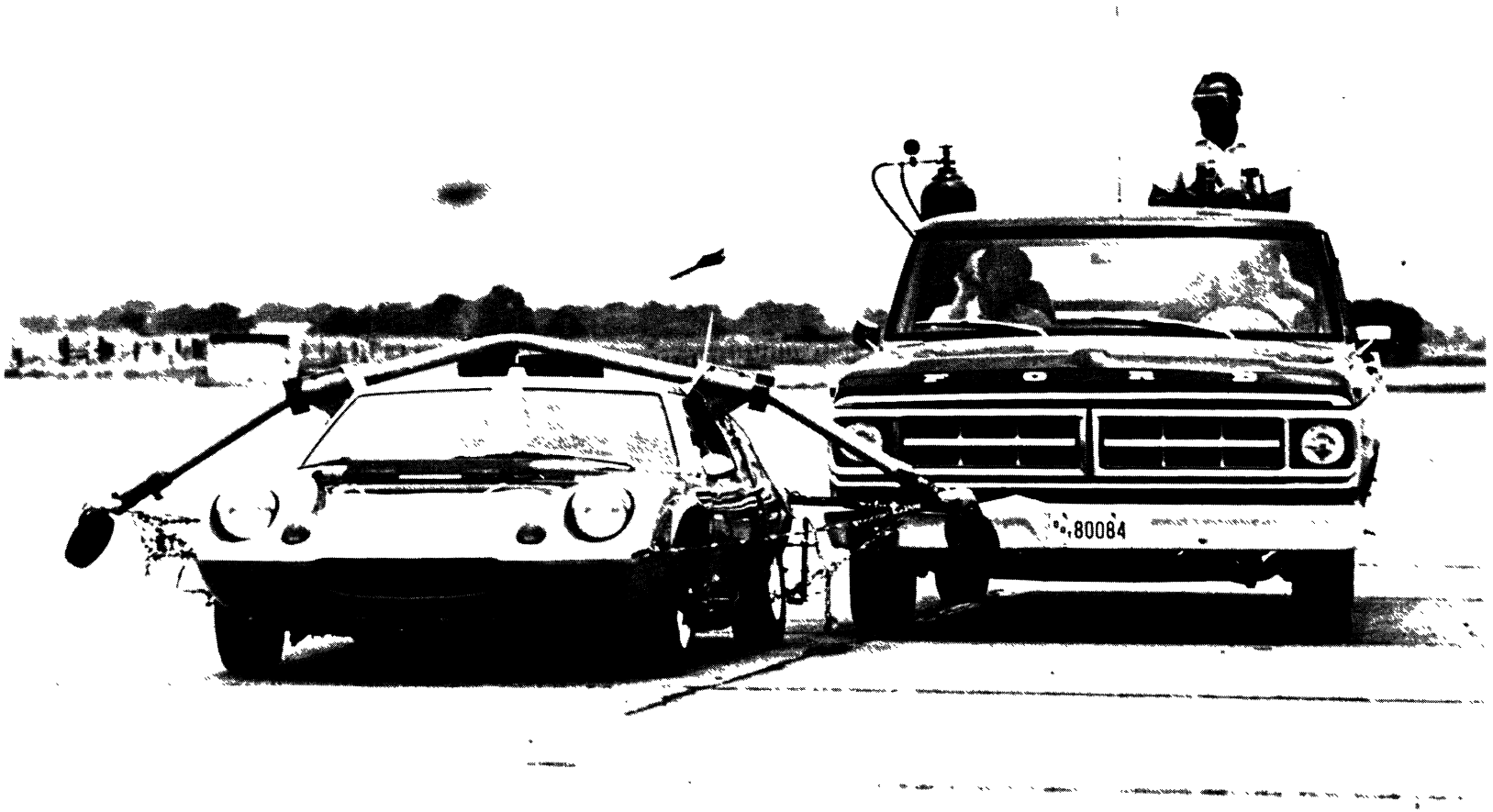

Figure VI-13.
Operation of the automatic controller in
a vehicle with manual transmission.

APPENDIX VII

TEST PROCEDURE SPECIFICATIONS

In this appendix, the specific procedures used in conducting the full scale tests are presented. For each of the six maneuvers the following items are identified:

1. "Initial Conditions" indicate the steady-state conditions from which the limit maneuver portion of the test begins.
2. "Incremental Controls" identifies the index variables with which the test is sequenced.
3. "General Constraints" specify the preliminary steps to be observed prior to test initiation, as well as certain constraints to be observed during the test sequence.
4. "Minimum Signals Required" lists those input and response variables which are critical to the proper interpretation of the experimental results, and thus must be recorded.
5. "Procedure" specifies the sequence of steps to be observed during the execution of the test maneuvers.

Note that the procedures involve certain specifications which assume that the tests are being conducted with the use of the test apparatus identified in this report.

VHTP #1 - STRAIGHT-LINE BRAKING

Initial Conditions: V_o = 40 mph

δ_{sw} = 0°

Incremental Controls: P_B-- Brake Line Pressure

General Constraints:

1) All brake lines are to be controlled by one pressure limiter assembly.

2) Brake lining temperatures are not to exceed 250°F, prior to any run.

Minimum Signals Required: A_x, V_5, W_1, W_2, W_3, W_4, MC

Procedure:

1. Set initial brake line pressure level to 200 psi.
2. Approach test pad above initial velocity.
3. Manually initiate test mode.
4. Coast down to initial velocity.
5. Rapidly depress brake pedal to the physical limit of its stroke, holding steering wheel fixed.
6. Allow vehicle to decelerate to a complete stop and hold for 2 seconds minimum after any pitch motion has settled out.
7. Terminate test mode.
8. Increase brake line pressure by 100 psi increments and repeat steps 2 through 7 until a positive wheel lockup is detected, above 10 mph.

9. Decrease brake line pressure by 100 psi and execute steps 2 through 7 twice.

10. Increase brake line pressure by 25 psi increments and repeat steps 2 through 7 twice at each pressure setting until two wheels indicate positive wheel lockup above 10 mph.

VHTP #2 - BRAKING IN A TURN

Initial Condition: V_o = 40 mph

δ_{sw} = angle required for initial lateral acceleration to be 0.3g.

Incremental Controls: P_B-- Brake Line Pressure

General Constraints:

1) All brake lines are to be controlled by one pressure limiter assembly.

2) Brake lining temperatures are not to exceed 250°F, prior to any test run.

3) Perform trial tests to determine steering wheel angle required to obtain initial lateral acceleration of 0.3g at 40 mph.

Minimum Signals Required: A_x, A_y, r, V_5, W_1, W_2, W_3, W_4, MC

Procedure:

1. Set initial brake line pressure to 200 psi.

2. Approach test pad above initial velocity.

3. Manually initiate test mode.

4. Rapidly apply steering input to limit stop.
5. Coast down to initial velocity.
6. Rapidly depress brake pedal to the physical limit of its stroke, holding steering wheel fixed.
7. Allow vehicle to decelerate to a complete stop and hold for 2 seconds minimum after any pitch motion has settled out.
8. Terminate test mode.
9. Repeat steps 2 through 8 for opposite polarity steering input.
10. Increasing brake line pressure in 100 psi increments, repeat steps 2 through 9 until a positive wheel lockup is detected above 10 mph.
11. Decrease brake line pressure 100 psi and repeat steps 2 through 8 twice for each steering polarity until 2 wheels on a single axle indicate positive wheel lockup above 10 mph.

VHTP #3 - TURNING ON A ROUGH ROAD

Initial Condition: V_o = 30 mph

δ_{SW} = Angle required for initial lateral acceleration to be 0.4g.

Incremental Controls: Three road disturbance grids fundamental frequencies of 9, 11, and 14 Hz.

General Constraints:

1) Perform trial tests to determine steering wheel angle required to obtain initial lateral acceleration of 0.4g at 30 mph.

2) Velocity and lateral acceleration initial conditions are to be achieved upon initial contact with the disturbance grid.

3) Road disturbance grids are to be laid out as in Figure VII-1.

Minimum Signals Required: A_x, A_y, r, V_5, MC

Procedure:

1. Approach the test area above the initial velocity.
2. Manually initiate test mode.
3. Apply steering input to limit stop, timed to aim the vehicle at the center of the first grid.
4. Manually lift fifth wheel prior to traversing grids.
5. Terminate test mode after exiting from the grid and prior to changing the steering angle.
6. Each of the three grids (of 9, 11, and 14 Hz construction) is to be successfully traversed five times. A successful traversal requires that all four wheels contact all grid elements.

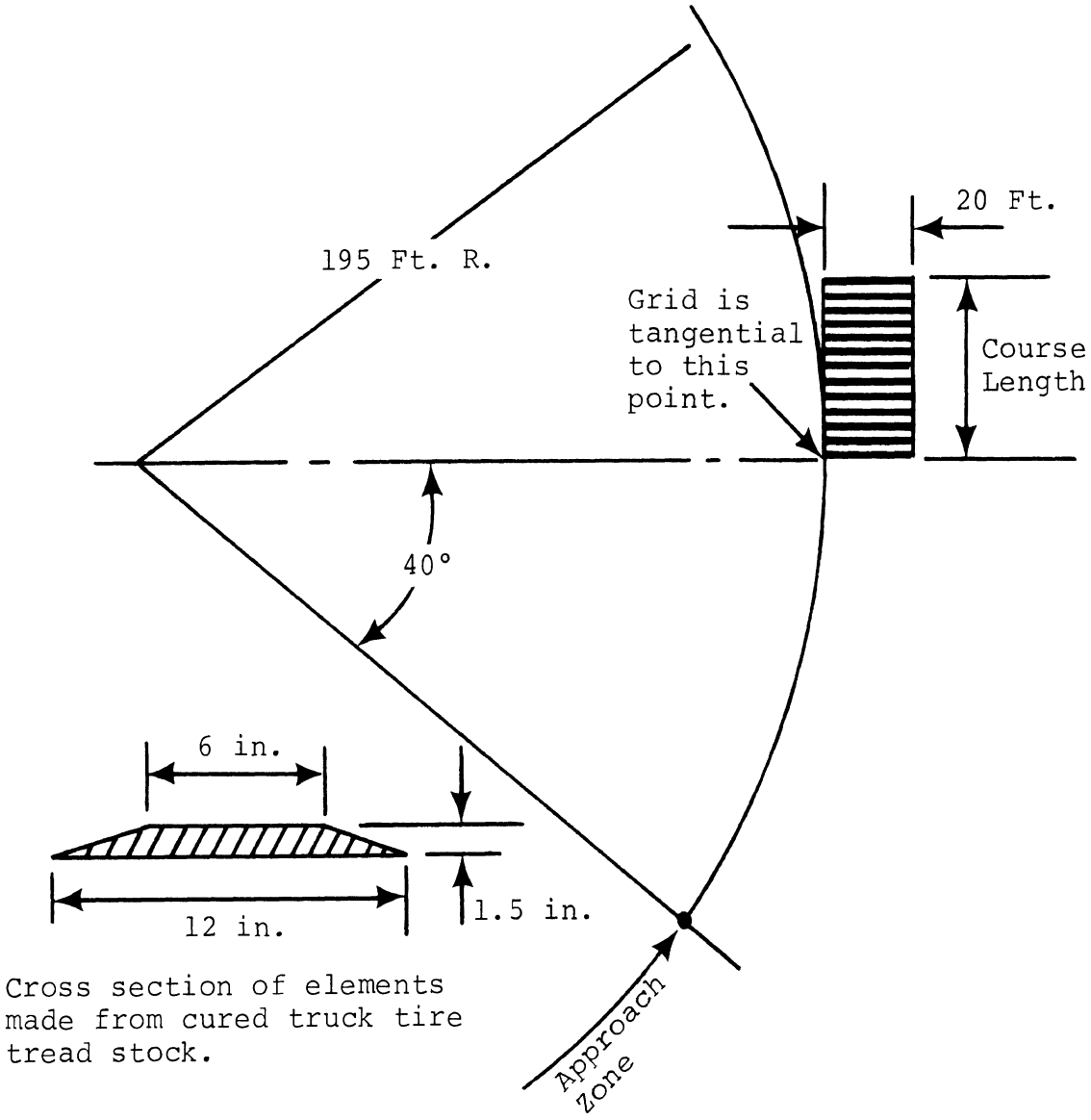

Cross section of elements made from cured truck tire tread stock.

Fundamental Frequency	9 Hz	11 Hz	14 Hz
Center Spacing - Feet	4.8	4.0	3.14
Course Length - Feet	38.4	40	40.8

Figure VII-1

Road Disturbance Course Layout

VHTP #4 - TRAPEZOIDAL STEER

Initial Conditions: V_o = 40 mph

$\delta_{sw} = 0°$

Incremental Controls: $\delta_{sw} = N_g \frac{\ell}{10} \sigma'$

for σ' = 4,6,8,12,16,20,24

where ℓ = wheel base in feet

N_g = overall steering ratio

General Constraints:

1) All function generator time settings are fixed for all vehicles.

Steer Trapezoid Start = 1.00 sec (100)
Ramp Time = .40 sec (40)
Steer Trapezoid Stop = 4.50 sec (450)
Total Time = 5.50 sec (550)

} Note: Controller settings refer to the HSRI Automatic Vehicle Controller

2) All unused function generator controls are to be set at zero magnitude, with start times set at values greater than 9.00 sec (900).

Minimum Signals Required: A_x, A_y, r, V_5, MC

Procedure:

1. Knowing the overall steering ratio, compute δ_{sw} for first σ value, and set trapezoid level accordingly.
2. Set steering trapezoid controls for 0.4 second ramp time, with δ_{sw} polarity to "left turn."
3. Maneuver vehicle with drone controls into approach path above initial velocity criterion.

4. Initiate function generator cycle. (Tape recorder, test mode and maneuver execution cycle automatically.)

5. Execute maneuver twice (steps 3 and 4) for a left turn and twice for a right turn.

6. Compute δ_{sw} value for the next σ' value and execute steps 2 through 5 until all σ' values have been executed.

VHTP #5 - SINUSOIDAL STEER

Initial Conditions: V_o = 45 mph (1 complete run set)

V_o = 60 mph (1 complete run set)

$\delta_{sw} = 0°$

Incremental Controls: 1) V_o = 45, 60 mph

2) $\delta_{sw} = \frac{66}{V} \frac{\ell}{10} \sigma \ N_g$

for σ = 2,4,6,8,10,12,14,16,18

where V = Initial velocity in ft/sec

ℓ = wheel base in ft.

N_g = overall steering ratio

General Constraints:

1) All function generator time settings are fixed for all vehicles:

Steer Start = 1.00 sec (100)
Sine Period = 2.00 sec (200)
Total Time = 5.00 sec (500)

2) All unused function generator controls are to be set at zero magnitude with start times set at calues greater than 9.00 sec (900).

3) Each initial velocity threshold is a separate test sequence.

4) This test is not to be executed when wind velocity normal to the initial path exceeds 15 mph.

Minimum Signals Required: A_x, A_y, r, V_5, MC

Procedure:

1. Knowing the steering gear ratio and vehicle wheel base, compute δ_{sw} for the first velocity and first σ value.
2. Set first initial velocity threshold on function generator.
3. Set steering sinusoid controls for 2.0 sec. period, sinusoid amplitudes equal to the calculated δ_{sw}, and "left turn" polarity.
4. Maneuver vehicle with drone controls into approach path.
5. Initiate function generator cycle. (Tape recorder, test mode and maneuver execution cycle automatically.)
6. Execute maneuver twice (steps 4 and 5) for both polarities of sinusoidal control.
7. Repeat steps 3 through 6 for each σ' value.
8. Repeat steps 2 through 7 for each V_o value.

VHTP #6 - DRASTIC STEER AND BRAKE

Initial Conditions: V_o = 50 mph (1 complete set)

V_o = 60 mph (1 complete set)

$\delta_{sw} = 0°$

Incremental Controls: 1) V_o = 50, 60 mph

2) $\delta_{sw} = \delta_{sw}^* \gamma$

for γ = 0.75, 1.00

and $\delta_{sw}^* = 360(\frac{N_g}{22.5})\ (\frac{\ell}{10})$

3) Brake release times, selected after viewing response data in procedure steps #9 and #16

General Constraints:

1) These function generator time settings are fixed for all vehicles:

   Steer Start = 1.00 sec (100)
   Sine Period = 2.00 sec (200)
   Total Time = 5.00 sec (500)
   Brake Ramp = 0.05 sec (005)

2) Brake application and release times are "tuned" to the vehicle response.

3) All unused function generator controls are to be set at zero magnitude with start times set at values greater than 9.00 sec (900).

4) The brake force should be large enough to lock all four wheels but shall not exceed 250 lbs.

Minimum Signals Required: A_x, A_y, r, V_5, $\dot{\phi}$, MC

Procedure:

1. Set first initial velocity threshold.
2. Knowing the overall steering ratio and vehicle wheel base (see Table I-3), compute δ_{sw}*.
3. Set steering sinusoidal controls for a 2.0 second period with first half amplitude set to (δ_{sw}* times first γ value) and second half amplitude set to zero.
4. Set δ_{br} controls to zero.
5. Maneuver vehicle with drone controls into approach path above initial velocity criterion.
6. Initiate function generator cycle.
7. Repeat steps 5 and 6.
8. Examine the response data from the previous two runs, determining the time at which the yaw rate time history was seen to have reached 95% of its peak value.
9. Select brake application time, t_5, to coincide with timing of 95% peak yaw rate value, and brake release time, t_6, equal to (t_5+2.0).
10. Set brake ramp time to 0.050 sec.
11. Set brake level for amplitude of full brake pedal stroke, with force not to exceed 250 lbs.
12. Maneuver vehicle with drone controls into approach path above initial velocity criterion.
13. Initiate function generator cycle.
14. Repeat steps 12 and 13.

15. Play back tape recorder signal of roll rate, ϕ, onto the pen recorder, along with function generator time base, t_{ac}.

16. Examine the response data from the previous two runs, determining the values for brake release time, t_6, from the roll rate response. Two release timings are to be selected, t_p and t_z, coinciding with 2nd sympathetic polarity peak and 3rd zero crossing, respectively.

17. Set brake release time, t_6 to t_p; repeat steps 5 and 6 twice for each value of γ.

18. Set brake release time, t_6 to t_z; repeat steps 5 and 6 twice for each value of γ.

19. Repeat steps 17 and 18 for second velocity threshold.

20. A rollover is counted and logged if an outrigger wheel touches the test surface. A rollover occurrence terminates the test sequence.

APPENDIX VIII

DATA ACQUISITION AND ANALYSIS

TRANSDUCER CAPABILITIES AND CALIBRATION

The various signals recorded on the magnetic tape are listed in Table VIII-1 with their nominal ranges. These signals are also identified by vehicle test system. For many of these components, secondary or back-up hardware were available and utilized to cope with equipment breakdowns.

Each transducer signal was routed through circuits in the interface module to standardize the voltage calibration levels for both systems. The signal levels were adjusted to yield a full scale calibration level of 71% of the linear dynamic range of the tape recorders. The block diagrams of Figures VIII-1 and VIII-2 illustrate the complete systems used to record data.

All of the transducers were calibrated for physical units during vehicle change-overs. Each type of transducer required a separate calibration technique:

1. Accelerometers - The Humphrey Inertial Package was suspended on a "sine table" and incremented through several inclination angles. The appropriate component of the gravity vector was determined for each inclination angle and tabulated to provide the physical reference levels, in g's, for determination of each accelerometer gain.

2. Rate Gyros - Rate gyros were mounted on the sine table and allowed to oscillate in simple harmonic motion. A calibrated rotary potentiometer, providing the time history of angular displacement was recorded together with the rate gyro output on a light-beam oscillograph. The resulting displacement and rate

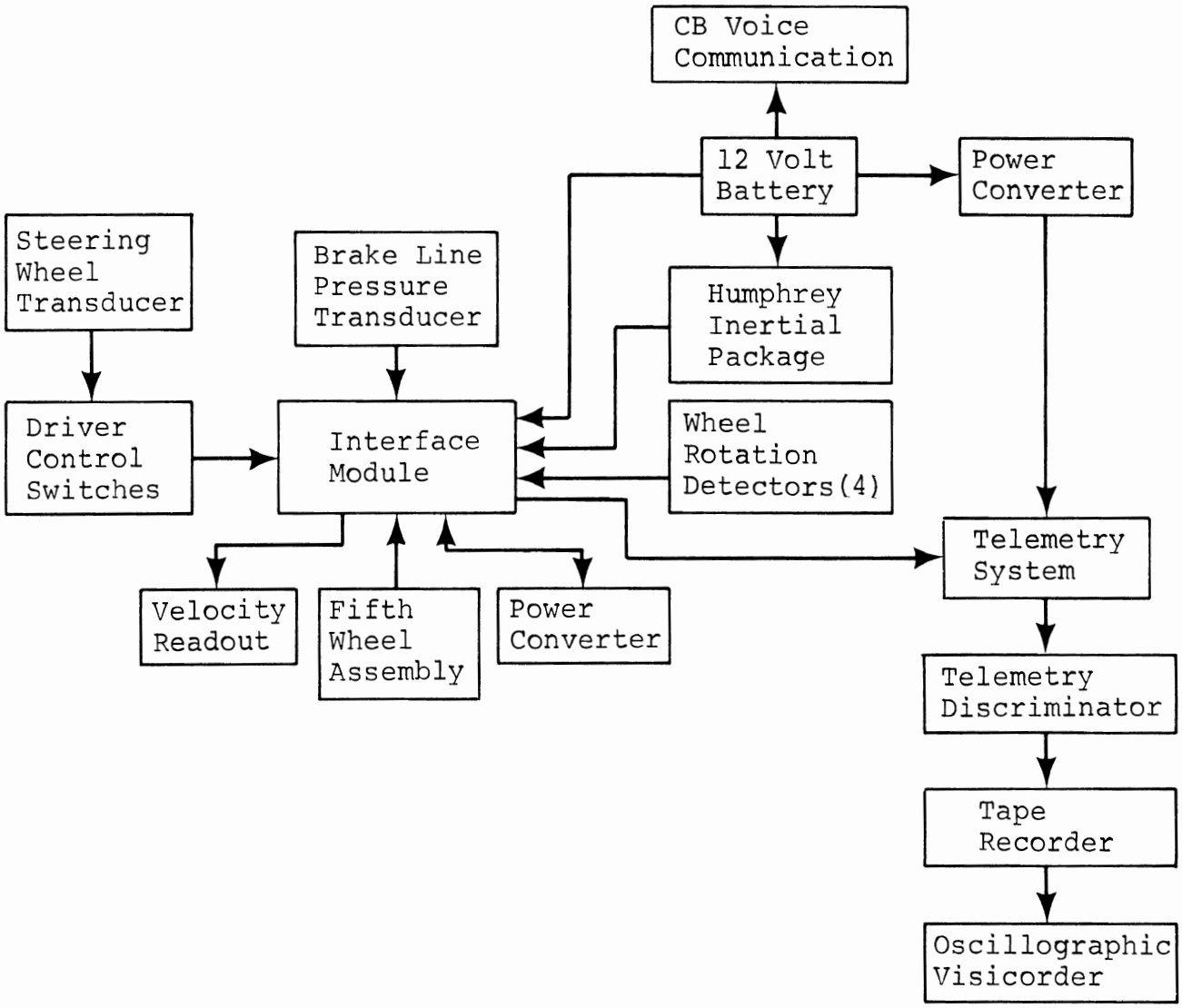

Figure VIII-1

Instrumentation Block Diagram - Driver System

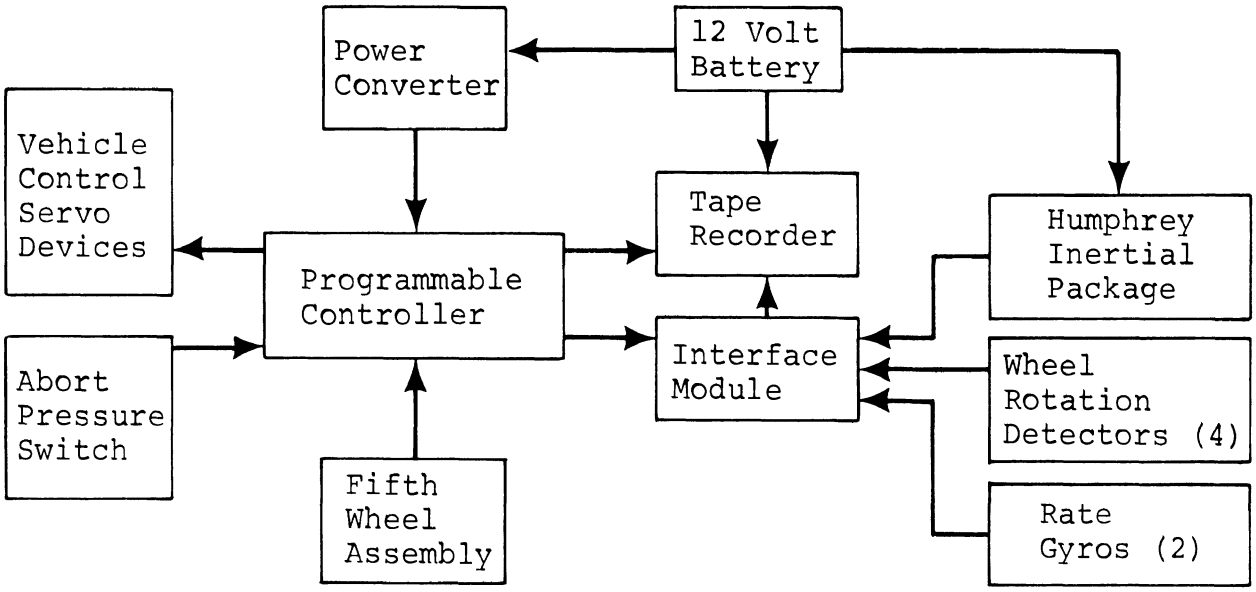

Figure VIII-2

Instrumentation Block Diagram - Automatic System

TABLE VIII-1

TRANSDUCER DESCRIPTION

Tape Channel	Signal Symbol	Transducer Device	Transducer Range	System	FSC Value
1	A_x	Humphrey Inertial Package	±2.0 g	AC-DR	1.00 g
2	A_y	Humphrey Inertial Package	±2.0 g	AC-DR	1.00 g
3	r	Humphrey Rate Gyro	±90 deg/sec	AC-DR	60.0 deg/sec
4	V_s	Tracktest Fifth Wheel	0-100 mph	AC-DR	50 mph
5	δ_{SW}	Geared Rotary Potentiometer	±900°	AC-DR	500 deg
6	W_1+W_2	Interface Wheel Rotation Circuit	N/A	AC-DR	4.0
7	W_3+W_4	Interface Wheel Rotation Circuit	N/A	AC-DR	4.0
8	P_b	Brake Line Pressure Potentiometer	1500 psi	DR	1000 psi
9	δ_{BR}	Linear Potentiometer	6" Extension	AC	5"
10	F_{BR}	Lebow Load Cell	500 lbs	AC	250 lbs
11	t_{AC}	Function Generator Time Ramp	0-10 sec	AC	10 sec
12	$\dot{\phi}$	AST Rate Gyro	±40 deg/sec	AC	40 deg/sec
13	ψ_H	Humphrey Inertial Package	360° Continuous	DR	360 deg.
14	Control	Interface Circuit	N/A	AC-DR	2.0

N/A Implies Not Applicable

sinusoids are related by the simple harmonic motion equations:

$$\theta = A \sin(\omega t)$$

$$\dot{\theta} = A\omega \cos\left(\omega t - \frac{\pi}{2}\right)$$

The oscillograph traces are then analyzed for period and amplitude of oscillation to determine the voltage calibration in deg/sec.

3. Fifth Wheel - A digital readout device is attached to a fifth wheel pulse-type tachometer. Driving over a measured mile, the fifth wheel tire inflation pressure is adjusted to yield 5280 pulses, or 1 pulse per foot. These pulses are compared against a crystal-controlled time base in a digital tachometer circuit to yield miles per hour. Then the analog tachometer voltage for the fifth wheel is measured at several steady velocity conditions, using the concurrent digital tachometer output as reference.

4. Control Inputs - The various potentiometer devices--steering wheel and brake pedal displacement--are simply calibrated against visual reference with a pointer or tape measure.

5. The Lebow Load Cell for brake force was provided with a shunt resistor for calibration. In this case, no physical load reference was effected at each recalibration of the device.

6. The wheel rotation circuit and control mode levels are functionally checked but are not calibrated.

Additional calibrations included periodic maintenance on the tape recorders and telemetry system according to the respective manufacturers' recommendations. All calibrations were performed with the equipment running in the test vehicle. Various calibrations were also performed as internal adjustments in the automatic controller: velocity threshold, sine period, radio drone gains, abort threshold levels, and calibration of the adjustable command levels on the programmable control. The final calibration activity prior to testing involved the precise setting of the full scale calibration voltage reference generated by the interface module.

TEST EXECUTION

During the test sequencing, the vehicle control inputs were incremented through the various levels as discussed in Appendix VII. After recording the pre-calibration modes, the data was recorded for a typical sample:

1. Automatic System - The test operator maneuvers the vehicle into the approach lanes to the skid pad. The on-board tape recorder begins recording when the function generator is armed. This provides a run-up time prior to the maneuver initiation as the vehicle coasts down through the velocity threshold. The recorder automatically shuts off at the end of function generator time ramp.
2. Driver System - The test vehicle driver approaches the test pad in the same manner and he gives a verbal command on the citizen's band radio to the base station telemetry operator. The base tape recorder is thus started a few seconds

prior to test execution. Following the termination of test mode, controlled by a switch near the driver, the tape recorder is manually turned off.

Oscillograph traces of the raw data were created simultaneously with tape data recording during the driver tests. Data tapes from the automatic system tests were also "dumped" regularly on the base station equipment to verify the continued proper functioning of the system and transducers.

HYBRID ANALYSIS AND DIGITIZATION

HYBRID SYSTEM. The FM magnetic data tapes were processed on the HSRI Hybrid Computer facility. This facility consists of an Applied Dynamics AD-4 analog computer and an IBM 1800 digital computer. Various peripheral devices are associated with each basic computer as shown in Figure VIII-3.

1. Ampex FR 1900 FM 14-channel tape machine for reproducing data tapes.
2. Hewlett-Packard 101A Dual Beam Oscilloscope for monitoring tape data and validity checks.
3. Brush Mark 200 Recorder (2), total of 16 channels for plotting time history data.
4. Hewlett-Packard 2FA Dual Pen X-Y plotter for plotting trajectory data.
5. HSRI hybrid interface unit for hybrid communication signals and data transfer.
6. IBM 1442 card reader-punch for input data.
7. IBM 1443 line printer for listing edited tape files.
8. IBM 2401 Type I tape drive, 9 track, 800 BPI, for digitized data storage.

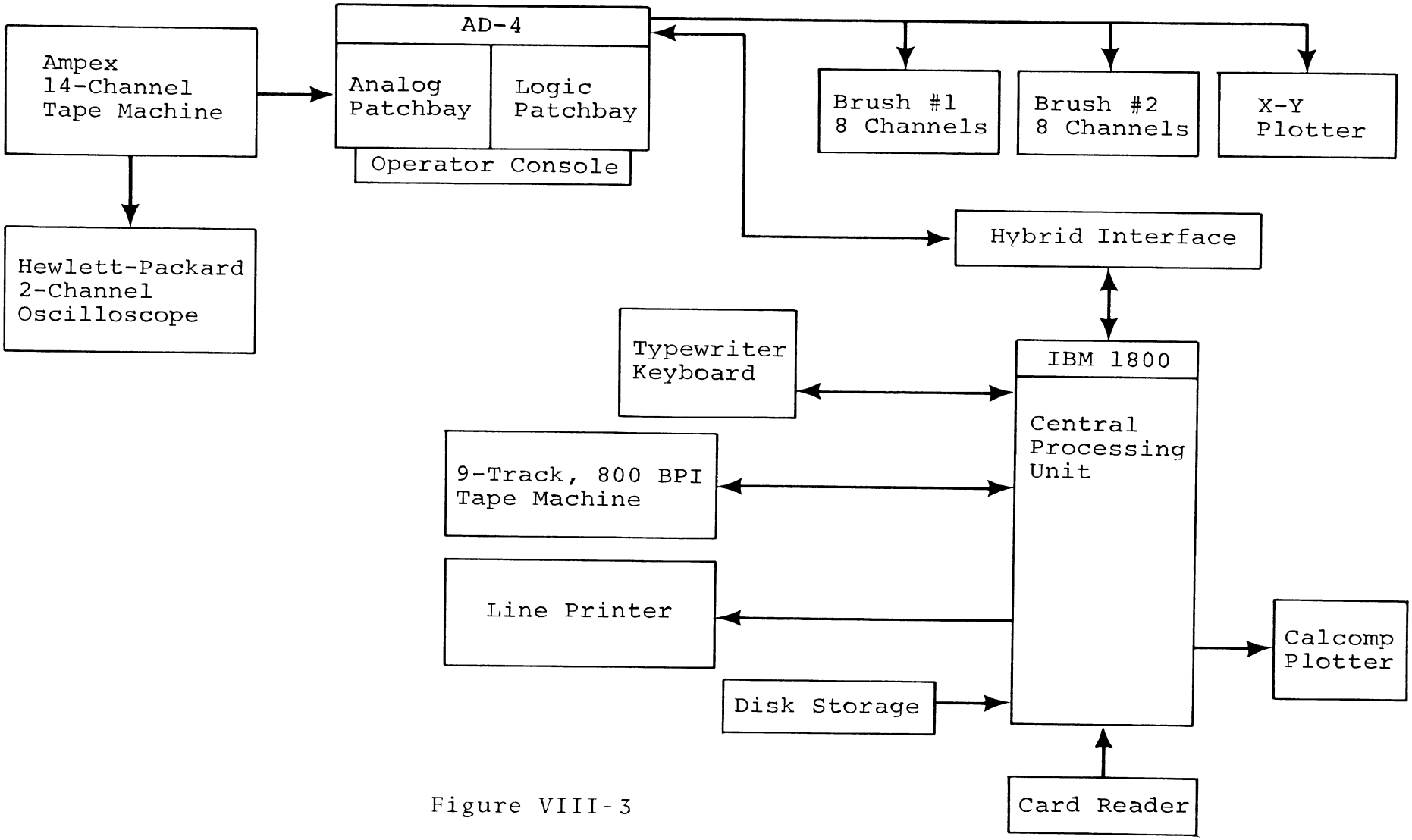

Figure VIII-3

Hybrid Data Processing Equipment

9. IBM 1810 disc drives for program storage.

10. IBM 1816 printer keyboard for operator interaction and control of the program sequence.

11. Calcomp 565 digital plotter for final analysis and validity checks.

The basic program is designed to be highly interactive. Each of these hardware devices is utilized at the appropriate times in the program sequence. The program sequence is directed by the operator and can be interrupted at any time.

TEST SEQUENCE MODE CONTROL

A test sequence is defined to be a single car executing a single maneuver in a single condition. Each test sequence, recorded on magnetic tape, was prefaced by initialize sequence (IS) mode and concluded by end of sequence (EOS) mode. In addition, the three calibration modes (Zero Calibration (ZC), Full Scale Calibration (FSC), and Zero Data (ZD)) were recorded immediately following IS mode. All vehicle test runs were recorded in "data" mode. These five modes are switch-selected on the interface module. A sixth mode, test mode, is generated uniquely in each vehicle series at a time immediately preceding the control input application. A typical test sequence would be recorded as follows:

1.	Initialize Sequence	30 seconds
2.	Zero Calibration	30 seconds
3.	Full Scale Calibration	60 seconds
4.	Data - Zero Data	30 seconds
5.	Data - Test Mode	as required
6.	End of Sequence	30 seconds

NOTES:

(1) Zero data is recorded while the vehicle is standing still on a level surface with all instrumentation activated.

(2) Test mode was initiated when the vehicle was traveling in a straight line above the initial velocity requirements, 2 seconds prior to control input execution.

(3) Every data sample recorded on the tape, including all sequencing and calibration modes, was assigned a unique sample number on the log sheets.

(4) All transducer calibrations are referenced as FSC equivalents. The transducer signals gathered and their calibration levels are listed in Table VIII-1.

A typical data sequence would be analyzed as shown in Figure VIII-4. During the initial phases of the program execution, the digital computer has main control over the analog; during the actual data analysis, the analog computer has main control. Modified sequencing or control mode selection can be selected at the operator's discretion by manually over-riding the automated logic sequencing during the data analysis phase. Several error recovery options are also included to aid in rapid trouble shooting of any unanticipated problems. Program-generated comments and operator control options are listed on the typewriter-keyboard to document the processing and catalog the digitized tapes.

ANALOG ANALYSIS

The data signals recorded on the magnetic tape fall into four basic categories:

BASIC DIGITAL BLOCK DIAGRAM
TYPICAL SEQUENCING

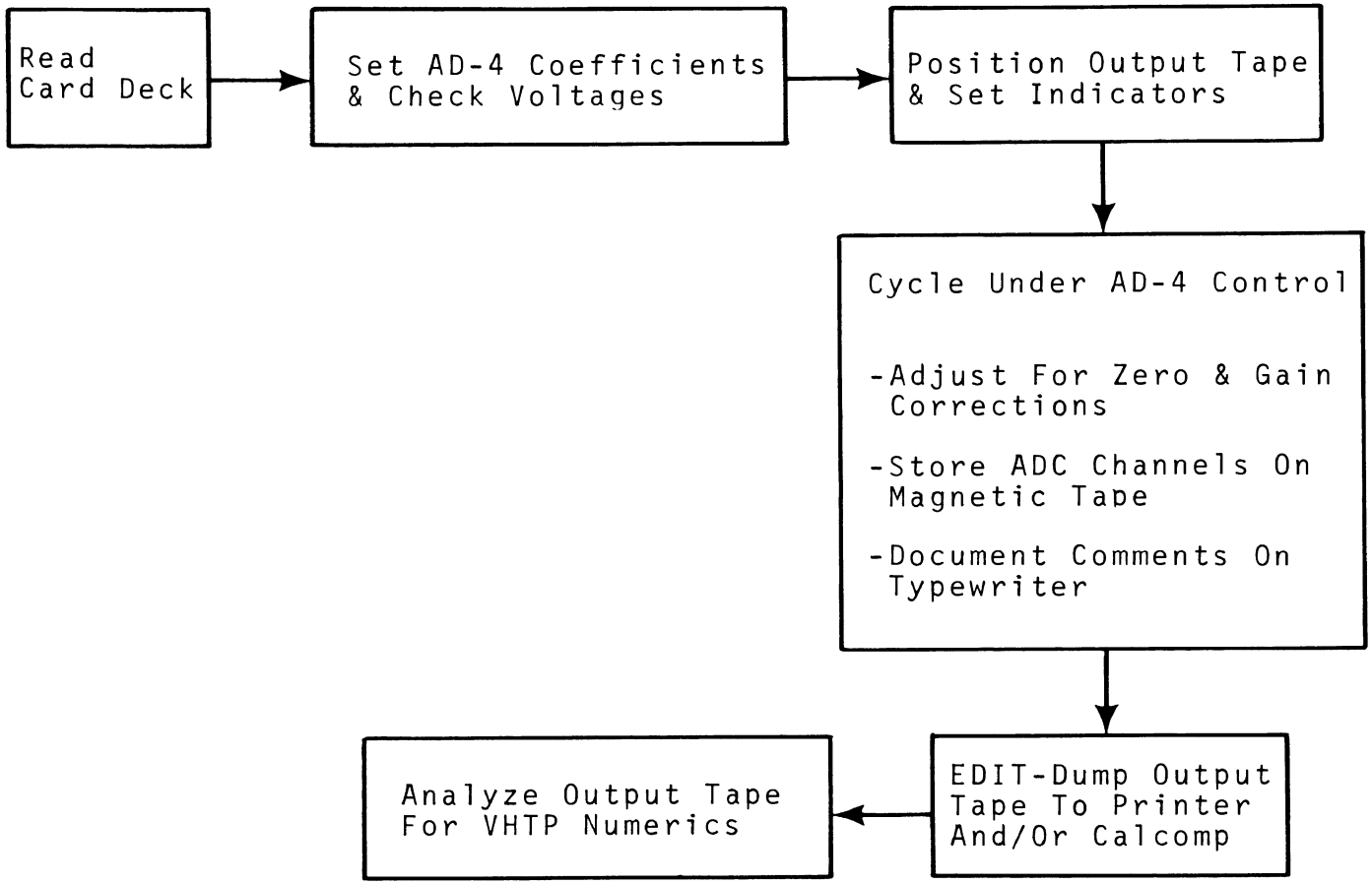

Figure VIII-4.

1. Primary vehicle response data to be analyzed with basic kinematics equations.
2. Vehicle control inputs and informational data.
3. Analog multiplexed wheel rotation detectors to be decoded and reconstructed as time signals.
4. Control channel logic to be decoded for mode control.

A basic functional block diagram for the analog computer is shown in Figure VIII-5. All data signals are initially processed through data calibration circuits, which provide necessary zero and gain corrections and filtering.

The primary vehicle response data is processed with the following equations:

$$-V_x = \int (A_x + V_y r)\,dt$$

$$V_y = \int (A_y - V_x r)\,dt$$

$$\psi = \int r\,dt$$

$$\phi = \int \dot{\phi}\,dt$$

$$x = \int (V_x \cos\psi - V_y \sin\psi)\,dt$$

$$y = \int (V_y \cos\psi + V_x \sin\psi)\,dt$$

$$\tan\beta = V_y / V_x$$

$$1/R = \frac{\dot{\beta} + r}{(V_x^2 + V_y^2)^{1/2}}$$

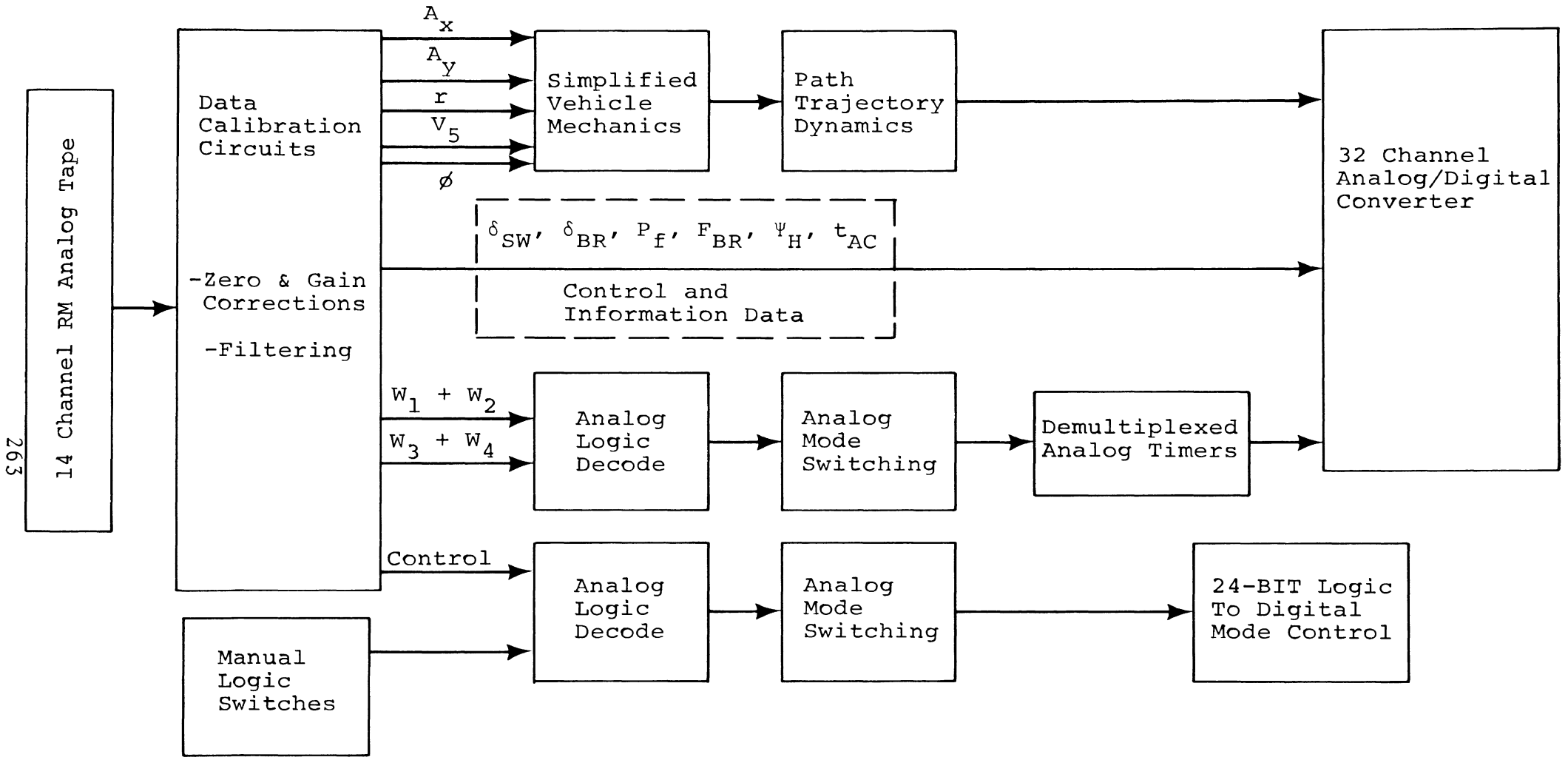

Figure VIII-5

Basic Analog Block Diagram

Definition of these terms can be found in Table VIII-2. All of these computations are initiated at the beginning of test mode by logical switching; all integral computations are initialized at zero except for V_x, which is initialized by the instantaneous fifth wheel velocity, V_5.

The wheel rotation detectors are triggered by light-sensitive photo-cells to create discrete voltage levels. Each wheel generates a square wave with a period equal to the wheel's rotational period; the square waves from an axle of wheels are assigned different magnitudes and then added together (analog multiplexed) to form one signal and conserve tape channels. This combined signal is de-multiplexed by the analog logic; the multiplexed signal drives analog comparators set to detect thresholds between the four possible voltage values. The logic states of the comparators are combined and used to trigger time duration amplifiers synchronously with wheel rotation rates.

The control channel information is decoded in a manner similar to the wheel rotation signals. The control signal is a DC voltage with a unique value for each mode. This signal drives a set of analog logic elements to switch states in the vehicle mechanics circuits, control the peripheral equipment and signal the digital computer.

TYPICAL SEQUENCE

It will be illustrious to consider the computer activities for a typical sequence. As shown in Figure VIII-4, the digital computer has primary control in the initial phases. Parameter data is read from punched cards to identify the analog elements in use and to specify various data values for filtering effects, calibration magnitudes, etc. The digital computer then sets the analog coefficient devices to the proper magnitudes and performs a static check of all

analog voltage elements to test the analog circuit. When these steps are completed satisfactorily, the analog and digital tape machines, the Brush recorders and X-Y plotter are readied. Main control is then passed to the analog computer and decoded logic signals, based on the control channel, control the sequence.

The first expected mode is Initialize Sequence (IS). During IS, the digital computer stores certain control indicators on the magnetic tape and sets internal logic switches for later reference.

During Zero Calibration (ZC) mode, the digital computer reads the initial analog stage ten times and computes the necessary voltage offset to correct for tape machine and signal processing errors. The offset values are set into the analog and the voltages are read again as a check. All of this information is also stored on the digital output tape.

During Full Scale Calibration (FSC) mode, the digital computer again reads the initial analog stages ten times and computes the gains through these amplifiers. The desired gain is known from the input deck; the actual gain will be slightly wrong due to variations in the complete system hardware. Gain control potentiometers are reset to correct for these errors and the voltages are read again as a check. All of this information is also stored on the digital output tape.

During Zero Data (ZD) mode, the digital computer repeats the procedure and equations of the ZC mode. Voltage offset errors generated by the transducers are nulled at this time.

The hybrid system is now ready for vehicle test samples. The next mode is data and the digital computer switches to read the 32 ADC channels. At the start of test mode, these channels are digitized and stored on the magnetic tape at a

rate of 50 samples per second per channel until the end of the test mode. Table VIII-2 identifies the samples stored. This digitizing process creates an output tape file for each test sample.

Upon encountering End of Sequence (EOS) mode, the digital computer closes the magnetic tape output, clears certain indicators and prompts the operator to initiate the next test sequence or branch elsewhere. Validity checks may be performed by dumping the digital tape file data to the main printer or creating digital plots.

DIGITAL ANALYSIS AND NUMERIC DEFINITION

The output of the analog-to-digital conversion process consists of digital magnetic tapes containing the 32 digitized variables stored in sequential files. Each data file represents one test sample and contains a discretized time history of each of the 32 variables. At the beginning of each file is a header record containing information on that file's contents. The information contained in this header gives the type of maneuver being performed, the vehicle identification, the condition code, the sample number, the test and processing dates, the file number, the number of records or data points in the file, and the file type. Calibration data associated with each data sequence is stored in calibration files before and after every sequence of data files.

The structure of the digital processing programs is shown in Figure VIII-6. The overall operation is controlled by a main-option control program which reads the header record of a file and determines what branching or tape control is required. At the next lowest level are six subprograms which are accessed from the main-option control program. Each subprogram performs the required numeric calculations

TABLE VIII-2. IDENTIFICATION OF VARIABLES

Identification Number	Symbol	Description
1	A_x	Longitudinal acceleration
2	A_y	Lateral acceleration
3	r	Yaw rate
4	V_5	Fifth wheel velocity
5	δ_{sw}	Steer wheel angle
6	W_1+W_2	Multiplexed wheel rotations, front axle
7	W_3+W_4	Multiplexed wheel rotations, rear axle
8	P_b	Brake line pressure
9	F_{BR}	Brake pedal force
10	δ_{BR}	Brake pedal position
11	tac	Time base of automatic controller
12	$\dot{\phi}$	Roll rate
13	ψ_H	Vehicle heading angle, as measured
14	CONT	Control channel (MC)
15	t_{AD}	Time base on AD-4
16	REF	AD-4 voltage reference
17	V_x	Longitudinal vehicle velocity, body axis
18	V_y	Lateral vehicle velocity, body axis
19	x	x-Displacement, fixed axis
20	y	y-Displacement, fixed axis
21	ψ	Vehicle heading angle, as computed
22	Tanβ	Tangent of vehicle sideslip angle
23	β	Vehicle sideslip angle
24	$\dot{\beta}$	Derivative of vehicle sideslip angle
25	W_1IND	Wheel rotation indicator, left front

TABLE VIII-2. (Cont)

Identification Number	Symbol	Description
26	W_2IND	Wheel rotation indicator, right front
27	W_3IND	Wheel rotation indicator, left rear
28	W_4IND	Wheel rotation indicator, right rear
29	$\dot{x}$	x-Direction velocity, fixed axis
30	$\dot{y}$	y-Direction velocity, fixed axis
31	1/R	Path curvature
32	ϕ	Roll angle

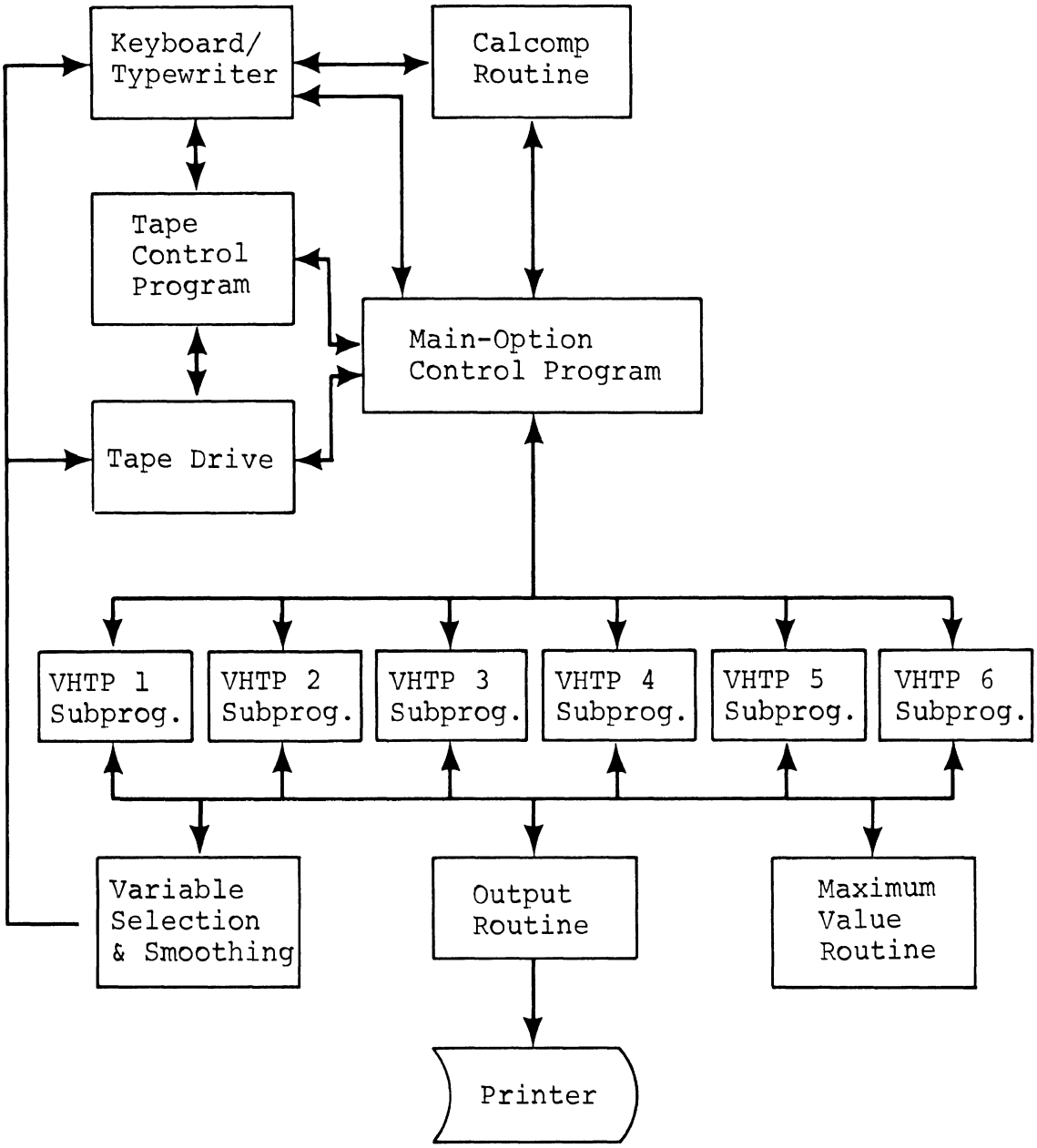

Figure VIII-6

BLOCK DIAGRAM OF DIGITAL PROGRAM STRUCTURE

associated with a particular VHTP maneuver. These subprograms, in turn, interact with various subroutines which are used for smoothing, finding maximum values, and printing out the results.

The processing operation is completely automatic with no need for any operator interaction. The numerics computed for each VHTP test sample are printed out in tabular form on the line printer during this mode. However, the processing may be interrupted at any time and controlled completely from the keyboard/typewriter, with additional options available such as Calcomp plotting of any two variables, complete control of the tape unit, and arbitrary subprogram branching.

The following sequence is typical of the operations that the digital processing program performs. The main-option control program first reads the header record of the present file and determines whether or not it is a data file. If it is not (hence, a calibration, initialize sequence, or end of sequence file), it skips over the present file to the next file. Once a data file is encountered, the program determines what type of maneuver is being performed and then branches to the subprogram associated with that particular VHTP maneuver. The VHTP subprogram identifies the variables needed for its particular numeric calculations and passes this information to the variable selection and smoothing subroutine, which reads these required variables from the tape to core storage, smooths, and returns them to the VHTP subprogram. The VHTP subprogram then performs the necessary numeric calculations, using these smoothed variables, and outputs the results to the line printer. Program control is then returned to the main-option control program which reads the next file header record, and the above cycle is repeated.

If the processing is interrupted for keyboard/typewriter control, the variables used in numeric calculations for the last data file remain in core storage and are not lost until the next file is processed. This eliminates any requirement to re-position the tape and read data that normally would have been lost upon completion of the calculations of the last file. Hence, many operations may be performed on this same data from the keyboard/typewriter such as Calcomp plotting, printing, searching for maximum values, or even further smoothing.

The following defines and explains the individual numerics that were calculated for each VHTP maneuver:

VHTP 1: a) $(A_x)_{ave} = \frac{1}{t_1 - t_o} \int_{t_o}^{t_1} A_x \cong \frac{1}{i} \sum_{i=1}^{n} A_{x_i}$

= average longitudinal deceleration.

where

A_x is the longitudinal deceleration

A_{x_i} is the discretized representation of longitudinal deceleration

t_o is the initial time at V = 35 mph

t_1 is the final time at V = 10 mph

i is the integer count of data points over the summation interval

V is the velocity

t is time

VHTP 2: a) $(A_x)_{ave} = \frac{1}{t_1 - t_o} \int_{t_o}^{t_1} A_x \, dt \cong \frac{1}{t_1 - t_o} \sum_{i=1}^{n} A_{x_i}$

= average longitudinal deceleration

where

A_x, A_{x_i}, t_1, t_o, i, V, t are defined the same as under VHTP 1 a).

VHTP 2: b) $R_o(\frac{1}{R})_{av} = \frac{(\frac{1}{R})_{av}}{(\frac{1}{R})_o}$ = average path curvature ratio

where

$$(\frac{1}{R})_{av} = \frac{1}{1} \int_{t_2}^{t_2+1} (\frac{1}{R}) dt \cong \frac{1}{s_f} \sum_{i=1}^{s_f} (\frac{1}{R})_i$$

$$(\frac{1}{R})_o = \frac{1}{R}\Big|_{t_2} \cong (\frac{1}{R})_i \quad , \quad i=0$$

and,

$(\frac{1}{R})_i$ is the discretized representation of path curvature

$(\frac{1}{R})$ is path curvature

$(\frac{1}{R})_o$ is the path curvature at the time the brakes are applied

$(\frac{1}{R})_{av}$ is the average path curvature for 1 second after the brakes are applied

t_2 is the time the brakes are applied

t_2+1 is the one second following brake application

s_f is the digitizing rate in samples/second.

VHTP 2: c) $\beta_p(t)$ = Maximum absolute value of sideslip angle.

where

t is defined over the interval $[t_2, t_2+1]$

t_2, t_2+1 are defined as under b).

VHTP 2: d) $\dot{\beta}_p(t)$ = Maximum absolute value of rate of change of sideslip angle.

where

t is defined over the interval $[t_2, t_2+1]$

t_2, t_2+1 are defined under b).

VHTP 3: a) $R_o(\frac{1}{R})_{av} = \frac{(\frac{1}{R})_{av}}{(\frac{1}{R})_o}$ = average path curvature ratio.

where

$$(\frac{1}{R})_{av} = \frac{1}{1}\int_{t_3}^{t_3+1} (\frac{1}{R})dt \cong \frac{1}{s_f}\sum_{i=1}^{s_f} (\frac{1}{R})_i$$

$$(\frac{1}{R})_o = \frac{1}{R}\Big|_{t_3} \cong (\frac{1}{R})_i \quad , \quad i=0$$

and,

$(\frac{1}{R})$, $(\frac{1}{R})_i$ are defined the same as under VHTP 2 b).

t_3 is the time the vehicle enters the grid.

t_3+1 is the time 1 second after the vehicle enters the grid.

$(\frac{1}{R})_{av}$ is the average of $\frac{1}{R}$ over the above defined interval $[t_o, t_o+1]$.

$(\frac{1}{R})_o$ is the value of $\frac{1}{R}$ at the time the vehicle enters the grid.

VHTP 3: b) $\beta_p(t)$ = Maximum absolute value of sideslip angle.

where

t is defined over the interval $[t_3, t_3+1]$.

t_3, t_3+1 are defined as in a).

VHTP 3: c) $\dot{\beta}_p(t)$ = Maximum absolute value of rate of change of sideslip angle.

where

t is defined over the interval $[t_3, t_3+1]$.

t_3, t_3+1 are defined as in a).

VHTP 4: a) A_{yp} = Maximum lateral acceleration over the entire maneuver time interval.

VHTP 4: b) r_p = Maximum yaw rate over the entire maneuver time interval.

VHTP 4: c) $R_o(\frac{1}{R})_{av} = \frac{(\frac{1}{R})_{av}}{(\frac{1}{R})_o}$ = Average path curvature ratio.

where

$$(\frac{1}{R})_{av} = \frac{1}{2}\int_{t_4}^{t_4+2} (\frac{1}{R})dt \cong \frac{1}{2s_f}\sum_{i=1}^{2s_f} (\frac{1}{R})_i$$

$$(\frac{1}{R})_o = \frac{1}{R}\Big|_{t_4} \cong (\frac{1}{R})_i \ , \quad i=0$$

and

t_4 is the time of the steering input

t_4+1 is the time 2 seconds after the steering input

$(\frac{1}{R})_{av}$ is the average path curvature over the above defined interval $[t_4, t_4+1]$

$(\frac{1}{R})_o$ is the path curvature at t_o.

VHTP 4: d) $\beta_p(t)$ = Maximum absolute value of sideslip angle over t.

where

t is defined over the interval $[t_4, t_4+2]$

t_4, t_4+2 defined as in c).

VHTP 4: e) $\dot{\beta}_p(t)$ = Maximum absolute value of rate of change of sideslip angle over t.

where

t is defined over the interval $[t_4, t_4+2]$

t_4, t_4+2 defined as in c).

VHTP 4: f) $\Delta\beta = \beta_p(t) - \beta(t_4)$

where

t is defined over the interval $[t_4, t_4+2]$

$t_4 m t_4+2$ defined as in c)

$\beta(t_4)$ = the value of sideslip at t_4.

VHTP 5: a) $$\Delta = \frac{1}{T}\int_{t_5}^{t_5+T} |y-12|dt \cong \frac{1}{T\cdot s_f}\sum_{i=1}^{T\cdot s_f} |y_i-12|,$$

for right-left steer.

$$= \frac{1}{T}\int_{t_5}^{t_5+T} |y+12|dt \cong \frac{1}{T\cdot s_f}\sum_{i=1}^{T\cdot s_f} |y_i+12|,$$

for left-right steer.

where

t_5 is the time of the steering input

T is the length of time of the maneuver, usually 3.4 seconds

y is the time history of the lateral displacement of the vehicle after t_5

y_i is the discretized representation of y

s_f is the digitizing rate.

VHTP 5: b) $\beta_p(t)$ = Maximum absolute value of sideslip angle.

where

t is defined over the interval $[t_5, t_5+T]$

t_5, t_5+T defined as in a).

VHTP 5: c) $\Delta\psi(t_5+T)$ = Heading angle at the time (t_5+T)

where

t_5, T are defined as in a).

VHTP 6: a) ϕ_{max} = Maximum absolute value of roll angle over the entire maneuver time interval.

APPENDIX IX

TIRE LATERAL FORCE INVESTIGATION

BACKGROUND

In the pilot test phase of the VHP and S/SS programs, vehicle response data from trapezoidal steer tests were gathered which indicated a large variation in peak lateral acceleration capability over a two-week period. A later set of tests on another vehicle operated over a three-week period confirmed the previous response variations. Since this variability seriously degrades the viability of the limit performance measurement procedures, a research study was undertaken to identify the causative factors contributing to the non-repeatable response. It was hypothesized that the magnitude of the variability could only be explained by a major change in conditions at the tire-road interface. Thus, the research effort was designed to investigate the relationship between peak lateral force capability of the tire and each of three potential test variables: tire wear, surface wetness, and pavement temperature. Experiments directed toward the investigation of each factor will be treated here individually.

INVESTIGATION INTO THE RELATIONSHIP BEWTEEN TIRE SIDE FORCE CAPABILITY AND TIRE TREAD WEAR

Since the trapezoidal steer maneuver and both other automatically controlled vehicle handling test procedures involve repetitive testing with the tires experiencing large sideslip angles, a considerable degree of tire wear is

incurred as a result of the test process. The character of this type of wear is quite different from that obtained in normal driving. The most rapid changes in tread profile take place at the outside shoulder and sometimes further up the sidewall.

In recognition of the multi-variable character of vehicle testing, it was determined that specific findings on tire properties could only be obtained through experiments with tight control on condition variables. The HSRI Mobile Tire Tester was used as the experimental apparatus for a) providing, in a controlled fashion, a vertical load and slip angle to a tire such that it could be incrementally worn in a manner analogous to that obtained in testing the vehicle, and b) for gathering tire side force data concurrent with the wearing process.

The first two tires subjected to this experiment were a Uniroyal L78-15 Fastrak and a Goodyear F78-14 Polyglas. These tires were provided as original equipment on the two test vehicles with which variability in trapezoidal steer data had been first observed. Each tire was subjected to a sequence of runs over both concrete and asphalt by which the Mobile Tire Tester, travelling at 40 mph, lowers the tire onto the pavement at a 20° slip angle and a selected large vertical load. Tire tread profiles were measured by use of a contour copying device and reproduced versus average side forces for each data sample, in Figure IX-1. Data sets were gathered in groups of 4 runs each, designated as a "lap" of the Mobile Tire Tester involving a path over the TTI facility as shown in Figure IX-2. The very first piece of data with the new tire, then, is on concrete, followed by two runs on asphalt, and one more on concrete.

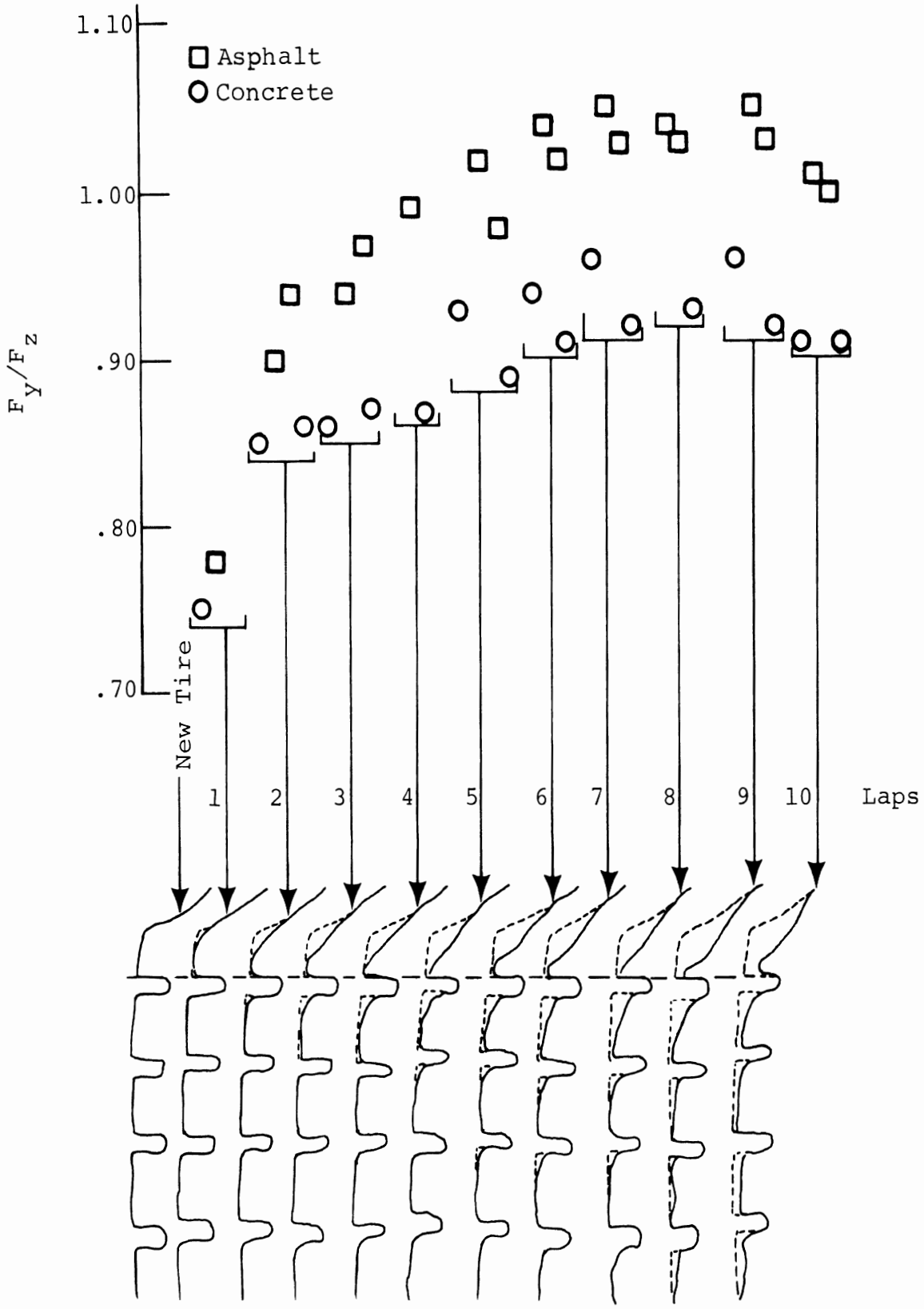

Tread Profile - Outside Shoulder
α=20° F_z=1550 Uniroyal L78-15 Fastrak
Tire Sample No. 1

Figure IX-1

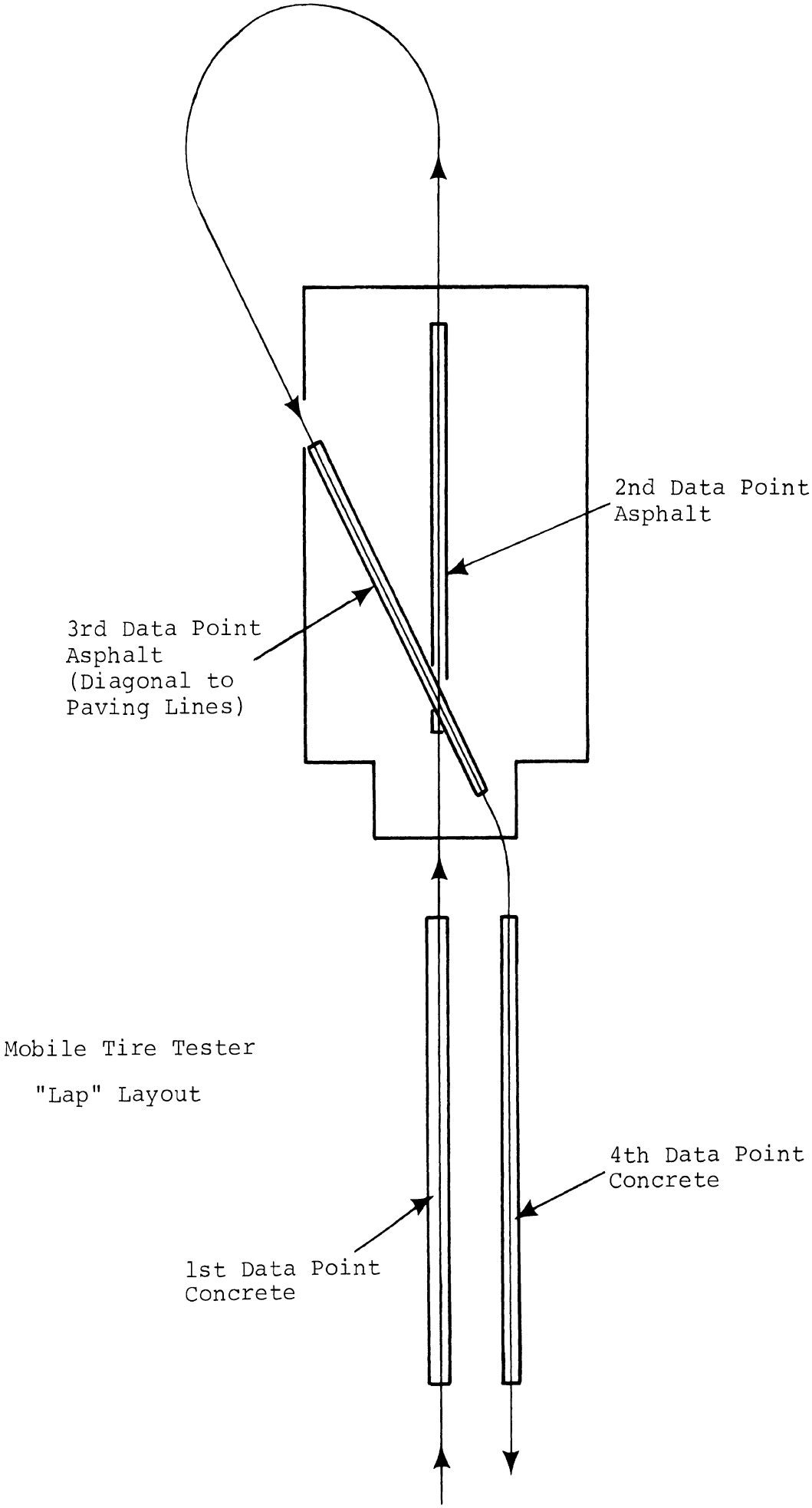
2nd Data Point
Asphalt
3rd Data Point
Asphalt
(Diagonal to
Paving Lines)
Mobile Tire Tester
"Lap" Layout
4th Data Point
Concrete
1st Data Point
Concrete

Figure IX-2

The tire data shown in Figure XI-1 thus indicates a significant rise in side force capability with increased wear. It is apparent that the first data point, on concrete, represents a condition whereby a significant improvement in the tire's lateral force capability is taking place, even as the run progresses over 9 seconds, see Figure XI-3. Note in Figure IX-3 that the force is increasing as runs progress on both concrete and asphalt.

This remarkable result was confirmed with a second Uniroyal L78-15 Fastrak to assure that the general finding was not, for some reason, atypical. (See Figure IX-4.) A similar wear sensitivity (force increase) characteristic was then obtained with the Goodyear F78-14 Polyglas tire. (Figure IX-5). It is presumed that, although the first concrete data point is consistently the lowest force on Figures IX-1, 4, and 5, the wearing process is the dominant influence. If the first run had been over asphalt, the lowest force would be expected to have been observed there also.

Additional force data was taken on asphalt for these two tire types, at slip angles of α = 5, 10, 15, 20°, after they had been worn. This data was needed to determine the adequacy of the α = 20° choice in representing peak force capability during the wear experiments. In Figure IX-6, both tires are seen to be operating at approximately peak side force at α = 20°.

CORRELATION OF MOBILE TIRE TESTER RESULTS WITH VEHICLE TESTS

Trapezoidal steer tests were conducted to determine the extent to which vehicle test results could be shown to correlate with the Mobile Tire Tester data (concerning

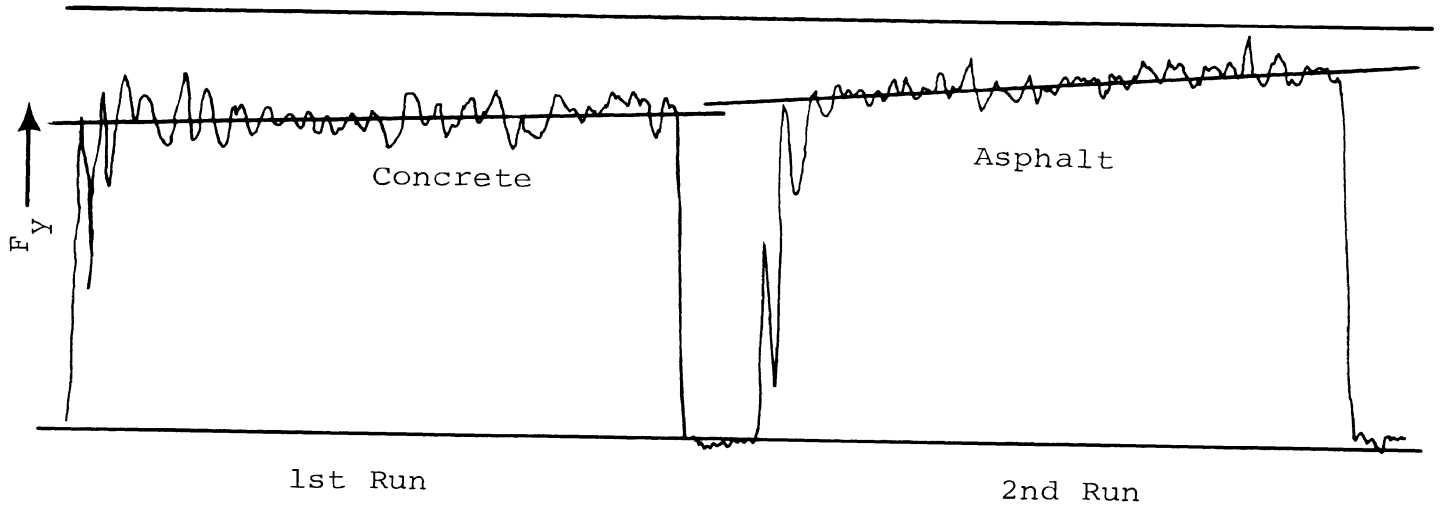

Uniroyal L78-15
Fastrak

Figure IX-3

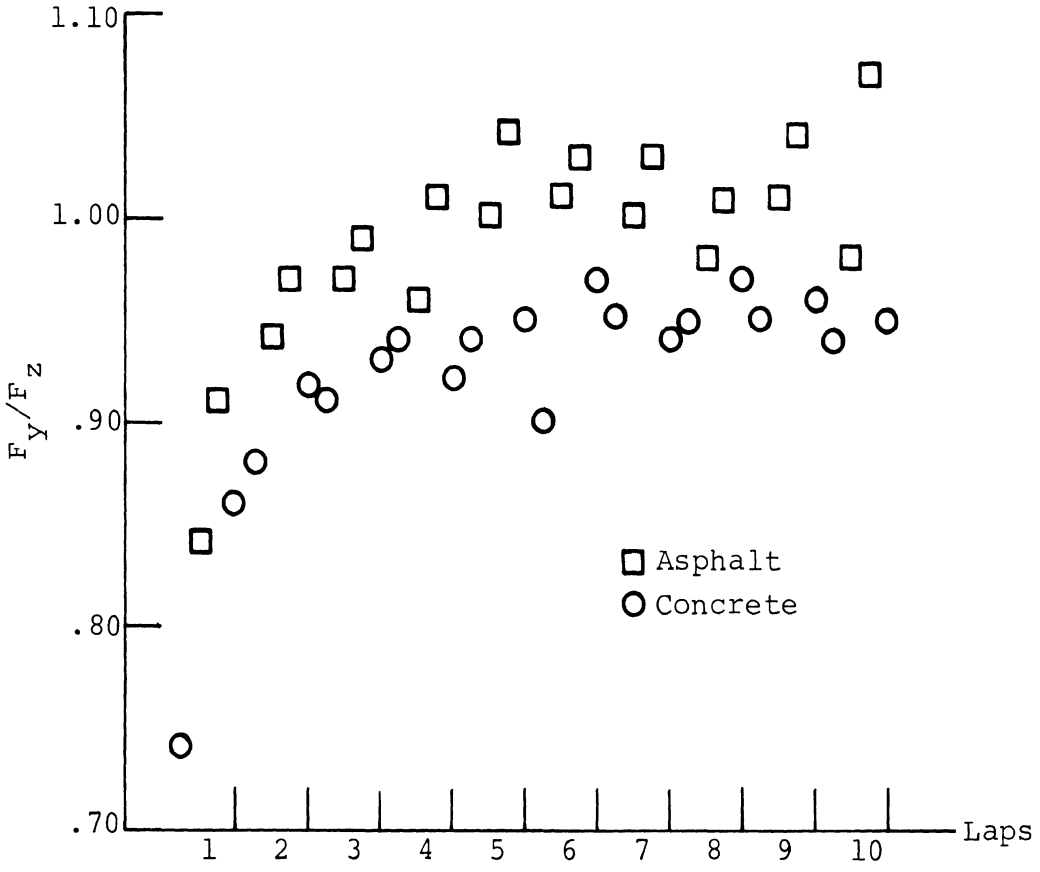

Lateral Force/Wear Data
Mobile Tire Tester
α=20° F_z=1550 lbs. 27 psi 40 mph
Uniroyal L78-15 Fastrak
Tire Sample No. 2
Chevrolet

Figure IX-4

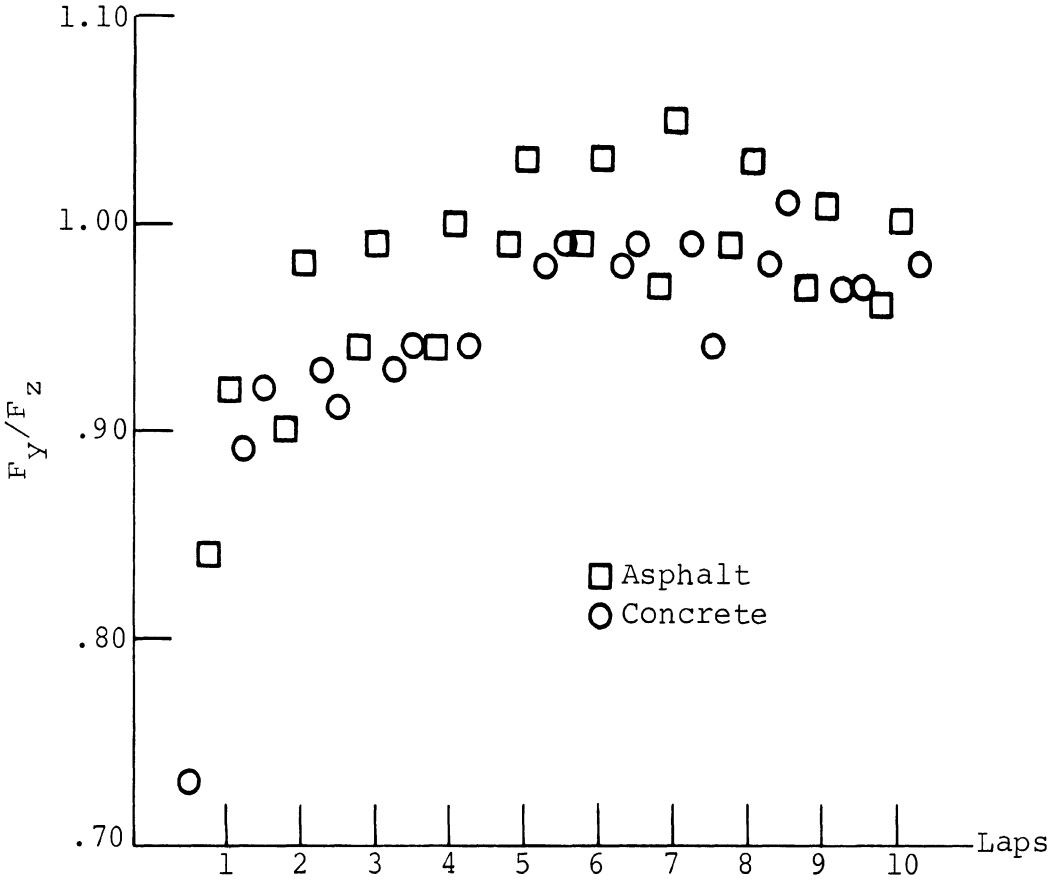

Lateral Force/Wear Data

Mobile Tire Tester

α=20° F_z=1200 lbs. 26 psi 40 mph

Goodyear F78-14 Polyglas

Coronet

Figure IX-5

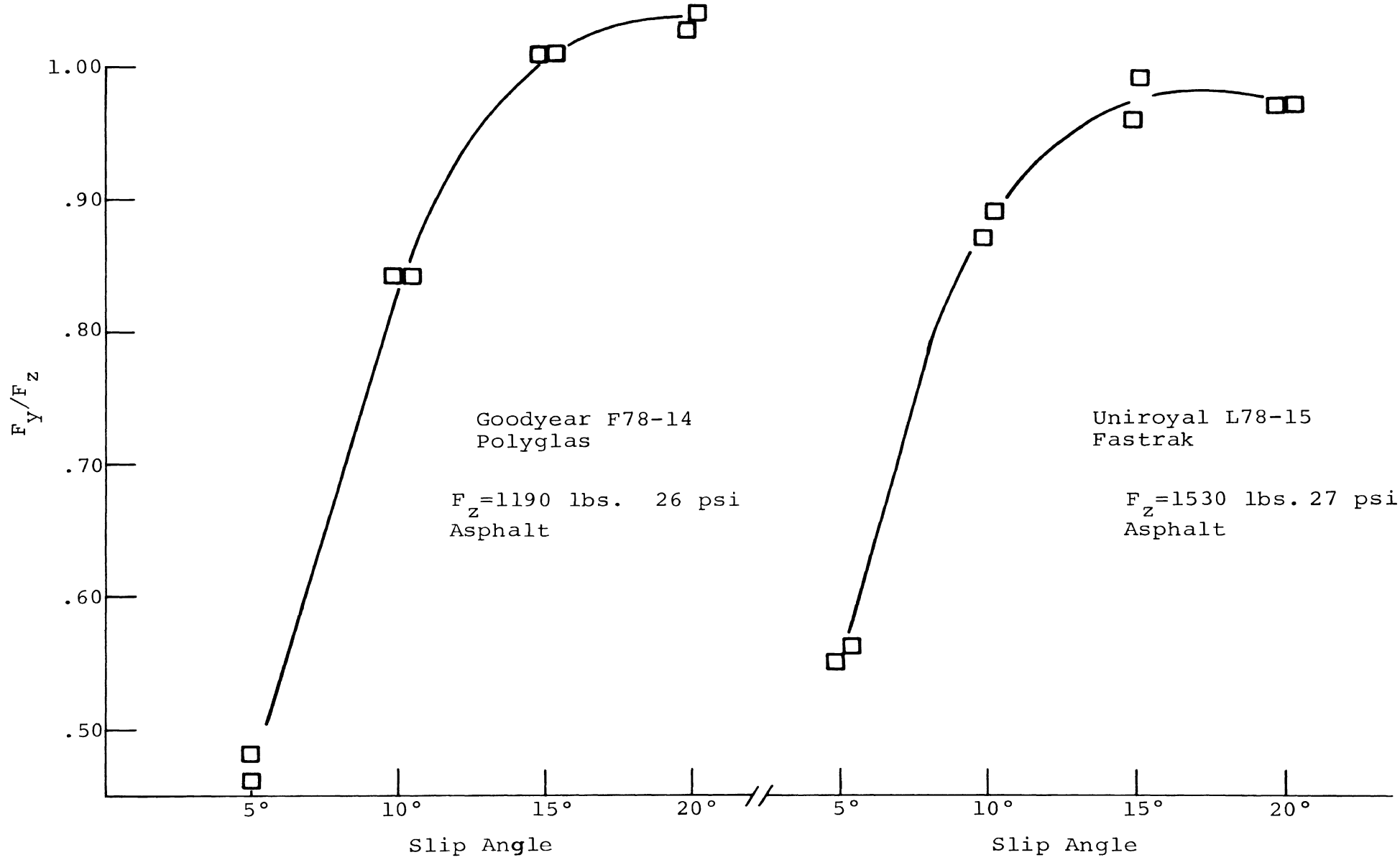
1.00
.90
.80
.70
.60
.50
F_y/F_z
Goodyear F78-14
Polyglas
F_z=1190 lbs. 26 psi
Asphalt
Uniroyal L78-15
Fastrak
F_z=1530 lbs. 27 psi
Asphalt
5°
10°
15°
20°
Slip Angle
5°
10°
15°
20°
Slip Angle

Figure IX-6

tire wear sensitivity). A trapezoidal steer sequence was performed on a Dodge Coronet with Goodyear F78-14 Polyglas tires that had been heavily worn due to previous testing, followed by a sequence with worn rear but new front tires (the term "new tires" always refers to tires that have been broken in with 100 or 200 miles of "normal" driving). Peak lateral accelerations achieved are plotted versus steer angle in Figure IX-7. The worn tire sequence was run going up in steer level and the new-front, worn-rear tire condition was run starting with the highest steer level and going down. The first two (left turn) runs with 2 new tires show a .23g lower acceleration response than was obtained at the highest steer level with all worn tires. The slight increase in lateral acceleration at the next lower steer level with 2 new tires appears to indicate the increased force potential of the new tires with cumulative wear. At the conclusion of this sequence a significant alteration in tire properties was evident from the elevated performance obtained in six more runs at the highest steering level. (These six runs are shown in the hexagon in Figure IX-7.)

The wear/side force data from the Mobile Tire Tester was more directly correlated with data gathered using a Chevrolet Station Wagon, equipped with a set of (4) new Uniroyal L78-15 Fastrak tires. Trapezoidal steer responses were obtained at the highest level of steering used in the procedure (i.e., $\delta_{SW} = 400°$) employing alternating sets of three left and three right turns on both asphalt and concrete. These data are plotted in Figure IX-8 and show that the tire wearing process is accompanied by large changes in the value of peak lateral acceleration.

A degradation in directional stability appears to result from the wearing process as quantified by the data in Figure IX-9, depicting an increasing spin-type response on

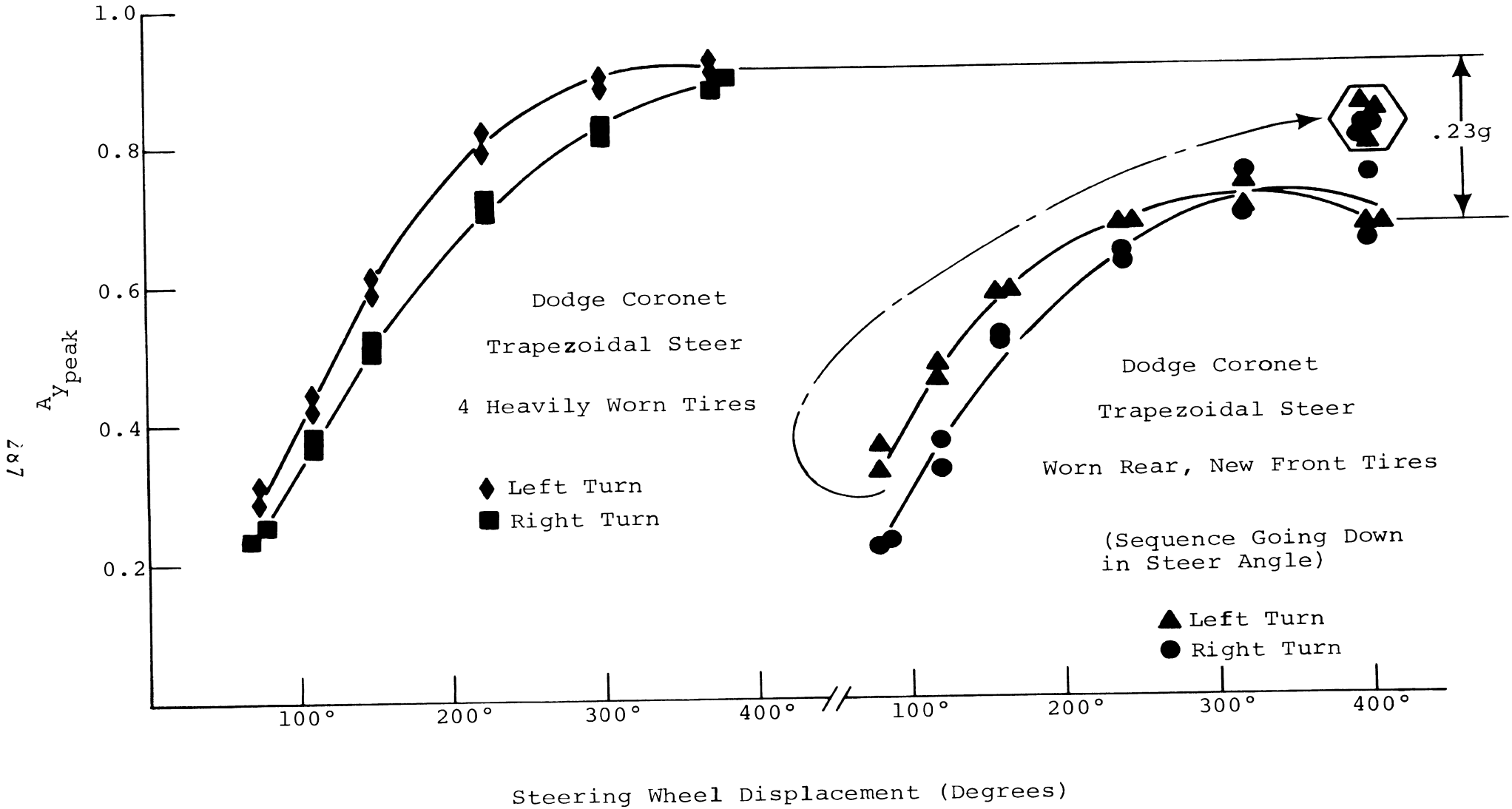
1.0
0.8
0.6
0.4
0.2
$A_{y_{peak}}$
Dodge Coronet
Trapezoidal Steer
4 Heavily Worn Tires
Left Turn
Right Turn
.23g
Dodge Coronet
Trapezoidal Steer
Worn Rear, New Front Tires
(Sequence Going Down
in Steer Angle)
Left Turn
Right Turn
100°
200°
300°
400°
100°
200°
300°
400°
Steering Wheel Displacement (Degrees)

Figure IX-7

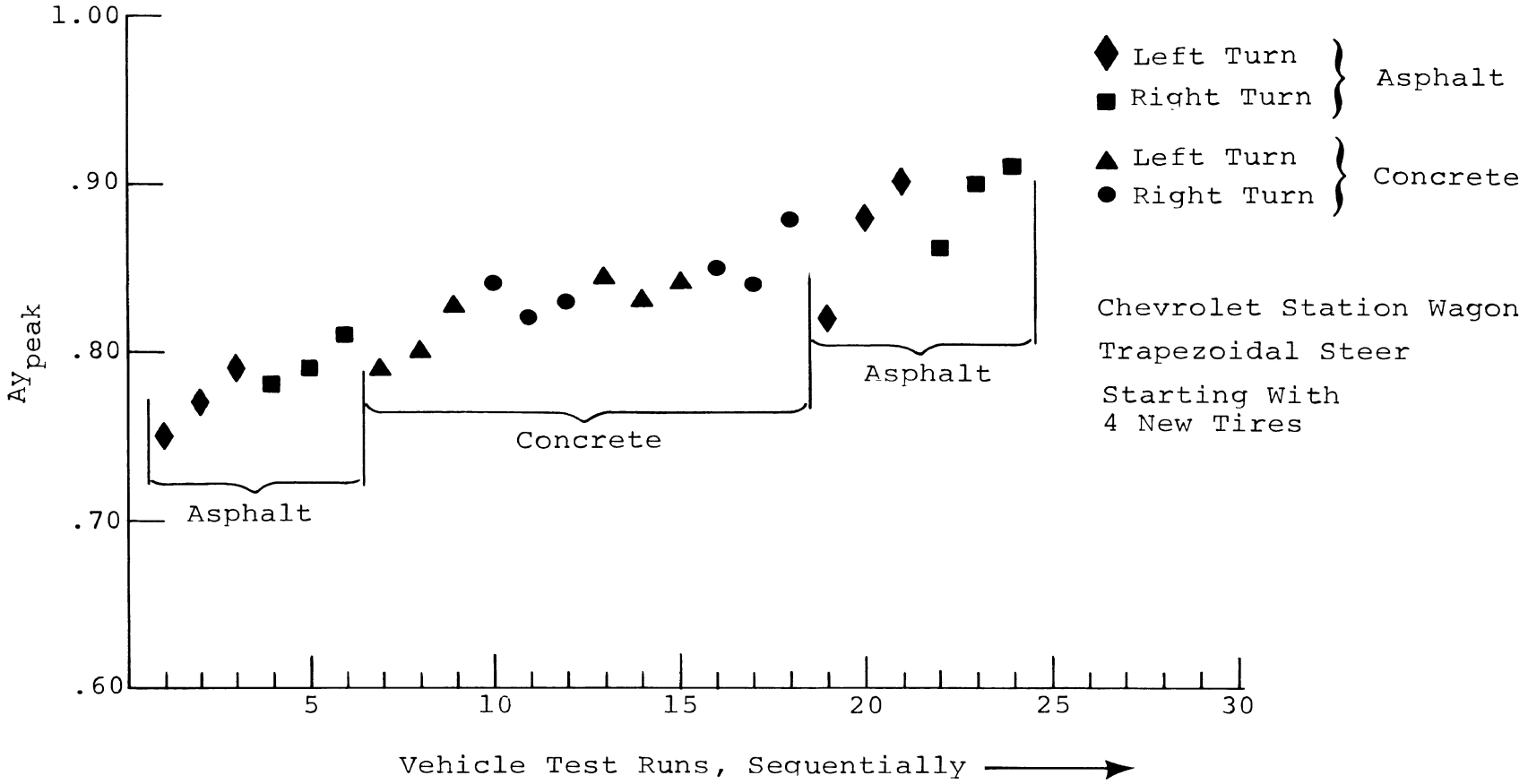
1.00
.90
.80
.70
.60
Ay_{peak}
5
10
15
20
25
30
Vehicle Test Runs, Sequentially
Left Turn
Right Turn
Asphalt
Left Turn
Right Turn
Concrete
Chevrolet Station Wagon
Trapezoidal Steer
Starting With
4 New Tires
Asphalt
Concrete
Asphalt

Figure IX-8

asphalt (increasing peak value of vehicle sideslip angle). This result is attributed to the higher rate of wear occurring on the front tires resulting from the large load transfers caused by the roll stiffness of the front suspension. A similar manifestation of the effectiveness of tire wear distribution in destabilizing the limit turning response also appears in Figure IX-9, where data is presented for tests performed with worn tires installed on the front wheels and new tires on the rear axle. After a few spin-out responses, the new rear tires show an apparent trend toward more wear, and thus greater vehicle stability.

The results obtained with the Mobile Tire Tester and the test results obtained with the Chevrolet and Dodge show very clearly that the tire wear produced in the trapezoidal steer maneuver has a very large influence on the maximum side forces produced by the tires and, consequently, has a large influence on the peak lateral accelerations that are attained, including the character of the total vehicle response.

Data obtained recently from the flat bed tire test machine at General Motors Proving Ground also indicate a significant change in lateral tire force capability as a function of wear. In the GM work, tire wear was achieved by shaving the tread surface and thus substantial wear of the tread face was incurred, in a manner more analogous to normal driving wear. Although the conditions are not the same and not directly comparable to the MTT results, the same trend is evident. Expressed in similar terms, the GM data shows an increase in F_y/F_z, normalized lateral force, from .69 to .81 over the full range of tire wear.

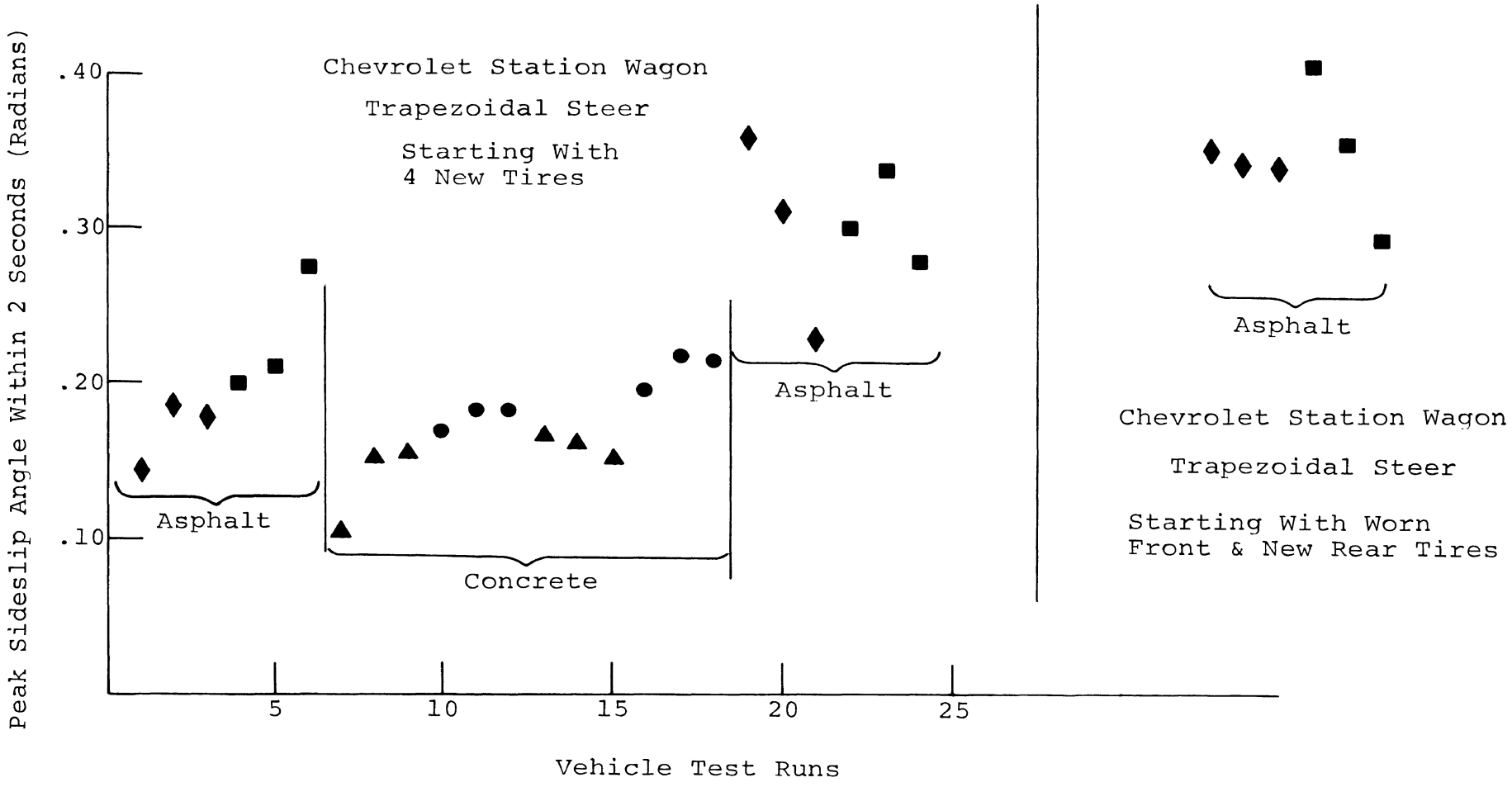
Peak Sideslip Angle Within 2 Seconds (Radians)
.40
.30
.20
.10
Chevrolet Station Wagon
Trapezoidal Steer
Starting With
4 New Tires
Asphalt
Concrete
Asphalt
Asphalt
Chevrolet Station Wagon
Trapezoidal Steer
Starting With Worn
Front & New Rear Tires
5
10
15
20
25
Vehicle Test Runs

Figure IX-9

INVESTIGATION INTO THE RELATION BETWEEN TIRE SIDE FORCE CAPABILITY AND SURFACE DRYING TIME

The drying time experiment consisted of: (1) wetting one-half of the skid pad with a water truck, (2) measuring maximum normalized tire side force with the Mobile Tire Tester at several times and at several locations as the pad was drying and (3) measuring peak lateral acceleration obtained with the Chevrolet Station Wagon in a limit trapezoidal steer maneuver as the pad was drying.

The west (low side) of the asphalt test pad was heavily wetted by making a series of parallel passes over the length of the skid pad with the watering truck. The Mobile Tire Tester tests and the vehicle tests started as soon as possible after the water truck had finished. The water depth over the wetted portion of the skid pad varied considerably due to small unevenness in the pad surface caused by the asphalt laying process. Almost immediately after wetting there were areas of standing water and areas of asphalt which were discolored from wetting but over which no water was standing.

The Mobile Tire Tester was used to make side force measurements on areas of the asphalt skid pad with differing water conditions. Tests were made in areas of standing water, in areas discolored by wetting, and in areas which had never been wetted. The tests were made using a Chevrolet Station Wagon tire operated at 20° slip angle and 40 mph. The results are summarized in Table IX-1. The normalized lateral force capability of the surface varied from 0.56 to 0.80 at two different locations on the surface just after it had been wetted. In just less than two hours after the surface had been wetted almost all of the standing water was gone. A section of asphalt which was still discolored from wetting had a normalized lateral force capability of

about 0.83. The asphalt which appeared dry after having been wetted had a normalized lateral force capability of 0.96 which was identical to the normalized lateral force capability of the portion of the skid pad which had never been wetted.

Simultaneously with these tire tests, trapezoidal steer maneuvers were conducted with the Chevrolet Wagon on the skid pad. The test results are presented in Figure IX-10. Note that, before the pad was wetted, the maximum lateral acceleration obtained in a series of 6 trapezoidal steer maneuvers varied from 0.84 to 0.87g. After the pad was wetted, the maximum lateral acceleration obtained in 6 trapezoidal steer tests varied from 0.65 to 0.78g. (This spread in values demonstrates the variability in lateral force capability resulting from variations in water depth.) The maximum lateral acceleration obtained in tests performed approximately 2 hours after wetting the surface varied from 0.825 to 0.86g, indicating that the surface had essentially recovered its "dry" friction properties.

On the basis of these findings, it is concluded that vehicle testing can commence after a rain when the pavement appears to be dry, that is, the asphalt is no longer discolored from wetting.

TABLE IX-1. SUMMARY OF MTT (MOBILE TIRE TESTER) WET TEST DATA, F_y/F_z

Time	Wet (Standing Water)	Discolored From Wetting (Partially Wet)	Appears Dry After Wetting	Not Wetted (Dry Surface)
0:00	0.56	0.80		0.98 0.98
0.15	0.60	0.81		0.98
0:55	0.56 0.59	0.86 0.84		
1:40		0.83 0.84	0.96 0.96	
1:50				0.96 0.96

Asphalt Skid Pad
40 mph
1550 lbs. Load, F_z
20° Slip Angle
"20%" Worn Chevy S.W. Tire, Tire #1

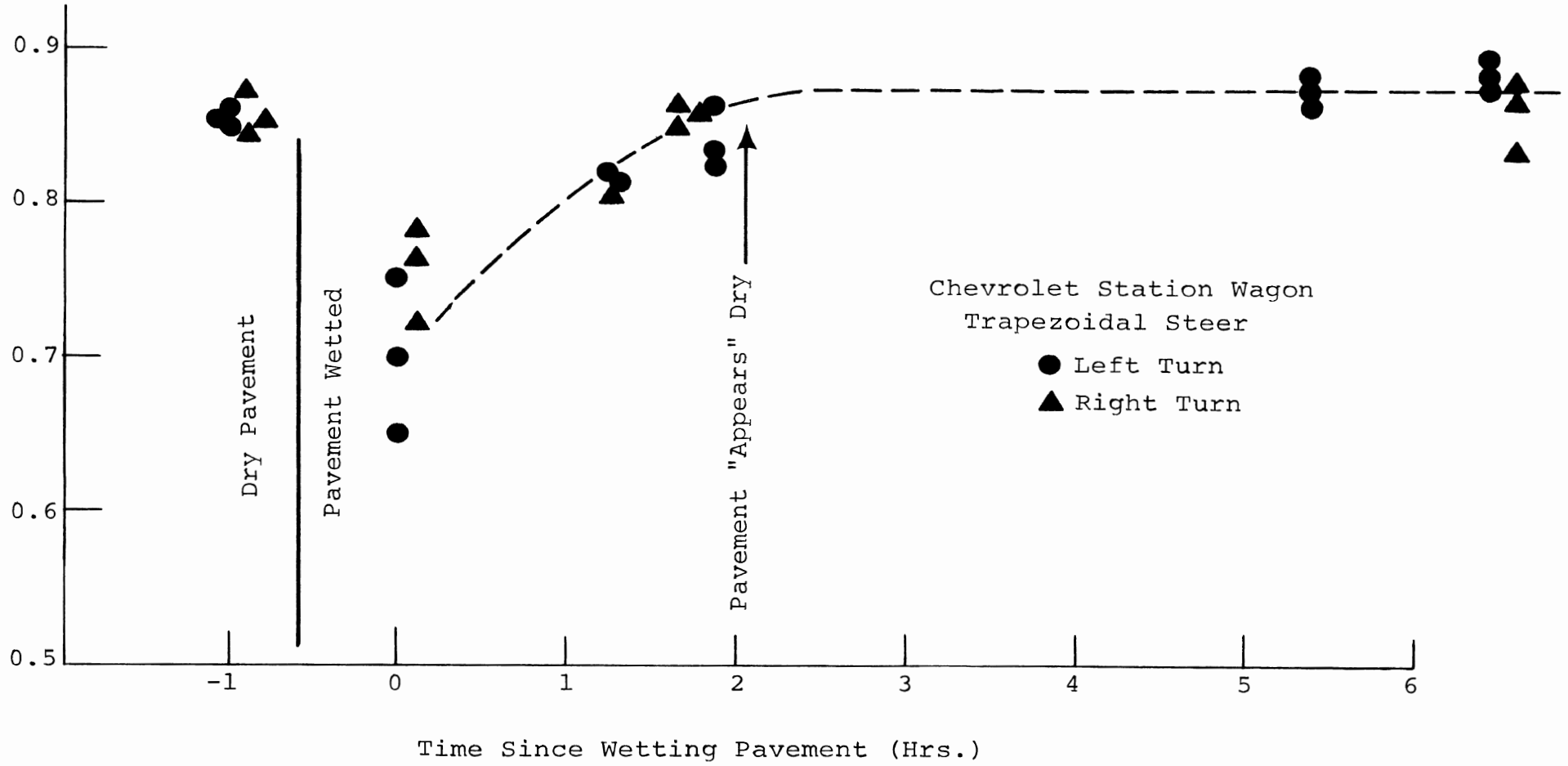
0.9
0.8
0.7
0.6
0.5
Ay_{peak} (g's)
Dry Pavement
Pavement Wetted
Pavement "Appears" Dry
Chevrolet Station Wagon
Trapezoidal Steer
Left Turn
Right Turn
-1
0
1
2
3
4
5
6
Time Since Wetting Pavement (Hrs.)

Figure IX-10

INVESTIGATION INTO THE RELATION BETWEEN TIRE LATERAL FORCE CAPABILITY AND PAVEMENT SURFACE TEMPERATURE

To obtain test data over a wide range of asphalt pad temperatures, tire force measurements and trapezoidal steer maneuvers were performed with the Chevrolet Wagon over a period of 7 days, morning and afternoon. It is clear that this experiment involved uncontrolled variables since environmental factors such as humidity and wind could have been changing over this period. However, all of the tires were well worn and thus tire wear is not believed to have been a significant factor in these tests. The pad was not wetted during this period.

The test results for the asphalt pad are shown on Figure IX-11. Similar results are shown for the concrete pad in Figure IX-12. It is seen that there is very little change in peak lateral acceleration produced in a trapezoidal steer maneuver when the asphalt pad temperature varied from 83°F to 119°F. On the basis of these data it is concluded that pad surface temperature does not have a significant influence on the peak lateral acceleration that can be attained by a vehicle. It can also be concluded that any other environmental factors such as humidity or wind which may have been varying to some extent over the seven-day-period did not have a significant effect on the test data. Thus no test constraint involving surface temperature was adopted.

LATERAL FORCE CAPABILITY AS EFFECTED BY TIRE WEAR AND TEMPERATURE EFFECTS AS RELATED TO PAVEMENT TYPE

The test results showing the influence of tire wear, as given in Figures IX-1, 4, 5, and 14 through 23, were obtained on both concrete and asphalt surfaces. While the

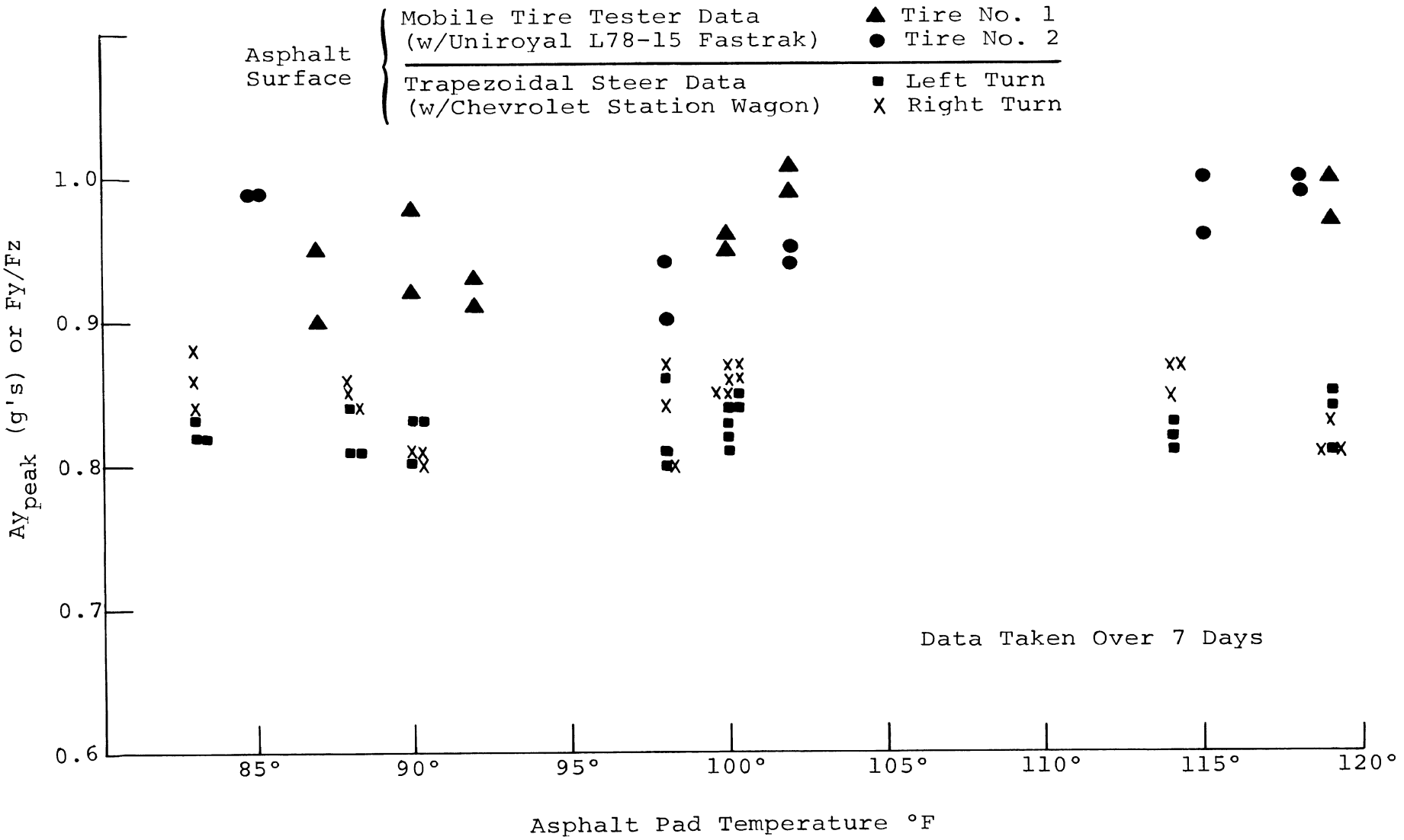
Asphalt Surface
Mobile Tire Tester Data (w/Uniroyal L78-15 Fastrak)
Trapezoidal Steer Data (w/Chevrolet Station Wagon)
Tire No. 1
Tire No. 2
Left Turn
Right Turn
Data Taken Over 7 Days
Ay peak (g's) or Fy/Fz
1.0
0.9
0.8
0.7
0.6
85°
90°
95°
100°
105°
110°
115°
120°
Asphalt Pad Temperature °F

Figure IX-11

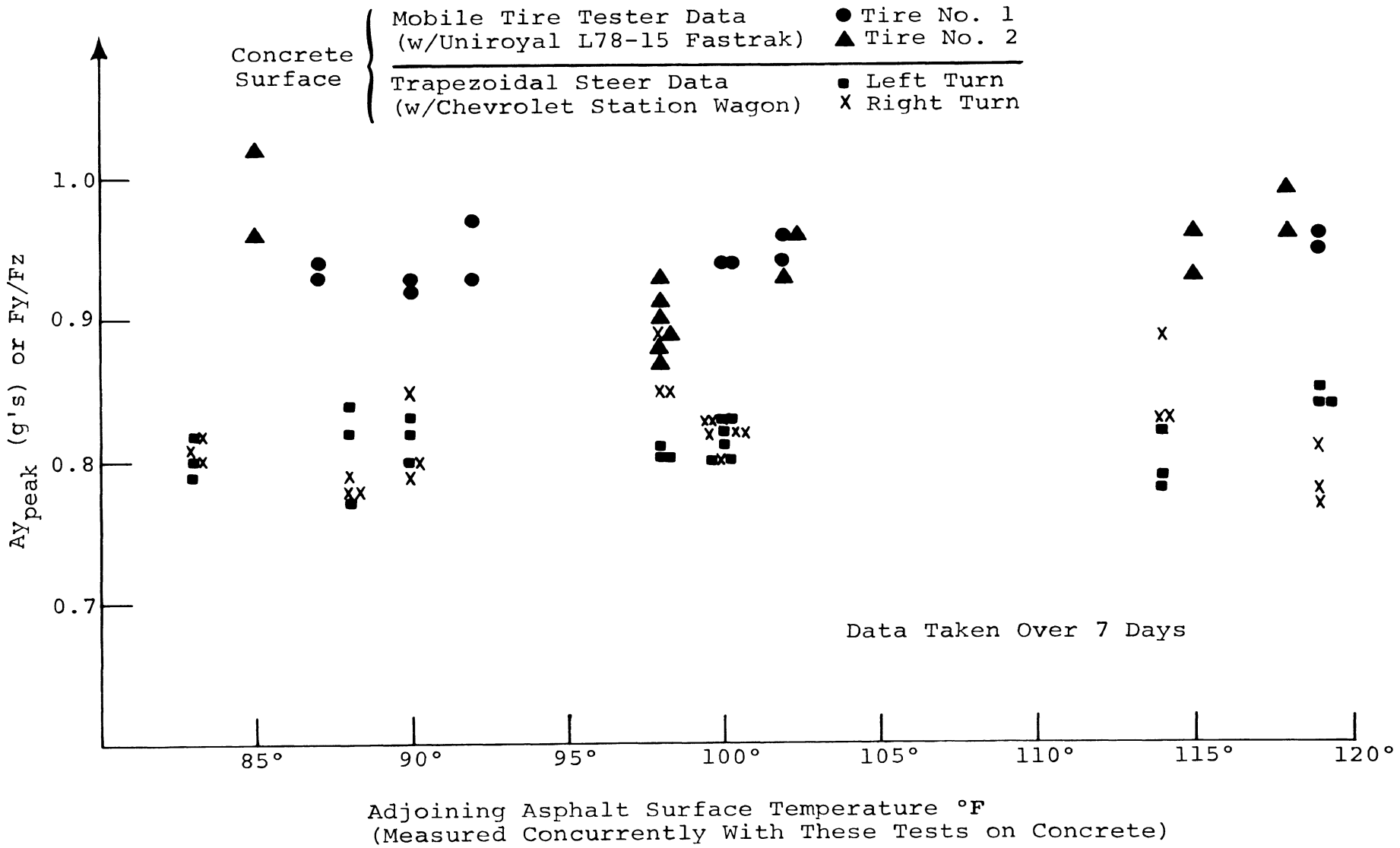
Concrete Surface
Mobile Tire Tester Data (w/Uniroyal L78-15 Fastrak)
Tire No. 1
Tire No. 2
Trapezoidal Steer Data (w/Chevrolet Station Wagon)
Left Turn
Right Turn
Data Taken Over 7 Days
Aypeak (g's) or Fy/Fz
1.0
0.9
0.8
0.7
85°
90°
95°
100°
105°
110°
115°
120°
Adjoining Asphalt Surface Temperature °F
(Measured Concurrently With These Tests on Concrete)

Figure IX-12

asphalt produces a slightly higher lateral force than the concrete for almost all of the tires tested, there does not appear to be any significant difference between the two surfaces with respect to the manner in which tire wear progresses.

Pad temperature does not have a significant influence on lateral force capability of tires operating on the asphalt surface. Unfortunately, the temperature of the concrete surface was not measured directly. However, the results given in Figure IX-13 indicate that temperature change was not a significant factor influencing the developed lateral force during the seven-day measurement period.

In summary, no tire wear or temperature factors have been identified as a basis for selecting a concrete surface over an asphalt surface for vehicle test purposes.

CONCLUSIONS BASED ON THE INVESTIGATION

The results obtained with the Mobile Tire Tester and the test results obtained with the Chevrolet and Dodge show very clearly that:

1. The tire wear produced in the trapezoidal steer maneuver has a very large influence on the maximum side forces produced by the tires and consequently has a large influence on the peak lateral accelerations that are attained. Additionally, the character of the limit response of the vehicle can alter markedly as dissimilar tire wear rates are accrued at front and rear.

2. The pad surface temperature varying over the range (83°F to 119°F) has no first order influence on peak side force.

3. The influence of surface wetness following a rainfall can be presumed negligible upon recovery of apparent dryness, i.e., no pavement discoloration.

APPLICATION OF LATERAL FORCE VERSUS WEAR FINDINGS

Since tire lateral force, and consequently vehicle lateral acceleration, has been shown to increase rapidly with severe cornering wear, it was necessary to establish a tire wearing procedure to eliminate large variations in vehicle test results. Based on Figures IX-1 and IX-8, it was estimated that the tire wear effects produced in 20 trapezoidal steer maneuvers is equivalent to the amount of tire wear produced during one "lap" of the MTT, as defined in Figure IX-2. The resultant procedure was determined in a two step process.

The first step necessitated gathering the tire wear data for all of the vehicles in the sample in a controlled fashion with the MTT. Test conditions for each of 12 tires measured were:

1. 20° slip angle
2. 40 mph steady velocity
3. Tire inflation pressure set to average of front and rear values specified for the respective test vehicle
4. Normal load

$$F_z = .30[\text{Vehicle Weight} + 300] + 50 \text{ lbs.}$$

Under these conditions, lateral force data was collected for all sample tires over 10 "laps" of the MTT. The range of this data is summarized in Figure IX-13. The bars indicate the range of data collected for each test tire. The separate data points collected during each run for all tires are shown in Figures IX-14 to IX-23.

This data was then analyzed and tabulated to determine the number of laps required for the ratio, F_y/F_z, to stabilize within 5% of its long-term average value. Based on the correlation data taken with the Chevrolet Brookwood, this yields an equivalent number of limit trapezoidal steer maneuvers required. Table III-2 presents a listing of the pertinent tire wear-in values for each of the measured tires.

TABLE IX-2. TIRE WEAR-IN DATA

Vehicle	Tire	Asphalt Long-Term F_y/F_z	No. Laps To Wear In To Within 0.05	Equivalent Limit Trapezoidal Steer Maneuver
VW	Continental 560-15	1.07	1.0	20
Imperial	Goodyear L84-15	0.99	2.0	40
Mercedes	Firestone 735-14	1.00	0	20 (min.)
Lotus	Dunlop 144 HR13	0.81	0	20 (min.)
*Austin	Dunlop 595-12	0.59	1.5	30
Gremlin	Goodyear F60-15	1.08	2.0	40
Trans-Am	Goodyear F60-15	0.88	1.5	30
Toyota	Dunlop 155-13	0.81	0	20 (min.)
Galaxie	Uniroyal F78-15	1.07	2.0	40
Toronado	Firestone J78-15	0.99	1.5	30
Coronet	Goodyear F78-14	1.00	2.5	50
Brookwood	Uniroyal L78-15	1.02	2.5	50

It is interesting to note the wide variation in the number of runs required to wear-in these different types of tires. It is also interesting to note that these tires seem to divide into 4 ranges of lateral force capability. The VW, Gremlin, and Galaxie tires have very large lateral force capability ($F_y/F_{z_{max}} \doteq 1.07$). The Imperial, Mercedes, Toronado, Coronet, and Brookwood tires have large lateral force capability ($.99 \leqq F_y/F_z \leqq 1.02$). The Lotus, Trans-Am, and Toyota tires have relatively low lateral force capability ($0.81 \leqq F_y/F_z \leqq 0.88$). The Austin tire was measured to have an exceptionally low lateral force capability, although it is suspected that this property is indicative of a side force/slip angle relation which peaked at substantially below $\alpha = 20°$, such that the indicated force level does not represent "peak" side force.

The second phase of this procedure requires that the vehicle be tested with the number of "equivalent trapezoidal steer" runs shown in Table IX-2 prior to collecting the limit performance data. The conduct of this preliminary set of trapezoidal steer tests, designated as tire break-in tests, was given additional constraints:

1. The minimum number of test runs was chosen to be 20, although MTT data showed no wear effect for certain tires.

2. Tires were cross-rotated after 20 runs if additional limit break-in tests were required.

3. Vehicle response data was recorded during the break-in tests for all vehicles with the automatic test package instruments.

4. All test tires were originally broken in with a minimum of 100 miles of standard driving, prior to initiating any of the wear-in tests.

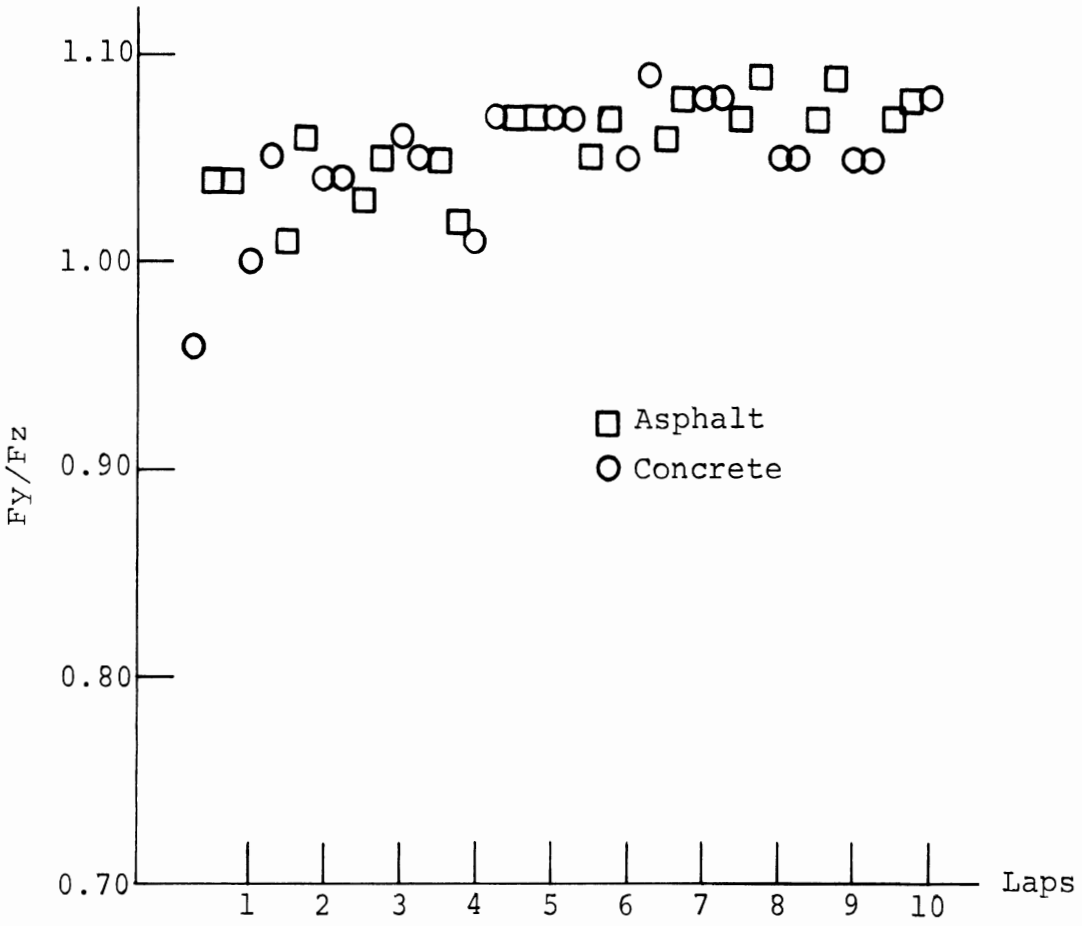

Lateral Force/Wear Data, Mobile Tire Tester, Continental 560-15 (VW).

α=20°, F_z=730, 22 psi, 40 mph

Figure IX-14

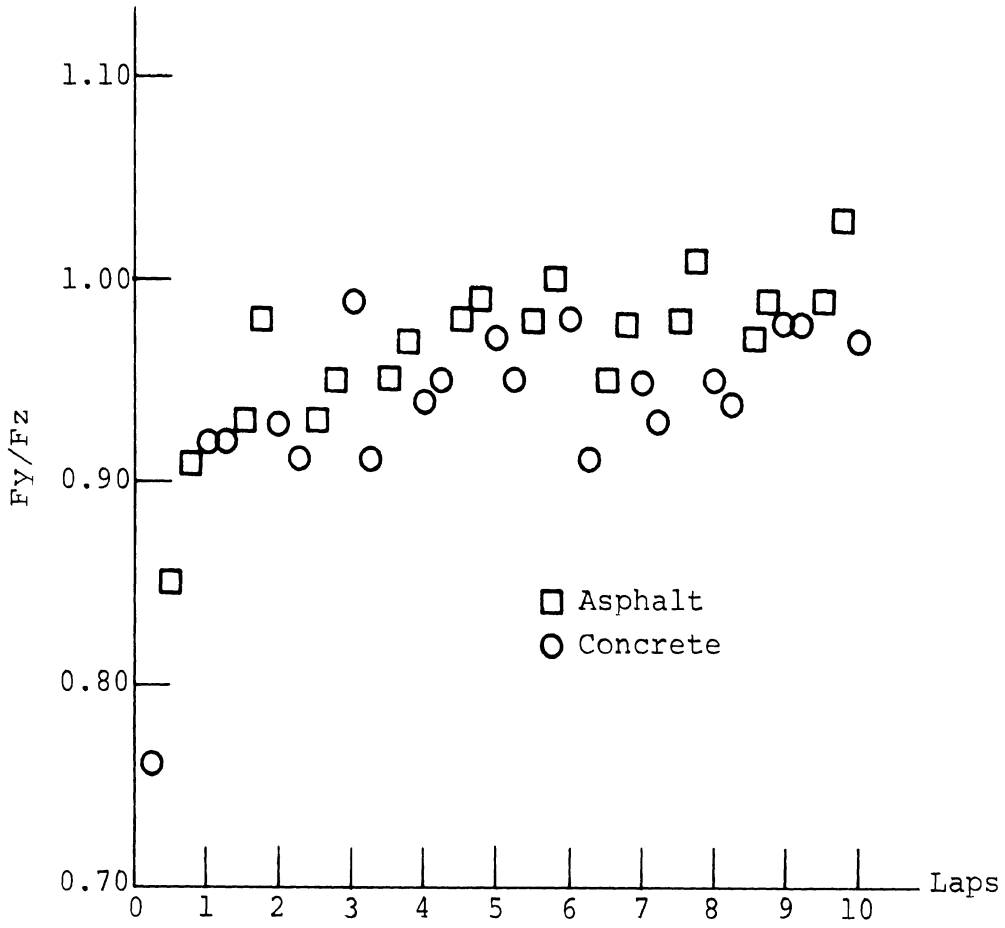

Lateral Force/Wear Data, Mobile Tire Tester, Goodyear L84-15 (Imperial).

α=20°, F_z=1580, 23 psi, 40 mph

Figure IX-15

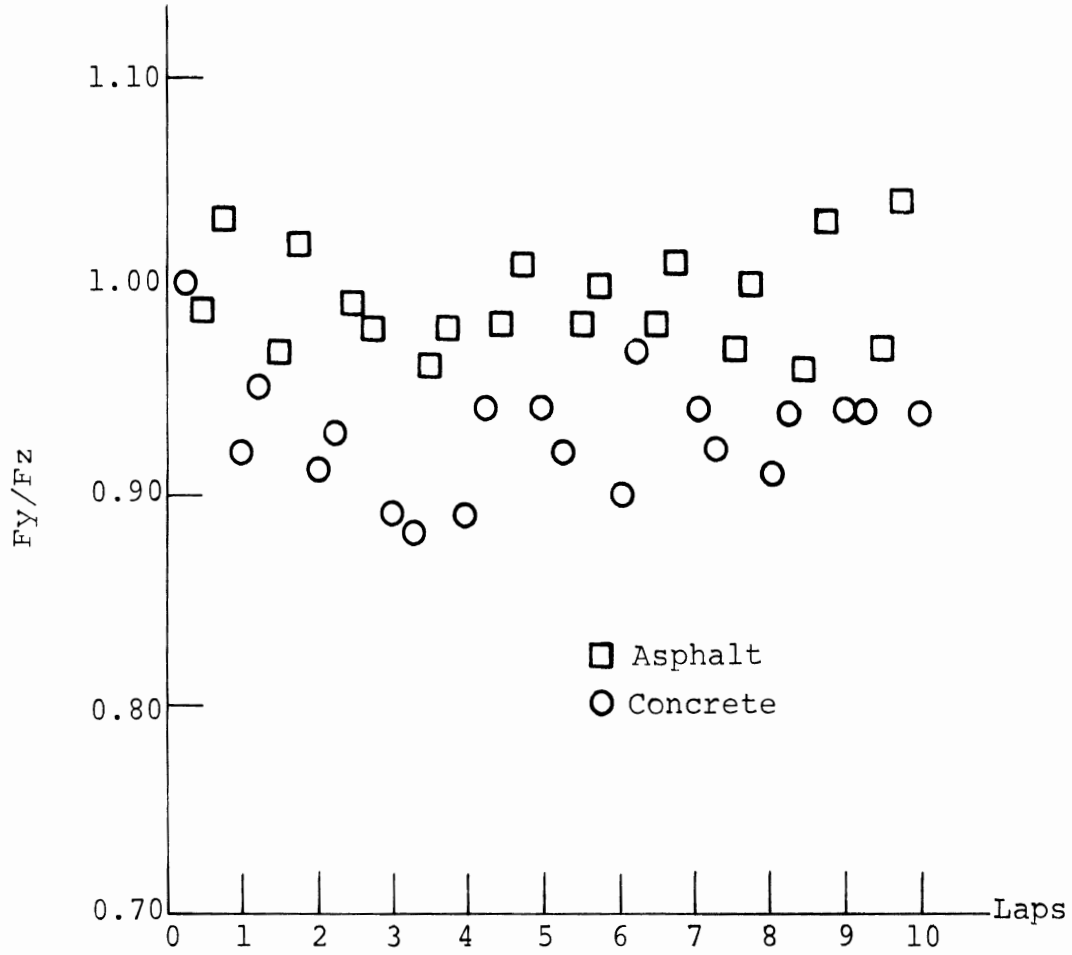

Lateral Force/Wear Data, Mobile Tire Tester, Firestone 735-14 (Mercedes).

α=20°, F_z=1300, 32 psi, 40 mph

Figure IX-16

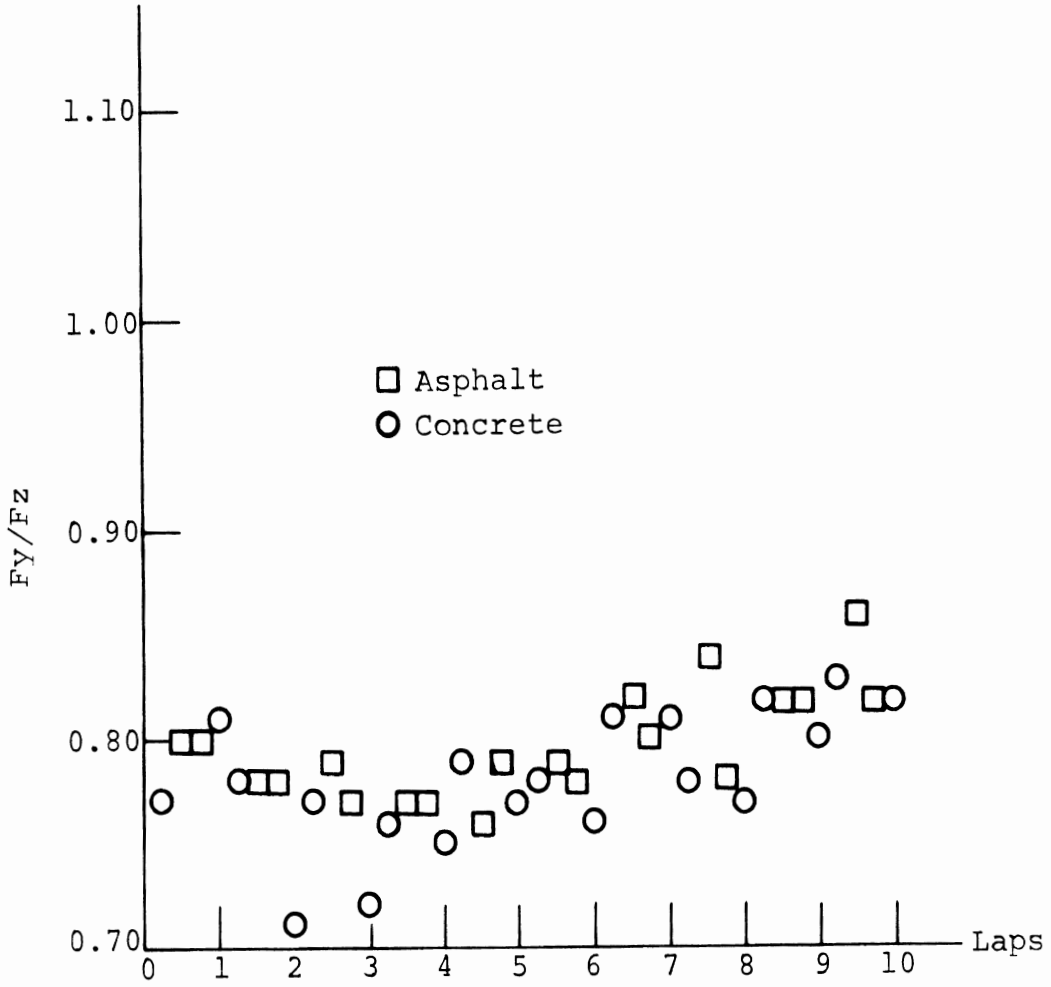

Lateral Force/Wear Data, Mobile Tire Tester, Dunlop 155 HR13 (Lotus).

α=20°, F_z=630, 22 psi, 40 mph

Figure IX-17

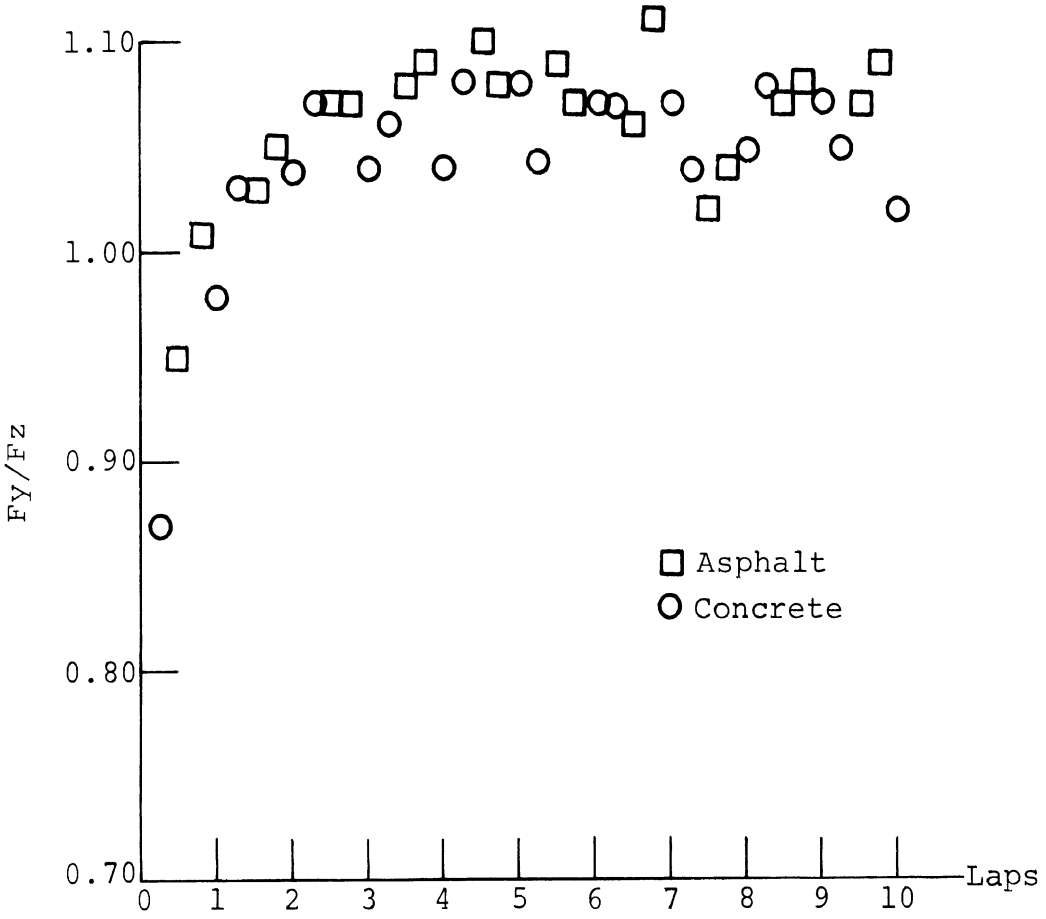

Lateral Force/Wear Data, Mobile Tire Tester, Goodyear 645-14 (Gremlin).

α=20°, F_z=900, 28 psi, 40 mph

Figure IX-18

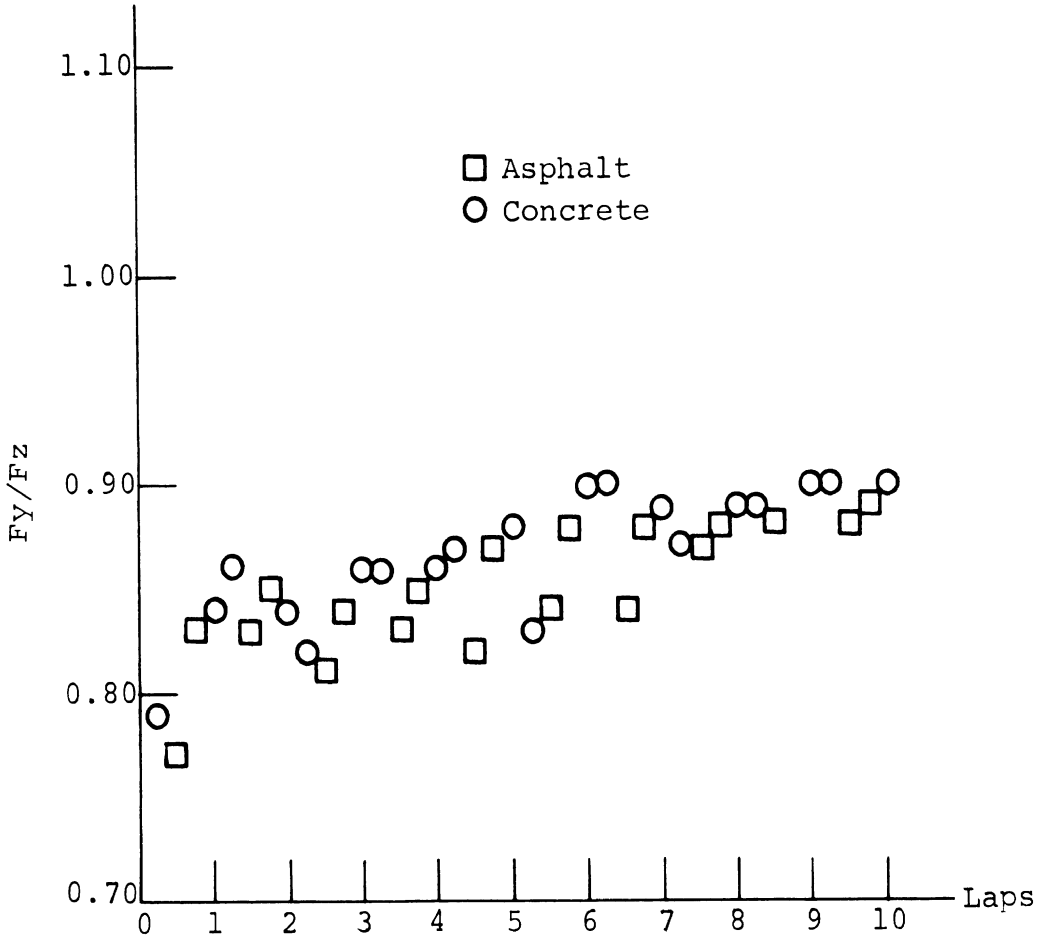

Lateral Force/Wear Data, Mobile Tire Tester, Goodyear F60-15 (Trans Am).

$\alpha=20°$, $F_z=630$, 22 psi, 40 mph

Figure IX-19

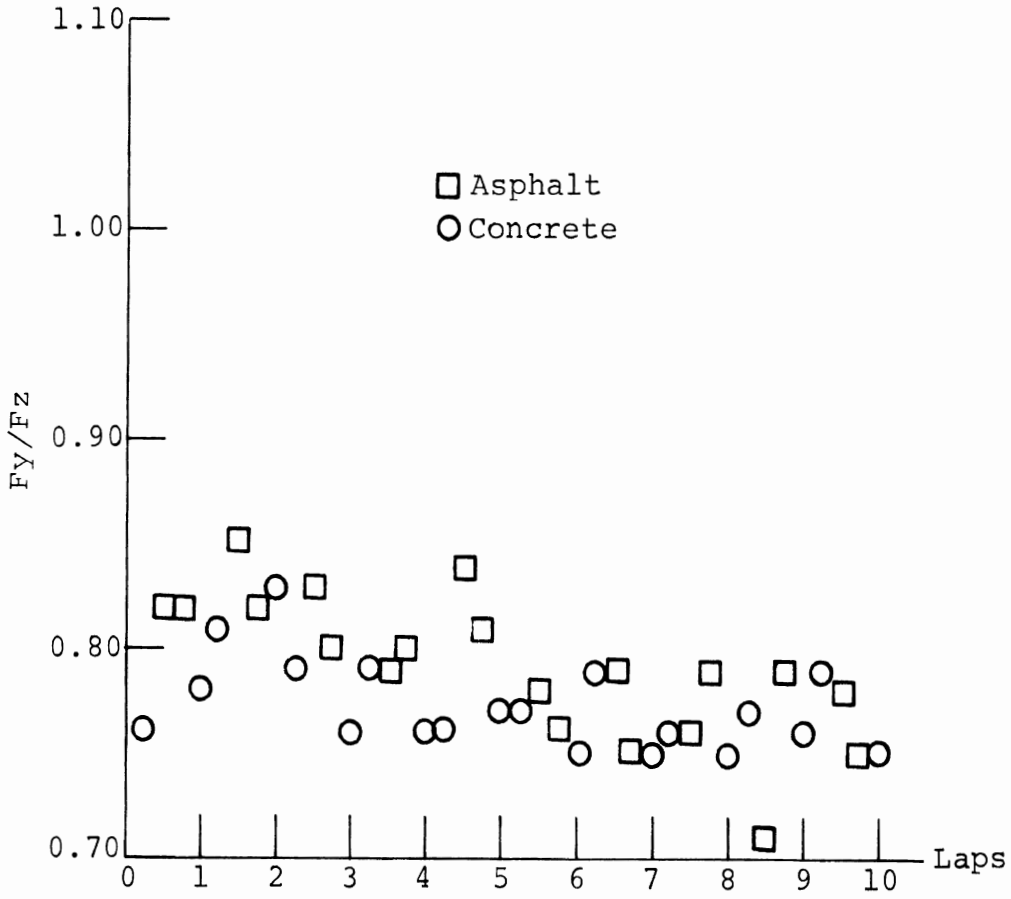

Lateral Force/Wear Data, Mobile Tire Tester, Dunlop 155-13 (Toyota).

α=20°, F_z=710, 22 psi, 40 mph

Figure IX-20

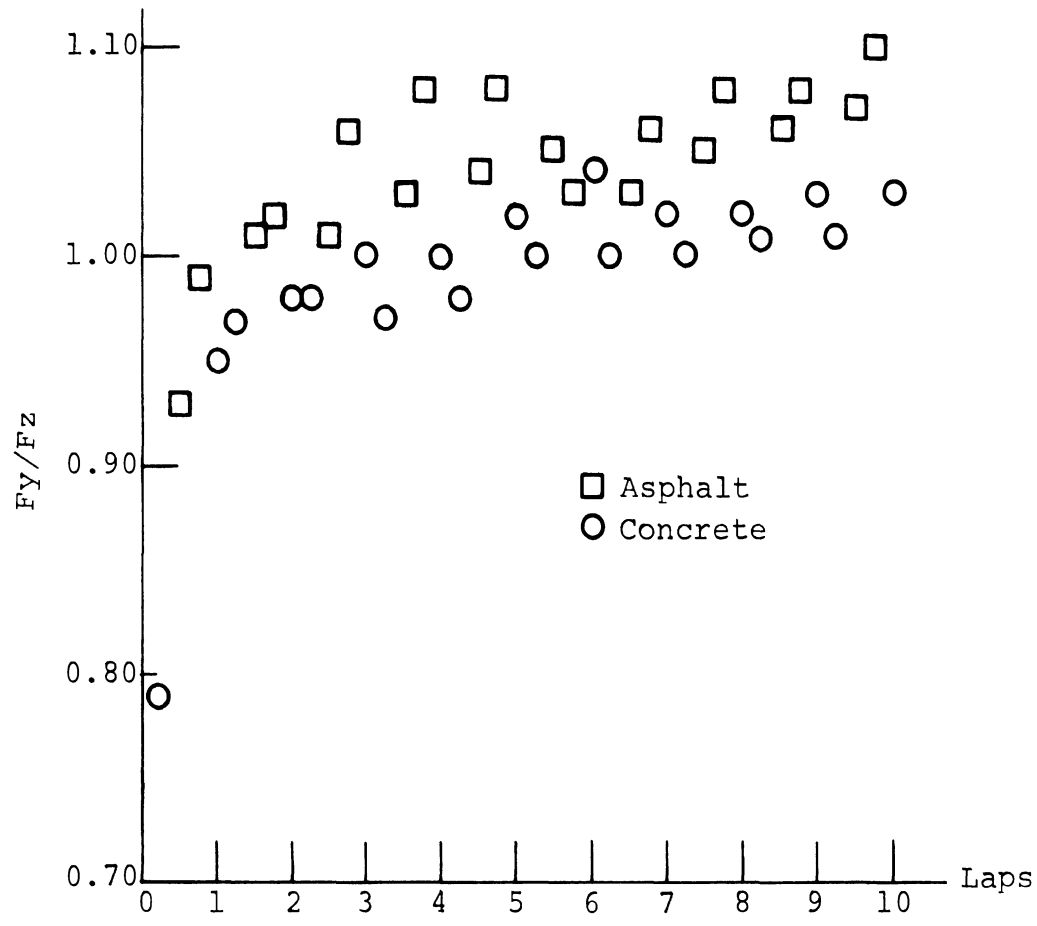

Lateral Force/Wear Data, Mobile Tire Tester, Uniroyal F78-15 (Galaxie).

α=20°, F_z=1310, 28 psi, 40 mph

Figure IX-21

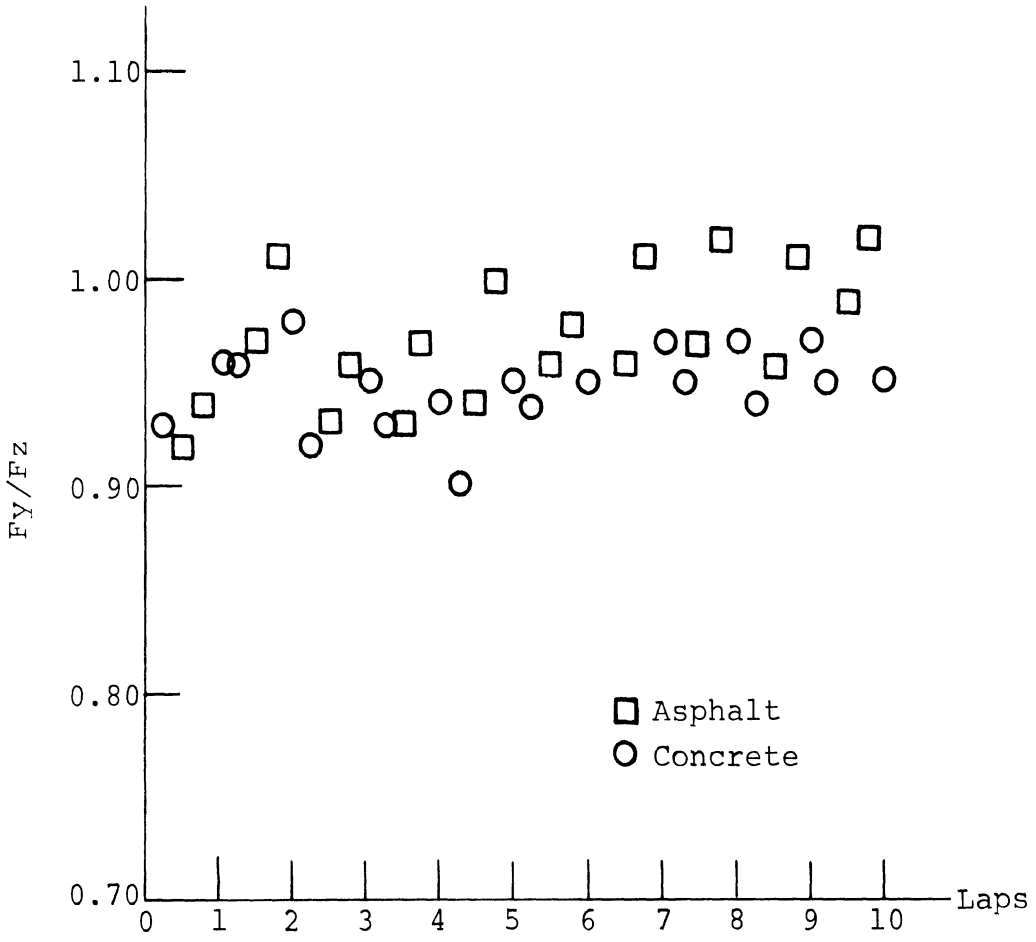

Lateral Force/Wear Data, Mobile Tire Tester, Firestone J78-15 (Toronado).

α=20°, F_z=1570, 24 psi, 40 mph

Figure IX-22

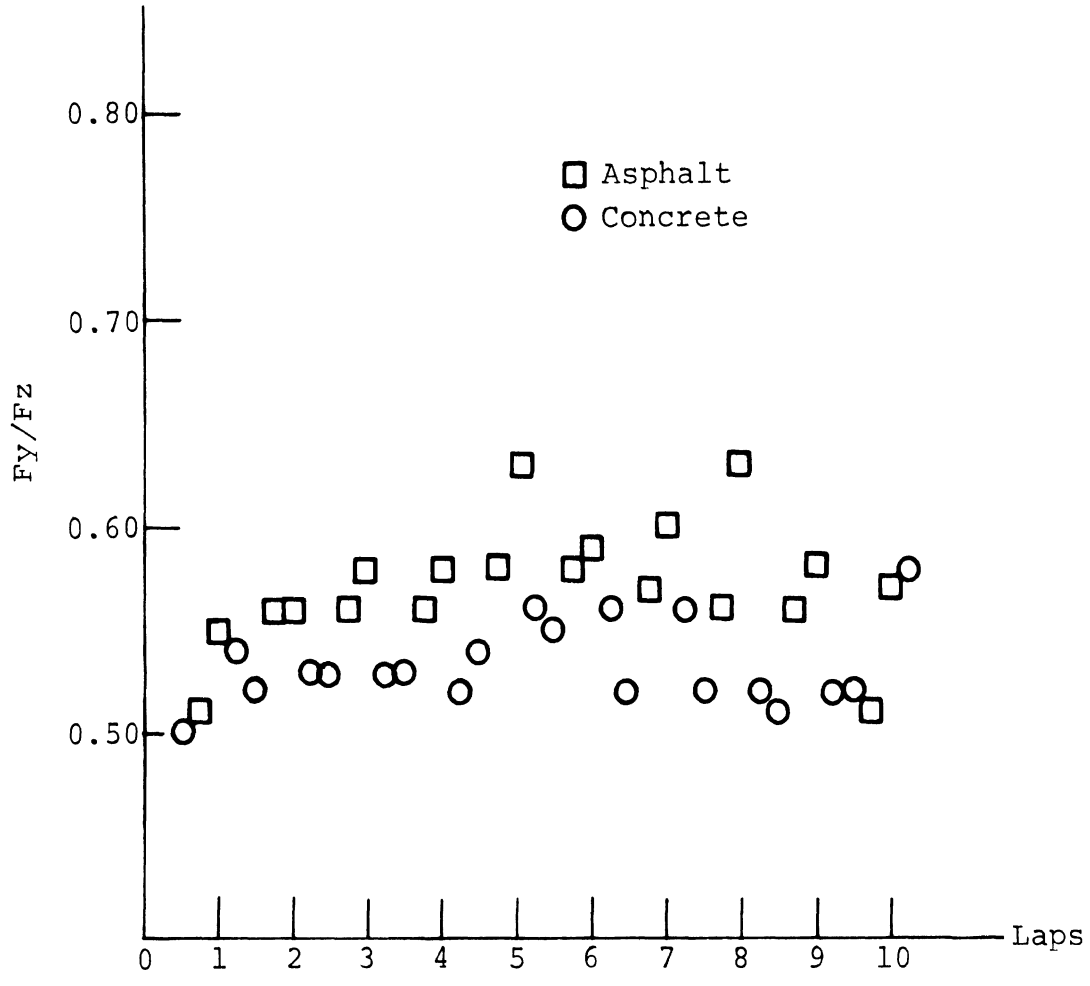

Lateral Force/Wear Data
Mobile Tire Tester
Dunlop 5.95-12 (Austin)
α=20°, F_z=750, 28 psi, 40 mph

Figure IX-23